



---

# Towards a Green Optical Internet

---

**MADUSHANKA NISHAN DHARMAWEERA *B.Eng (Hons)***

SUBMITTED IN TOTAL FULFILMENT OF THE REQUIREMENTS FOR THE DEGREE OF  
DOCTOR OF PHILOSOPHY

*Department of Electrical and Computer Systems Engineering*  
SCHOOL OF ENGINEERING  
MONASH UNIVERSITY

JULY 2014

---

# Towards a Green Optical Internet

---

MADUSHANKA NISHAN DHARMAWEERA *B.Eng (Hons)*

Increasing electricity consumption significantly affects all nations from environmental, social, and economic perspectives. Among the contributors to this problem is rising power consumption of the Internet's backbone network due to expanding Internet traffic volumes.

This thesis addresses the power consumption minimization problem of the Internet's backbone network. Existing solutions to reduce power consumption are identified and categorized into four approaches of network redesign, traffic engineering, power-aware networking, and load-adaptive operation.

Network redesign solutions either modify core nodes by incorporating advanced devices or optimize the physical link topology. Traffic engineering solutions aggregate multiple traffic flows into fewer streams using wavelength/waveband grooming. Power-aware networking solutions vary the operating states of network devices according to traffic variability. Load-adaptive operation solutions use high-rate network devices with Mixed Line Rates (MLR) to serve traffic.

To reduce power consumption of an Optical Circuit Switched (OCS) network, each chapter derives solutions from one or more approaches. First, network redesign and traffic engineering solutions are combined to develop a novel sparse grooming algorithm. The proposed algorithm selectively places core routers to reduce power consumption by 688 kW over a traditional network.

Second, network redesign and power-aware networking solutions are integrated to develop two novel strategies that use different algorithms to reduce cost and power consumption of a survivable network. Cost is reduced by 40% and power consumption is reduced by 1.3 MWh in a day.

Third, the effect of grouping policy and band size and configuration design parameters on power consumption of a waveband-groomed network is analyzed. Proposed algorithms show that power consumption of this Band Switched Network (BSN) can be reduced in different traffic environments by using specific design parameters.

Fourth, traffic engineering and load-adaptive operation solutions are combined to develop three new schemes and two algorithms that assign line rates and wavelengths/wavebands in the network, respectively. Power consumption of this MLR-based BSN reduces by 80% and 17% over two Single Line Rate (SLR)-based traditional networks.

Lastly, solutions from network redesign and power-aware networking are integrated to develop a novel burst assembly scheme that reduces power consumption of a sleep-mode-enabled Optical Burst Switched (OBS) network by approximately 0.5 kW than when traditional schemes are used.

I declare that, to the best of my knowledge, the research described herein is original except where the work of others is indicated and acknowledged, and that the thesis has not, in whole or in part, been submitted for any other degree at this or any other university.

Under the Copyright Act 1968, this thesis must be used only under the normal conditions of scholarly fair dealing. In particular, no results or conclusions should be extracted from it, nor should it be copied or closely paraphrased in whole or in part without the written consent of the author. Proper written acknowledgement should be made for any assistance obtained from this thesis.

I certify that I have made all reasonable efforts to secure copyright permissions for third-party content included in this thesis and have not knowingly added copyright content to my work without the owner's permission.

Signature \_\_\_\_\_

Date \_\_\_\_\_

---

---

# Acknowledgments

---

I take this opportunity to express my gratitude to the people without whose support and encouragement this thesis would not have been possible. First, I offer my most sincere thanks to my main supervisor, Dr. Rajendran Parthiban, for providing continuous support and guidance towards the successful completion of my Ph.D. thesis. Your years of mentoring and invaluable advice have helped me grow as a researcher.

I would also like to thank my co-supervisor, Dr. Ahmet Sekercioglu, for tirelessly supporting me despite the distance and for introducing me to LaTeX and Mendely. I'm thankful to Mr. Nader Kamrani, Dr. Vineetha Kalavally, and Dr. Hisham Jaward for their constructive feedback and suggestions to improve my work.

Words cannot express how grateful I am to my parents, grandparents, and in-laws for their love, support, and prayers. Amma & Thaththa, I'm deeply indebted to you both for all of the sacrifices that you have made for me. I'm thankful to my sister and brother-in law, Himali and Iresh, and my sister-in law and fiance, Devangi and Rangika, for believing in my ability to do well and cheering me on throughout my Ph.D. journey.

Thanks to all my colleagues for making my Ph.D. journey a truly memorable experience. I'm not likely to forget our intense gaming sessions and our time together in the Monash University Postgraduate Association executive committee. So a very special thanks to Kasun, Mukund, JJ, Chew Yee, Vero, Shan, Yasir, Jason, Rish, Jon, Kokum, Koh, Boon Ean, Timothy, Mah, and Ajay. Thanks also to all my friends here in my second home, Malaysia, and back home in Sri Lanka.

Most importantly, I would like to acknowledge my beloved wife, Hasuli, without whom the completion of this thesis would not have been possible. You gave me an overwhelming sense of love, confidence, and strength and stood by my side at every stage of this journey. It was you who encouraged me to never give up during challenging times and supported me the most in reaching the chequered flag. Hurrah! It's time to travel!

---

---

# Contents

---

<b>1</b>	<b>Introduction</b>	<b>1</b>
1.1	Looking ahead . . . . .	1
1.2	Focus of the thesis . . . . .	3
1.2.1	Backbone networks . . . . .	3
1.2.2	Power consumption of backbone networks . . . . .	4
1.2.3	Problem definition . . . . .	7
1.3	Organization of the thesis . . . . .	8
1.4	Contributions of the thesis . . . . .	10
1.5	Publications . . . . .	13
<b>2</b>	<b>Approaches for Reducing Power Consumption of Backbone Networks</b>	<b>15</b>
2.1	Introduction . . . . .	15
2.2	Architecture of the backbone network . . . . .	18
2.3	Network redesign approach . . . . .	19
2.3.1	Core node redesign . . . . .	20
2.3.1.1	Evolution of core nodes . . . . .	21
2.3.1.2	Electronic vs. optical buffering . . . . .	24
2.3.1.3	Electronic vs. optical processing . . . . .	25
2.3.1.4	Electronic vs. optical switching . . . . .	26
2.3.1.5	Networks with Hybrid Core Nodes . . . . .	27
2.3.2	Physical link topology redesign . . . . .	28
2.3.3	Network redesign approach: Summary of findings . . . . .	30
2.4	Traffic engineering approach . . . . .	31
2.4.1	Wavelength grooming for static traffic . . . . .	33
2.4.2	Wavelength grooming for dynamic traffic . . . . .	36
2.4.3	Waveband grooming . . . . .	38
2.4.4	Traffic engineering approach: Summary of findings . . . . .	41
2.5	Power-aware networking approaches . . . . .	45
2.5.1	Power-aware network design . . . . .	46
2.5.2	Power-aware routing . . . . .	47
2.5.3	Reconfiguration . . . . .	49
2.5.4	Sleep mode of operation . . . . .	51
2.5.5	Limitations of power-aware networking . . . . .	52
2.5.6	Power-aware networking approach: Summary of findings . . . . .	53
2.6	Load-adaptive operation approaches . . . . .	56
2.6.1	Mixed Line Rate . . . . .	57
2.6.2	Adaptive Line Rate . . . . .	58
2.6.3	Load-adaptive operation approach: Summary of findings . . . . .	61

2.7	Adopting the four approaches in real networks . . . . .	63
2.7.1	Approaches adopted in industrial research projects . . . . .	63
2.7.2	Approaches adopted by vendors and carriers . . . . .	64
2.7.3	Summary of approaches adopted in real networks . . . . .	66
2.8	Conclusion . . . . .	67
<b>3</b>	<b>Sparse Grooming in OCS Networks</b>	<b>70</b>
3.1	Introduction . . . . .	70
3.2	Overview of relevant work . . . . .	71
3.3	Network model . . . . .	72
3.3.1	Traffic generation . . . . .	72
3.3.2	Grooming procedure . . . . .	73
3.3.3	Power consumption . . . . .	75
3.4	Problem definition . . . . .	76
3.4.1	Inputs . . . . .	77
3.4.2	Assumptions . . . . .	77
3.4.3	Goal . . . . .	78
3.5	Methodology . . . . .	78
3.6	Evaluation of results . . . . .	79
3.7	Summary of findings . . . . .	83
<b>4</b>	<b>Traffic-Dependent Link Optimization</b>	<b>86</b>
4.1	Introduction . . . . .	86
4.2	Overview of relevant literature . . . . .	87
4.3	Network architecture . . . . .	91
4.3.1	Network operations . . . . .	91
4.3.2	Power consumption of WDM-layer equipment . . . . .	93
4.3.3	Costs of WDM-layer equipment . . . . .	93
4.4	Problem formulation . . . . .	94
4.4.1	Input parameters . . . . .	95
4.4.2	Variables . . . . .	96
4.4.3	Objectives . . . . .	97
4.4.4	Constraints . . . . .	97
4.5	Heuristic algorithms . . . . .	100
4.5.1	Link-Reducing algorithm . . . . .	100
4.5.2	Multi-Objective algorithm . . . . .	102
4.5.3	Long Fiber Removal algorithm . . . . .	106
4.5.4	Incremental and Greenfield heuristic strategies . . . . .	107
4.6	Reducing deployment cost or CAPEX . . . . .	108
4.6.1	Experiment environment . . . . .	108
4.6.2	CAPEX minimization . . . . .	109
4.6.2.1	Power consumption . . . . .	111
4.6.2.2	Transmission distance . . . . .	113
4.6.2.3	Comparison of cost, power consumption and delay . . . . .	113
4.7	Reducing power consumption during low-load periods . . . . .	114
4.7.1	Comparison of MO algorithm with near-optimal results . . . . .	114
4.7.2	Comparison of MO algorithm with other criteria-based algorithms . . . . .	114
4.7.2.1	Switching off active fibers . . . . .	115
4.7.2.2	Reducing the length of active fibers . . . . .	116
4.7.2.3	Reducing the number of regenerators used . . . . .	117
4.7.2.4	Reducing CAPEX . . . . .	118
4.7.2.5	Reducing daily/monthly power consumption and OPEX . . . . .	118

4.8	Summary of findings . . . . .	121
<b>5</b>	<b>Designing Power-Efficient Band-Switched OCS Networks</b>	<b>122</b>
5.1	Introduction . . . . .	122
5.2	Design parameters: Grouping policy, band size and band configuration . . . . .	125
5.3	Network model . . . . .	126
5.3.1	Node architecture . . . . .	127
5.3.2	Modelling power consumption . . . . .	128
5.4	Problem framework . . . . .	130
5.4.1	Input parameters . . . . .	131
5.4.2	Notations . . . . .	132
5.4.3	Variables . . . . .	133
5.4.4	Objective . . . . .	133
5.4.5	Constraints . . . . .	134
5.4.5.1	Set of general constraints . . . . .	134
5.4.5.2	Constraints on regenerators . . . . .	135
5.4.5.3	Constraints on fibers . . . . .	136
5.4.5.4	Constraints on waveband switching . . . . .	136
5.4.5.5	Port numbers . . . . .	137
5.4.6	Existing heuristics . . . . .	138
5.5	Balanced-Path Light-Splitting algorithm . . . . .	138
5.5.1	Stage 1: Balanced-Path routing . . . . .	139
5.5.2	Stage 2: Light-Splitting wavelength/waveband assignment . . . . .	139
5.6	Evaluation of results . . . . .	144
5.6.1	Experiment procedure . . . . .	145
5.6.2	Input parameters . . . . .	146
5.6.3	General trend . . . . .	147
5.6.4	Impact of BG on different-sized networks . . . . .	150
5.6.5	Impact of BG on different traffic models . . . . .	151
5.6.6	Effect of grouping policy . . . . .	152
5.6.7	Effect of band size . . . . .	156
5.6.8	Effect of band configurations . . . . .	158
5.7	Summary of findings . . . . .	161
<b>6</b>	<b>MLR-Based Band Switched OCS Networks</b>	<b>163</b>
6.1	Introduction . . . . .	163
6.2	Overview of related work . . . . .	164
6.3	Network models . . . . .	166
6.4	Problem framework . . . . .	168
6.4.1	Input parameters . . . . .	169
6.4.2	Notations . . . . .	170
6.4.3	ILP variables . . . . .	171
6.4.4	Objective . . . . .	171
6.4.5	Constraints . . . . .	172
6.4.5.1	Set of general constraints . . . . .	172
6.4.5.2	Constraints on regenerators . . . . .	173
6.4.5.3	Constraints on fibers . . . . .	174
6.4.5.4	Constraints on waveband switching . . . . .	174
6.4.5.5	Port numbers . . . . .	175
6.5	Heuristic Approaches . . . . .	176
6.5.1	Notations . . . . .	176
6.5.2	Stage 1: Path selection using Balanced-Path routing . . . . .	177

6.5.3	Stage 2: Line rate assignment . . . . .	178
6.5.3.1	Minimize transponder and regenerator power consumption using MTR . . . . .	178
6.5.3.2	Minimize transponder power consumption using MT . . . . .	179
6.5.3.3	Combining MTR and SLR using HMTR . . . . .	179
6.5.4	Stage 3: Wavelength and waveband assignment using Lightpath Splitting . . . . .	180
6.6	Evaluation of results . . . . .	184
6.6.1	Power consumption of transponders . . . . .	185
6.6.2	Power consumption of regenerators . . . . .	187
6.6.3	Power consumption of amplifiers . . . . .	189
6.6.4	Power consumption of optical switch ports . . . . .	190
6.6.5	Total power consumption . . . . .	192
6.7	Summary of findings . . . . .	193
<b>7</b>	<b>Sleep-Mode-Enabled OBS Networks</b>	<b>195</b>
7.1	Introduction . . . . .	195
7.2	Network model . . . . .	197
7.2.1	Burst assembly router . . . . .	198
7.2.2	OBS core router . . . . .	199
7.2.3	Operation of a sleep-mode-enabled OBS network . . . . .	201
7.2.4	Power consumption model . . . . .	203
7.3	Problem definition . . . . .	205
7.3.1	Input parameters . . . . .	205
7.3.2	Assumptions . . . . .	206
7.3.3	Goals . . . . .	206
7.4	Methodology . . . . .	206
7.4.1	Strategy 1: Increase the Threshold Releasing Criterion . . . . .	207
7.4.2	Strategy 2: Concatenate multiple bursts into a single burst . . . . .	208
7.4.2.1	Destination- and Path-based Segmentation burst assembly scheme . . . . .	210
7.4.2.2	Testing the condition . . . . .	211
7.5	Evaluation of results . . . . .	213
7.6	Summary of findings . . . . .	214
<b>8</b>	<b>Conclusion</b>	<b>217</b>
8.1	Looking back . . . . .	217
8.2	General approach . . . . .	220
8.3	Summary of key findings . . . . .	222
8.3.1	Sparse grooming in OCS networks . . . . .	222
8.3.2	Traffic-dependent link optimization . . . . .	224
8.3.3	Designing power-efficient band-switched OCS networks . . . . .	225
8.3.4	MLR-based band-switched OCS networks . . . . .	225
8.3.5	Sleep-mode-enabled OBS networks . . . . .	226
8.4	Expected future work . . . . .	226
8.4.1	Sparse grooming in OCS networks . . . . .	226
8.4.2	Traffic-dependent link optimization . . . . .	227
8.4.3	Designing power-efficient band-switched OCS networks . . . . .	227
8.4.4	MLR-based band-switched OCS networks . . . . .	228
8.4.5	Sleep-mode-enabled OBS networks . . . . .	228

---



---

## List of Figures

---

1.1	The fundamental architecture of a backbone network . . . . .	4
1.2	The evolution from PtP-WDM networks to optical backbone networks . . . . .	5
2.1	Constituent devices of an optical backbone network . . . . .	19
2.2	Different core node architectures . . . . .	22
2.3	Two different physical topologies connecting 7 core nodes . . . . .	29
2.4	Comparison of the three wavelength grooming schemes . . . . .	34
2.5	Aggregating traffic at multiple granularities by an MG-OXC of a Band Switched Network (BSN) . . . . .	39
2.6	Switching nodes into sleep mode to reduce power consumption. . . . .	45
2.7	A backbone network using load-adaptive techniques: The size of the circles are proportional to their capacity and line rates; the dotted and solid lines indicate light- and heavy-loaded links, respectively. . . . .	57
2.8	Rates assigned by SLR, MLR, and ALR techniques when transporting 50 Gbps of traffic from node $i$ to $j$ . . . . .	59
3.1	General architecture of the Internet . . . . .	73
3.2	Example illustrating grooming performed at different core nodes . . . . .	74
3.3	Initial topology of the network . . . . .	76
3.4	Final topology of the network containing a single grooming node . . . . .	77
3.5	The initial network topology . . . . .	81
3.6	The resultant network topology . . . . .	83
3.7	Power consumed by the network when core nodes in different locations are equipped with core routers . . . . .	83
3.8	Power consumed by the core routers and physical (WDM) links with different grooming nodes . . . . .	84
3.9	Total power consumption with and without grooming nodes . . . . .	84
4.1	General architecture of the backbone network . . . . .	92
4.2	CAPEX against increasing $W$ . . . . .	109
4.3	Number of fibers/links against increasing $W$ . . . . .	110
4.4	Total length of the fibers/links against increasing $W$ . . . . .	111
4.5	Number of hops travelled by traffic demands against increasing $W$ . . . . .	112
4.6	Power consumption against increasing $W$ . . . . .	112
4.7	The number of switched-on fibers remaining against traffic variations . . . . .	116
4.8	The total length of switched-on fibers remaining against traffic variations . . . . .	117
4.9	The number of regenerators used against traffic variations . . . . .	118
4.10	Breakdown of CAPEX . . . . .	119

4.11	Percentage power consumption of network devices using the MO algorithm with peak-hour traffic) . . . . .	120
4.12	Power consumption against increasing time . . . . .	120
5.1	Comparison of C1 and C2 configurations with a uniform BS of 2 . . . . .	126
5.2	The architecture of a three-layer MG-OXC containing AOWCs and AORs . . . . .	127
5.3	Representation of (i) the initial topology $G$ , (ii) initial virtual topology $LL$ , (iii) updated $LL$ , and (iv) updated $WL$ . . . . .	140
5.4	An illustrative example of waveband assignment using Algorithms 4 and 5 . . . . .	144
5.5	Different combinations of design parameters with BG = <i>SE-BS2</i> highlighted . . . . .	145
5.6	$Rt$ , obtained for different combinations of band size and grouping policy (i.e., BG) on the <b>NSF</b> network with a <b>uniform</b> traffic model, plotted against increasing traffic volume . . . . .	148
5.7	$Rt$ , obtained for different BG on the <b>NSF</b> network with a <b>gravity</b> traffic model, plotted against increasing traffic volume . . . . .	148
5.8	$Rt$ , obtained for different BG on the <b>EON</b> network with a <b>uniform</b> traffic model, plotted against increasing traffic volume . . . . .	149
5.9	$Rt$ , obtained for different BG on the <b>EON</b> network with a <b>gravity</b> traffic model, plotted against increasing traffic volume . . . . .	149
5.10	$Rt$ , averaged over the range of traffic volumes distributed using the <b>uniform</b> traffic model, plotted against every BG on the <b>NSF</b> and <b>EON</b> networks . . . . .	151
5.11	$Rt$ , averaged over the range of traffic volumes distributed using the <b>gravity</b> traffic model, plotted against every BG in the <b>EON</b> and <b>NSF</b> networks . . . . .	152
5.12	$Rt$ of combinations <i>SE-BS4</i> and <i>INT-BS4</i> plotted against increasing traffic volumes on the <b>NSF</b> network using the <b>uniform</b> traffic model . . . . .	153
5.13	$Rt$ of combinations <i>SE-BS2</i> and <i>INT-BS2</i> plotted against increasing traffic volumes on the <b>NSF</b> network using the <b>gravity</b> traffic model . . . . .	154
5.14	Device power consumption plotted against increasing traffic volume for each grouping policy on the <b>NSF</b> network, using a <b>uniform</b> traffic model . . . . .	155
5.15	Power savings of a BSN using the <b>INT</b> grouping policy with respect to <i>different BS</i> and a <b>uniform</b> traffic model on the <b>NSF</b> network . . . . .	156
5.16	Power savings of a BSN using the <b>SE</b> grouping policy with respect to <i>different BS</i> and a <b>gravity</b> traffic model on the <b>NSF</b> network . . . . .	157
5.17	Total power consumption of the MG-OXCs and amplifiers, using SE and INT grouping policies with C1 and C2 configurations, plotted against three band sizes . . . . .	159
5.18	Power consumption of the MG-OXCs, using SE and INT grouping policies with C1 and C2 configurations, plotted against three band sizes . . . . .	159
5.19	Power consumption of the amplifiers, using SE and INT grouping policies with C1 and C2 configurations, plotted against three band sizes . . . . .	160
5.20	Power consumed by amplifiers and the individual devices of MG-OXCs, using C1 and C2 configurations with INT grouping policy and BS = 4, when total network traffic is 25 Tbps. . . . .	161
6.1	Serving two connection requests $(s_1, d)$ and $(s_2, d)$ in an SLR-based WSN/BSN . . . . .	167
6.2	Serving two connection requests $(s_1, d)$ and $(s_2, d)$ in an MLR-based WSN/BSN . . . . .	168
6.3	Three rate assignment choices for $t^{sd}$ of 30 Gbps . . . . .	179
6.4	Assignment of rates for $t^{sd}$ of 150 Gbps using the HMTR algorithm . . . . .	180
6.5	Representation of (i) the actual topology $G$ , (ii) initial $LL$ , (iii) updated $LL$ , and (iv) $WL$ . . . . .	181
6.6	Power consumption of transponders at every traffic volume (Tbps) in all test networks . . . . .	186

6.7	Power consumption of regenerators at every traffic volume (Tbps) in all test networks . . . . .	188
6.8	Power consumption of optical amplifiers at every traffic volume (Tbps) in all test networks . . . . .	189
6.9	Number of optical switch ports consumed by SLR-based networks at every traffic volume (Tbps) . . . . .	190
6.10	Number of optical switch ports consumed by MLR-based networks at every traffic volume (Tbps) . . . . .	191
6.11	Combined power consumption of <i>optical switch ports</i> and <i>wavelength converters</i> at every traffic volume (Tbps) in all test networks . . . . .	192
6.12	Total power consumption of the WDM-layer devices of all test networks at every traffic volume (Tbps) . . . . .	193
7.1	The fundamental architecture of an OBS network . . . . .	196
7.2	Key devices and operations of a burst assembly router and an OBS core router . . . . .	196
7.3	Power consumption at different operating states of a device in a sleep-mode-enabled OBS network . . . . .	197
7.4	The architecture of an OBS burst assembly router . . . . .	198
7.5	Block diagram of an OBS core router . . . . .	200
7.6	A simple example of a sleep-mode-enabled OBS network . . . . .	203
7.7	Relationship between power consumption, TRC, and traffic arrival rate . . . . .	209
7.8	Relationship between queueing delay, TRC, and traffic arrival rate . . . . .	210
7.9	An example of a <i>traditional</i> OBS network which accommodates traffic between node pairs $(s, d_1)$ and $(s, d_2)$ that arrives at a rate of $R^{sd_1}$ and $R^{sd_2}$ , respectively, using the <b>DEB burst assembly scheme</b> . . . . .	211
7.10	An example of an OBS network which accommodates traffic between node pairs $(s, d_1)$ and $(s, d_2)$ that arrives at a rate of $R^{sd_1}$ and $R^{sd_2}$ , respectively, using the <b>DPS burst assembly scheme</b> . . . . .	212
7.11	Power consumption of the router ports at every test instance when bursts are generated with the DEB and DPS schemes . . . . .	215
7.12	Average burst queueing delay at every test instance . . . . .	216

---

---

## List of Tables

---

2.1	Comparison between this study and available surveys . . . . .	17
2.2	Power consumption values of backbone network devices . . . . .	20
2.3	Power consumption of electronic, optical, and hybrid core nodes . . . . .	32
2.4	A summary of power-reducing grooming efforts . . . . .	44
2.5	A summary of research on power-aware networking . . . . .	54
2.6	A broad comparison of SLR, MLR, and ALR approaches. . . . .	62
3.1	Parameter values . . . . .	81
3.2	Traffic between access routers of different cities (in Gbps) . . . . .	82
4.1	Key differences between the present study and past research . . . . .	90
4.2	Power consumption of network devices . . . . .	93
4.3	Normalized price model of network equipment . . . . .	94
4.4	A simple comparison of IS and GS heuristics . . . . .	113
4.5	Comparison of results with MO and near-optimal (NO) results . . . . .	115
4.6	Cost of a network designed to serve peak hour traffic optimized with different heuristic algorithms . . . . .	119
5.1	Testing every BG in Figure 5.5 with different networks, traffic models, and traffic volumes . . . . .	146
5.2	Power consumption of network devices . . . . .	147
6.1	Rated power consumption of WDM-layer devices . . . . .	185
6.2	Percentage reduction in power consumption (%) of devices in each network, averaged over the considered traffic range, relative to highest power consumption . . . . .	187
7.1	Power consumption of the devices in a burst assembly router as a percentage of its total power consumption . . . . .	201
7.2	Power consumption of the devices in an OBS core router with 4 line cards as a percentage of its total power consumption . . . . .	202
7.3	Values assigned to the parameters . . . . .	208
7.4	Max. and Min. traffic arrival rates and burst threshold of the test network . . . . .	214
8.1	Key differences across research problems . . . . .	223

---

# Acronyms

---

ALR	Adaptive Line Rate
A-OCS	All-Optical Circuit Switched
A-OLS	All-Optical Label Switching
AOR	All-Optical Regenerator
AOWC	All-Optical Wavelength Converter
AWG-TWC	Arrayed-Waveguide-Gratings with Tunable Wavelength Converter
BBR	Bandwidth Blocking Ratio
BCP	Burst Control Packet
BG	Band size-Grouping policy combination
BL	Burst Length
BoB	Burst-of-Bursts
BP	Balanced-Path (routing algorithm)
BPHT	Balanced-Path routing with Heavy Traffic first (algorithm)
BPLS	Balanced-Path Light-Splitting (algorithm)
BS	Waveband or Band Size
BSN	Band Switched Network
BTF	Band-to-Fiber (multiplexer)
BTW	Band-to-Wavelength (de-multiplexer)
BuS	Burst Switch
BXC	Band Cross-Connect
C1,C2	Waveband Configurations
CAPEX	Capital Expenditure
CMOS	Complementary-symmetry Metal-Oxide Semiconductor
DAC	Drop-And-Continue
DB	Direct Bypass
DEB	Destination-Based (burst assembly scheme)
DEMUX/D-MUX	De-multiplexer
D-OXC	Drop-And-Continue-enabled Optical Cross Connect
DPS	Destination- and Path-based Segmentation (burst assembly scheme)
DPSF	Disjoint-path Power Savings Factor (criteria-based heuristic algorithm)
DTBA	Dynamic Time-Based Assemble
DTU	Data Transmission Unit
DWDM	Dense Wavelength Division Multiplex
EAR	Energy-Aware Routing
EA-RWA	Energy-Aware Routing and Wavelength Assignment
EER	Energy-Efficient Routing
EON	European Optical Network

---

EOP-A	Electro-Optic-Phased Array
EPAR	Energy-Profile-Aware Routing
EPS	Electronic Packet Switch
EWA	Energy Watermark Algorithm
EXC	Electronic Cross Connect
FA	First Approach
FCR	Fully-Constrained Reconfiguration
FDL	Fiber Delay Line
FF	First-Fit (wavelength assignment scheme)
FTB	Fiber-to-Band (de-multiplexer)
FXC	Fiber Cross-Connect
GA	Genetic Algorithm
GS	Greenfield Strategy
HCN	Hybrid Core Node
HMTR	Hybrid of Minimize Transponder and Regenerator power consumption (heuristic)
HOS	Hybrid Optical Switched
HOXC	Hybrid Optical Cross Connect
HWA	Hierarchical Waveband Assignment (algorithm)
I/O	Input-Output
ICT	Information and Communication Technology
ILA	In-Line Amplifier
ILP	Integer Linear Programming
INT	Intermediate (waveband grouping policy)
IP	Internet Protocol
IP-OTN	IP over Optical Transport Network
IS	Incremental Strategy
ITU	International Telecommunication Union
JET	Just-Enough-Time (one-way reservation protocol)
LAP-FF	Least-Additional-Power First-Fit
LBC	Load-Based Cost
LCP	Least-Congested Path
LCW	Least-Cost Wavelength
LF	Least Utilized Fiber (criteria-based heuristic algorithm)
LFA	Least-Flow Algorithm
LFR	Long Fiber Removal (algorithm)
LL	Lightpath Layer
LLPR	Least-Loaded Path Routing
LR	Link-Reducing (algorithm)
LS	Light-Splitting (algorithm)
MA	Most Amplifiers (criteria-based heuristic algorithm)
mAOR	Multi-wavelength All-Optical Regenerator
MBSN	Mixed/Multi-Line-Rate-based Band Switched Network
MEMS	Micro-Electro-Mechanical-Systems
MG-OXC	Multi-Granular Optical Cross Connect
MHB	Multi-Hop with Bypass
MILP	Multiple Integer Linear Programming
MinL	Minimize Lightpaths
MinP	Minimize Power
MinT	Minimize Transponders
MLR	Mixed/Multi-Line Rate

---

MO	Multi-Objective (algorithm)
MRR	Micro-Ring Resonator
MSGPE	Multi-hop Survivable Grooming with Power Efficiency
MSPP	Multi-Service Provisioning Platform
MT	Minimize Transponder power consumption (heuristic)
MTR	Minimize Transponder and Regenerator power consumption (heuristic)
MUP	Most-Used Path
MUX	Multiplexer
MWSN	Mixed/Multi-Line-Rate-based Wavelength Switched Network
MXHF	Maximizing Hop First
NB	No Bypass
NGN	Next-Generation Network
NIC	Network Interface Card
NO	Near-Optimal
NSF	National Science Foundation
OBS	Optical Burst Switching
OCS	Optical Circuit Switching
OE	Opt-Edge
O-E	Optical-to-Electrical
O-E/E-O	Optical-to-Electrical or Electrical-to-Optical
OLS	Optical Label Switch/Switching
ONP	Optical Networking Platform
O-OFDM	Optical Orthogonal Frequency Division Multiplexing
OPEX	Operational Expenditure
OPS	Optical Packet Switching
OSC	Optical Supervisory Channel
OXC	Optical Cross Connect
PA-RWA	Power-Aware Routing with Wavelength Assignment
PEGA	Power-Efficient Grooming Algorithm
PHY	Physical Layer (transceivers)
PIC	Photonic Integrated Circuit
PoA	Post-Amplifier
PPS	Photonic Packet Switch
PrA	Pre-Amplifier
PtP	Point-to-Point
PtP-WDM	Point-to-Point Wavelength Division Multiplexing
QoS	Quality of Service
RAM	Random Access Memory
RIG	Robust Integrated Grooming
RS	Rate-Adaptive Scaling
RWA	Routing and Wavelength Assignment
SA	Second Approach
SB	Switch Block
SBSN	Single-Line-Rate-based Band Switched Network
SCU	Switch Control Unit
SE	Same-Ends (waveband grouping policy)
SEON	Spectrum Elastic Optical Network
SinPR	Single Path Routing
SLOB	Slow-Light Optical Buffer
SLR	Single Line Rate

---

SOA-GA	Semiconductor-Optical-Amplifier Gate Array
SPR	Shortest Path Routing
SPT	Shortest Path Tree
SSE	Sleep-State Exploitation
SSGPE	Single-hop Survivable Grooming with Power Efficiency
Start-SH&ReR	Start Single-Hop and Re-Route
SWSN	Single-Line-Rate-based Wavelength Switched Network
TA	Third Approach
T-AOR	Total number of single-wavelength and multi-wavelength All-Optical Regenerators
TAP-BR	Time-Aware Provisioning with Bandwidth Reservation
TATG	Time-Aware Traffic Grooming
TDS	Time-Driven Switching
TEER	Telecommunications Energy Efficiency Ratio
TP-FF	Two-Phased First-Fit
TRC	Threshold Releasing Criterion
TU	Terminal Unit
TWC	Tunable Wavelength Converter
UR	Unconstrained Reconfiguration
VROOM	Virtual Routers On The Move
VTCR	Virtual-Topology-Constrained Reconfiguration
WAPG	Waveband Assignment with Path Graph (heuristic)
WC	Wavelength converter
WDM	Wavelength Division Multiplexing
WL	Waveband Layer
WSN	Wavelength Switched Network
WTB	Wavelength-to-Band (multiplexer)
WXC	Wavelength Cross-Connect
XPM	Cross-Phase Modulation

---

# INTRODUCTION

---

## 1.1 Looking ahead

The *International Energy Outlook 2013* projects that electricity consumption will increase by 93% between 2010 and 2040 [1]. Telecommunication networks consumed well over 250 TWh of power in 2012 [2], accounting for 2% of global electricity consumption [3]. On the 22nd of September 2012, *The New York Times* reported that the Internet was responsible for consuming 30 billion watts of electricity in 2011, which is roughly equivalent to the output of 30 nuclear power plants [4].

As electricity consumption mounts, non-renewable fossil fuels, which are still the primary energy source for electricity [1], are depleting and raising the cost of electricity [2,5]. Greater combustion of fossil fuels and resultant emissions are also contributing to the elevation of the global carbon footprint [6]. In 2010, *The Guardian* reported that the Internet alone produced 300 million tonnes of  $CO_2$  per year, which is as much as all the coal, oil and gas burned in Turkey or Poland in one year [7]. Therefore, it is imperative that electricity consumption be minimized to reduce its far-reaching impact on the economy and the environment. The onus is on the telecommunications industry to reduce electricity or power consumption, especially if the latter's advancement is not to be constrained by its high power consumption in the near future [8].

The Internet is generally split into three different domains, namely, the access, metro, and core network [9]. Considering the similarity in estimated traffic volumes of the metro and core networks [10], it is argued that the two networks can be merged to form a single backbone network [11]. The Internet is then considered to comprise the access and backbone networks. The access network presently consumes the most power of the two networks [9]. However, as network traffic exceeds the zettabyte threshold and increases by threefold over the next few

years [12], power consumption of the backbone network is expected to soon surpass that of the access network [8,9,13].

A backbone network consists of high capacity core nodes and optical fiber links. Today, most backbone networks are commonly referred to as Point-to-Point Wavelength Division Multiplexing (PtP-WDM) networks. In a PtP-WDM network, traffic is exchanged between core nodes, consisting of core routers, via point-to-point (PtP) lightpaths established in the form of wavelengths. Using Wavelength Division Multiplexing (WDM), multiple wavelengths are combined into a single optical fiber. Core routers primarily rely on electronic technology, thus consuming a substantial amount of electricity, dissipating heat, and possessing limited switching capacity [11, 14, 15]. Due to these limitations of the core routers, it is difficult to scale PtP-WDM networks to serve future traffic demands [11]. To overcome such limitations, backbone networks are gradually evolving from PtP-WDM to optical backbone networks. Optical backbone networks take the form of Optical Circuit Switching (OCS), Optical Burst Switching (OBS), and Optical Packet Switching (OPS) networks. Power consumption of these optical networks have been heavily scrutinized in recent years [16, 17], and numerous solutions to reduce power consumption of these networks have been developed. We categorize the power-efficient solutions developed in relevant studies into four main approaches:

1. **Network redesign:** Designing power-efficient networks using optical and electronic technologies;
2. **Traffic engineering:** Developing energy-aware traffic grooming schemes;
3. **Power-aware networking:** Switching devices between different operating states;
4. **Load-adaptive operation:** Adopting rate-adaptive and mixed-line rate techniques.

In brief, solutions that have been developed using the network resign approach reduce power consumption by appropriately modifying the core nodes and the fiber link topology. Solutions that have used the traffic engineering approach reduce power consumption by efficiently managing traffic flows. Solutions that have been developed using the power-aware networking approach minimize power consumption by dynamically changing the operating state of network devices. Lastly, solutions that have been devised using the load-adaptive operation approach adjusts the operational speeds or capacities of network devices to draw less power. An in-depth analysis of the solutions developed under the four approaches leads us to the following questions:

- How much power can be reduced by modifying core nodes and links?
- How can traffic flows be efficiently managed to minimize power consumption of backbone networks?
- How much more power can be reduced by changing the operational state of network devices without disrupting network operations?
- Could we combine one or more of the above approaches be combined to attain further reduction in power consumption? If so, how much more power can be reduced?

This thesis seeks to provide answers to the above questions and offer new insight into how future optical backbone networks can be designed to minimize power consumption over current PtP-WDM networks.

## 1.2 Focus of the thesis

This section provides the background of the thesis, and defines the problem addressed in this work. we address.

### 1.2.1 Backbone networks

The fundamental architecture of a backbone network is depicted in Figure 1.1. Core nodes are interconnected via links. Optical fibers are housed within the conduit of every link that is laid underground. Each optical fiber is equipped with multiple opto-electronic devices. The type of backbone network (i.e., PtP-WDM, OCS, OBS or OPS) determines the constituent devices of a core node.

Internet Protocol (IP) traffic, originating at the access network, reaches the backbone network via access routers. Access networks communicate with each other through core nodes. *Local traffic from/to the access network is added to the backbone network and dropped from the backbone network via source and destination core nodes of respective local sites. Source and destination core nodes are jointly referred to as edge nodes. Traffic from one edge node to another passes through intermediate core nodes.*

The core nodes of a PtP-WDM network consist of core routers. To minimize Optical-to-Electrical or Electrical-to-Optical (O-E/E-O) signal conversions and electronic traffic processing, the core nodes in an optical backbone network are equipped with optical devices. As

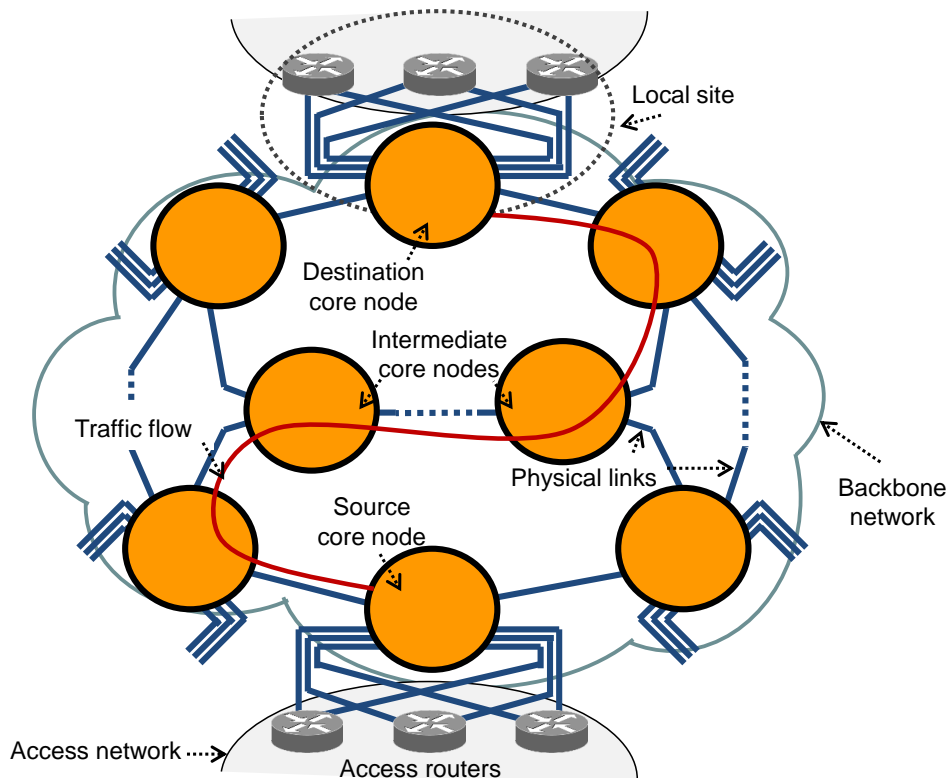


Figure 1.1: The fundamental architecture of a backbone network

backbone networks evolves from PtP-WDM networks to OCS networks, as shown in Figure 1.2, core nodes in the latter would contain Optical Cross Connects (OXCs). Similarly, in OBS and OPS networks, core nodes consist of OBS core routers/burst switches and optical/photonic packet switches, respectively.

### 1.2.2 Power consumption of backbone networks

Power consumption of an optical backbone network (i.e., OCS, OBS or OPS) is equivalent to the sum of power consumed by its constituting devices [18]. To reduce its power consumption, it is then necessary to optimize the *number, configuration, speed/capacity, and operating duration* of network devices. In this thesis, we analyze a number of key concepts that shows potential in reducing power consumption of optical backbone networks.

To achieve high power efficiency, power consumption of network devices should be proportional to their actual load (i.e., power-load proportionality) [19]. Yet, the majority of network devices consume a fixed amount of power regardless of their actual utilization. Hence, power consumption of a backbone network can be modelled by assuming that devices either comply with power-load proportionality [8] or consume a fixed amount of power [20].

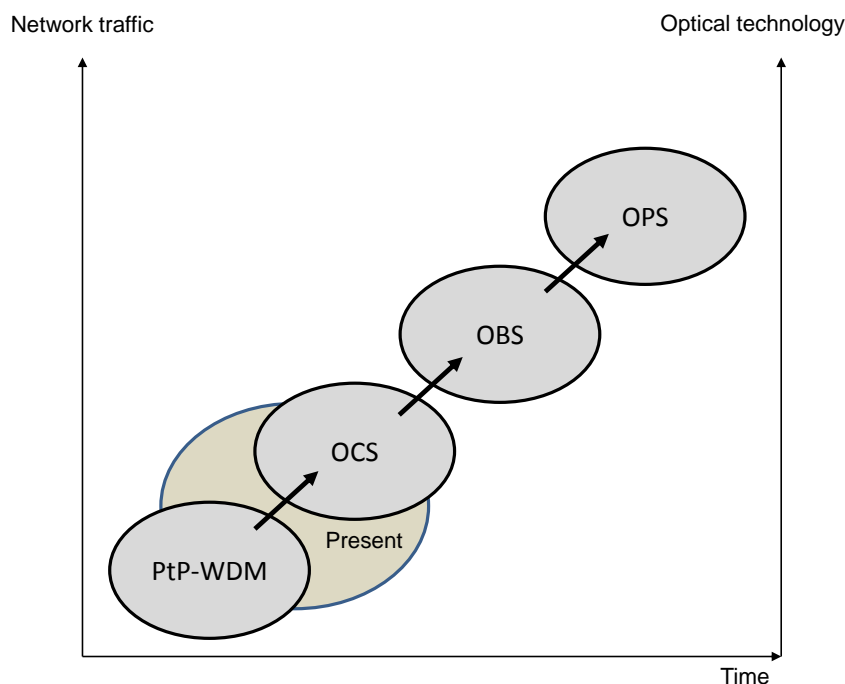


Figure 1.2: The evolution from PtP-WDM networks to optical backbone networks

In a PtP-WDM network, pass-through traffic traversing an intermediate core node is converted from the Optical to Electrical (O-E) domain and is processed by the core router. A considerable amount of power is consumed by the O-E converters [21]. Since core routers have to process both local and pass-through traffic, a PtP-WDM network is required to provision high-capacity core routers. High-capacity core routers consume a significant amount of power and dissipate considerable heat [14, 15]. These problems make it challenging to scale the core nodes of PtP-WDM networks to serve increased traffic demands of the future.

To reduce traffic processing and minimize O-E/E-O conversions, in an OCS network, pass-through traffic is switched from an incoming fiber to an outgoing fiber by an OXC using a single Input-Output (I/O) port pair. Similarly, in an OBS network, pass-through data bursts are switched all-optically. In both OCS and OBS networks, when the need arises, a wavelength assigned to incoming traffic/bursts can be converted to another using advanced all-optical wavelength converters (AOWCs) [22]. The transmission reach of a lightpath in an OCS network can be increased by using all-optical regenerators (AORs) [22]. It is evident that, by gradually moving away electronic technologies and increasing reliance on advanced optical technologies, core nodes could minimize O-E/E-O conversions and reduce power consumption of backbone networks.

In both PtP-WDM and optical backbone networks, physical links could be designed to mimic a ring, star, or mesh topology. By taking into consideration the heterogeneous nature of traffic in the network, the link topology can be designed to minimize the amount of traffic traversing intermediate core nodes and optical fibers, thereby reducing power consumption [23].

To reduce costs of maintenance and upgrades, backbone networks are typically designed to accommodate traffic demands of the foreseen future [24, 25]. As such, network devices are generally over-provisioned when a backbone network is first deployed. However, fluctuations are often observed in network traffic during the course of a day. Under these circumstances, some devices are under-utilized during certain time periods. By allowing selected devices to operate in low-power-consuming sleep or switch-off states, power consumption of under-utilized devices and, thus, the backbone network can be minimized in these time frames.

In most backbone networks today, heterogeneous traffic demands between different core nodes are served using devices that operate at the same speed [26]. In such networks, traffic is exchanged between different core nodes via wavelengths travelling at a Single Line Rate (SLR). Since the power consumption of network devices is closely related to their operating speeds [18], unnecessary electricity waste can be minimized by serving traffic demands with devices that operate at matching speeds [26]. These devices would then operate at mixed or multi-line rates (MLR) [26].

Network device usage can be reduced by using different traffic grooming techniques to manage traffic flows. Traffic grooming can be performed at both wavelength and waveband granularity. Wavelength grooming is the process of aggregating several traffic flows into a single wavelength, and waveband grooming groups several wavelengths into a single waveband. An OCS network that uses wavelength grooming is referred to as a wavelength switched network, while an OCS network that utilizes waveband grooming is referred to as a waveband switched network. In a wavelength-switched network, a pass-through wavelength is switched by an OXC using a single I/O port pair [27]. In a waveband-switched network, a pass-through waveband is switched by a single I/O port pair of a Multi-Granular OXC (MG-OXC) [27]. Wavelength grooming increases wavelength utilization and, thereby, reduces power consumption of the I/O ports of core routers and OXCs. It can be performed at all node sites (full grooming) or at selected locations (sparse grooming). Waveband grooming reduces power consumption of the I/O ports of MG-OXCs [28]. By equipping MG-OXCs with advanced AOWCs

---

and AORs [29,30], further reductions in power consumption can be expected.

### 1.2.3 Problem definition

In this thesis, we address the power consumption minimization problem of optical backbone networks. Particular emphasis is given to OCS and, to a lesser extent, OBS networks. Different optimization processes are developed using the four approaches - network redesign, traffic engineering, power-aware networking, and load-adaptive operation - to reduce power consumed by network devices. Solutions are provided in the form of analysis and developed algorithms. Results are presented as absolute and relative power consumption values.

The inputs of the power consumption minimization problem are core node sites, the initial link topology, and a static traffic matrix. Each optimization process begins by modelling power consumption of the backbone network. While the general architecture of the backbone remains consistent across relevant studies reviewed, significant differences are observed in the technologies and constituent devices of the core nodes and physical links. Furthermore, discrepancies are often observed in reported power consumption values. Therefore, a single power consumption model cannot be applied to different backbone networks.

Through the optimization process, we calculate the number and placement of network devices, measure the usage of elements in every network device, analyze the configuration of the link topology, and compute the speeds/capacities/operating durations of network devices.

While reducing power consumption is the main objective of our thesis, we also take heed of the importance of maintaining Quality of Service (QoS) and reducing cost. In this thesis QoS is measured in terms of traffic latency, transmission delay, signal degradation due to cross-talk and non-linear affects, network survivability, and link resilience among others. The solutions developed in this thesis, therefore, not only reduce power consumption of the backbone network but also minimize any adverse impact on QoS parameters.

Taking the above discussion into account, we address the following power consumption minimization problems:

1. How can core nodes be selectively equipped with core routers to minimize power consumption of an OCS network?
2. How much electricity and cost can be reduced in an OCS network by appropriately configuring physical links?

3. How can waveband grooming effectively incorporate the advanced features of MG-OXC's and all-optical technologies to minimize power consumption of an OCS network?
4. How can waveband grooming and MLR be combined to reduce power consumption of an OCS network?
5. How much more power can be minimized in an OBS network by using the sleep mode of operation?

### 1.3 Organization of the thesis

The chapters in this thesis are organized in the following manner.

**Chapter 2 - Approaches in reducing power consumption of backbone networks** - carries out a comprehensive survey of the most relevant research efforts on minimizing power consumption of backbone networks. Important studies are categorized into four broad approaches - network redesign, traffic engineering, power-aware networking, and load-adaptive operation - based on similarities in developed solutions. Significant findings of these studies and their limitations are discussed, while also evaluating the technological differences between similar work. This chapter also provides an overview of how solutions developed under the four approaches are gathering pace among prominent research bodies, device manufacturers, and network operators. The chapter concludes with a summary of relevant techniques that will be adopted in the ensuing chapters to address the five power consumption minimization problems defined earlier.

**Chapter 3 - Sparse grooming in OCS networks** - analyses how sparse grooming can be utilized to reduce power consumption of an OCS backbone network. Prior research on sparse grooming mostly focuses on maximizing cost benefits and devotes little attention to the increasing power consumption issue. Combining elements of the network redesign and traffic engineering approaches, this chapter presents a novel technique that reduces power consumption by appropriately selecting the grooming sites of a given OCS network. We use the developed technique to provide the solution to research problem 1.

**Chapter 4 - Traffic-dependent link optimization** - investigates how cost and power consumption of an OCS backbone network can be reduced by appropriately configuring physical links according to predicted future traffic demand and hourly traffic demand, respectively. Two algorithms are developed in this chapter using network redesign and power-aware networking

---

approaches to reduce cost and power consumption of an OCS network that is resilient against link failure (i.e., a *survivable* backbone network). After specifying the appropriate power consumption model, future traffic demand, and hourly traffic variations, this chapter compares the two proposed algorithms in the context of cost and power consumption reduction. This comparison demonstrates that the developed algorithms using power-aware networking and network redesign approaches, respectively, provides long-term and short-term cost and power consumption benefits.

**Chapter 5 - Designing power-efficient band switched OCS networks** - evaluates power consumption of an OCS backbone network that uses waveband grooming and employs advanced three-layer MG-OXCs equipped with all-optical devices. Specifically, this chapter assesses how a waveband switched backbone network can be designed to consume less power than a traditional wavelength switched network under different traffic environments. After mathematically defining the power consumption minimization problem of a waveband switched network, a novel heuristic algorithm is proposed. Results obtained by using the developed algorithm in this chapter demonstrates that, by appropriately selecting design parameters according to network size and traffic environment, a considerable amount of power can be reduced.

**Chapter 6 - MLR-based band switched networks** - addresses the power consumption minimization problem of an OCS network that combines traffic engineering (specifically, waveband grooming) and load-adaptive operation (specifically, MLR) approaches. The power consumption minimization problem of an MLR-based waveband switched network is represented using a mathematical model. To be able to solve the problem in feasible time on large-scale networks, three rate assignments schemes and a waveband assignment heuristic are then proposed in this chapter. By comparing the MLR-based waveband switched networks against other network types in this chapter, the obtained results show that this network consumes less power than others.

**Chapter 7 - Sleep-mode-enabled OBS networks** - examines the power consumption minimization problem of a sleep-mode-enabled OBS backbone network. This chapter shows how OBS networks could use power-aware networking to maximize power savings without incurring excessive transmission delays. After specifying the power consumption model of the sleep-mode-enabled OBS network, a novel burst assembly algorithm is presented. The proposed algorithm reduces power consumption by minimizing the number of transitions be-

tween different operating states of network devices.

**Chapter 8 - Conclusion** - summarizes the main findings of this thesis and highlights intended future work.

## 1.4 Contributions of the thesis

The contributions of each chapter in this thesis are listed and explained in detail below.

1. In Chapter 2, we comprehensively review existing studies that are relevant to power consumption of backbone networks and classify solutions developed in these studies into four main approaches. We name these approaches as (1) network redesign (2) traffic engineering, (3) power-aware networking, and (4) load-adaptive operation. From this review, we uncover several gaps in the extant literature that are highlighted below.
  - (a) Core nodes of OCS and OBS networks can be designed to consume less power by combining all-optical and electronic technologies (i.e., hybrid technology). However, prior studies have not evaluated power consumption of optical backbone networks that use a mix of optical and hybrid core nodes.
  - (b) A vast number of studies reduce deployment cost or Capital Expenditure (CAPEX) of networks by minimizing the number of physical links and their placement. However, only a limited number of studies optimize link placement in networks to minimize network power consumption.
  - (c) Past research has not analyzed how power consumption of waveband switched networks using all-optical devices can be reduced.
  - (d) Sleep-mode of operation can be adopted to reduce power consumption of both OCS and OBS networks. Yet, only a handful of studies *jointly* evaluate cost and power consumption of sleep-mode-enabled *survivable* OCS networks. Existing studies also do not consider the effect of queuing delay in sleep-mode-enabled OBS networks.
  - (e) MLR-based wavelength switched networks consume less power than 10 Gbps and 40 Gbps SLR-based wavelength switched networks. However, power consumption of MLR-based *waveband* switched networks has not been previously evaluated.
2. We reduce power consumption of an OCS network by placing core routers at selected core node sites (Chapter 3). In this chapter, we carry out the following tasks:

- 
- (a) Model power consumption of an OCS network, assuming that network devices comply with power-load proportionality.
  - (b) Show that it is infeasible to place core routers at *all* core node sites of an OCS network (full grooming).
  - (c) Demonstrate that power consumption can be reduced by only placing core routers at core node sites that process relatively less traffic and are situated farther from other sites.
  - (d) Propose an algorithm that selectively places core routers, thereby reducing power consumption by approximately 688 kW over a network employing full grooming.
3. We reduce both cost and power consumption of a survivable OCS network by configuring physical links according to the traffic load (Chapter 4). In this chapter, we perform the following tasks:
- (a) Model cost and power consumption of physical links in a survivable OCS network.
  - (b) Show that cost and power consumption of an OCS backbone network can be substantially reduced by deploying a minimum number of links and transporting traffic using fewer optical fibers.
  - (c) Develop an algorithm using elements of the network redesign approach to minimize the number of physical links, thereby reducing initial CAPEX.
  - (d) Develop an algorithm using elements of the power-aware networking approach to reduce the number of optical fibers needed to transport traffic, thereby reducing power consumption and resultant Operational Expenditure (OPEX). The proposed algorithm reduces power consumption by 1.3 MWh during the course of a single day and 40 MWh in an entire month.
4. We evaluate the reduction in power consumption of a waveband switched backbone network that employs advanced three-layer MG-OXCs (Chapter 5). In this chapter, we carry out the following tasks:
- (a) Model the power consumption minimization problem of a waveband switched network that employs three-layer MG-OXCs equipped with all-optical devices.
  - (b) Develop an algorithm to reduce power consumption by assigning wavebands in the OCS network.

- 
- (c) Analyze the impact of a range of design parameters on power consumption of the waveband switched network. Specifically, we look at how waveband size, waveband grouping policy, and waveband configurations affect power consumption of different-sized networks at various traffic volumes and using distinct traffic distribution models.
  - (d) Show that, regardless of network size, power consumption can be reduced by (1) grouping wavebands at both source and intermediate core nodes, (2) grouping only a few wavelengths at low traffic volumes, and (3) grouping a higher number of wavelengths at peak traffic volumes.
  - (e) Show that a waveband switched network provides significant power savings over a wavelength switched network at high traffic volumes and when traffic is distributed using the gravity traffic model.
5. We reduce power consumption of an MLR-based waveband switched network by appropriately assigning line rates and efficiently grouping traffic into wavebands (Chapter 6). In this chapter, we perform the following tasks:
- (a) Model the power consumption minimization problem of an MLR-based waveband switched network.
  - (b) Develop three rate assignments schemes and evaluate power consumption of the network using each rate assignment scheme.
  - (c) Develop a novel algorithm to assign wavebands in an MLR-based waveband switched network.
  - (d) Demonstrate that an MLR-based waveband switched network, optimized with the proposed rate assignment scheme and waveband assignment heuristic, offers 64.78% and 17% power savings over 10 Gbps and 40 Gbps SLR-based wavelength switched networks.
6. We reduce power consumption of a sleep-mode-enabled OBS network by reducing the number of transitions that network devices undergo from one operating state to another (Chapter 7). In this chapter, we carry out the following tasks:
- (a) Develop a novel burst assembly scheme to reduce the state transitions while ensuring acceptable burst queuing delay.

- (b) Show that burst length needs to be optimized to 1 Mb to jointly minimize power consumption and queueing delay.
- (c) Demonstrate that the proposed burst assembly scheme reduces power consumption by combining multiple bursts into one and transporting the single burst without unduly prolonging queueing delay.
- (d) Show that the developed scheme reduces power consumption by 0.48 kW, on average, over traditional burst assembly schemes.

## 1.5 Publications

1. M. N. Dharmaweera, R. Parthiban, and Y. A. Sekercioglu, "Towards a power-efficient backbone network: The state of research," *IEEE Communications Surveys & Tutorials*, vol. PP, no. 99, pp. 1-30, 2014.
2. M. N. Dharmaweera, R. Parthiban, and Y. A. Sekercioglu, "Reducing power consumption in multi-line rate-based band switched networks," submitted to *Optical Switching and Networking Journal* [under review].
3. M. N. Dharmaweera and R. Parthiban, "Reducing power consumption in an optical circuit-switched core network by switching-off amplifiers," in *Proceedings of the 22nd Wireless and Optical Communication Conference (WOCC)*, Chongqing, China, 2013, pp. 532-537.
4. M. N. Dharmaweera, R. Parthiban, and Y. A. Sekercioglu, "Waveband grouping policies for reducing energy consumption in optical internet backbone networks," in *Proceedings of IEEE TENCON*, Cebu, Philippines, 2012, pp. 1-6.
5. M. N. Dharmaweera, R. Parthiban, and Y. A. Sekercioglu, "A novel burst assembly method for energy saving in burst switching networks," in *Proceedings of IEEE TENCON*, Cebu, Philippines, 2012, pp. 1-5.
6. M. N. Dharmaweera, R. Parthiban, and Y. A. Sekercioglu, "Multi-constraint physical topology design for all optical networks," in *Proceedings of the 18th International Conference on Telecommunications (ICT)*, Ayia Napa, Cyprus, 2011, pp. 463-469.

7. M. N. Dharmaweera, R. Parthiban, and Y. A. Sekercioglu, "Effect of sparse grooming on power consumption of optical networks," in Proceedings of the 1st Workshop on Green Computing Middleware (GCM), Bangalore, India, 2010, pp. 27-32.

# APPROACHES FOR REDUCING POWER CONSUMPTION OF BACKBONE NETWORKS

---

## 2.1 Introduction

Mounting economic and environmental concerns about the increasing power consumption of the Internet have propelled major Information and Communication Technology (ICT) companies and research bodies to foster initiatives towards the development of power-efficient Internet networks [31–33]. The numerous power-efficient solutions developed have been comprehensively reviewed in three important research surveys published between 2010 and 2012 [34–36]. The solutions developed can be classified into four main approaches, which have been explored to differing degrees in each of the three surveys:

1. **Network redesign:** Designing power-efficient networks using optical devices and modifying physical topology;
2. **Traffic engineering:** Developing energy-aware traffic grooming schemes;
3. **Power-aware networking:** Switching devices between different operating states;
4. **Load-adaptive operation:** Changing speeds/rates of network devices to match traffic dynamics.

The literature survey presented in this chapter differs from previous surveys in three aspects.

First, this survey devotes attention to existing research efforts on reducing power consumption of the integrated core and metro networks that is known as the backbone network [11]. The decision for this choice was based partly on predictions by Cisco that the volume of global Internet traffic would exceed the zettabyte threshold [12] and on the knowledge that, at such high

traffic volumes, power consumption of the backbone network is expected to surpass that of the access network [37]. Current evidence points to the dominance of wired and wireless access networks in the Internet's power consumption. However, while power consumption of access networks is proportional to the number of subscribers, power consumption of the backbone network is dependent on traffic volume [37] which, as previously mentioned, is expected to soon exceed the zettabyte threshold. At such high traffic volumes, power consumption of the backbone network is very likely to overtake power consumption of the access networks [8,9]. Baliga et al. [8] report that, as the access rate per household exceeds 100 Mbps, the backbone network would consume 34.5% of total network power, provided that power efficiency of network devices increases by 10% per annum. In a more recent study, Kilper et al. [38] estimate that power consumption of the backbone network (10.5 W/Mbps) will surpass that of the fixed-access network (8 W/Mbps) beyond the year 2020. Considering the technology of 2008, Tucker et al. [9] show that the backbone network consumes more power than access networks as the average access rate per user exceeds 4 Mbps. Furthermore, to make things more challenging, the backbone network is only expected to gain an increment of 64% in power efficiency in the year 2020 relative to 2010, while wired and wireless access networks are expected to gain an increase of 449% and 1043% in power efficiency, respectively.

Second, the work presented in this chapter is the first literature survey that reviews recent research efforts in reducing power consumption of the backbone network alone. Based on similarities among developed solutions in the literature, this survey categorizes these recent research efforts into the four aforementioned approaches. By solely concentrating on the backbone network, the present survey is able to provide a comprehensive analysis of concepts, findings, and limitations of prior work and report power-saving results in terms of absolute values and percentages. It reviews novel concepts such as optical circuit/burst/packet-switched networks, hybrid networks, topology optimization techniques, waveband grooming, spectrum elastic networks, and multi-line rates in the context of reducing backbone network power consumption. Table 2.1 shows the key concepts reviewed under each approach in this study vis-à-vis those addressed in existing surveys by Zhang et al. [34], Bolla et al. [35], and Bianzino et al. [36]. Furthermore, while these three surveys only examine studies published until 2011, this survey extends this body of literature to include more recent studies published after 2011.

Third, certain solutions reviewed in the three surveys, although power-efficient, cannot be effectively implemented due to limitations such as space and cost constraints. This survey,

Table 2.1: Comparison between this study and available surveys

Approach	Key concepts	This study	Bolla et al. [35]	Bianzio et al. [36]	Zhang et al. [34]
1	Electronic vs. optical technologies	✓	✓		✓
	Point-to-point WDM networks (PtP-WDM)	✓			
	Optical circuit switched networks (OCS)	✓			
	Optical burst switched networks (OBS)	✓		✓	
	Optical packet switched networks (OPS)	✓			
	Physical topology optimization	✓			
2	Wavelength grooming	✓		✓	✓
	Waveband grooming	✓			
3	Switch-off/Sleep-mode operation	✓	✓	✓	✓
	Re-configuration cost	✓			
	Handling drawbacks	✓	✓	✓	✓
4	Single and Mixed Line Rates (SLR/MLR)	✓			✓
	Adaptive Line Rate (ALR), Elastic and SEON networks	✓	✓	✓	✓
	Compare SLR, MLR, and ALR	✓			

Note: Approach numbered 1,2,3, and 4 refer to network redesign, traffic engineering, power-aware networking and load-adaptive operation, respectively.

in contrast, explores how alternative mechanisms that are developed to achieve other objectives, such as reducing cost and increasing bandwidth utilization, can be integrated with the proposed power-efficient solutions to overcome their inherent limitations.

We begin this survey by presenting an overview of the Internet’s backbone network, its devices, and their respective power consumption values in Section 2.2. Subsequent sections are devoted to a critical analysis of the relevant literature and a summary of the key findings from the four approaches. These findings are then related to the research problem(s) stated in Section 1.2.3.

The first approach, network redesign, is discussed in subsection 2.3 where, first, core node redesign using electronic and all-optical technologies is examined and, second, the possibility of optimizing link topology to reduce power consumption is assessed. The second approach, traffic engineering, is examined in subsection 2.4 where we investigate how wavelength and waveband grooming schemes could be used to reduce backbone network power consump-

tion. Subsection 2.5 discusses the power-aware networking approach where the possibility of conserving power at the device level by dynamically switching on and switching-off network devices is explored. The fourth approach, load-adaptive operation, is examined in subsection 2.6 where we review load-adaptive techniques such as Adaptive Line Rates (ALRs) and Mixed Line Rates (MLRs), in terms of power consumption, and their drawbacks. Subsection 2.7 evaluates the practical relevance of the four approaches and, finally, subsection 2.8 presents important conclusions that are drawn from this survey chapter.

## 2.2 Architecture of the backbone network

The fundamental architecture of a backbone network comprising core nodes and links is depicted in Figure 2.1. Core nodes are interconnected via bundled optical fibers that are installed within conduits. A conduit connecting two core nodes is referred to as a physical link or a WDM link. In existing backbone networks, which are mostly PtP-WDM, core nodes consists of core routers, whereas in advanced optical backbone networks (i.e., OCS), core nodes consist of both core routers and OXCs. As illustrated in Figure 2.1, the optical backbone network (i.e., OCS) can be split into “IP” and “WDM” layers. IP traffic originating at the access network is processed, switched, and aggregated by core routers using high-speed electronics. Electronic signals emanating from the core routers are converted into optical wavelengths by O-E/E-O converters that reside within transceivers or transponders. Using the WDM technique, multiple wavelengths are bundled into individual optical fibers. Traffic is switched from one fiber to another via I/O ports of the OXC. Note that the core node architecture of OBS and OPS optical backbone networks, which differ from that of OCS, would be explained in Section 2.3.1.

An optical fiber is equipped with a Pre-Amplifier (PrA) and a Post-Amplifier (PoA) at either end. A set of evenly-spaced In-Line Amplifiers (ILAs) are placed along the fiber. If the need arises, an incoming wavelength could be converted to another using a Wavelength Converter (WC). Relevant wavelengths can be regenerated to extend the reach of a lightpath by using a Regenerator (Rg). In the example illustrated in Figure 2.1, the wavelength carrying pass-through traffic is converted to another (solid line to dotted line) by the WC and is then regenerated by the Rg.

Power consumption values of optical backbone network devices are shown in Table 2.2. Discrepancies are observed in the reported power consumption values of the same device from

different manufacturers. In general, high-capacity devices consume more power than low-capacity devices, but with a declining power-to-capacity ratio (i.e., volume discount [26, 39]). In comparison to other network devices, core routers consume a significant amount of power. A detailed list of power consumption values of backbone network devices can be found in [18,40]

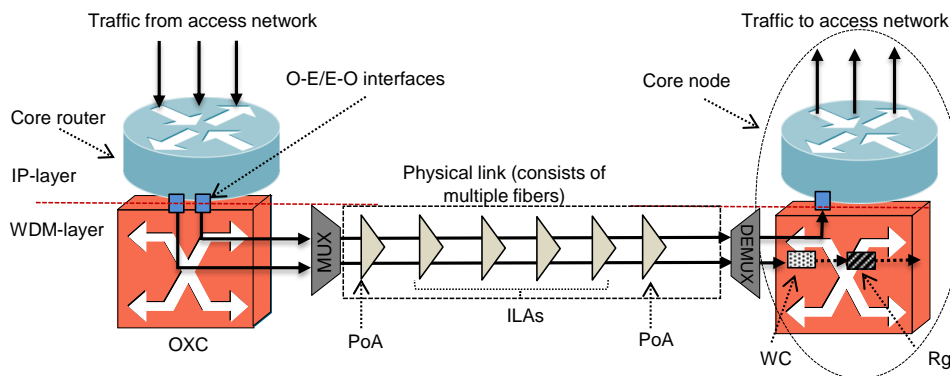


Figure 2.1: Constituent devices of an optical backbone network

## 2.3 Network redesign approach

Power consumption of the backbone network can be reduced by re-designing its two main constituent devices - core nodes and physical links - to be more power-efficient.

Core nodes have primarily relied on electronic technology, while physical links mainly run on optical technology [9]. However, electronic devices of core nodes are now gradually being replaced by high-speed optical switching devices in order to increase network capacity and speed [9,53]. While most researchers agree that optical devices are faster than electronics, they remain sceptical about their power-saving abilities [16,54,55]. These scholars argue with evidence that electronic devices consume less power than optical devices [9, 16, 17, 50, 55–58]. Nevertheless, as will be discussed in Section 2.3.1 below, certain limitations of electronic technology, which are inevitable in the future, signify that core nodes would eventually rely on optical technology. Solutions then need to be developed to increase power efficiency of optical technologies that replace electronics in core nodes. These solutions are summarized in subsection 2.3.1.

Another critical means of reducing power consumption of the backbone network is physical topology redesign by optimizing the assignment of physical links [59]. This means that net-

Table 2.2: Power consumption values of backbone network devices

Device	Product	Capacity	Power Cons.
Core router	Cisco CRS-1	1.2 Tbps	9.63 kW [41]
	Cisco CRS-3	4.4 Tbps	12.3 kW [42]
	Juniper T1600	1.6 Tbps	8.35 kW [43]
	Juniper T4000	4 Tbps	9.83 kW [43]
Transponder	Fujitsu Flashwave 7200	2.5 Gbps	37.2 W [44]
	Fujitsu Flashwave 7200	10 Gbps	68.5 W [44]
	Transmode 10G tunable	10 Gbps	25 W [44]
OXC	Cisco 40-channel OXC	2-degree	400 W [44]
	Cisco 80-channel OXC	2-degree	550 W [44]
Amplifiers	Cisco ONS 1454 PrA/PoA	1 fiber	78 W [44]
	Alcatel LM1600 ILA	1 fiber	52 W [44]
	Cisco ONS 1454 ILA	1 fiber	46 W [44]
	Infira Erbium-Doped Fiber Amp. (EDFA)	1 fiber	106 W [44]
Regenerator	Cisco optical regenerator	2.5 Gb/s	100 W [40]
	iLynx Regenerator	2.5 Gb/s	8 W [40]
	40G electronic regenerator	40 Gb/s	126 W [45]
	All-optical regenerator (AOR)	1 wavelength	6 W to 80 W [46–48]
Converter	Tunable Wavelength Converter (TWC)	1 wavelength	500 mW -800 mW [49,50]
	Fixed Wavelength Converter (FWC)	1 wavelength	600 mW [50]
	All-optical wavelength converter (AOWC)	1 wavelength	2 W [51,52]

work operators must take power consumption into consideration when designing the physical topology in addition to infrastructure cost [60,61], Quality of Service (QoS) constraints (e.g., delay, signal loss, and resilience) [62,63], and geographical constraints [64]. The existing literature on power-efficient physical topology redesign is reviewed in Section 2.3.2.

### 2.3.1 Core node redesign

This section first explains how core nodes are evolving from PtP-WDM networks to advanced optical backbone networks. We then comparatively analyze available and prospective electronic and all-optical technologies in core nodes that can reduce power consumption of backbone networks.

### 2.3.1.1 Evolution of core nodes

In PtP-WDM networks, IP packets, which are also known as Electronic Packet Switches (EPS), transit across multiple electronic core routers (also known as Electronic Packet Switches (EPS)) connected via point-to-point WDM links [9, 56]. An electronic core router is predominantly composed of Complementary-symmetry Metal-Oxide Semiconductor (CMOS)-based electronic devices, which come in many forms and perform different tasks, such as converting signals between electrical and optical domains (i.e., O-E/E-O conversion), buffering, processing, and switching.

The commercially-available single-shelf Cisco CRS-3 electronic core router consumes 12.2 kW of electricity and has a maximum switching capacity of 4.4 Tbps [42]. Although switching capacity of an electronic core router can be increased by combining multiple shelves [65], the result is an increase in power consumption due to provisioning of additional interfacing devices and the need for a much larger cooling system [56]. For example, in comparison to 9.6 kW of power consumed by a single-shelf Cisco CRS-1, a 72-shelf Cisco CRS-1 consumes 800 kW of power. If current technologies prevail, Aleksic [14,15] predicts that future electronic core routers with a maximum switching capacity of 1 Pbps will consume 10 MW or more power.

Advancements in electronic technology [6, 66, 67] creates a belief that each new generation of electronic core routers will be more power-efficient [16, 55, 58, 68]. Higher power efficiency is made possible by the development of small-sized, high-capacity semiconductors. For example, the most recent 14 nm Intel Broadwell CPU is 30% more power-efficient than the existing 22 nm Haswell CPU [69]. However, some researchers believe that CMOS scaling may halt in the near future [70, 71], making it a challenge to further increase the power efficiency of semiconductors without incurring large production costs [72].

To provide an overview of a PtP-WDM network, a simple example is shown in Figure 2.2a. Here, three sub-wavelength connections are transported from node  $i$  to nodes  $j$  and  $k$ . The solid lines indicate optical lightpaths, while dotted lines indicate electronically-processed signals. The white dotted squares represent electronic IP packets. Notations E-O and O-E denote electrical-to-optical and optical-to-electrical conversions, respectively. Pass-through traffic is electronically processed at the intermediate node  $j$ .

Due to the forecasted halting of CMOS scaling and resultant inability to further exploit power efficiencies of electronic devices, optical devices are gradually being introduced into core nodes. By replacing core routers with OXCs, a PtP-WDM network can be transformed into

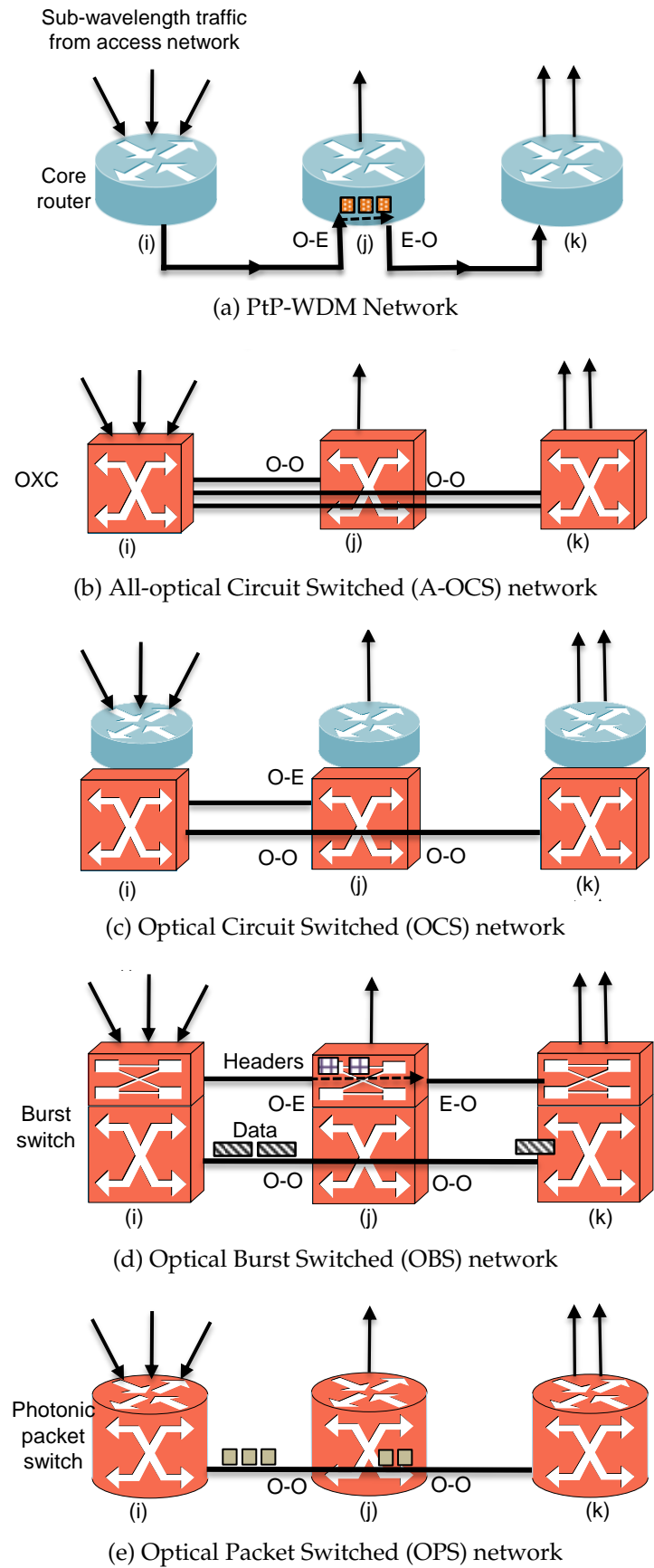


Figure 2.2: Different core node architectures

an All-Optical Circuit Switched (A-OCS) network, as depicted in Figure 2.2b. Replacing a core router with an OXC is advantageous in eliminating the capacity bottleneck caused by electronic processing. Yet, the OXC fails to efficiently utilize available bandwidth when traffic arrives from the access network at sub-wavelength granularity [11]. For example, in Figure 2.2b, the A-OCS network accommodates incoming traffic using 5 wavelengths instead of 2 wavelengths used in the PtP-WDM network (Figure 2.2a). To increase bandwidth utilization, core nodes of OCS networks today are often provisioned with both core routers and OXCs [11], as illustrated in Figure 2.2c. Such OCS networks could be referred to as IP over Optical Transport Networks (IP-OTNs) [11].

In the evolution of optical switching technologies [9], OBS follows OCS (both A-OCS and IP-OTN) [9]. Burst switching was first used in the early 1980s [73] to statistically multiplex data in traditional PtP-WDM networks. As illustrated in Figure 2.2d, a core nodes in an OBS network consists of a Burst Switch (BuS). A data burst is generated by aggregating multiple IP packets. The header is sent ahead to the burst on a separate wavelength. Figure 2.2d provides a simple example of an OBS network. At intermediate nodes, the header (illustrated by a checkered square) is processed by the electronic devices, and the burst (illustrated by rectangles with stripes) is switched by the optical devices. OBS allows multiple bursts to share the capacity of a single wavelength, thereby increasing bandwidth utilization.

OPS networks appear to be the last frontier of the optical switching technology evolution [9]. Research on OPS networks first began in the 1990s and test-bed experiments were performed towards the end of the same decade [73]. OPS networks mimic the operation of PtP-WDM networks, and their similarities can be observed in Figures 2.2a and 2.2e. In an OPS network, core nodes consist of Photonic Packet Switches (PPS). Replicating the core routers' function of electronic processing, PPS optically buffer, process, and switch IP packets (illustrated by the solid grey squares) at intermediate nodes.

In order to replace electronic core routers with optical core nodes in OCS, OBS, and OPS networks, power-efficient optical devices are expected to perform the tasks of buffering, processing, and switching. In the following subsections, we review technologies, architectures, and alternative mechanisms that could be used to develop power-efficient optical core nodes.

### 2.3.1.2 Electronic vs. optical buffering

In an electronic core router, buffers are used to temporarily store IP packets as the control information is processed [70, 74, 75]. Being able to store IP packets is critical in avoiding wavelength contentions and performing packet synchronization, especially in PtP-WDM networks [70, 74, 75]. In the electric core router, buffers are realized using electronic random access memory (RAM) technology [56]. In an optical core node, buffering could be realized using Fiber Delay Lines (FDLs) [56, 68, 76] or Slow-Light Optical Buffers (SLOBs) [76, 77].

In comparison to proposed all-optical buffering technologies, such as FDL and SLOB, RAM technology not only provides more capacity (e.g., RAM used in line cards of the Cisco CRS-1 has a capacity of 4 Gb), but also consumes less power [56]. However, the capacity bottleneck of electronics constrains the maximum achievable store-and-retrieve speed of RAMs [78]. In [56], Tucker et al. report that FDL-based optical buffers consume 40 mW of power in comparison to 8 mW of power consumed by CMOS-based RAMs when the buffer capacity is 40 Mb. Among the optical buffering technologies, FDLs consume less power (approximately 44 pW) than SLOBs (approximately 80 mW) when the buffer capacity is 400 kb [56]. However, FDLs are considered infeasible due to their large physical size [56, 76]. In an interesting study, Yoo et al. [70] analyze the power consumption of FDL-based cascaded, serial, and parallel optical buffers. Their results show that cascaded optical buffers consume only 1 kW of power in comparison to 35 kW of power consumed by electronic RAMs. However, due to complexity of the associated control circuitry, the OPS network utilizing the cascaded optical buffers consumes 347 kW of power in comparison to 317 kW consumed by the PtP-WDM network.

Since optical buffers consume more power, optical core nodes can exploit wavelength and space domain contention resolution schemes [79, 80] to perform the necessary functions using a limited number of buffers [79–82]. In [83, 84], wavelength conversion is used to minimize buffering and reduce power consumption of an OPS network. Wavelength conversion can be performed using both electronic and optical converters [22]. The ability to serve multiple wavelengths simultaneously, using a single device, is an advantage of all-optical converters over their electronic counterparts. Recent studies show that all-optical wavelength converters (AOWCs) consume less power than electronic converters [22, 85–88]. According to [51, 52], an AOWC consumes only a trace amount of power between 0.7 and 2 W, approximately. Moreover, the use of AOWCs can be minimized by appropriately assigning wavelengths. Thus, OCS and OBS networks can prove to be power-efficient networks when implemented with limited

buffering.

Unlike in a PtP-WDM network, intermediate core nodes of an OCS network do not possess buffers or fast switches [9, 14, 15]. As a result, they consume less power than electronic core routers in a PtP-WDM network [89]. According to Shuping et al. [90], intermediate core nodes of an OBS network also consume less power than the electronic core routers in the PtP-WDM network. However, burst assembly routers of an OBS network, which serve to aggregate multiple IP packets into bursts, require large buffers, thus consuming a significant amount of power than electronic core routers at the network edge.

### 2.3.1.3 Electronic vs. optical processing

In a PtP-WDM network, an IP packet is formed by combining the payload (i.e., packet content) and the header (i.e., packet information) in a series. At an intermediate node, the header is processed, while the packet is momentarily stored in the RAM. Unlike in an electronic core router of a PtP-WDM network, optical core nodes, in general, do not possess a mature buffering technology like RAM. Therefore, in place of the electronic packet-header-processing mechanism, Optical Label Switching (OLS) can be adopted in optical core nodes to reduce power consumption of OCS, OBS, and OPS networks [70, 74, 75].

Optical labels that perform the task of a header can be sent parallel to the payload on a separate wavelength. Since a label carries only a small amount of data, it could be converted and processed by low-power CMOS-based electronics working at moderate speeds. As the payload is transported separately, it can be switched by an optical switch using minimum optical buffering [70, 74, 75]. Resultantly, an OLS-based OPS network, for example, consumes less power (e.g., 16.8 kW) compared to a buffered OPS network (e.g., 347 kW) in a similar traffic environment [70, 74, 75]. However, OLS continues to use electronic devices, requiring O-E/E-O conversion. Hence, it may be beneficial to replace OLS with All-Optical Label Switching (A-OLS) [21, 70], which does not involve electronics, in order to further reduce power consumption.

The process of traffic grooming in PtP-WDM and OCS (i.e., IP-OTN) networks is performed by electronic devices. In OBS networks, on the other hand, traffic grooming is an integrated functionality as a wavelength is shared among multiple bursts. However, optical core nodes of an OPS network lack a viable all-optical traffic grooming mechanism. Given this limitation, Musumeci et al. propose a novel Time-Driven Switching (TDS) technique for grooming

in optical core nodes [91,92]. TDS exploits the time coordination of network elements to optically switch and groom sub-wavelength traffic tributaries. Results indicate that TDS-based all-optical traffic grooming consumes 55% less power than electronic grooming [91,92].

#### 2.3.1.4 Electronic vs. optical switching

In large electronic core routers, switching is performed by CMOS-based fast switches [93,94]. In an optical core node, a fast switch can be constructed using Semiconductor-Optical-Amplifier Gate Arrays (SOA-GAs), a Micro-Ring Resonator (MRR), Arrayed-Waveguide-Gratings with Tunable Wavelength Converters (AWG-TWCs), and Electro-Optic-Phased Arrays (EOP-As) [16,50,56,68].

It is quite often suggested that SOA-GA and EOP-A fast switches consume more power in comparison to CMOS-based electronic switches [50]. The MRR fast switch consumes less power than an electronic switch; yet, large scale implementation of the MRR is challenging due to difficulties in controlling resonance wavelengths [50]. The results presented in [50] indicate that, in the year 2020, electronic, SOA-GA, AWG-TWC, MRR, and EOP-A switches will consume 10 kW, 100 kW, 7 kW, 8 kW, and 10 MW of electricity, respectively, while providing a throughput of 1 Pbps. Among the available optical fast switches, AWG-TWC consumes the least amount of power [16,50,56,68,95,96]. In [97,98], Aleksic et al. reports that the AWG-TWC switch consumes 25% less power than a SOA-GA switch. However, practical application of AWG-TWC switches is still pending due to the unavailability of rapid Tunable Wavelength Converters (TWCs) [50,56]. Because optical fast switches are driven by electronic circuits, in [50], Tucker concluded that it is important to reduce power consumption of the electronic drive circuits in order to increase power efficiency of the optical fast switches and, thus, optical core nodes.

While fast optical switches are essential in OPS networks, slow optical switches (such as Micro-Electro-Mechanical-Systems (MEMS) switches) can still be used in OCS and OBS networks given that the bursts are long [99]. Different measurements of power consumed by MEMS switches have been provided in past studies. For example, in [16], MEMS switches consume less than 10 pJ/b of power. In [100], an  $80 \times 80$  port MEMS switch consumes 8.5 W of power. According to Murakami et al. [101], a 3D-MEMS optical switch consumes 8 kW (1/7th of an electronic slow switch) of power per 1000 ports and provides a total switching capacity of 1 Tbps.

### 2.3.1.5 Networks with Hybrid Core Nodes

A Hybrid Core Node (HCN) consists of a hybrid core router that is assigned an electronic RAM, electronic packet processor, and an optical switch [102]. While packet processing, grooming, buffering, and controlling are performed by electronic circuitry, switching is performed by optical switches. According to [102,103], a hybrid core router consumes only  $5.6 \times 10^{-10}$  W per bit of transmitted traffic in comparison to  $1 \times 10^{-9}$  W of power consumed by a Cisco CRS-1 core router. Nonetheless, regular use of E-O and O-E converters in the hybrid core router restricts its maximum achievable power efficiency.

An HCN with a different architecture is used in [104, 105] to reduce power consumption of Hybrid Optical Switched (HOS) networks. A core node of an HOS network consists of an electronic or SOA-GA fast switch and a MEMS slow optical switch [106–110]. When traffic arrives at a core node, the control plane decides if traffic should be switched fast or slowly. By re-directing circuit-oriented traffic and long data bursts to the slow optical switch, the load on the power-hungry fast switch is reduced, thus reducing overall power consumption. As pointed out in [108] and [106], if an HOS network is employed with SoA-GA fast switches, power consumption can be reduced by 1000% over ordinary PtP-WDM networks and by 600% over an HOS network with electronic fast switches. In two separate studies, an HOS network with SOA-GA fast switches and an HOS network with electronic fast switches were found to consume 9 and 2 times less power [109] and produce 10 and 3 times less  $CO_2$  than a PtP-WDM network, respectively [107].

An optical core node of an OCS network (i.e., IP-OTN) that consists of an OXC and a core router could also be regarded as an HCN, since it involves both electronic traffic processing and optical switching. In such networks, an HCN can be constructed with opaque, transparent or translucent architectures [111–113]. According to [111–113], core nodes of the translucent architecture are the most power-efficient. The work in [111] indicates that an OCS network provisioned with translucent core nodes consumes 60% less power in comparison to PtP-WDM networks with electronic core routers. This is partly due to the fact that wavelength regeneration and switching in translucent core nodes are performed within the OXC. In order to further reduce power consumption in a translucent core node, wavelength regeneration can be performed using an AOR that only consumes 50-80 W of power [46–48] in comparison to 100 W of power consumed by an electronic Rg (i.e., a back-to-back transponder) [18, 44]. Multi-wavelength all-optical regenerators (mAORs) are currently being developed in research labo-

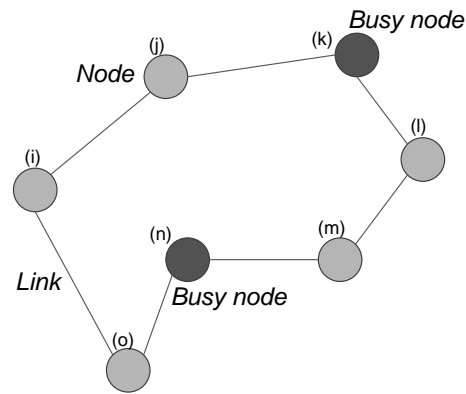
ratories [114–117]. An mAOR performs the task of several regenerators using a single chassis and cooling system, thus consuming less power.

### 2.3.2 Physical link topology redesign

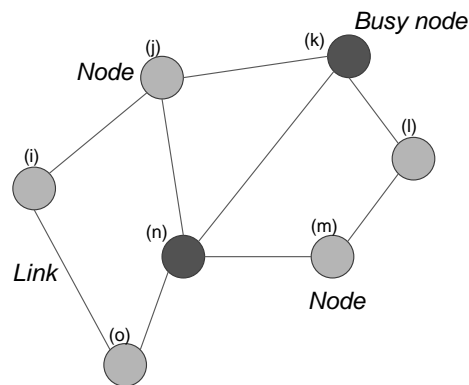
As high cost makes it impractical to modify the physical topology of an existing backbone network, new backbone networks need to be designed using the greenfield approach (i.e., a design on which no prior restrictions are imposed due to the absence of pre-existing infrastructure) in order to reduce power consumption [59]. Deployment cost (i.e., CAPEX) of an optical backbone network is dominated by the link laying cost. Therefore, to reduce cost, core nodes need to be interconnected via a minimum number of links.

In Figure 2.3a and Figure 2.3b, we depict two different physical topologies designed to minimize cost and power consumption, respectively. Nodes  $n$  and  $k$  are located in high-population cities and, thus, they source (i.e., add) and sink (i.e., drop) more traffic (busy nodes). The ring topology in Figure 2.3a costs less as it has fewer links. Yet, the partial mesh topology in Figure 2.3b consumes less power than the ring topology in Figure 2.3a as busy nodes of the former are directly connected to other nodes. Therefore, traffic travels via a smaller number of links and fibers and through a minimum number of intermediate core nodes in the partial mesh topology.

While the majority of the existing literature attempts to reduce cost and packet loss as well as ensure resilience of the physical topology, a few studies seek to optimize power consumption of the backbone network. Dong et al. [118] developed a Multiple Integer Linear Programming (MILP)-based formulation to optimize the physical topology of the National Science Foundation (NSF) network and reduce its power consumption. Their experiments show that the proposed scheme reduces power consumption by 10% without increasing the number of physical links. It is also highlighted that if the network is allowed to use a full mesh topology or a star topology, power consumption could be reduced by a staggering 95% and 92%, respectively. The authors also investigate the possibility of optimizing the physical topology by accounting for the presence of renewable energy sources in the network. The resultant network offers 10% of power savings over their initially proposed network. Further analyzing the results of [118], it becomes evident that a network optimized to consume less power will also be cost-effective. Nevertheless, one drawback of the proposed optimization scheme is the increase in propagation delay.



(a) A Ring network



(b) Optimized partial mesh topology

Figure 2.3: Two different physical topologies connecting 7 core nodes

Carmello et al. [119] propose a multi-objective evolutionary algorithm to optimize the physical topology. The algorithm attempts to simultaneously minimize cost, blocking probability, and power consumption by configuring the physical topology and node capacities. The authors pronounce their work as the first to jointly analyze these three aspects under a single objective function. To measure power consumption, Carmello et al. consider normalized power consumption values of transmitters, amplifiers, and OXCs. After running the algorithm multiple times, they obtained a variety of network solutions, some of which are successful in reducing cost and power consumption, but at the expense of high blocking probability [119]. Thus, a trade-off between reducing cost, power consumption, and blocking probability is noted.

Reducing cost and power consumption of the backbone network by optimizing the physical topology, using two separate objective functions, is also studied in [23]. Here, the authors investigate the problem of designing a cost-efficient physical topology with the explicit objective of minimizing power consumption. The topology design problem is solved using Integer

Linear Programming (ILP) formulations while considering the realistic Single Path Routing (SinPR) constraint [23]. SinPR constrains traffic between a node pair to travel along a fixed route. Alternatively, if the SinPR constraint is relaxed, traffic between a node pair can take multiple routes. The simulation results in [23] indicate that the proposed model is cost-efficient and only consumes 26.5% of extra power in comparison to topologies optimized by the relaxing the SinPR constraint.

### 2.3.3 Network redesign approach: Summary of findings

The increasing production cost of semiconductors [72] and possible end of Moores law [70,71] motivate network operators to shift from electronic core routers to optical ones. Our review of the state-of-the-art research uncovered some of the key limitations of existing optical core nodes, and provides potential alternative solutions to these limitations below:

- The unavailability of a feasible buffer technology is the main drawback of optical core nodes, especially in PPS. High-capacity FDLs and slow-light buffers consume more power than RAMs and are space-consuming. It is thus important to minimize the use of buffers in optical core nodes. This can be achieved by using AOWCs and space domain contention (deflection-routing) resolution schemes. A-OLS and TDS can also be adopted in optical core nodes to minimize the need of optical buffers to increase power efficiency. OCS and OBS networks can thus be realized using a limited number of buffers.
- High power consumption of fast optical switches poses a challenge to the realization of optical core nodes, particularly in OPS networks. Both OCS and OBS networks can use MEMS-based slow optical switches that consume less power than both fast optical switches and electronic switches.
- Combining the best of both technologies, HCNs consume less power than electronic core routers and are least susceptible to the limitations of optical buffers, processors, and fast switches. AORs can be used in hybrid translucent core nodes to further increase power savings.

In Table 2.3, we provide a brief summary of power consumption of electronic, all-optical, and hybrid core nodes. Specifically, for each network, we highlight the buffering, processing, and switching technologies that are used in their respective core nodes and explain how they com-

pare against each other in terms of power consumption. We also report the key limitations of these technologies.

We previously highlighted in subsection 2.3.1 that core nodes of PtP-WDM networks will gradually evolve into those of OCS and OBS networks in the near future due to advancements in all-optical technologies. It is then important to focus on developing novel mechanisms to reduce power consumption of OCS and OBS networks. Core nodes of OCS and OBS networks can rely on hybrid technology to minimize power consumption and increase capacity. While buffering, processing, and grooming could be realized using electronic technology, switching, contention resolution, and regeneration could be performed using all-optical technology. Among the examined HCN architectures, we are inclined to believe that translucent core nodes would be the way forward.

Finally, our review shows that optimizing the physical topology is also critical in reducing power consumption, as past research provides evidence that an optimized network topology accommodates traffic using fewer devices. Then, to maximize power savings and reduce operational cost in the future, network operators may opt to replace legacy network topologies with newly-designed topologies.

## 2.4 Traffic engineering approach

An alternative approach to the reduction of power consumption of backbone networks is to minimize the use of network devices (e.g., fibers, ports, traffic processors) by employing traffic grooming approaches [8, 9, 13]. Recall that core nodes communicate with each other through lightpaths established in the form of wavelengths. By aggregating multiple low-granularity traffic flows into few, high-granularity traffic flows, traffic grooming cuts down the number of wavelengths traversing the backbone network, thereby lowering the demand on network resources [121–124]. Traffic grooming is performed at wavelength, waveband, and fiber granularities [125, 126]. The process of aggregating sub-wavelength traffic (i.e., IP packets) into a single wavelength is referred to as wavelength grooming, and aggregating multiple wavelengths into a single waveband is referred to as waveband grooming. A network that utilizes wavelength grooming is referred to as a Wavelength Switched Network (WSN) and a network that uses waveband grooming is known as a Band Switched Network (BSN).

In a backbone network, where core nodes consist of core routers and OXCs, wavelength

Table 2.3: Power consumption of electronic, optical, and hybrid core nodes

Network type	PtP-WDM	OCS		OBS	OPS
Node type	EPS	OXC	Hybrid	BuS	PPS
<i>-Advantages</i>	Mature electronic technology, supports connectionless IP traffic, high bandwidth utilization	Mature optical technology, fully transparent data transmission	Combines the best of electronic and optical technologies	Connectionless transparent data transmission, supports statistical traffic grooming	Mimics PtP-WDM using all-optical technology, supports statistical traffic grooming, connectionless data transmission
<i>-Limitations</i>	Increased complexity, power consumption, cost, heat dissipation, and footprint of high-capacity core routers	Low bandwidth utilization, latency caused by two-way reservation process	Complexity associated with optical electronic integration, increased cost	Complex burst assembly algorithms, uses a separate control wavelength channel, latency due to offset time	Lacks feasible optical buffering and processing technologies
<b>Buffers</b>	Electronic RAMs	No data buffering	Electronic RAMs	No buffering*	FDLs, SLOBs
<i>-Pwr. cons.</i>	Lower than FDLs and SLOBs at high capacities	NA	Same as RAMs	NA	Lower than RAMs at lower capacities
<i>-Limitations</i>	Store/retrieve speed is restricted by speed of electronics	NA	Same as RAMs	NA	Infeasible physical size, high intrinsic loss
<b>Processors</b>					
<i>-Data processing</i>	Use electronics	NA	Use electronics	NA	All-optical packet processing which is yet to be developed
<i>-Control info.</i>	Use electronics	Use electronics or OLS, A-OLS			
<i>-Resolve contentions in</i>	Time domain	Space and wavelength domains	Time, space, and wavelength domains		
<i>-Pwr. cons.</i>	O-E/E-O converters consume high power	OLS and AOWCs consume less power than electronic header processing and contention resolution methods			A-OLS, FDLs, and AOWCs consume less power than their electronic counterparts
<i>-Limitations</i>	Limited speed of electronics	Limited packet/header penetration only allows simple operations, space domain contention resolution may cause traffic synchronization problems in OPS networks			
<b>Switches</b>	Electronic fast switches	MEMS-based slow switches		Electronic/optical fast switches** or MEMS-based slow switches***	SOA-GA, AWG-TWC, MRR, and EOP-A fast switches
<i>-Pwr. cons.</i>	Consume less power than SOA-GA and EOP-A fast switches	Consume less power than optical and electrical fast switches			MRR and AWG-TWC consume more power than electronic and other optical fast switches
<i>-Limitations</i>	Switching speed is restrained by the limited speed of electronics	High switch configuration time, slow switching speeds only suitable for connection-oriented traffic or large bursts			SOA-GA and EOP-A consume high power, MRR is impractical due to difficulties in controlling resonance wavelengths, AWG-TWC is dependent on the development of rapid TWCs

Note: \* OBS edge routers contain electronic or all-optical buffers, \*\* Fast switches are used in [90, 120], \*\*\* MEMS is used in [99].

grooming can be performed using three different schemes, namely, No Bypass (NB), Direct-Bypass (DB), and Multi-Hop with Bypass (MHB) [127]. These three wavelength grooming schemes are explained using Figure 2.4. With NB, sub-wavelength traffic is first aggregated into

point-to-point lightpaths. At each intermediate core node, as shown in Figure 2.4a, the wavelengths of point-to-point lightpaths are then O-E converted, disassembled into sub-wavelength traffic (i.e., IP packets), and electronically processed by the intermediate core routers. With DB, sub-wavelength traffic between every node pair is groomed into dedicated end-to-end lightpaths. As shown in Figure 2.4b, wavelengths of an end-to-end lightpath is switched by the OXC of each intermediate core node, avoiding electronic processing (also referred to as optical bypassing). With MHB, as shown in Figure 2.4c, sub-wavelength traffic that shares a set of physical links in the same route, with a minimum hop distance of two, are aggregated into a multi-hop lightpath.

In the example depicted in Figure 2.4, NB, DB, and MHB wavelength grooming schemes produce 3, 2, and 2 lightpaths and consume 12, 14, and 10 OXC input/output ports (denoted as '1'), respectively. The three schemes also consume 6, 4, and 4 core router ports (denoted as '0') and process a total of  $3.5\lambda$ ,  $2\lambda$ , and  $2.5\lambda$  wavelength traffic, respectively. While it appears that the MHB scheme produces fewer wavelengths and consumes fewer ports, the DB scheme involves less traffic processing. Given the benefits and trade-off related to each wavelength grooming scheme, it is important to know how the three grooming schemes affect power consumption of the backbone network and how they can be improved to consume less power.

### 2.4.1 Wavelength grooming for static traffic

Power consumed by different wavelength grooming schemes has been analyzed by past studies in both static and dynamic traffic environments. A static traffic model is used when information about connection requests is available and when network traffic shows minimum variation over long periods of time [128]. The primary objective of most studies using a static traffic model has been to identify the most power-efficient wavelength grooming scheme in a static traffic environment [129–132]. However, notable differences among these studies are the core node architecture, power consumption values of network devices, the optimization technique, and their inter-relationships.

In [130], the authors used MILP-based optimization techniques and heuristic-based algorithms to demonstrate that MHB consumes 45% less power compared to NB. A similar conclusion is drawn from the ILP-based work in [129] whose results indicate that MHB consumes 28% and 53% less power compared to NB in the European Optical Network (EON) and the NSF

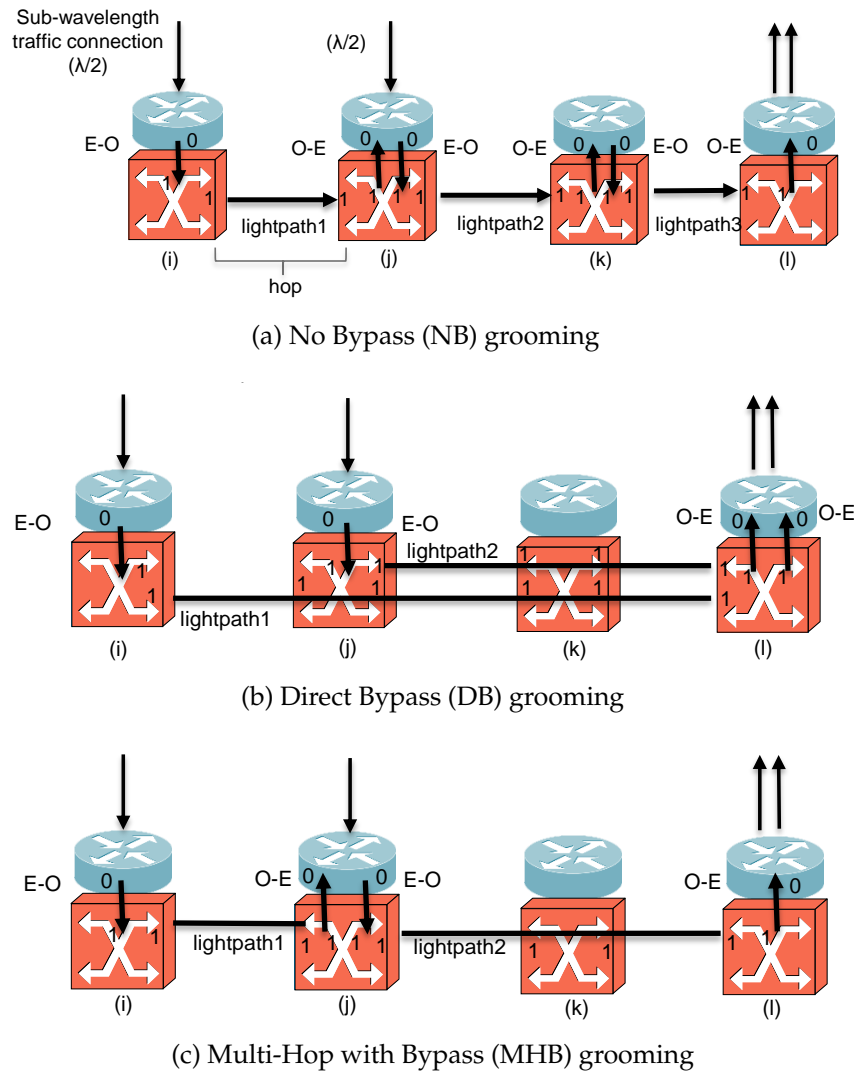


Figure 2.4: Comparison of the three wavelength grooming schemes

network, respectively. We observe that the MHB scheme tends to send traffic connections via longer paths, which elevates power consumed by the transport system. However, this increase is compensated by minimizing both electronic processing and the number of active transponders, through the establishment of fewer lightpaths, which helps to save power.

Depending on the wavelength grooming scheme used, a core node will consist of different devices. While NB grooming is performed by electronic devices, DB and MHB grooming require both electronic and optical devices. In [131], it is clear that MHB consumes less power when electronic and optical devices have comparable power consumption values. If electronic devices are more power-hungry, then of the three grooming schemes, DB consumes the least amount of power. Referring to our example in Figure 2.4, DB consumes 4 electronic core router ports and processes 2 wavelength traffic connections compared to 6 and 3.5 by NB and 4 and 2.5

by MHB. On the contrary, if optical devices are more power-hungry, then NB looks to be the most power-efficient wavelength grooming scheme. Based on this analysis, we contend that selection of the appropriate wavelength grooming scheme should be based on actual power consumption values of both electronic and optical devices.

Yetginer et al. [132] evaluated the power consumption of three different wavelength grooming strategies (MinL, MinP and MinT) with respect to increasing network traffic. The first strategy, denoted as Minimize Lightpaths (MinL), is developed to optimize the number of lightpaths in the network, similar to the MHB grooming scheme. The second strategy, Minimize Transponders (MinT), optimizes the network to use a minimum number of transponders and electronic processing, resembling the DB grooming scheme. The third strategy, known as Minimize Power (MinP), combines MinL and MinT to achieve a balance between reducing the number of lightpaths and transponders. The authors discovered that the largest reduction in power consumption can be achieved by optimizing the network using MinP. When network traffic is low, MinT and MinL consume 95% and 10% more power compared to MinP, respectively. Conversely, when network traffic is high, MinT and MinL consume 2.5% and 5% more power compared to MinP, respectively. Between MinT and MinL, the former is more power-efficient when network traffic is high and the latter when network traffic is low. The reason is that, at high traffic loads, MinL cannot further increase lightpath utilization because only a limited bandwidth (i.e., available capacity) remains under-utilized in end-to-end lightpaths. On the other hand, when network traffic is low, several sub-wavelength traffic connections can be groomed into a single lightpath, thereby reducing the use of transponders and maximizing optical bypass.

Similar to the MinP strategy proposed in [132], Coiro et al. [133] developed a heuristic algorithm which effectively combines DB with MHB. The objective of the proposed algorithm is to reduce the amount of power consumed by line cards connected to the fibers. In the first stage of the algorithm, traffic is routed along paths on a virtual topology that is derived using the DB grooming scheme. The algorithm then eliminates unnecessary links (i.e., effectively switches off line cards) by re-routing traffic and re-grooming wavelengths using the MHB grooming scheme. Re-routing paths are selected based on a cost function which takes into account the number of new line cards that need to be switched on and the load distribution in the fibers. By minimizing the cost function, the proposed scheme is able to groom and route traffic using a minimum number of fibers. The results in [133] indicate that the proposed algorithm attains

an 80%-95% increase in power efficiency over a network using only DB grooming. This work highlights the potential of MHB in reducing power consumption of line cards by grooming traffic into fewer wavelengths and accommodating them through a limited number of optical fibers.

#### 2.4.2 Wavelength grooming for dynamic traffic

The dynamic nature of the Internet demands frequent alteration of network connections. Thus, connection requests arrive randomly and last for varying time periods. Under such conditions, all connection requests cannot be served concurrently as in static traffic models, but would have to be dealt with individually. Past research efforts on traffic grooming with dynamic traffic models propose several approaches to reduce power consumption that we label as First, Second, and Third approaches.

The First Approach (FA) attempts to groom new connections into existing lightpaths [5,127, 134, 135], thereby reducing the activation of new network devices and lightpaths. The Second Approach (SA) follows the first approach but allows existing lightpaths to be re-configured when necessary [136]. The Third Approach (TA) is similar to the first approach, but does not allow resource-holding time to be extended [137–139]. It is important to keep in mind that the first two approaches, FA and SA, do not account for time and are, thus, oblivious to resource-holding times.

Using the FA approach, Xia et al. developed a power-aware grooming algorithm [5, 127]. As the authors demonstrate, grooming new connection requests into existing lightpaths is done at the expense of additional electronic processing. Contrarily, if a new lightpath is established for each new request, extra devices need to be activated (e.g., transponders, receivers). Using an auxiliary graph and arc weight assignment technique, the proposed power-aware traffic grooming algorithm accommodates traffic demands by activating a minimum number of network devices without excessively increasing electronic processing. In comparison to DB and NB grooming schemes, the proposed algorithm reduces power consumption by 28% and 12%, respectively. The proposed algorithm is also able to reduce the Bandwidth Blocking Ratio (BBR) by using network devices more efficiently.

Similarly, in [134], the authors developed a dynamic, energy-aware traffic grooming scheme. By optimizing an energy-cost function, the proposed scheme saves as much as 30% of power compared to MHB and NB. In designing the cost function, the authors account for the

power consumption of core node devices. By minimizing the energy-cost function, connection requests are accommodated via the path that consumes the least amount of power. When network traffic is low, the proposed grooming scheme aggregates new connection requests into existing lightpaths, minimizing the need to activate new devices. When network traffic is high, new lightpaths are initiated as existing lightpaths will have run out of bandwidth.

One of the major drawbacks of wavelength grooming is that it involves electronic processing at aggregation and de-aggregation nodes. With the aim of reducing electronic processing at de-aggregation nodes, Farahmand et al. [140] introduce a new type of OXC which supports a Drop-And-Continue (DAC) functionality. The proposed DAC-enabled OXC (D-OXC) allows a lightpath to be shared among many connection requests whose destination is located along the route of the lightpath. At intermediate nodes, groomed traffic is dropped from the lightpath using passive devices of the D-OXC. Electronic processing is then limited to the source nodes. The D-OXCs were tested with several grooming schemes based on the FA [140]. Their results show that, by grooming new connection requests onto existing lightpaths with the objective of minimizing electronic processing or the number of logical hops, power consumption can be reduced by 80%. However, grooming traffic with different objectives, such as to minimize the initiation of new lightpaths or to minimize the travelling distance of connection requests, fails to offer similar power savings.

Guo et al., in [136], discern that the SA is more effective in reducing power consumption over the FA approach in a dynamic traffic environment. In their proposed Power-Efficient Grooming Algorithm (PEGA), new connection requests are groomed onto existing lightpaths unless existing lightpaths lack capacity, at which point new lightpaths are established. Unlike with the FA approach, as in [5, 127, 134], however, the PEGA reconfigures (i.e., splits and re-grooms) existing lightpaths whenever necessary in order to increase power savings.

A network device, when activated, consumes a fixed amount of power and continues to draw power as long as the device remains active. In a network where traffic is represented using a dynamic model, a connection request only lasts for a brief interval. Certain devices could then be de-activated the moment a connection terminates unless they serve another connection request. The third traffic grooming approach (i.e., TA) not only reduces device activations but also decreases the time that devices remain active. Shuqiang et al. [138] suggest that if grooming new connections onto existing lightpaths forces devices to remain active for much longer than necessary, power consumption would escalate. Alternatively, if new connections can be

groomed onto lightpaths without lengthening the time that the devices remain active, power consumption can be reduced. Taking the above into account, Time-Aware Traffic Grooming (TATG) was proposed in [137, 138]. The TATG heuristic consumes less power than the DB and MHB grooming schemes when network traffic is low, but consumes more when network traffic is high.

In [139], the authors developed a similar TATG scheme by taking into account the connection holding time and power consumption of network devices. Wavelength converters were used to maximize lightpath re-use and reduce BBR. Their experiments indicate that the proposed grooming scheme consumes less power than both DB and MHB. An important point to note is that the MHB grooming scheme, which is shown to be the most power-efficient in a static traffic environment, comes second to TATG schemes proposed under the TA in [137, 138] and [139] in a dynamic traffic environment. This is due to the fact that both DB and MHB do not use time-domain information unlike TATG.

Applying the TATG concept in the Spectrum Elastic Optical Network (SEON) [141, 142], Zhang et al. [143] propose a Time-Aware Provisioning with Bandwidth Reservation (TAP-BR) protocol. The TAP-BR protocol incorporates both time and bandwidth information to facilitate power-efficient traffic grooming. To further reduce power and increase resource utilization, it grooms the majority of new traffic demands onto existing lightpaths that last long durations. Simulation results in [143] indicate that the proposed TAP-BR protocol in the SEON consumes 68%, 51% and 27% less power than the NB, DB and MHB grooming schemes, respectively.

### 2.4.3 Waveband grooming

Even with wavelength grooming, a large number of lightpaths would continue to enter the backbone network as network traffic continues to grow. Consequently, high-capacity OXCs are essential to carry out switching [100]. However, as reported in [144, 145], high-capacity OXCs are expensive, complex, have poor scalability, and consume more power. In order to reduce the amount of switching by the OXCs, waveband grooming [125, 145, 146] can be used.

A waveband is generated by aggregating a set of wavelengths using either Same-Ends (SE) or Intermediate (INT) waveband grouping policies. With the SE grouping policy, a waveband is generated at the source node, whereas with the INT grouping policy, a waveband can be generated at either the source or an intermediate node. At an intermediate node, a waveband is switched by a single I/O port. Band Switched Network (BSN) refers to a backbone network

that utilizes waveband grooming. In a BSN, OXCs are replaced with a Hybrid Optical Cross Connect (HOXC) or a Multi-Granular Optical Cross Connect (MG-OXC) [27, 147]. A detailed survey of different node architectures, grouping policies, and band configurations of BSNs is presented by Wang and Cao in [27]. Figure 2.5 shows how traffic grooming is performed in a BSN. The core node consists of an MG-OXC that is comprised of wavelength, band, and fiber cross-connects [27]. At the core node, 8 sub-wavelength traffic connections are groomed into four wavelengths, which are then multiplexed into two wavebands. The two wavebands are subsequently multiplexed into a single fiber using the WDM technique.

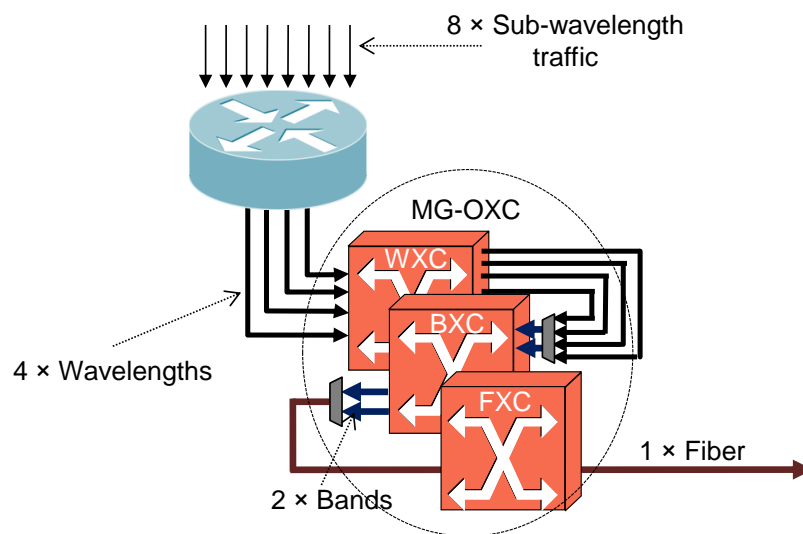


Figure 2.5: Aggregating traffic at multiple granularities by an MG-OXC of a Band Switched Network (BSN)

Waveband grooming is often used concurrently with wavelength grooming schemes to achieve different objectives. In [28], Hou et al. developed a novel Robust Integrated Grooming (RIG) scheme that jointly reduces power consumption and port consumption in dynamic traffic environments. To reduce power consumption of the electronic devices in the BSN (e.g., transponders and router ports), traffic is aggregated into fewer wavelengths using RIG. Then, by grooming these wavelengths into wavebands, RIG minimizes the use of optical switching ports. In comparison to existing state-of-the-art robust algorithms [148], the proposed RIG algorithm is 15% more power-efficient and consumes 32% fewer switching ports. Extending this work, Hou et al. developed the Maximizing Hop First (MXHF) heuristic in [149] to reduce both power consumption and switching ports in a network serving dynamic, multi-granular connection requests (e.g., OC-1, OC-3 and OC-12). The proposed MXHF heuristic adopts the

MHB grooming scheme to improve power efficiency and the INT waveband grouping policy to reduce the number of switching ports. Simulations show that the MXHF heuristic is more power-efficient than other robust algorithms proposed in [150].

Survivable BSNs (i.e., BSNs that are resilient against device failures) are studied in [144] and [151]. Extending this prior work, the authors in [152] developed two heuristic wavelength routing algorithms, namely, Single-hop Survivable Grooming with Power Efficiency (SSGPE) and Multi-hop Survivable Grooming with Power Efficiency (MSGPE), to provide resilience against link failures and to reduce power consumption. While link resilience is guaranteed using a dedicated path protection scheme, power consumption is reduced through wavelength grooming. Waveband grooming is utilized to reduce optical switching ports. Results show that MSGPE is 200% and 130% more power-efficient than SSGPE when experimented on the USA network and NSF network, respectively. However, the authors in [28, 149, 152] intentionally omitted the power consumption of optical switching ports from their calculations, assuming their power consumption to be negligible [149]. Therefore, in [28, 149, 152], waveband grooming did not appear to have an impact on network power consumption. Nevertheless, it is our understanding that power savings, albeit limited, may be offered by reducing the number of optical switching ports.

While minimizing the amount of switching by OXCs remains the primary objective of waveband grooming [126, 153–155], the latter could also be used to reduce power consumption [156–158]. In their pioneering work [126, 153–155], Hou et al., Guo et al., and Wang et al. developed integrated grooming schemes by combining wavelength and waveband grooming to reduce the number of optical switching ports of HOXCs. Hou et al. [156] are the first to jointly analyze port cost and power savings in a BSN. The authors first developed an ILP formulation to reduce both switching ports and power consumption of a BSN [156]. As the developed ILP formulation is only solvable for small networks, the authors then proposed two heuristic schemes. Their results show that the SE grouping policy consumes less power, but more switching ports, than the INT grouping policy. INT consumes more power as it requires more electrical processing. The reason is that lightpaths need to be assigned appropriate wavelengths in order to be grouped into wavebands at intermediate nodes. However, as HOXCs do not possess wavelength converters at the optical switch [156], lightpaths have to enter the electronic layer, increasing the amount of electrical processing. On the other hand, SE consumes less power as waveband grouping does not occur at intermediate nodes. It is also observed

that increasing waveband granularity raises power consumption.

In a separate study, Wang et al. [157] obtained identical results after experimenting with both static and dynamic traffic models. Considering their results and that of Hou et al. [156], we contend that SE grouping is more power-efficient than INT and that a small band size is more favourable in reducing power consumption. However, it is unclear if the above statement holds true for BSNs employing MG-OXCs instead of HOXCs or when optical switches are provisioned with AOWCs.

While [157] and [156] experiment on BSNs with HOXCs, [158,159] analyze power consumption of BSNs with MG-OXCs. According to their survey [27], Wang et al. report that the three-layer MG-OXC provides the most switching port savings. Recent efforts in [158–160] provide some interesting insights into power consumption of a BSN employing three-layer MG-OXCs. To understand the relationship between power consumption and a range of design parameters (e.g., wavelength capacity (denoted as ‘C’), waveband size (‘W’), number of wavebands per fiber (‘B’), and number of fibers per unidirectional physical link (‘F’)), Naas et al. [158,160] carried out several experiments on the NSF network and EON. Their experiments reveal that, with the selection of an optimum C-W-B combination (that is a function of the network topology, network traffic, and fiber capacity), the BSN consumes, on average, 50% less power than ordinary IP-over-WDM networks (with wavelength grooming only) under both fiber-scarce and fiber-plentiful situations.

In another study, Naas et al. [159] analyze how the optical reach of lightpaths would affect power consumption and cost of a BSN. Their results show that increasing the optical reach of a lightpath beyond a certain threshold would considerably elevate cost, despite reducing power consumption by a small percentage. It is then important to pinpoint the threshold that provides the optimum balance between cost and power consumption. However, if the MG-OXC is provisioned with AORs [22, 161], wavelengths can be regenerated within the optical switch without involving electronic processing, and the results obtained in [159] might not hold true.

#### **2.4.4 Traffic engineering approach: Summary of findings**

Important conclusions drawn from the reviewed literature are summarized in Table 2.4. In Table 2.4, the studies examined are first categorized according to the grooming technique (i.e., wavelength or waveband grooming) and the nature of traffic requests (i.e., static or dynamic

traffic models). The considered core node architecture and relevant power-related findings are then presented.

By aggregating traffic into fewer wavelengths, wavelength grooming reduces power consumption of amplifiers and line cards. It also helps to minimize the O-E/E-O interfaces required to add and drop traffic between the WDM and IP layers of the backbone network. However, wavelength grooming involves traffic processing, which results in power-hungry O-E/E-O conversions. Thus, if not handled appropriately, wavelength grooming could result in increased power consumption. Among the available wavelength grooming schemes, MHB consumes the least amount of power under static traffic environments in experiments performed in most studies. However, DB is more effective when electronic devices (e.g., O-E/E-O converters, core routers) consume a significant amount of power compared to optical devices. Under dynamic traffic environments, time-aware wavelength grooming schemes (e.g., TATG, TAP-BR) show superior results in reducing power consumption of backbone networks. To minimize power consumption under dynamic traffic environments, traffic needs to be served using a smaller number of network devices that remain active for a minimum duration.

Waveband grooming is the process of aggregating multiple wavelengths into a single waveband which is switched using a single I/O pair of an OXC. As I/O ports consume a small amount of power, waveband grooming is believed by researchers to have a minimum impact on reducing power consumption. Therefore, most researchers do not quantify actual power savings from using waveband grooming. However, as reported in [113, 162], ports in the switching layers of a three-layer MG-OXC are equipped with pre/post amplifiers, add/drop multiplexers, and modules for termination of the Optical Supervisory Channel (OSC). Thus, Murakami et al. [101, 163] shows that an I/O port consumes approximately 8 W of power, which is not negligible. Furthermore, translucent OXCs in the future would not only perform switching but may also convert and regenerate wavelengths using both single-wavelength and multi-wavelength all-optical devices [22, 114, 116, 161, 164]. *If multi-wavelength devices could be used to convert and regenerate wavebands without demultiplexing them into individual wavelengths, we believe that waveband grooming would be able to offer greater power savings, although this has yet to be investigated. We also believe that more research should be conducted to quantify the actual power savings of BSNs employing different MG-OXCs and various design parameters (e.g., grouping scheme, band size).*

In summary, traffic grooming is the process of aggregating multiple low-granularity traffic

into few high-granularity traffic flows. Traffic grooming plays an important role in reducing power consumption by increasing resource (e.g., bandwidth, capacity) utilization and minimizing the use of network devices. To maximize power reduction, traffic can be groomed at both wavelength and waveband granularities. Inclusion of all-optical devices would also help to increase power savings offered by traffic grooming.

Table 2.4: A summary of power-reducing grooming efforts

Granularity	Traffic model	Policy	Core node	Outcome(s)	Studies
Wavelength Grooming	Static	NB, DB, MHB	Core router + OXC, Digital Cross Connect (DXC) + Optical Add/Drop Multiplexer (OADM)*	Out of three schemes, MHB is more power-efficient	[129, 130], [131]*
			Core router + OXC, Digital Cross Connect (DXC) + OXC*	A combination of DB and MHB offer excellent power savings	[133], [132]*
			Core router + OXC, Core router only *	FA is more power-efficient than NB, DB and MHB	[5, 127], [134]*
Waveband grooming	Dynamic and static	FA, SA, TA	Core router + OXC	SA is more power efficient than FA	[136]
			Core router + OXC	TA is more power-efficient than DB and MHB.	[137, 138, 143] and [139]
			Electronic Cross Connect (EXC) + a three-layered MG-OXC	If $C$ , $W$ , $B$ , and $F$ design parameters are selected correctly, a network employing waveband grooming consumes 50% less power than a network that only relies on wavelength grooming.	[158–160]
Waveband grooming	Dynamic and static	MHB combined with INT	Core router + HOXC	Power consumption is reduced by limiting IP-layer electronic processing.	[28, 148–150, 152]
			SE and INT	SE consumes less power than INT.	[156, 157]

## 2.5 Power-aware networking approaches

When designing a backbone network, typically, capacities of network devices are dimensioned to support peak-hour traffic [138]. However, according to [165,166], network traffic experiences cyclic variations. During early morning hours or after midnight, when network traffic is low [166], certain devices needlessly consume and waste a significant amount of power without performing any task.

According to many scholars [167–170], unnecessary power waste can be curtailed by shutting down network devices or switching them into low-power-consuming sleep mode (i.e., idle state). A simple scenario of the sleep mode of operation is presented in Figure 2.6. By switching nodes  $j$  and  $l$  (the dotted circles) into sleep mode, power consumption is reduced at nodes  $j$  and  $l$  and links connecting node pairs  $(i,j)$ ,  $(j,k)$ , and  $(k,l)$  (dotted lines). In order for network devices to be shut off or switched off, network architecture and routing protocols need to be modified [167], leading to the development of power-aware networking schemes. Over the past years, a number of such schemes have been developed [169, 171–175], which can be categorized into power-aware network designs and power-aware routing protocols.

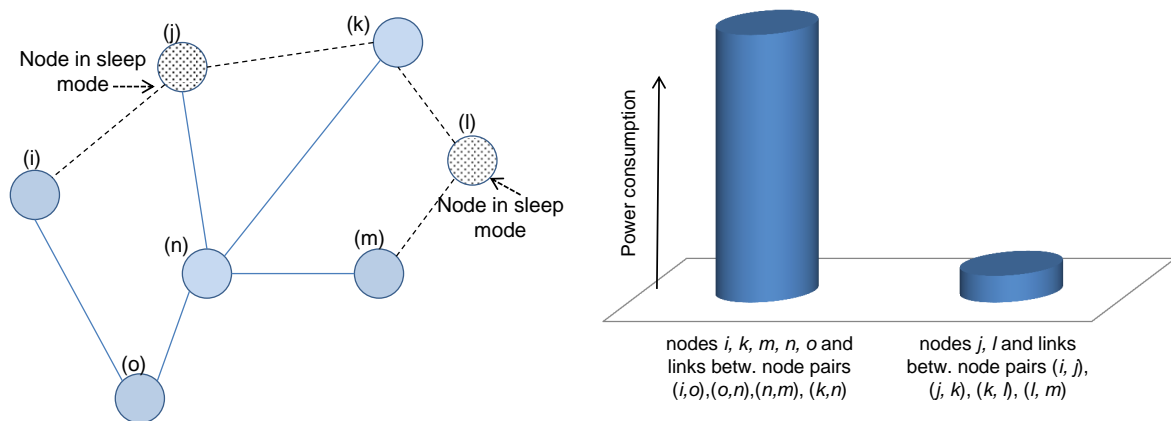


Figure 2.6: Switching nodes into sleep mode to reduce power consumption.

By minimizing the use of network devices, traffic grooming schemes explained in Section 2.4 and power-aware networking schemes discussed in this section share a common outcome of reduced power consumption. However, their fundamental objectives differ. The primary objective of traffic grooming is to reduce the number of lightpaths, while that of power-aware networking is to shut down as many devices as possible. To achieve the latter objective, power-aware networking, performed by optimizing a cost function using either integer programming

techniques or heuristic algorithms, serves traffic using fewer network devices.

### 2.5.1 Power-aware network design

Power-aware networking schemes, specifically the sleep mode of operation, were first adopted in Ethernet and Local Area Networks [168, 176, 177], and most schemes were developed by considering daily traffic variations. In 2008, power-aware networking was introduced to backbone networks by Chabarek et al. [173]. Chabarek et al. measured power consumption of two widely-used Cisco routers and then determined the optimum router-configuration at each core node in the tested network for different network traffic levels, creating a power-aware network design. Subsequently, specific line cards and router chassis were switched off by routing traffic using a power-aware routing scheme. The end result produced a 2% and 65% increase in power savings in a 12-node network with 24 and 134 links, respectively. The authors highlight that a larger number of links provides an opportunity to save more power and ensure robustness against link failure [173].

Power consumption of network devices can be represented using different energy models [178, 179]. In [178], device power consumption is modelled using linear, logarithmic, cubic, and on-off energy profiles [178]. By taking these energy profiles into consideration, the authors developed an Energy-Profile-Aware Routing (EPAR) scheme that was optimized using integer programming [178]. The objective of this algorithm is to force the routing of traffic via the most power-efficient network devices. Results show that the EPAR offers a 10%, 10%, 0% and 35% increase in power efficiency over the Shortest Path Routing (SPR) scheme when network devices use on-off, logarithmic, linear, and cubic energy profiles, respectively.

The authors of [179] developed a green power-aware routing scheme by assuming three different energy profiles (energy-agnostic, idleEnergy, and fully-proportional). A device with an energy-agnostic profile always stays powered-on, while a device with an idleEnergy profile may operate in off, idle, and fully-on states. The authors [179] developed an ILP formulation to reduce power consumption while satisfying QoS constraints on maximum link utilization. Their results show that devices with the idleEnergy profile consume, on average, 0.2% less power than devices with the energy-agnostic profile. Although devices with the fully-proportional energy profile consume the least amount of power, such devices are not available today. The study further indicates that using devices with an idleEnergy profile to reduce power consumption has a limited impact on QoS, but may raise some reliability issues. It is

noted that switching off nodes (although impractical, as nodes always generate and receive traffic) has a higher potential in reducing power consumption than switching off links.

### 2.5.2 Power-aware routing

Research on power-aware routing protocols has garnered considerable interest in recent times. In [172], the authors developed three different power-aware routing schemes and investigate the power efficiency of each. The main objective of the study is to accommodate a given set of traffic demands (when network traffic load is low) using a minimum number of line cards. This is the first study to investigate the impact of re-routing traffic in IP and WDM layers, individually, on power consumption.

The first routing scheme proposed in [172] uses virtual (at IP layer) and physical routing paths that are both fixed. The second scheme allows flexibility in the virtual routing paths, while the physical paths remain fixed. The third scheme allows changes to be made to both virtual and physical routing paths. Using MILP optimization techniques, the three schemes are compared in terms of power consumption with respect to network traffic variations. The results demonstrate that the first, second, and third schemes offer a 40%, 63%, and 66% increase in power efficiency, respectively, when the network traffic load is 5 Tbps. These findings show that power savings arise from jointly re-configuring routes on the IP and physical layers that allows more devices to be switched off. This work is comprehensively discussed again in [180].

In another study published in 2010 [181], the authors developed a three-phase Energy-Aware Routing (EAR) heuristic algorithm that reduces power consumption by switching off links in the network. The developed algorithm allows a subset of routers to connect to other nodes using Shortest Path Trees (SPT) and forces the remaining nodes to utilize these SPTs to route traffic instead of creating their own, thereby increasing link re-use. The proposed EAR algorithm is able to switch off up to 60% of existing links and evenly distribute traffic on links that remain switched on.

Chiaraviglio et al. [171, 182, 183] reduces power consumption by selectively switching off network devices according to traffic variations during the day. In [171, 183], Chiaraviglio et al. first defined an analytical model and a cost function by taking into account the power consumption of nodes and links. They then proposed a heuristic algorithm, after showing that optimizing the analytical model runs into the multi-commodity flow problem that makes solving it within a feasible time period difficult. The heuristic algorithm, which is tested on

synthetic and realistic networks, identifies and switches off nodes and links when network traffic is low. In the first stage of the algorithm, nodes are sorted and switched off in succession using four sorting criteria, namely, random, least-link, least-flow, and Opt-Edge (OE). While least-link takes into account the number of links that are attached to each core node, least-flow accounts for the amount of traffic that flows through each core node. On the other hand, OE considers the redundancy of edge nodes. In the second stage, links are sorted and switched off using the random and least-flow sorting criteria. Power consumption values are obtained from experimenting with different combinations of node and link sorting criteria. The obtained results indicate that 50% of core nodes and 30% of links can be switched off by using a sorting criteria combination of OE for nodes and least-flow for links.

In a recent study, Coiro et al. [174] developed an algorithm that reduces power consumption by switching off individual fiber links depending on network traffic variation. This is the first study to jointly analyze power consumption and network resilience. To conserve power, links are sorted and removed using three different criteria. First, authors switch off fibers according to the Most-Amplifier (MA) criterion. Then, the difference between the number of amplifiers in the removed fiber and the number of amplifiers in fibers constituting the working path is used as the second sorting criterion. To offer resilience against link failure, working paths are protected by backup paths. Lastly, as the third criterion, the fibers are sorted according to the difference between the number of amplifiers in the removed fiber and the number of amplifiers in the fibers that constitute the backup path. Results indicate that the third criterion reduces the most amount of power (35% reduction) in comparison to the first two criteria. Contrarily, the MA criterion reduces the least amount of power. The novel heuristic algorithm, proposed by the same authors in [133], achieves power efficiency between 80% and 100% depending on the traffic load. This new algorithm that is named Start Single-Hop and Reroute (Start-SH&ReR), first grooms traffic demands using the single-hop wavelength grooming scheme (i.e., DB scheme), and then switches off unnecessary links by reconfiguring traffic demands using the MHB grooming scheme.

Power-Aware Routing with Wavelength Assignment (PA-RWA) was first investigated in [184]. Two heuristics were developed to perform routing and wavelength assignment in separate stages and reduce power consumption in a network with a static traffic matrix. Routing is performed using the Most-Used Path (MUP) algorithm where lightpaths are forced to share links. Wavelengths are assigned using the Two-Phased First-Fit (TP-FF) algorithm that gathers

lightpaths into fewer fibers. Extending this work, in [185], Coiro et al. developed a Load-Based Cost (LBC) routing algorithm and two wavelength assignment schemes, namely, Least-Cost Wavelength (LCW) and Least-Additional-Power First Fit (LAP-FF). By taking into account link load and power consumption information, the LBC routing algorithm routes traffic via a reduced number of links. LCW and LAP-FF consider the wavelength load within each fiber and try to provision new lightpaths along used fibers without activating new fibers and allowing low-utilized fibers to be switched off.

To validate their performance in terms of power consumption, the LBC routing algorithm is compared against SPR, Least-Congested Path (LCP), and MUP algorithms, while LCW and LAP-FF are compared against the TP-FF algorithm. Results indicate that, among the routing algorithms, LBC and SPR consume less power at high traffic loads, while LBC and MUP consume less power at low to moderate traffic loads. Power efficiency of LBC is found to be between 85% and 95% at varying traffic loads. However, LCP offers the best results in terms of traffic blocking. Among the wavelength assignment schemes, TP-FF consumes more power than LAP-FF and LCW schemes, with LCW consuming 10% less power than LAP-FF.

Contrary to the idea of switching off links (i.e., destructive mechanism), authors of a recent study [175] developed a novel scheme where additional links in the network are activated or switched on (i.e., constructive mechanisms) based on the traffic load [175]. The results obtained in this study show that the proposed switch-on scheme is more power-efficient in comparison to available switch-off schemes. On average, the switch-on scheme provides 15% savings in power consumption, while switch-off schemes only offers 11% savings during the course of a day. On the negative side, the proposed switch-on algorithm employs a higher number of low-speed transponders that increases cost, which is also a critical factor.

### 2.5.3 Reconfiguration

The reconfiguration cost of power-aware routing was first studied by Zhang et al. [186]. They propose three power-aware routing schemes, namely, Unconstrained Reconfiguration (UR), Virtual-Topology-Constrained Reconfiguration (VTCR), and Full-Constrained Reconfiguration (FCR), to save power by shutting down idle line cards and chassis of routers based on network traffic variation. At each traffic interval, the network is optimized with the UR, VTCR, and FCR schemes, individually, using MILP. The UR scheme allows lightpaths to be re-routed and devices to be re-configured (i.e., switched on or off) at each traffic interval. With VTCR, the

network is first optimized to carry maximum traffic. As traffic decreases, lightpaths are re-routed and excess devices are switched off appropriately. However, new devices would not be switched on. Lastly, FCR does not allow lightpaths to be re-routed and only excess devices can be switched off. Comparing the three schemes, it is clear that the UR scheme consumes the least power but involves more lightpath re-routing and device reconfiguration. On the other hand, VTCR consumes almost the same amount of power as UR, but involves less re-routing and re-configuration. FCR eliminates re-routing and involves even fewer re-configuration, but still consumes 22.36% more power than UR and FTCCR. Hence, the most favoured scheme to curtail power consumption and reduce re-routing and reconfiguration is the VTCR power-aware routing scheme.

In [187], the authors investigate the possibility of switching off links during periods of low traffic while limiting the number of configurations allowed within a day. Unlike their previous work [171, 174, 183], where network resources freely switch between different operating states at the end of each hour, in this particular study [187], the number of resource reconfigurations per day is restricted to a maximum of three. Based on random graph theory, traffic variations, and QoS constraints, the developed model produces power savings even with the limited configurations allowed.

In a related study [188], Bonetto et al. developed three different algorithms, namely, LFA (Least Flow Algorithm), GA (Genetic Algorithm), and EWA (Energy Watermark Algorithm) by extending past efforts in [183, 189, 190] to jointly reduce power consumption and re-configuration cost. This is also modelled as an MILP formulation in [191]. LFA, first introduced in [183], sorts links according to utilization and then switches them off in succession. GA, first introduced in [189], optimizes the network at lightpath level by using a meta-heuristic that is based on the principal of natural evolution, a set of parameters, and a fitness value defined as a function of power consumption and re-configuration cost. EWA, derived from the work of [192], uses lightpath utilization information to identify and switch off line cards [190]. The three algorithms are tested on three different networks using actual traffic information. Results show that a substantial amount of power can be saved while keeping the reconfigured cost low. GA and EWA produce higher power savings and involve smaller re-configuration costs than LFA.

## 2.5.4 Sleep mode of operation

Most power-aware routing schemes are developed for IP-OTN networks where core nodes consist of an electronic core router and/or an OXC. However, in 2009, Bathula et al. [193] reduced power consumption of an OBS network by turning a selected set of core nodes into sleep mode at random intervals. To be able to route traffic and ensure QoS requirements during these intervals, they developed an Energy-Efficient Routing (EER) heuristic. Their results indicate that a 40% increase in power efficiency can be obtained by allowing nodes to sleep and routing traffic using EER at the cost of a slight increase in request blocking and end-to-end delay, in comparison to an OBS network without sleep mode of operation.

Most recently, Yang et al. [120, 194] show that sleep-mode-enabled burst switches consume less power than electronic core routers. Certain components of these sleep-mode-enabled burst switches can sleep (i.e., they are in a low-power-consuming state) while waiting for the next burst. According to Yang et al. [120, 194], to efficiently manage the individual elements, the nodes have to be provisioned with a sleep-wake controller. Although inclusion of an additional controller seems to increase power consumption initially by 1.3 times, a drastic reduction of operational power consumption is achieved by allowing elements of core nodes to sleep. Kang et al. propose burst assemble [195, 196] and wake-transition decision-making [197] algorithms, which maximize power savings of sleep-mode-enabled burst switches by allowing components to sleep for long durations.

In [196], the authors find that a substantial amount of power can be saved in a sleep-enabled OBS network if traffic shares self-similar characteristics. It is also noted that provisioning of larger bursts allows core node elements (e.g., line cards) to remain in a sleep state for longer durations, resulting in reduced power consumption. By increasing the burst assemble time threshold from 0.01 ms to 1 ms, extra 10% of power can be saved when traffic exhibits high self-similarity. In comparison to PtP-WDM networks, OBS networks consume between 5% and 35% less power [196]. The proposed Dynamic Time-Based Assemble (DTBA) algorithm in [195] adjusts the burst assemble time or length according to the nature of traffic to maximize the sleeping duration of core node elements. In another important study [197], Kang et al. propose fixed-time and fixed-length sleep-awake algorithms to reduce power consumption by minimizing unnecessary transitions between different working states. The two algorithms achieve a maximum combined power saving of 30%.

### 2.5.5 Limitations of power-aware networking

Prior to implementing the switch off/sleep mode of operation in a network, a number of uncertainties need to be resolved. As pointed out in references [169,198], elements that are switched off or are in sleep mode lose their presence, literally “falling off” the network unless the network state is frequently monitored [199]. This could lead to transitory network instabilities and reduced reliability. To solve this issue, a proxy is introduced to perform the tasks of the switched-off or sleeping devices. The devices could then move from a low power mode to an active mode when it either receives a wake-up signal from the proxy device or after a pre-configured time elapses.

To switch devices between different operating modes, routers need to process and make controlling decisions instantaneously. Else, the switching delay between different operating modes would result in traffic loss and QoS degradation. Although available commercial routers do not possess the ability to control the operating state of individual devices, recent developments in router technologies [200] and emerging 802.3az standards that demand a faster transition time between modes (a minimum wake-up time of 3 s in a 10 Gbps link) [35] make it more possible that future devices can quickly adapt to traffic variations.

Nevertheless, the inclusion of additional electronic controlling and monitoring circuitry is likely to elevate power consumption of core routers [120,194]. Furthermore, when a device switches between different operating modes, it also experiences a transition period. According to [170,199], the device consumes a considerable amount of power during this transition period and, thus, overall reduction in power is much less than anticipated.

Many of the proposed schemes increase power efficiency either by switching off the whole device [171,174,175] or by switching off only certain elements of the device [120,194]. In [201], an interesting approach is proposed which could resolve some of the uncertainties involved in applying power-aware networking schemes in the backbone network. The authors exploit two well-known features where decoupling physical elements of a device from its virtual functionalities and resources, allows the latter (virtual) feature to be migrated onto other active elements of the same device. This indicates that a device with multiple modules can de-activate some modules and transfer their work load to residual modules within the same device. The proposed mechanism [201] allows components/elements of a core router (e.g., line cards) to be switched off selectively without incurring service interruptions. Only allowing modules to be switched off negates the likelihood of a node (i.e., a core router) falling off the network, as in the

---

case of [171], thereby ensuring its presence. The ability to carry out line-card transitions with total IP transparency is considered to be the most innovative part of this proposed scheme. This concept has its similarities with the novel idea introduced in [202], which performs the migration of virtual routers from one physical router to another. The proposed concept, known as VROOM (Virtual Routers on the Move), reduces power consumption of the core network by shutting down some of the routers.

### **2.5.6 Power-aware networking approach: Summary of findings**

To provide an overview of this section, we summarize the relevant findings in Table 2.5. Studies are categorized according to their power-related objective and optimization technique used. The outcomes of these studies are also briefly explained.

Traditionally, the backbone network is over-provisioned to cater to peak traffic demand of the future. Hence, devices often remain underutilized during low traffic periods. Our review of the relevant literature reveals that power-aware networking shows great potential in reducing power consumption, especially during low traffic periods. Solutions that are developed using power-aware networking increase resource utilization and reduce device usage.

To offer significant reduction in power consumption, network devices should operate in multiple states. Past studies highlight that an effective monitoring mechanism is essential to allow devices to switch between different operating states without causing network instabilities. In developing power-aware networking schemes, greater effort needs to be put into minimizing re-configurations, network disruptions, and state transitions. Two solutions that have been introduced to prevent network instabilities, when implementing power-aware networking in the backbone network, are proxy methods and switching off individual modules rather than the device as a whole.

Table 2.5: A summary of research on power-aware networking

Focus	Method	Study	Objective	Outcome(s)
Power-aware network design		[173]	To select the most power-efficient router configuration	An appropriate router combined with power-aware routing offers power savings.
	ILP/MILP	[178]	To investigate the power consumption of four different energy profiles	Cubic energy profile consumes the least amount of power. On-off profile consumes the most.
		[179]	To investigate the power consumption of three different energy profiles	Devices with idleEnergy energy profile consume less power, are commercially available, and have less impact on link utilization.
Power-aware routing	MILP	[172, 180]	To reduce the number of line cards in use	Proposed three algorithms. Demonstrate that more power can be saved by re-configuring routes on IP and physical layers.
	Heuristics	[181]		The proposed algorithm can switch off 60% of links.
	MILP and Heuristics	[133] [174]	To switch off as many fiber links as possible	Achieves power efficiency between 80% and 100%. Reduces power consumption by 35% while guaranteeing resilience against link failure.
Power-aware routing	MILP and Heuristics	[171, 182, 183]	To selectively switch off nodes and links	The proposed algorithm can switch off 50% of core nodes and 30% of links
	Heuristics	[184]		The combination of MUP routing algorithm and TP-FF wavelength assignment scheme offers considerable power savings.
	MILP	[175]	To route and assign wavelengths to minimize device usage	The proposed 'switch-on' scheme is more power-efficient in comparison to available 'switch-off' schemes.
Power-aware routing	MILP and Heuristics	[185]		The proposed LBC routing algorithm combined with LCW wavelength assignment scheme offers between 85% and 95% increase in power efficiency.

Heuristics	[187]	To reduce the use of network devices and minimize reconfiguration cost	The developed model, based on random graph theory, produces power savings even with few reconfigurations allowed.
MILP	[186]		VTLR routing scheme reduces power consumption and minimizes re-routing.
MILP and Heuristics	[188, 191]	To reduce the use of network devices and minimize reconfiguration cost	GA and EWA produces higher power savings and incurs lower re-configuration cost than LFA.
Power-aware networking solutions for OBS networks	[120, 194–196]	To use sleep mode of operation to reduce power consumption of burst switches	Proposed burst assemble and wake decision-making algorithms and novel router architectures offer power savings in OBS networks.
	[169, 198, 199]		Suggest that switched-off devices will lose their presence in the network. A “proxy” is introduced to perform the tasks of the switched-off or sleeping devices.
Limitations of power-aware networking	[35, 200]	To propose solutions to the identified drawbacks of power-aware networking.	Emerging technologies and advancements can enable power-aware networking.
	[201, 202]		Only allows modules of a device to be switched off, while the device remains switched on and tasks are performed by residual modules.

## 2.6 Load-adaptive operation approaches

Depending on the application, population and time, traffic between nodes (i.e., connection requests) demand different capacities. Today, in most backbone networks, lightpaths are established using a Single Line Rate (SLR) (i.e., a single link rate) that takes a distinct value between 50 Mbps (i.e., Optical Carrier OC-1) and 40 Gbps (OC-768) [26, 203]. To enable more traffic connections to be carried by lightpaths at an envisioned line rate of 100 Gbps, advanced modulation formats and digital processing techniques are currently being developed [203, 204]. As repeatedly mentioned in [26, 205–209], backbone networks that rely on SLR show poor resource utilization and consume more power [26, 205, 210]. For example, if the selected line rate is 2.5 Gbps and 9 Gbps of traffic needs to be transported between a pair of nodes, multiple transponders and lightpaths are needed. On the other hand, if the selected line rate is 40 Gbps, transponders are underutilized and bandwidth of the lightpaths is wasted.

A closer look at the rated power consumption values of network devices in [44] reveals that low-capacity devices (or devices running at low operational speeds) consume less power. However, high-capacity devices consume less power per bit of transmitted traffic and, thus, offer a volume discount [5, 59]. To reduce power consumption then, it is preferable to deploy a minimum number of network devices with capacity that matches the actual need. For example, 9 Gbps of traffic transiting between a node pair can be served with a single 10 Gbps transponder, instead of using four 2.5 Gbps transponders.

To increase resource utilization and fully exploit the volume discount offered by high-capacity devices, Mixed/Multi-Line Rate (MLR) and Adaptive Line Rate (ALR) strategies can be adopted in heterogeneous backbone networks [39, 45, 170, 205–209]. These approaches were first used in Ethernet networks [206, 207], and are slowly progressing towards backbone networks [170]. Unlike with SLR, a backbone network that employs MLR may serve each traffic connection using a different line rate. However, line rates have to be selected from a discrete set of line rates (e.g., OC-48(2.5 Gbps), OC-192(10 Gbps), and OC-768 (40 Gbps)) and, thus, offer less flexibility. Alternatively, if the backbone network employs ALR, the line rate can be tuned according to the actual demand.

In Figure 2.7, we present a simple example of a backbone network using load-adaptive techniques (MLR or ALR). A core node is represented by a circle whose illustrated size is proportional to the traffic capacity served by that node and the line rates assigned to traffic connec-

tions originating from the same node. The dotted lines represent links that are lightly loaded and solid lines indicate links that are highly utilized. Basically, the load-adaptive technique allows the capacity of the nodes to be dynamically adjusted according to the demand. In comparison to Figure 2.6, instead of switching off the low-load nodes  $j$  and  $l$ , they will continue to work at a lower speed or capacity, maintaining their presence in the network.

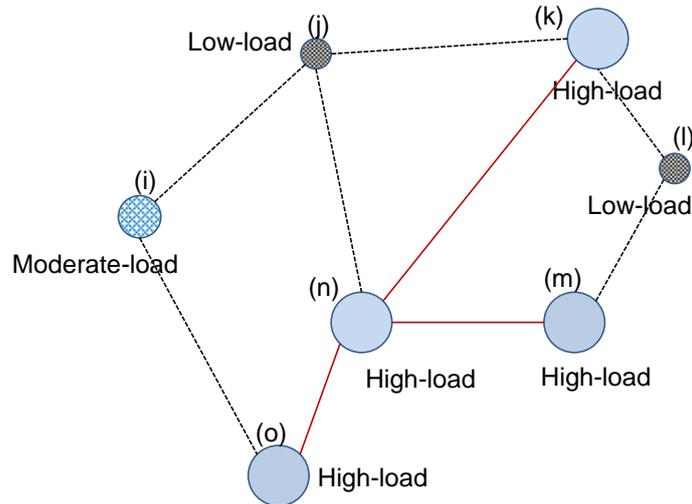


Figure 2.7: A backbone network using load-adaptive techniques: The size of the circles are proportional to their capacity and line rates; the dotted and solid lines indicate light- and heavy-loaded links, respectively.

### 2.6.1 Mixed Line Rate

At present, backbone networks can support a maximum line rate of 40 Gbps [26]. Following technological advancements, 100 Gbps and 400 Gbps line rates are soon to be a reality in the near future [26]. Considering the heterogeneous nature of traffic demands, multiple line rates should co-exist in the same backbone network. To this end, several studies investigate the possibility of adopting MLR in backbone networks [26, 39, 45, 59]. In [39], MLR is shown to minimize network cost compared to a network using SLR. However, as demonstrated in many studies [26, 39, 45, 211], co-propagating lightpaths at different line rates induces non-linear effects on each other (e.g., Cross-Phase Modulation (XPM)), which impairs signal quality. Consequently, high-capacity lightpaths assigned with a faster line rate need to be frequently regenerated after every few hundred kilometres. To increase the transmission reach of lightpaths in MLR-based backbone networks, dispersion management techniques, mixed-modulation formats, and channel input power management schemes have been proposed [39, 211, 212].

In a SLR-based backbone network, every transponder works at the same line rate of 10 Gbps, 40 Gbps, or 100 Gbps. As a result, when network traffic is high, a 10 Gbps SLR employs a large number of transponders, consuming more power. On the other hand, if network traffic is low, a significant amount of power is consumed unnecessarily by power-hungry transponders of a 100 Gbps SLR. However, if MLR is used in place of SLR, transponders of both low and high line rates can be employed according to the actual traffic demand, thereby reducing power consumption and increasing transponder utilization. However, signal degradation is critical in MLR-based backbone networks and, thus, high-capacity lightpaths may often need the service of a regenerator. Consequently, as shown in [26], when network traffic is high or when core nodes in the network are located far apart, a 100 Gbps SLR consumes less power than MLR [26]. While an SLR network designed to minimize power consumption also reduces network cost, a power-minimized MLR network would not necessarily minimize network cost [26].

Under dynamic traffic demands, line rates are frequently adjusted in an MLR network. As a result, lightpaths are repeatedly removed and reinstated using different line rates. However, to reduce both re-configuration cost and network disruptions, established lightpaths should remain intact when network traffic upgrades from one state to another. In [59], the authors investigate how this can be achieved in a MLR network while reducing both cost and power consumption. The study uses an MILP-based optimization scheme to find the optimum line rates that can serve different traffic connection requests. The maximum number of disruptions allowed between the current and ensuing state is assigned a value between 5 and 40. Power consumed is recorded against increasing network traffic. By allowing more disruptions to occur, the study shows that MLR is able to adjust line rates more efficiently, thereby reducing power consumption. By allowing 5 disruptions at a network traffic capacity of 250 Gbps and 40 disruptions when traffic capacity rises to 375 Gbps, MLR reduces power consumption by 4% and 6%, respectively, in comparison to zero disruptions.

### **2.6.2 Adaptive Line Rate**

ALR was first introduced by Nordman et al. [208] as a technique to reduce power consumption of Ethernet network interface cards (NICs). The authors in [206,207] then developed a number of practical algorithms to test and validate power savings offered by ALR. By changing the Ethernet line rate according to the link utilization factor, ALR allows network devices to work at a lower clock speed when network traffic is low and consume much less power. Although most

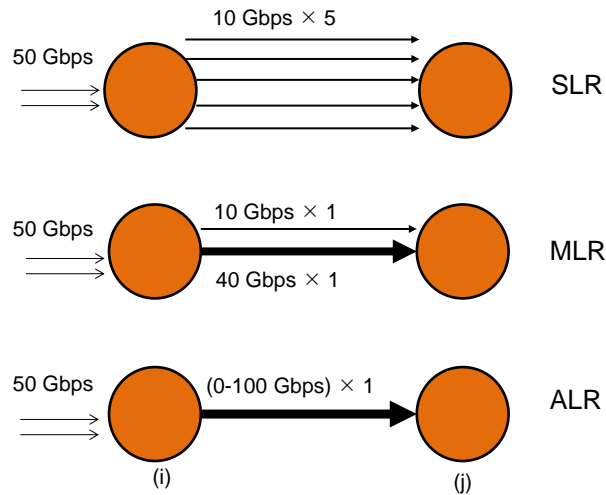


Figure 2.8: Rates assigned by SLR, MLR, and ALR techniques when transporting 50 Gbps of traffic from node  $i$  to  $j$ .

research on ALR is still at an experimental stage, Zhang et al. [213] succeeded in developing an ALR-enabled NIC. Thus, it is fair to believe that ALR-enabled backbone network devices would become commercially available in the near future.

ALR is commonly realized using the Optical Orthogonal Frequency Division Multiplexing (O-OFDM) technique. ALR can be applied to backbone networks using O-OFDM-based SEON [141], and power-related results available for such SEON networks are impressive. The experiments in [141,214] demonstrate that a tunable O-OFDM-based backbone network significantly reduces the need for transponders and wavelengths. Due to such power-saving benefits, SEON networks are frequently compared with SLR and MLR techniques. In an example that compares SLR, MLR, and ALR techniques, which is illustrated in Figure 2.8, 50 Gbps of traffic travels from node  $i$  to node  $j$ . If a single line rate of 10 Gbps is used, then a total of 5 lightpaths would be established. If MLR is used, then 2 lightpaths with different line rates can serve the traffic demand. On the other hand, with ALR, a single lightpath that has a variable capacity between 0 and 100 would accommodate the 50 Gbps traffic demand between the two nodes.

Nedeveschi et al. [170] compare the amount of power consumed by networks utilizing the sleep mode of operation (discussed in Section 2.5) and those using ALR. Their results indicate that enabling sleep mode offers higher power savings under bursty traffic environments as power consumption can be reduced during idle times between bursts. However, when the traffic load is low, the ALR technique offers more power savings. Nedeveschi et al. conclude that a combination of the two techniques could provide the best configuration in the context

of power efficiency. Analyzing the results obtained in [215,216], in which the authors develop a hybrid network by incorporating the abilities of sleep mode of operation and ALR, we are inclined to agree with Nedeveschi et al.'s conclusion. In a similar vein, the authors of [217] successfully formulate a hybrid network using ALR (referred to as rate-adaptive scaling (RS) in their study) and sleep mode of operation (referred to as sleep-state exploitation (SSE) in their study). In developing this hybrid network, the authors also consider time-related parameters incurred by a data packet that travels in the network. Although the hybrid network proposed in [217] was tested for resource utilization, its power consumption is yet to be examined.

In [209], the authors compare the power efficiency of backbone networks utilizing power-aware-routing (that allows more links to remain asleep) and rate-adaptive techniques (which are similar to ALR). The authors point out that if rate-adaptable devices consume a substantial amount of power at the start-up (i.e., instantaneous power at activation), then power-aware routing is a more power-efficient strategy. However, if devices consume relatively low power at the start, then higher power savings are offered by rate-adaptive techniques.

In [205], Klekamp et al. compare MLR and reach/rate-adaptive (i.e., ALR) techniques. Using the actual German50 network, projected line rates for 2010 and 2020, and power consumption values of core network devices (both IP and WDM), the authors conducted a heuristic-based experiment. Two different routing schemes (hierarchical and flat) were also used. The obtained results indicate that both MLR and ALR consume an equal amount of power at the IP layer. However, MLR consumes less power at the WDM layer than ALR. In separate studies [210,218], Klekamp et al. performed a similar experiment on the USA66 network. The results mirror that of [205] and demonstrate that MLR consumes approximately 15% less power in comparison to ALR in the Dense-WDM (DWDM) layer of the network. While MLR is more effective in reducing power consumption of the DWDM layer, the reach/rate adaptive method (i.e., ALR) greatly reduces the number of transponders and fibers used in the network. However, the cost associated with reach/rate adaptive networks is higher in comparison to MLR networks, as the former employs expensive rate-adaptive transponders.

Vizcaino et al. [219] also extensively study the difference in power consumption between O-OFDM, MLR, and SLR approaches. Considering a static traffic environment, Vizcaino et al. [219] demonstrate that MLR and O-OFDM techniques both consume a similar amount of power and outperform SLR. Despite their similarities, O-OFDM elastic networks offer power consumption improvements over MLR networks that utilize a 100 Gbps line rate. Taking a

step further, the same authors developed energy-aware heuristic algorithms in [220] to efficiently allocate resources under static and dynamic traffic environments for O-OFDM elastic networks and WDM networks employing SLR and MLR techniques. The proposed heuristics, when tested on a large-sized network (e.g., GANT2 network) under a static traffic environment, show that O-OFDM networks consume 37.5% and 50% less power in comparison to MLR and SLR. Similarly, when the three techniques are tested under a dynamic traffic environment, the O-OFDM network consumes approximately 50% and 100% less power in comparison to MLR and SLR. A similar pattern is also observed for the service blocking ratio, with the O-OFDM network sustaining the least amount of blocking and the SLR network incurring a higher blocking ratio.

Although SLR, MLR, and ALR are comparatively analyzed in terms of power efficiency and transponder cost in many previous studies, their effects on path protection or network resilience is only studied in [221]. The most widely-adopted approach in assuring network resilience is reserving resources on two non-overlapping routes for working and protection paths by considering peak traffic demands. Consequently, resilient networks consume more power than unprotected networks. In [221], Lopez et al. identify the most power-efficient solution between resilient networks adopting SLR, MLR, and ALR approaches, where ALR is implemented in O-OFDM-based SEON. The main objective of their study is to measure the increase in power efficiency of SLR-, MLR- and ALR-based networks by dynamically adjusting transponder capacities (traffic awareness) in the protection paths according to the hourly variability of network traffic. Evaluating the results in [221], we can observe that O-OFDM-based SEON saves up to 27% of power when network traffic is high. Within the range of tested traffic loads, ALR outperforms SLR and MLR by consuming the least amount of power. Between MLR and SLR networks, MLR consumes less power at low traffic loads. However, a 100 Gbps SLR consumes much less power than MLR at higher traffic loads, which is consistent with the results of [26].

### **2.6.3 Load-adaptive operation approach: Summary of findings**

Studies that examine load-adaptive approaches are summarized in Table 2.6 and categorized according to the specific technique examined (i.e., SLR, MLR, and/or ALR). A comparison of network power consumption using these three techniques is presented, with the outcomes of the comparison briefly explained. The key drawbacks of SLR, MLR, and ALR are also high-

Table 2.6: A broad comparison of SLR, MLR, and ALR approaches.

Focus	SLR	MLR	ALR/Elastic/SEON/Rate adaptive techniques
Function	Every lightpath is assigned the same line rate.	Each lightpath has the ability to select its speed from a set of discrete values.	Each lightpath has the ability to select its speed from a set of continuous values.
Power-related comparison vs SLR		MLR is more power-efficient at low network traffic volumes and when traffic volume is not an integer multiple of the selected SLR. [26,45,219,221]	ALR is more power-efficient than SLR at all volumes of network traffic [220,221].
Power-related comparison vs MLR	When network traffic volume is high and SLR is 100 Gbps, SLR consumes less power than MLR as a result of reduced regeneration. [26,45,220,221]		The IP layer of the backbone network consumes less power [205, 210, 218] with ALR than with MLR. ALR is more power-efficient when experimented using static or dynamic traffic models. [220,221]
Power-related comparison vs ALR	SLR consumes more power than ALR at all traffic volumes [26,45,220,221].	The WDM layer of the backbone network consumes less power with MLR than with ALR [205,210,218].	
Other drawbacks	Low transponder and lightpath utilization. High power consumption, especially when network traffic is high	Excessive use of regenerators by high-capacity lightpaths increases power consumption.	Requires expensive, power-hungry, bandwidth-adaptive long-reach transponders and add/drop multiplexers.

lighted.

In summary, to reduce bandwidth waste and exploit volume discount on power consumption of high-capacity transponders, traffic needs to be served using appropriate line rates by employing either MLR or ALR. The key conclusion that we draw from the reviewed literature is that MLR and ALR techniques consume less power than SLR. However, power consumption of MLR-based networks is affected by regenerator power consumption at high network traffic volumes. Hence, it is vital to develop new algorithms to assign an appropriate line rate to each lightpath depending on the actual traffic requirement. Although findings reveal, overall, that ALR consumes less power, it is important to recognize that these results have been obtained using approximated power consumption values for bandwidth-adaptive long-reach transponders and add/drop multiplexers which are still in the early stages of development.

## 2.7 Adopting the four approaches in real networks

In Sections 2.3, 2.4, 2.5, and 2.6, we discussed solutions developed by academic scholars to reduce backbone network power consumption using four main approaches. In this section, we survey how these proposed solutions are currently adopted by carriers/operators, vendors, and research bodies to increase power efficiency of backbone networks. We begin our survey by describing important research projects, which are funded by network operators and/or device manufacturers, and their findings. In no particular order, we demonstrate the critical role played by our four approaches in these projects and provide examples of their application in devices and technologies.

### 2.7.1 Approaches adopted in industrial research projects

To explore solutions to the increasing power consumption problem of backbone networks, UC Santa Barbara's Institute for Energy Efficiency convened a two-day technology round-table in February 2013, bringing together 27 industry leaders representing vendors (e.g., Cienna, Juniper, Cisco, Infinera), service providers (e.g., Verizon, Sprint, Deutsche Telekom), research institutes (e.g., GreenTouch by Alcatel Lucent, Infornetics Research), government laboratories (e.g., Energy Sciences Network), and renowned academics [222]. At the end of the two-day round-table discussions, the participants identified several key advancements that could be exploited in reducing backbone network power consumption. These advancements include integrating optical and electronic technologies at device and component levels (as discussed under *network redesign*), using optical switching and optical bypass strategies (as discussed under both *network redesign* and *traffic engineering*), and adjusting routing paths and increasing device utilization to make power consumption proportional to the traffic load (as discussed under *network re-design*), among others. The participants argue that load-adaptive approaches, such as gridless architecture (i.e., SEONs) and the use of high-speed line rates, cannot produce high power savings, even in another ten years, due to the non-linear Shannon limit of fibers.

In 2010, a team of researchers established a partnership with a group of device manufacturers to form the EConet project [223]. The primary objective of EConet is to develop novel solutions to reduce power consumption of the Internet by exploiting power-aware networking and load-adaptive operation. The developed solutions and technologies are evaluated using large-scale test-beds at the TELIT test plant, and two additional, small-scale test-beds at GRNET and

NASK sites with 'real-life' testing methodologies and instrumentation that are usually adopted for evaluating commercial network devices, before putting them into actual production .

The GreenTouch consortium, launched in 2010, provides a platform for innovative researchers, engineers, and technology experts from around the world to develop solutions to increase power efficiency of the Internet, by a factor of 1000, by 2015 [224]. GreenTouch targets the following areas in developing these solutions, which we have discussed under network re-design, power-aware networking, and load-adaptive operation approaches:

- reducing power consumption of network devices and components;
- adopting MLR;
- using sleep and low-power-consuming operating modes;
- optimizing the physical topology considering traffic fluctuations.

The GreenTouch white paper, issued after three years of project commencement, report that developments in the four areas would improve power efficiency in the year 2020 by 2.7%, 1.2%, 1.8%, and 1.1%, respectively, compared to 2010.

Researchers who are currently involved in Alcatel-Lucent's 'green research program', spearheaded by Bell Labs, expect to increase power efficiency of backbone networks by integrating electronic and optical technologies within a single device, optimizing the network architecture, and achieving proportionality between power consumption and minimizing capacity waste [225]. In a separate partnership with the University of Melbourne, Bell Labs explores how traffic grooming affects next-generation backbone networks and investigates how increased traffic volumes could be modulated into high-line rates without increasing power consumption.

In 2008, the International Telecommunication Union (ITU) made recommendations to minimize power consumption of Next-Generation Networks (NGNs) [226]. The use of network devices with multiple power modes (e.g., full power, low power, stand-by, and hibernation) was shown to have a great impact on reducing power consumption of both optical backbone and access networks.

### **2.7.2 Approaches adopted by vendors and carriers**

To conserve energy, vendors incorporate state-of-the-art optical and electronic technologies to produce high-capacity, low-power-consuming devices.

---

Cisco plans to tackle increasing power consumption of the Internet with a range of solutions that use novel concepts discussed under the network redesign approach. Each generation of Cisco products consumes less electricity per bit of transmitted data. For example, Cisco-CRS-3 consumes 2.8 nW/bit in comparison to 8 nW/bit consumed by the Cisco CRS-1 core router [41, 42]. Furthermore, each generation of Cisco core routers and products support increased throughput, work at higher speeds, and contain a large number of ports. Thus, more traffic can be transmitted via a smaller number of lightpaths and devices. These CRS routers help AT&T, a Tier 1 carrier in the U.S., to meet growing traffic demands while, at the same time, reducing electricity consumption [227]. In recognition of its outstanding contributions to conserving energy and reducing environmental impact, Cisco was awarded the Supplier Sustainability Award by AT&T in 2012 [227].

Juniper is another top-tier manufacturer that continues to deliver devices that provide increased throughput with high power efficiency by integrating advanced electronics with optical technology. For example, the Juniper Networks T1600 series core router has a maximum throughput of 1.6 Tbps, supports 10/40/100 Gbps line rates, and performs traffic aggregation, while consuming 40% less power than other competitive platforms. At present, Juniper products are utilized by Verizon, another Tier 1 carrier in the U.S., and Japan Inc.(III) to offer higher capacity and reduced power per gigabit of served traffic [228, 229].

Infinera uses the latest technology to produce devices that consume less electricity and comply with standards such as EU, WEEE, RoHS, and other global environmental regulations. To minimize O-E/E-O conversions and, thereby, reduce power consumption, Infinera integrates hundreds of optical functions into small-form photonic integrated circuits [230]. Lab demonstrations show that Infineras 400 Gbps Photonic Integrated Circuits (PICs) consume approximately 50% and 80% less power compared to today's 100 Gbps and 40 Gbps PICs [230].

While most vendors try to minimize power consumption by integrating optical and electronic technologies in their devices, a few others explore traffic engineering, power-aware networking, and load-adaptive operation approaches in their search for alternative solutions. Some examples of such efforts are explained below.

Fujitsu, a top-tier network device manufacturer, reported in 2010 that their market-leading FLASHWAVE 4500/9500 Multi-service Provisioning Platform (MSPP)/Packet Optical Networking Platform (Packet ONP) meets the standards defined by the Telecommunications Energy Efficiency Ratio (TEER) metric [231]. Furthermore, in 2012, Fujitsu developed two tech-

nologies, 'flexible optical node' and 'spectrum de-fragmentation technology', which allow the backbone network architecture to be dynamically altered (using power-aware networking ), as needed, to increase resource utilization and minimize power consumption by eliminating unnecessary network devices [232].

MRV is another network device manufacturer who ensures that its products adhere to standards defined by the TEER metric [233]. Using traffic engineering and power-aware networking approaches, the MRV LambdaDriver aggregates and transmits outgoing traffic via a reduced number of links and de-activates under-utilized links to reduce electricity consumption.

Huawei has begun to utilize power-aware networking and load-adaptive operation to develop power-efficient network solutions. In a more recent report, Huawei suggests that, to maximize power savings, a device has to operate in normal, idle, or battery modes as decided by the traffic flow. In collaboration with telecommunication operators from Spain, the United Kingdom, and Germany, Huawei performed a series of successful field trials for the realization of hybrid transport mechanisms using 10 Gbps, 40 Gbps, and 100 Gbps MLR [234].

Cienna uses its expertise in multi-layer switching, bandwidth-sharing, and high line-rate transmission to design and develop next-generation, power-efficient backbone networks. Using experimental results, in 2013, Steve Alexander, the Vice President and Chief Technological Officer of Cienna, demonstrated that MHB grooming is more effective in reducing power consumption than both NB and DB grooming schemes when traffic is transmitted using 10/40/100 Gbps SLRs [235]. Cienna's 10/40/100 Gbps coherent optical interfaces help COMCAST, one of America's largest Internet service providers, to increase power efficiency by reducing the number of network devices and optical regenerators [236].

### **2.7.3 Summary of approaches adopted in real networks**

In this section, we presented examples of real-life, industry application of the four main approaches discussed in this survey. Although the academic literature has not provided evidence of the utilization of the four approaches by carriers/operators in real networks, we were able to scour online resources to find evidence of vendors who incorporate one or more approaches in manufacturing their devices and carriers/operators who utilize such devices.

Vendors, operators, and researchers agree that the integration of optical and electronic technologies, which is a concept examined under the network redesign approach, is the most effective method to date in reducing power consumption. As a result, next-generation network

---

devices are produced by heavily integrating electronic and optical components. In addition, traffic engineering is often preferred as a method of increasing device utilization and promoting optical bypass. As previously discussed, new-generation core routers are capable of aggregating a large amount of traffic into fewer lightpaths. Finally, using field trials and experiments, vendors adopt MLR in backbone networks to increase resource utilization and reduce power consumption. To maximize power savings, next-generation devices are also designed to operate in multiple power modes.

## 2.8 Conclusion

Reducing power consumption of the backbone network is critical to the growth of the Internet. As of recent, we have observed a surge in the number of studies on reducing power consumption of the Internet's backbone network. However, in order to develop new energy-efficient architectures and mechanisms, it is first essential to develop a sound understanding of existing frameworks. This chapter aimed to provide a comprehensive review of the relevant literature by examining four main approaches to reduce power consumption of backbone networks.

We categorized the main power-reduction techniques used in the literature into four main approaches, namely, network redesign, traffic engineering, power-aware networking, and load-adaptive operation. We discussed the results of individual studies and compared the potential of their solutions to offer power savings against their inherent limitations. Our survey shows that integrating individual concepts across approaches offers promising results for the generation of power-efficient backbone networks. Lastly, we explained how particular solutions within each approach are currently adopted in real-life projects and devices by device manufacturers and network carriers.

First, this chapter showed that power-hungry electronics of backbone networks are gradually being replaced by all-optical devices. It is therefore envisioned that traditional PtP-WDM networks would be eventually replaced with OCS and OBS and networks in the near future. However, at present, translucent core nodes that rely on hybrid technology provide the most power savings. Wavelength grooming performed by the core router of translucent core nodes, plays a critical role in increasing bandwidth utilization and reducing power consumption. Yet it is unclear if translucent core nodes should be placed at all core node sites. Instead, the question that needs to be asked is *can more power be saved by placing core routers at few core node sites*

*while allowing other core node sites to remain all-optical?*. This question serves as research problem 1 in this thesis.

Second, this chapter revealed that physical topology optimization is advantageous in reducing cost and power consumption of next-generation backbone networks. While cost benefits are evaluated in many studies, only a handful of studies use physical topology optimization to reduce power consumption. On the other hand, power-aware networking approaches are heavily scrutinized in the context of power savings, and yet their cost benefits are not evaluated. How these two approaches would compare against each other in terms of cost and power consumption reduction is an important research problem that we seek to solve in this thesis. We also intend to find out *how much power can be reduced by using novel physical topology optimization techniques and power-aware networking approaches, individually or jointly*. This concern serves as research problem 2 in this thesis.

Third, we understand that many researchers believe waveband grooming to have a minimal effect on reducing power consumption. However, as discussed in Section 2.4, this belief only appears to be valid if I/O ports consume a negligible amount of power and MG-OXC are not provisioned with wavelength converters and regenerators. Considering recent advancements in all-optical technology reported in Chapter 2.3, we expect MG-OXC to be provisioned with all-optical wavelength converters and regenerators in the near future. Furthermore, as explained in Section 2.4, I/O ports do consume a certain amount of power. Indeed, it is then important to quantify the power savings of a BSN that utilizes advanced MG-OXC equipped with all-optical devices. It is also important to find out *how various design parameters (e.g., grouping scheme, band size) can be fine-tuned to increase power savings of a waveband switched OCS network*. These concerns serve as research problem 3 in this thesis.

Fourth, we discussed in this chapter that much-needed proportionality in the relationship between power consumption and network traffic can be achieved by deploying rate-adaptive networks and transponders with MLR or ALR. Although MLR and ALR show excellent results in reducing power consumption over SLR when applied in traditional wavelength switched OCS networks (i.e., WSNs), neither MLR nor ALR have been implemented in BSNs to reduce power consumption. Previously, a few studies demonstrate that MLR-based BSN offers cost benefits over SLR-based BSN [237, 238]. However, they did not compare *power consumption* of MLR-based BSN with SLR-based BSN or SLR-based WSN. *How wavebands with wavelengths of different line rates can be efficiently formed and reach limitations of multi-rate lightpaths be overcome to*

*reduce power consumption* are critical design problems of a MLR-based BSN. These issues serves as research problem 4 in this thesis.

Lastly, sleep-mode enabled OBS networks that combine core node redesign with power-aware networking have gained a considerable amount of attention in recent years. As reviewed in Section 2.5.4, researchers have proposed novel node architectures and burst assembly and burst releasing algorithms to reduce power consumption of sleep-mode enabled OBS networks. *How much more power can be reduced by extending and building on this past work by proposing novel algorithms* is the final important research problem 5 that is sought to be answered in this thesis.

---

# SPARSE GROOMING IN OCS NETWORKS

---

## 3.1 Introduction

Today, most backbone networks are classified as PtP-WDM networks [9]. In these networks, traffic traversing every core node is electronically processed by the core routers. As explained in Section 2.3.1 in the last chapter, high power consumption and capacity scaling issues are foreseen limitations of electronic core routers.

To reduce power consumption and to eliminate the capacity bottleneck of core routers, it is envisioned that core nodes will employ OXCs in place of core routers, transforming the backbone network from PtP-WDM to OCS [9], which is a step further in the evolution of backbone networks (see Figure 1.2). A-OCS and IP-OTN are two different implementations of an OCS network [11]. Figure 2.2b depicts how traffic is handled by core nodes of an A-OCS network, whose main limitation is the lack of grooming capability and resultant inability to utilize fiber bandwidth efficiently. Thus, an A-OCS network generally uses a higher number of optical fibers than a PtP-WDM network, and the cost and power consumption of these fibers are also expected to be higher.

To mitigate this drawback of the A-OCS network, IP-OTN employs hybrid core nodes (HCNs), as depicted in Figure 2.2c. Each HCN of an IP-OTN consists of an OXC and a core router. HCNs not only increase bandwidth utilization by grooming sub-wavelength traffic, but also reduce electronic processing and O-E/E-O conversions by serving pass-through traffic using optical devices. Thus, it is reasonable to assume that IP-OTNs consume less power than both PtP-WDM and A-OCS networks. Nonetheless, it is unclear if core routers need to be placed at all core node sites in the network to increase power savings. Core routers are expensive and consume a significant amount of power. In this chapter, therefore, we seek to reduce power consumption of an OCS network (specifically, IP-OTN), by selectively placing

---

core routers at core node sites, and provide a solution to research problem 1:

- How can core nodes be selectively equipped with core routers to minimize power consumption of an OCS network?

The remaining sections of this chapter are in the following sequence. First, we review the relevant literature in Section 3.2 and explain how our work differs from existing studies. Section 3.3 defines the general architecture of the backbone network, introduces the key devices, and explains the traffic model, grooming methods, power consumption model, and important assumptions. In Section 3.4, we present the problem that we intend to solve in this chapter and the algorithm developed is described in Section 3.5. The proposed algorithm is used to solve the problem and the results are evaluated in Section 3.6. The key results are summarized in Section 3.7.

## 3.2 Overview of relevant work

In much of the previous work, IP-OTNs are considered to have full grooming capability. Thus, every core node is provisioned with a core router [239–241]. As of recent, many researchers argue that provisioning core routers at every core node is infeasible [242, 243]. In order to determine which grooming nodes of a given IP-OTN are feasible to contain core routers, *sparse grooming algorithms* have been developed [244, 245]. Commencing with a network having full grooming capability or with a network having zero grooming capability, these developed algorithms selectively disable or enable certain core nodes to groom traffic. In [246], Zhu et al. formulated the problem using ILP and developed a heuristic to find the grooming nodes in a network with a static traffic matrix [246]. The sparse grooming algorithm developed in [243] by Wang et al. reduces cost by placing core routers at random locations using a dynamic traffic matrix. In [244], Shen et al. compare the cost of a network in which all core nodes have grooming or wavelength-conversion capabilities with a network in which only a sub-set of nodes have the grooming capability. In their most recent work [245], Shen et al. developed an algorithm to selectively enable a sub-set of core nodes to groom traffic and, thereby, reduce cost. The maximum number of grooming core nodes allowed in the network is a common input parameter of most developed algorithms [243, 244, 246]. However, in [247], Srinivasan et al. reduce cost by enabling just enough core nodes to groom traffic without limiting the maximum number of grooming nodes.

At the time this research was being undertaken, past research on sparse grooming, such as those mentioned above, mostly focus on maximizing cost benefits. There has also not been any recent work on this issue to the best of our knowledge. Hence, the work presented in this chapter is the first to investigate sparse grooming as a technique to reduce *power consumption* of an optical backbone network. The aim of this study is to reduce power consumption by selecting the best grooming sites of a given IP-OTN, thereby providing a solution to research problem 1.

### 3.3 Network model

Figure 3.1 depicts the general architecture of the full network that carries Internet traffic among users of a country. The access routers and core nodes are situated in different locations of the country. In Figure 3.1, the access routers and core nodes are interconnected by physical links that consist of optical fibers. Network traffic originates and terminates at the access routers. Access routers communicate with one another via lightpaths established between core nodes of the backbone network, and a lightpath is realized using wavelengths. The O-E/E-O interfaces of core and access routers are assumed to be capable of transmitting wavelengths over ultra-long-distances without the need to regenerate signals at intermediate nodes. Each optical fiber is also assumed to accommodate a fixed number of wavelengths.

#### 3.3.1 Traffic generation

As explained in [11,247,248], Internet traffic can be represented using the gravity model. The gravity model uses population and distance information in computing traffic between different locations. Traffic  $t_{sd}$  between two access routers  $s$  and  $d$ , which reside in two different population centres (i.e., inter-city traffic)  $i$  and  $j$ , respectively, is computed using Equation 3.1 below;

$$t_{sd} = \frac{k\mathcal{Y}_i\mathcal{Y}_j}{d_{sd}^\phi} \quad (3.1)$$

where  $\mathcal{Y}_i$  and  $\mathcal{Y}_j$  are the populations at population centres  $i$  and  $j$ , respectively. Notation  $d_{sd}$  denotes the distance between the two population centres. Exponent  $\phi$  is defined by traffic type.  $\phi$  is assumed to be equal to 2 in order to accommodate both voice and data type traffic [11,247,249]. Factor  $k$  is a constant that is chosen based on empirical traffic values and used to determine inter-city traffic [125].

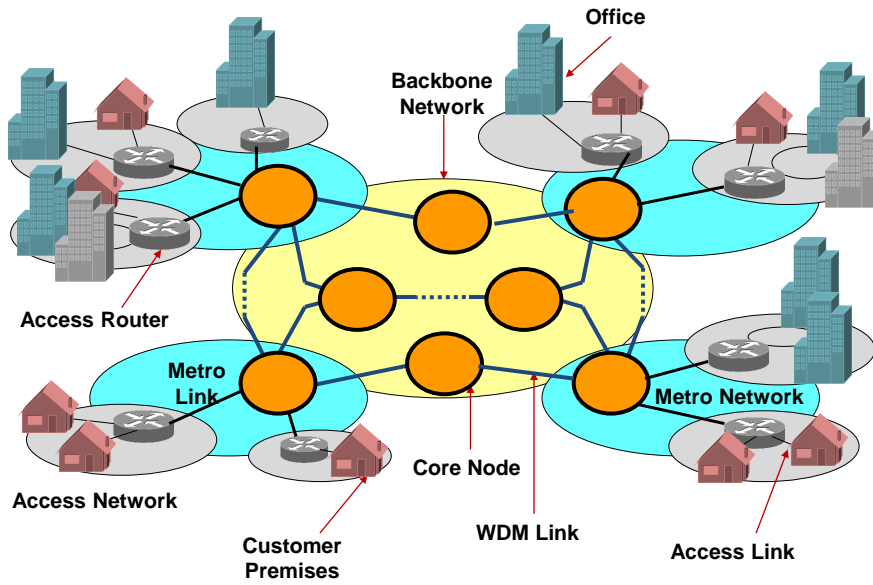


Figure 3.1: General architecture of the Internet

Traffic  $t_{sd}$  between access routers located in the same population centre  $i$  (i.e., intra-city traffic) is calculated using Equation 3.2.

$$t_{sd} = k_a \mathcal{I}_i^2 \quad (3.2)$$

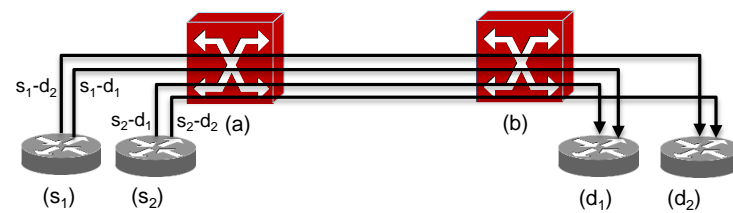
where,  $k_a$  is a constant found empirically [250] and is used to determine intra-city traffic.

### 3.3.2 Grooming procedure

In an IP-OTN, a core node is transformed into a *grooming node* by equipping it with a core router. Depending on the placement of the grooming core nodes, traffic sourced at the access routers can be accommodated via multiple wavelength channels.

If the network does not contain grooming nodes, sub-wavelength traffic between node pairs  $(s_1, d_1)$ ,  $(s_1, d_2)$ ,  $(s_2, d_1)$ , and  $(s_2, d_1)$  is accommodated via four end-to-end wavelength channels, as shown in Figure 3.2a. However, if node  $b$  is a grooming node, traffic to different access routers is groomed together. As shown in Figure 3.2b, traffic from the access routers of node  $a$  to the access routers of node  $b$  is then accommodated via 2 wavelengths. On the other hand, if node  $a$  is a grooming node, as shown in Figure 3.2c, traffic from the access router of node  $a$

to different destinations is groomed and transmitted together. Grooming node  $a$  grooms traffic according to the respective destination and accommodates the traffic along two wavelengths established between itself and the destination access routers. Finally, if both nodes  $a$  and  $b$  are grooming nodes, node  $a$  would groom incoming traffic, irrespective of the destination access router, and accommodate the groomed traffic via a single wavelength to the access routers of  $b$ , as shown in Figure 3.2d. Node  $b$  would then separate the incoming traffic and transmit them to the respective access routers.



(a) Without grooming nodes

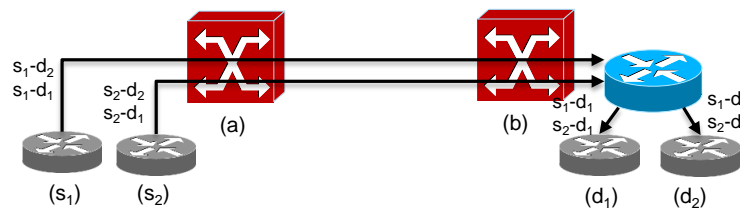
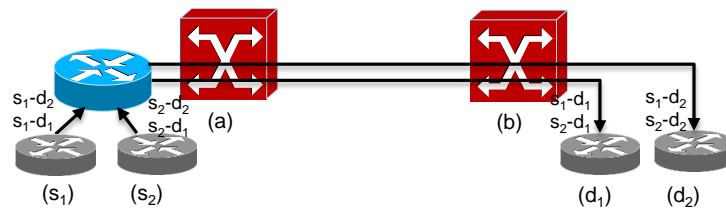
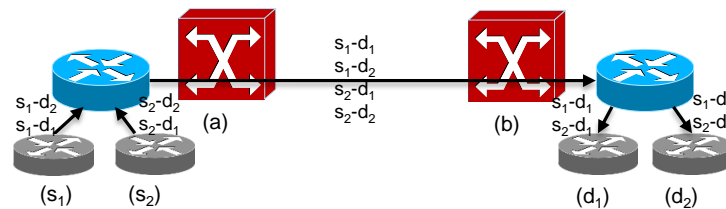
(b) Core router at node  $b$ (c) Core router at node  $a$ (d) Core routers at node  $a$  and  $b$ 

Figure 3.2: Example illustrating grooming performed at different core nodes

### 3.3.3 Power consumption

Power consumption of a backbone network is equivalent to the sum of power consumed by its core nodes and physical links. The values reported in Table 2.2 show that core routers and O-E/E-O interfaces (e.g., transponders, line cards) consume a significant amount of power. Core routers are assumed to be fully loaded, signifying that traffic processors and O-E/E-O interfaces are embedded within the core routers [93]. In contrast to fully-loaded core routers, OXCs are considered to consume a negligible amount of power by researchers [28, 149, 152] as well as in this thesis, specifically because they are not equipped with wavelength converters or regenerators. Therefore, power consumption of a core node is modelled in this thesis using only reported power consumption values of a fully-loaded Cisco CRS-1 core router.

Studies reveal that power consumption of a core router is dependent on the amount of traffic switched by it [8, 14, 18]. Hence, power consumption of a core router at node  $a$  ( $P_{c_a}$ ) is approximated as a function of the total switching capacity, which is defined in Equation 3.3 [13].

$$P_{c_a} = 4 \times \frac{\rho_a}{\psi} \times \Omega \quad (3.3)$$

In Equation 3.3, notation  $\rho_a$  denotes the amount of traffic switched by the core router of node  $a$ . Constant  $\Omega$  denotes power consumption of a fully-loaded core router when serving a maximum of  $\psi$  traffic. Factor 4, in front, is the product of:

- Factor of 2 to account for the power required for cooling [8],
- Factor of 2 to account for redundancy [8].

Each physical link has a fixed number of optical fibers, and each optical fiber accommodates a fixed number of wavelengths. To be able to serve traffic, the optical fiber needs to be equipped with terminal systems, PrAs and PoAs, and ILAs [8]. The number of fibers used to accommodate traffic across a link is strongly dependent on the number of wavelengths travelling through it. Therefore, a link that serves a large number of wavelengths will use more fibers which, in turn, will increase power consumption of the terminal systems, PrAs and PoAs, and ILAs. Therefore, power consumption of a physical link is closely related to the length and number of wavelengths travelling through it [13].

Following the work of [8, 13], we model power consumption of a physical link ( $P_{w_i}$ ) connecting nodes  $a$  and  $b$  using the reported power consumption of the Fujitsu Flashwave 7700

transport system [251] and the relationship defined in Equation 3.4.

$$Pw_i = 4 \times \omega_{ab} \times \Lambda \quad (3.4)$$

The parameter  $\Lambda$  is the cumulative power per wavelength channel [8]. Factor 4, in front, accounts for the power required for cooling and redundancy [8]. Notation  $\omega_{ab}$  denotes the number of wavelength channels passing through the link connecting nodes  $a$  and  $b$ .

### 3.4 Problem definition

The goal of this study is to reduce power consumption of an IP-OTN. To achieve this goal, we attempt to place core routers at selected core nodes. The initial network topology, depicted in Figure 3.3, does not contain grooming core nodes. By applying the proposed sparse grooming algorithm, we transform the initial network topology into an IP-OTN with sparse grooming, as shown in Figure 3.4. The inputs parameters, assumptions, and goal can be expressed in subsections 3.4.1, 3.4.2, and 3.4.3.

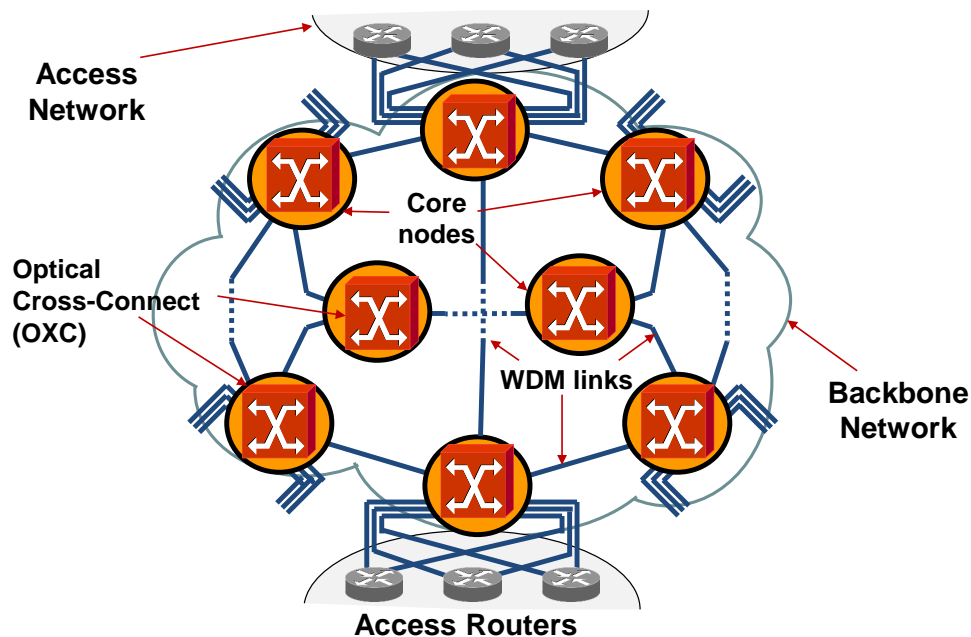


Figure 3.3: Initial topology of the network

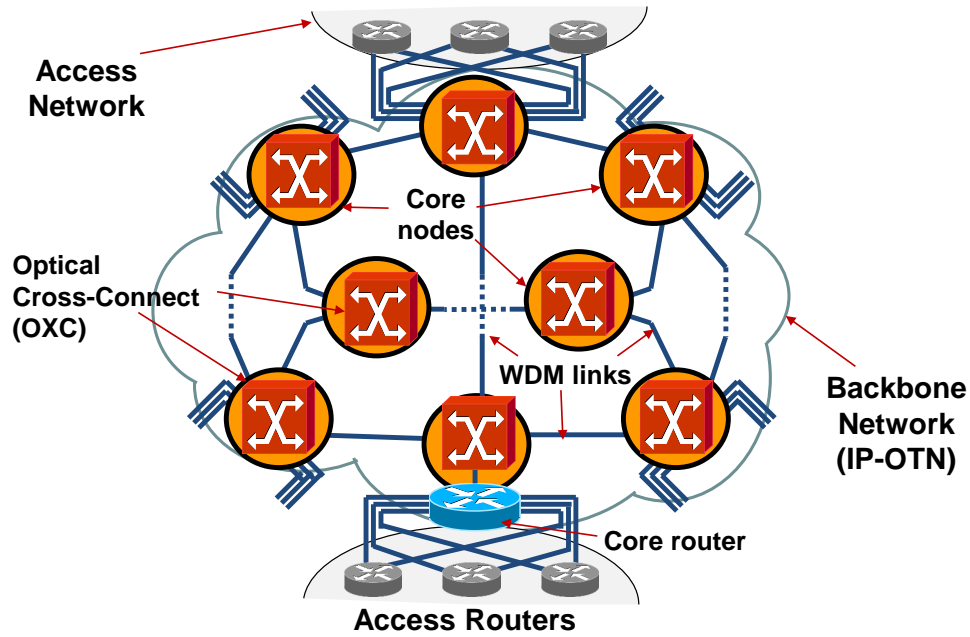


Figure 3.4: Final topology of the network containing a single grooming node

### 3.4.1 Inputs

- The physical topology  $G = (V, E)$  consists of  $V$  set of network elements (such as core nodes and access routers) and  $E$  set of physical links. The total number of access routers is denoted by  $N$  and the total number of core nodes is denoted by  $M$ .
- Each physical link carries  $F$  number of fibers and every fiber can accommodate a maximum of  $W$  wavelength channels. The maximum capacity of each wavelength is  $C$ .
- Traffic between access routers is represented by an  $N \times N$  static traffic matrix where, for example, the cell with traffic  $t_{sd}$  (located at row  $s$ , column  $d$ ) denotes traffic travelling from access routers  $s$  to  $d$ .
- The length of each physical link (e.g., link  $l_{ij}$ , connecting nodes  $i$  and  $j$ ) is known a-priori.

### 3.4.2 Assumptions

- As a static traffic matrix is assumed, the  $N \times N$  traffic matrix remains fixed for the entire optimization process.
- The OXCs cannot perform wavelength conversion, thus preserving the wavelength continuity constraint.

- Network topology is dimensioned and traffic routes are established and known a-priori. A path may exist between any two core nodes.
- Access routers and core routers can aggregate sub-wavelength traffic into fewer light-paths (i.e., grooming).
- Pass-through traffic is switched directly by the OXC at every intermediate core node.

### 3.4.3 Goal

- The goal is to produce a new topology  $G^* = (V^*, E)$ , where a subset of core nodes in  $V^*$  are equipped with core routers, while the links  $E$  remain identical to those of the initial topology  $G$ .
- Grooming nodes are placed at selected locations to minimize the combined power consumption of the core routers and physical links, as defined in Equation 3.5. Since OXCs consume a negligible amount of power in comparison to core routers and amplifiers, power consumption of the OXCs is not considered in Equation 3.5 [18,26,28].

$$\text{Minimize} \quad \sum_{\forall i \in V} P c_i + \sum_{\forall j \in E} P w_j \quad (3.5)$$

## 3.5 Methodology

Our proposed algorithm transforms an A-OCS network into an IP-OTN and determines the grooming nodes. The initial topology of the A-OCS backbone network that consists of access routers and OXCs is shown in Figure 3.5. The access routers connected to a core node are considered to be child elements of the respective core node. Traffic between access routers is generated using the gravity model described in Section 3.3.1. The traffic is exchanged between access routers via core nodes along the shortest path that is found using Dijkstra's algorithm. Wavelengths are assigned using the First Fit (FF) wavelength assignment scheme [252].

The pseudo code of the method that we use to determine the grooming nodes is presented in Algorithm 1. The initial network topology  $G$ , the traffic matrix generated using the gravity model, and the routing paths found using the shortest path algorithm are considered to be input parameters of the algorithm.

In the initial topology of the A-OCS backbone network, traffic between access routers is accommodated via end-to-end wavelengths. Power consumption of the A-OCS network with the

initial topology is calculated and saved as  $P_{\text{Init}}$ . The algorithm produces a search list ( $\text{OXC}_{\text{Set}}$ ) of every OXC in this initial topology.

From the search list  $\text{OXC}_{\text{Set}}$ , an OXC (e.g.,  $\text{OXC}_i$ ) is chosen and temporarily equipped with a core router. The links are re-connected and the network topology is updated. Depending on the placement of grooming node(s), sub-wavelengths are groomed to minimize the number of wavelengths, as explained in Section 2.4. Power consumption of the network ( $P_i$ ) is calculated and stored in the list  $P_{\text{OXC}}$  together with the respective OXC. The core router is then removed from  $\text{OXC}_i$  and the network topology is reverted to its previous state. This process is repeated with every OXC in the search list  $\text{OXC}_{\text{Set}}$ .

Next, the OXC that consumes the least power in the list  $P_{\text{OXC}}$  is selected and denoted as Sel-OXC (e.g.,  $\text{Sel-OXC} = \text{OXC}_j$ ). If the network consumes less power when Sel-OXC is equipped with a core router, the core node of Sel-OXC is permanently provisioned with a core router and  $P_{\text{Init}}$  is updated. The corresponding OXC of Sel-OXC (e.g.,  $\text{OXC}_j$ ) is then removed from the search list  $\text{OXC}_{\text{Set}}$ .

The above process is repeated until all OXCs in the search list ( $\text{OXC}_{\text{Set}}$ ) are evaluated or until the list  $P_{\text{OXC}}$  does not contain any OXC that consumes less power than  $P_{\text{Init}}$ .

### 3.6 Evaluation of results

To assess the effectiveness of the proposed method in reducing power consumption of an OCS backbone network, simulation-based experiments are performed on a small-scale network topology. The network topology, which is adopted from the work in [239,253], is generated for Australia. The network consists of 20 OXCs (i.e., core nodes) and 102 access routers. Every physical link is allotted 100 optical fibers ( $F = 100$ ) to prevent wavelength exhaustion. Each optical fiber supports up to 250 wavelengths ( $W = 250$ ). The inter-city and intra-city traffic constants  $k$  and  $k_a$  are assigned the values 40 and 10, respectively. The initial topology is depicted in Figure 3.5. Values assigned for the different parameters in Equations 3.3 and 3.4 are reported in Table 3.1. Table 3.2 summarizes the traffic between access routers situated at different locations in Gbps, which is generated using the gravity model.

Figure 3.7 plots the total power consumed by the OCS backbone network when a core router is placed at different core node locations. The x-axis represents different core node locations and the dotted red line indicates the power consumed by the backbone network when groom-

**Algorithm 1:** Grooming node selection

```

input : The initial topology  $G$ , traffic matrix, routing paths
output: The new topology  $G^*$ 

1 begin
2    $OXC_{Set} = \{\forall x \in V : x \text{ is an OXC}\};$  // Search list
3    $OXC_{Groom} = \text{empty list};$  // An empty list
4    $P_{Init} = \text{Power consumption of the initial network topology}$ 
   // Test all node locations
5   while  $OXC_{Set}$  not empty do
6      $P_{OXC} = \text{empty list};$ 
   // For every OXC in search list
7     for  $i \in OXC_{Set}$  do
8       Remove all links from the respective child elements of  $i$ ;
9       Attach a core router to  $i$ ;
10      Re-connect the respective child elements to the core router;
11      Update the topology;
12      Assign traffic and perform grooming;
   // Measure network power consumption
13      $P_i = \text{Network power consumption};$ 
   // Update  $P_{OXC}$ 
14     Append  $\{i : P_i\}$  into  $P_{OXC}$ ;
15     Remove the core router and re-connect the child elements to  $i$ ;
16     Revert the topology
17   end
   // Find the grooming node that reduces the power
   // consumption the most
18   Sel-OXC = OXC $_j$  with the smallest  $P_j$  found in list  $P_{OXC}$ ;
19   if  $P_j < P_{Init}$  then
   // Update the list  $OXC_{Set}$ 
20     Remove Sel-OXC from  $OXC_{Set}$ ;
   // Update the list  $OXC_{Groom}$ 
21     append Sel-OXC into  $OXC_{Groom}$ ;
   // Update network power consumption
22      $P_{Init} = (P_j)$ ;
   // update network topology
23     Attach the core router to Sel-OXC;
24     Update the topology  $G = G^*$ 
25   end
26   else
   // End while
27      $OXC_{Set} = \text{empty set};$ 
28   end
29 end
30 Return  $G^*$ 
31 end

```

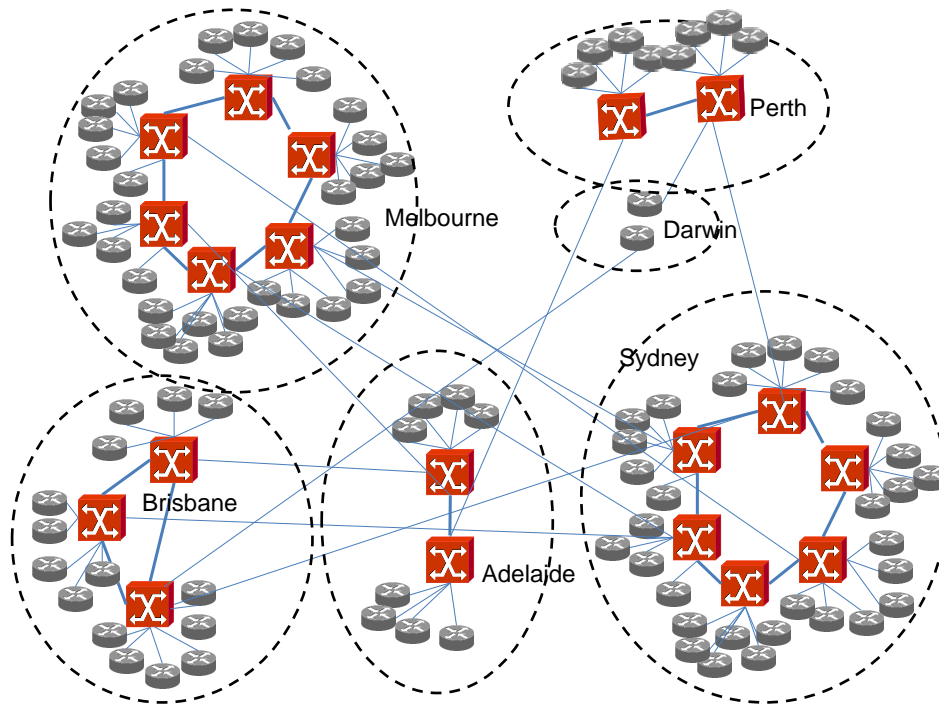


Figure 3.5: The initial network topology

ing nodes are not available. To obtain these results, Algorithm 1 repeats its process twice. At the end of the first iteration, a core router is placed at one core node in Perth. The second iteration results in another core router being placed at the second node in Perth. Algorithm 1 then exits and the resultant updated topology is shown in 3.6. It is observed from Figure 3.7 that the network consumes less power when core routers are attached to core nodes located in Perth. However, if core routers are placed at core nodes in any other city, an increase in power consumption is observed.

Table 3.1: Parameter values

Parameter	Value
$\psi$	640 Gbps [8]
$\Omega$	10.9 kW [8]
$\Lambda$	235 W [8]

The possible reason for the above outcome can be described using Figure 3.8 which depicts the power consumed by the core routers and the physical links, separately, at different

Table 3.2: Traffic between access routers of different cities (in Gbps)

	Sydney	Melbourne	Adelaide	Brisbane	Perth	Darwin
Sydney	122.75	738.96	102.36	416.68	13.16	1.04
Melbourne		99.90	309.08	95.76	16.56	0.92
Adelaide			10.12	23.96	8.24	0.45
Brisbane				22.71	5.04	0.56
Perth					13.82	0.48
Darwin						0.10

core node locations. Depending on the placement of the core router, physical links (denoted as WDM links) and core routers consume varying amounts of power. In general, power consumption of the backbone network is dominated by the physical links. Nevertheless, core routers consume a significant amount of power, especially when situated at core nodes in Melbourne and Sydney. Core nodes in Melbourne and Sydney have a higher degree of connectivity than those of other cities. As these two cities are located in close proximity to other cities, traffic between them and other cities travel a shorter distance. Therefore, reducing the number of wavelengths by grooming traffic at Melbourne and Sydney has only a limited impact on reducing power consumption of the physical links. Furthermore, as these cities are highly populated, they transmit and receive large amounts of traffic. Therefore, the grooming nodes of these two cities have to process a large amount of traffic and their core routers thus consume a significant amount of power. On the other hand, Perth is situated farther from other cities and generates less traffic. By placing grooming nodes in Perth, power consumption of physical links can be reduced considerably at the expense of only a slight elevation in core router power consumption.

Lastly, Figure 3.9 compares power consumption of the initial network and the final network modified by provisioning the core nodes in Perth with core routers. By placing grooming nodes in Perth, power consumption is minimized by 688 kW. Our findings, while preliminary, confirm that sparse grooming is indeed effective in reducing power consumption of an OCS backbone network. Interestingly, our findings that both core nodes located in Perth are grooming nodes are consistent with the cost-minimizing results of [239]. Thus, our algorithm can not only reduce power consumption but can also reduce network cost.

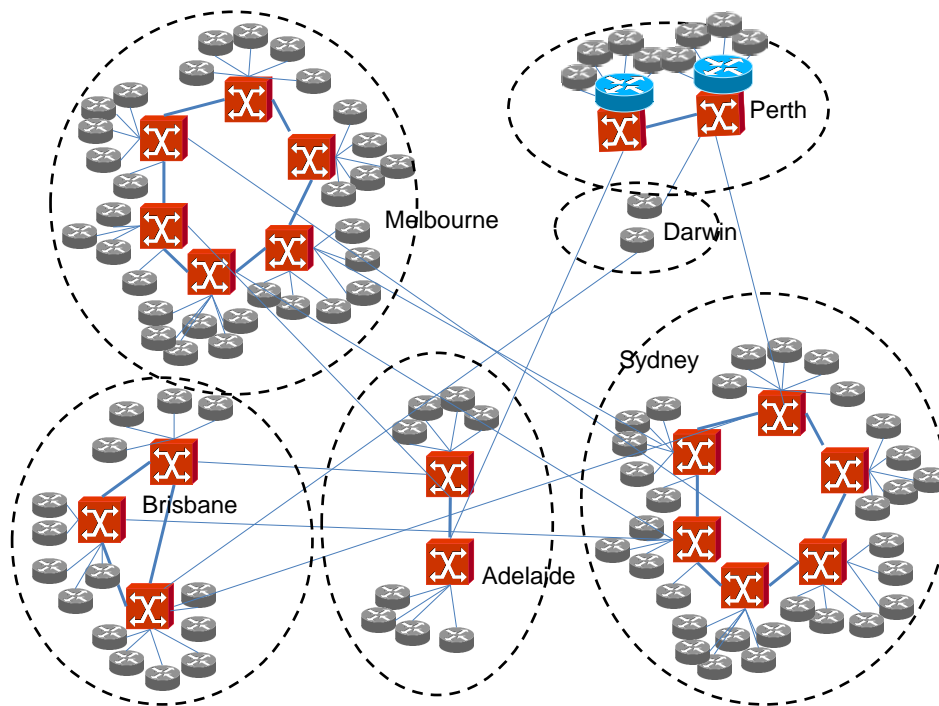


Figure 3.6: The resultant network topology

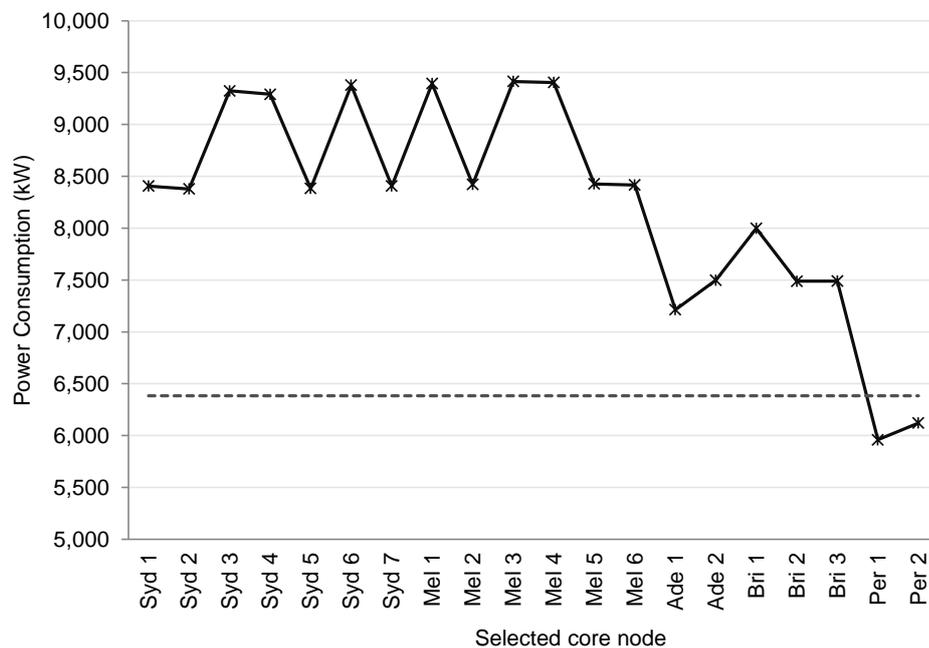


Figure 3.7: Power consumed by the network when core nodes in different locations are equipped with core routers

### 3.7 Summary of findings

All-optical core node technologies have achieved significant progress in recent years. However, HCNs that combine electronics with optical technologies are the preferred solution today. In

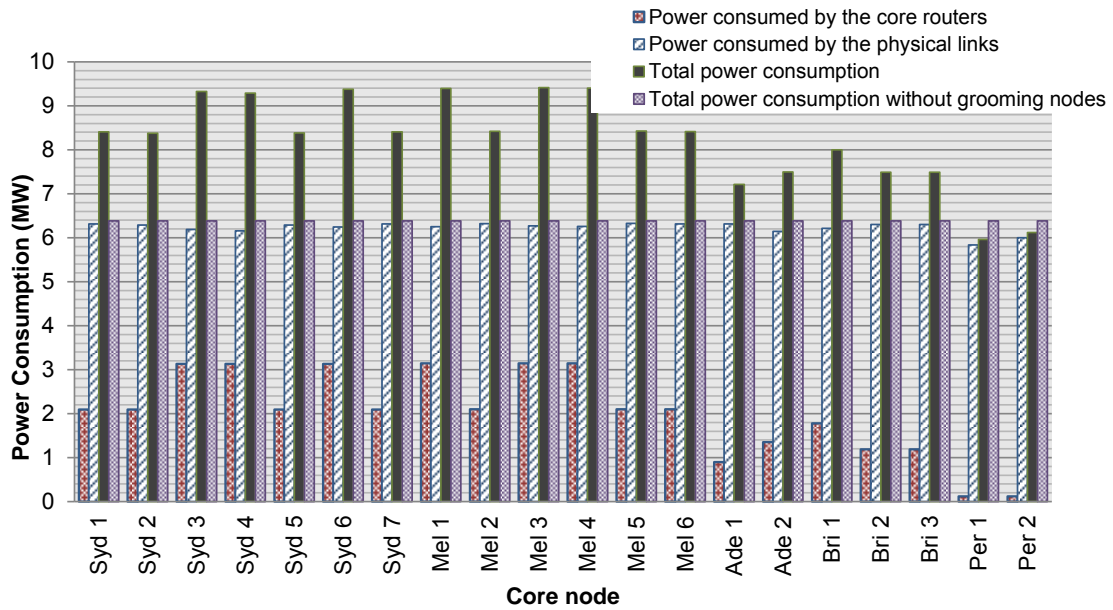


Figure 3.8: Power consumed by the core routers and physical (WDM) links with different grooming nodes

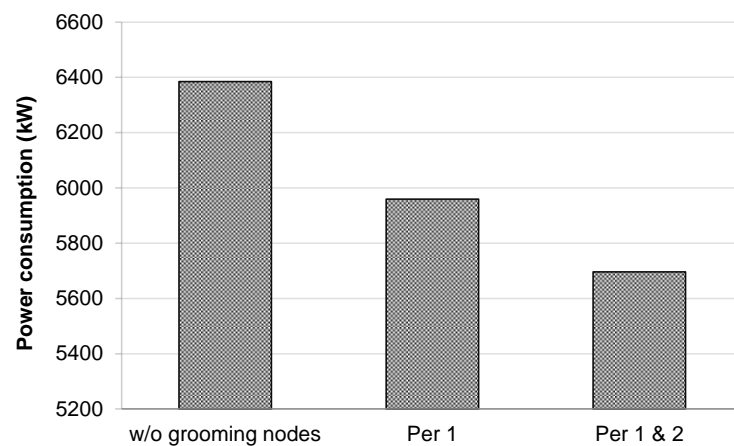


Figure 3.9: Total power consumption with and without grooming nodes

this chapter, we examined how power consumption can be minimized by appropriately provisioning all-optical and hybrid core nodes in a backbone network. Specifically, we were able to provide a solution to research problem 1 by identifying how much power could be reduced by selectively placing core routers at a subset of core node sites.

In an IP-OTN with full grooming capability, every core node consists of an OXC and a core router. A core node that is equipped with a core router is referred to as a grooming node. By provisioning grooming nodes, wavelength utilization is increased and traffic is transported using a minimum number of optical fibers. However, employing core routers at every core

node is infeasible, largely, due to cost constraints. Hence, researchers attempt to adopt sparse grooming in backbone networks. In this chapter, we propose and utilize a sparse grooming method to reduce power consumption of an OCS backbone network.

Most existing work on sparse grooming assumes that the number of grooming sites are known. Furthermore, most available studies evaluate cost, but not power consumption. The goal of this study was to identify and minimize the number of grooming nodes in an IP-OTN, thereby reducing power consumption. To achieve this goal, we formulated a method which is expressed as a heuristic algorithm. The proposed algorithm could be applied by future researchers to identify grooming nodes of a given IP-OTN.

Furthermore, we evaluated the performance of our algorithm by performing an experiment on an IP-OTN that interconnects core nodes located at different cities in Australia. The resultant network contains two grooming nodes and consumes approximately 688 kW less power than the initial network which does not have any grooming nodes. If sparse grooming is adopted, an IP-OTN will consume less power than an A-OCS network. However, if full grooming is adopted in an IP-OTN, our results show that an A-OCS network would consume less power than an IP-OTN.

In this chapter, we demonstrated that power consumption of the backbone network can be reduced by modifying core nodes. In the next chapter, we investigate how both power consumption *and* cost can be reduced by modifying physical links and their capacities following network traffic dynamics.

---

# TRAFFIC-DEPENDENT LINK OPTIMIZATION

---

## 4.1 Introduction

Increasing numbers of Internet users and bandwidth-intensive services dictate the growth of global Internet traffic. Rising traffic is driving the demand for more advanced high-capacity switching and transmission devices. These high-capacity devices are expensive [254] and consume a considerable amount of power [18]. Thus, network operators not only have to invest billions of dollars at the deployment stage of large-scale backbone networks [255], but also have to bear heavy operational costs. Network operators, therefore, find it increasingly important to reduce cost and power consumption of backbone networks in order to earn higher revenue and net profit.

As discussed in Sections 2.3 and 2.5 of Chapter 2, solutions using network redesign and power-aware networking approaches have been developed separately in a number of studies to reduce either cost or power consumption. Only a handful of researchers attempt to jointly reduce cost and power consumption using either approach [23, 119]. Furthermore, to date, no comparison has been undertaken between network redesign and power-aware networking approaches in terms of their potential for reducing cost and/or power consumption. In this thesis, we seek to address this gap in the literature by examining the cost and amount of power that can be reduced in a survivable OCS backbone network by using each of the two approaches. In doing so, we are able to provide solution(s) to research problem 2:

- How much electricity and cost can be reduced in an OCS network by appropriately configuring physical links (i.e., WDM links)?

The deployment cost or CAPEX of a backbone network is generally dominated by the labour cost associated with laying conduits (i.e., physical links) underground [24, 25]. To re-

duce recurring labour costs, an excessive number of optical fibers are installed in every conduit at the deployment stage [24,256]. To transport traffic, a requisite number of optical fibers are activated by equipping them with electronic devices like amplifiers) [256]. Inactive or spare fibers in every link are referred to as 'dark fibers' [24,25,256]. According to Ferreira et al. [25], network devices, with the exception of optical fibers, have an economical life span of five years. It is, therefore, natural to over-provision network devices to accommodate peak traffic demands of the future. While a certain level of over-provisioning is needed to ensure smooth network operation during traffic fluctuations and device failure, excess over-provisioning could result in increased cost and power consumption.

CAPEX can be reduced by dimensioning the network with a minimum number of conduits and optical fibers and fewer electronic devices. On the other hand, power consumption, and resulting OPEX, can be reduced by switching off redundant electronic devices [169,170].

Combining physical topology redesign and power-aware networking approaches, in this study, we seek to reduce the CAPEX of a backbone network by developing two strategies, namely, Incremental Strategy (IS) and Greenfield Strategy (GS). The proposed IS and GS heuristics reduce cost by combining physical topology redesign and power-aware networking approaches in different sequences. Power consumption of the dimensioned network is reduced using proposed the Multi-Objective (MO) algorithm. The IS and GS heuristics and the MO algorithm are explained, in detail, in Section 4.5. It is assumed in this study that core node locations are fixed and that core nodes remain active at all times [174,179].

## 4.2 Overview of relevant literature

In [118], Dong et al. reduce power consumption of the backbone network by configuring its physical topology. The power consumption minimization problem is modelled and optimized using an ILP formulation. However, the proposed optimization method can only produce significant power savings over the original network when traffic is processed at every core node (i.e., non-bypass (NB)). Moreover, the network optimized with the proposed scheme incurs a higher cost than the original network when traffic is distributed symmetrically. When calculating cost, Dong et al. do not take into account the conduit-laying cost. Furthermore, the proposed ILP-based optimization scheme cannot be used to reduce power consumption or cost of a *survivable* backbone network. Survivability is an important QoS parameter that needs to

be considered as the term 'survivable' describes a backbone network that is resilient against single-link failure.

Carmello et al. attempt to simultaneously minimize cost, blocking probability, and power consumption by configuring the physical topology and node capacities in [119]. To achieve this objective, a multi-objective evolutionary algorithm is proposed [119]. Cost and power consumption are measured using normalized values instead of actual values of respective network devices. The proposed algorithm generates a range of network solutions, some of which succeed in reducing cost and power consumption, although at the expense of high blocking probability [119]. However, the study considers neither network survivability nor traffic fluctuations.

With respect to hourly traffic variations [165], network devices are efficiently utilized during periods of peak traffic and underutilized during periods of low traffic [165]. Equipment utilization is thus estimated to be around 30-40%, on average, in large backbone networks [257]. When network traffic is low, underutilized devices continue to draw power. As advocated by many researchers [169–171, 174, 257], this unnecessary electricity waste can be reduced by switching off devices during low traffic periods. Taking heed of this advice, a number of different power-aware routing schemes [23, 257, 258] and capacity-dimensioning mechanisms [174,183] have been developed in recent years to reduce power consumption of backbone networks.

The Energy-Aware Routing and Wavelength Assignment (EA-RWA) algorithm proposed in [258] produces higher power savings over existing RWA schemes. Although the EA-RWA algorithm is believed to be capable of reducing cost [258], it is yet to be validated experimentally. Idzikowski et al. [23] reduce cost and power consumption by optimizing two separate objective functions using ILP formulations. The primary objective of their study is to reduce cost and power consumption of devices in both the IP and WDM layers. However, conduits were not included in their developed ILP formulation [23]. Fisher et al. [257] combine ILP formulations with simple heuristics to reduce power consumption of realistic, large backbone networks.

Despite this body of research on *non-survivable* networks, prior studies have not proposed or developed solutions to reduce the cost of *survivable* networks. Moreover, as routing paths need to be assigned intelligently, the proposed power-aware routing schemes in [23, 257, 258] cannot be implemented using conventional RWA schemes (e.g., shortest-path routing and first-

fit wavelength). As such, their solutions are complex and can only be solved using high-performance computer clusters and servers.

As previously discussed in Section 2.4, by grooming sub-wavelength traffic into fewer light-paths, a backbone network can serve traffic via a reduced number of active fibers. In [130], after providing the relevant mathematical model, the authors reduce power consumed by optical fibers using a heuristic algorithm that combines traffic grooming with power-aware routing. Their results show that an optical bypass strategy, implemented using DB or MHB grooming schemes, significantly reduces power consumption over the NB grooming scheme. Nevertheless, the study neither considers network survivability nor traffic variations. Moreover, the proposed algorithms cannot be used as a tool to dimension the physical link topology to reduce cost.

Capacity dimensioning is an intriguing approach to reduce power consumption. Beginning from the pioneering work in [259], a number of different capacity dimensioning solutions were developed in [252,260,261] to reduce network cost. In these studies, network cost is reduced by minimizing the number of active fibers. In [259] and [261], active fibers are reduced by optimizing the proposed ILP formulation in both survivable and non-survivable networks with and without wavelength conversion capabilities. In [252,260], the proposed heuristic algorithm exploits different combinations of routing (Shortest Path Routing (SPR) and Least-Loaded Path Routing (LLPR)) and wavelength assignment schemes (First-Fit (FF) and Most-Used (MU)) to reduce the number of active fibers. However, these studies reduce neither cost of conduits nor power consumption.

Capacity dimensioning is often performed using heuristic approaches [174,183]. The key advantage of heuristic-based capacity dimensioning over power-aware routing schemes is that the former is less complex and can be implemented using simple RWA schemes. In [183], the authors propose heuristic algorithms to identify and switch off nodes and active fibers during periods of low traffic. Using an iterative process, core nodes and active fibers are switched off according to the hourly traffic load. Similarly, in [186], Zhang et al. explore the possibility of switching off peripheral devices (e.g., line cards) of the core nodes during low traffic periods by grooming and re-routing traffic. However, the aforementioned work in [183,186] neither considers link resilience nor reduces network cost.

In [174], Coiro et al. developed a heuristic algorithm to reduce power consumption by dimensioning fiber capacity of the network according to a given traffic demand matrix. Their

results indicate that wavelength capacity of a fiber and the number of physical links/conduits in the network affect overall power consumption of the backbone network [174]. Although the proposed algorithm is shown to be effective in reducing power consumption [174], its impact on network cost is not evaluated. Furthermore, we believe that the proposed algorithms in [174] can be improved to provide higher power savings.

The novelty of the present study is its evaluation of cost and power savings that can be achieved in a survivable backbone network by using network redesign (specifically, physical topology redesign) and power-aware networking approaches while considering traffic variability. The main differences between relevant past literature and the present study are summarized in Table 4.1. In comparison to available solutions, the work proposed in this chapter can be adopted to reduce both cost and power consumption in survivable backbone networks using simple RWA schemes.

Table 4.1: Key differences between the present study and past research

Study	Objective: Reduce	Network	Solution	Approach
<b>Our study</b>	Pwr. cons. + Cost	Surv.	ILP + Heu.	Net. red. + P-awr. net.
Dong et al. [118]	Pwr. cons. + Cost	Non-surv.	ILP	Net. red.
Carmello et al. [119]	Pwr. cons. + Cost	Non-surv.	Heu.	Net. red.
Idzikowski et al., [23]	Pwr. cons. + Cost	Non-sur.	ILP	Net. red. + P-awr. net.
Maier et al., [259]	Cost	Surv. + Non-surv.	ILP	P-awr. net.
Miyao et al., [252,260]	Cost	Surv.	Heu.	P-awr. net.
Fisher et al., [257]	Pwr. cons.	Non-surv.	ILP	P-awr. net.
Konstantinos et al., [258]	Pwr. cons.	Non-surv.	ILP	P-awr. net.
Shen [130]	Pwr. cons.	Non-surv.	ILP	P-awr. net.
Zhang et al., [186]	Pwr. cons.	Non-surv.	ILP	P-awr. net.
Chiaraviglio et al., [183]	Pwr. cons..	Surv.	Heu.	P-awr. net.
Coiro et al., [174]	Pwr. cons.	Surv.	Heu.	P-awr. net.

**Note:** Pwr. cons. (Power consumption), Surv. (Survivable), Non-surv. (Non-survivable), Heu. (Heuristic), Net. red. (Network redesign approach) + P-awr. net. (Power-aware networking approach).

### 4.3 Network architecture

Figure 4.1 shows the considered architecture of the OCS backbone network. As described in Section 2.2 of Chapter 2, the WDM layer provides connectivity between core nodes (each consisting of a core router and an OXC) situated at different locations. OXCs are interconnected through physical links (i.e., conduits). Every physical link consists of multiple optical fibers. The node degree,  $N$ , of an OXC is the number of bi-directional fibers through which it connects to other OXCs [262,263]. A physical link can accommodate a maximum of  $F$  number of optical fibers. Each optical fiber can carry a maximum of  $W$  wavelengths. An activated optical fiber is equipped with ILAs and its ends are connected to a Terminal Unit (TU). As shown in Figure 4.1, a TU that comprises a multiplexer, demultiplexer, PrA and PoA serves 2 (input/output) fibers. To provide continuous amplification, ILAs are placed 80 km apart from each other on every optical fiber [174].

An optical fiber can support both bi-directional traffic (by bi-directional fibers) and uni-directional traffic (by uni-directional fibers) traffic. Inefficient capacity utilization and amplifier performance degradation are two main drawbacks of bi-directional fibers [264,265]. Hence, in the present study, the considered OCS network employs uni-directional fibers only. Two uni-directional fibers in opposing directions provide the service of a single bi-directional fiber. Unlike in Figure 2.1, the OXCs in 4.1 are not provisioned with wavelength converters. Thus, an end-to-end lightpath uses the same wavelength across multiple links (i.e., the wavelength continuity constraint).

#### 4.3.1 Network operations

Backbone network traffic can be modelled using either a static or dynamic traffic matrix [253, 266]. In this study, we deal with hourly traffic demands which are known a-priori. Thus, a static traffic matrix is considered in this study.

To accommodate a traffic demand (i.e., connection request) between two core nodes, an end-to-end lightpath(s) is established between them. A lightpath is routed along a logical circuit which comprises one or more physical links. Depending on the amount of traffic between a node pair, a lightpath may consist of one or more wavelengths. Wavelengths carrying pass-through traffic from incoming to outgoing fibers are switched by the OXC at the intermediate node. In the considered architecture, core routers and transponders process local add/drop

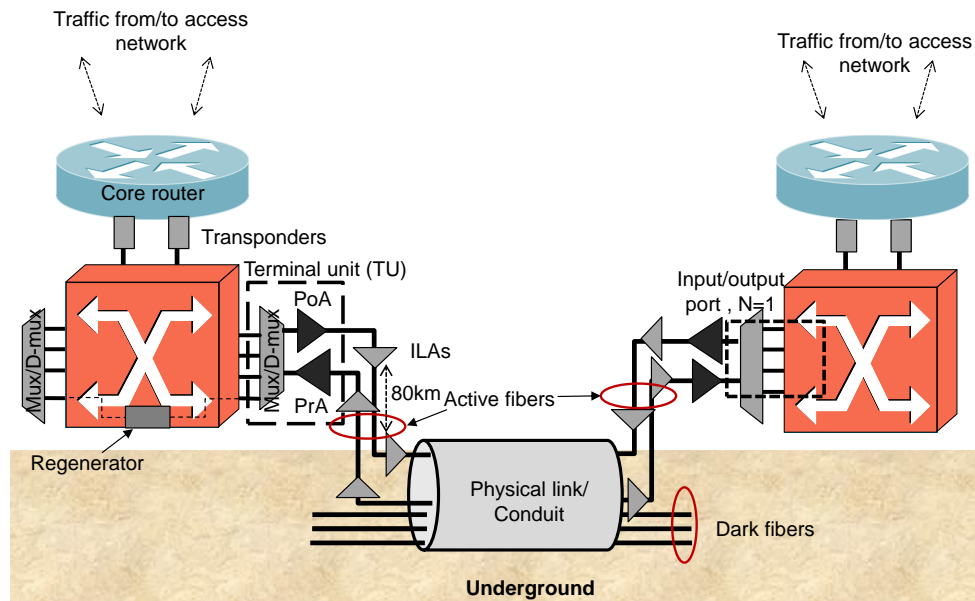


Figure 4.1: General architecture of the backbone network

traffic only. As a fixed amount of traffic flows between every node pair, core nodes remain switched on at all times [174, 179]. Therefore, the number and capacity of IP-layer devices cannot be optimized to reduce either cost or power consumption. Hence, in this study, we only seek to optimize WDM-layer devices.

Two important QoS constraints are considered in this work. First, transmission delay of every traffic demand needs to be minimal. Second, the network needs to be resilient against single-link failure (i.e., a survivable network). Transmission delay is measured in terms of the number of hops travelled by a lightpath. Reducing the number of hops is critical to lessen signal degradation that occurs due to crosstalk [267]. To reduce transmission delay (i.e., hop count), logical circuits or primary paths are established along the shortest routing path with sufficient bandwidth capacity. Note that every lightpath carrying traffic between a single node pair travels through the pre-defined single routing path only [23]. To provide protection against single-link failure, the primary paths are protected by link-disjoint backup paths [26]. Protection against link failure (i.e., link resilience) could be provided using either a dedicated-path protection scheme or a shared-path protection scheme. In this analysis, we use the shared-path protection scheme as it shows better performance in reducing the number of optical fibers [252, 260].

While routing is performed using the SPR algorithm, wavelengths are assigned using the simple, but effective, FF wavelength assignment scheme [268]. Traffic that travels to and from

two nodes also share the same shortest path. Although alternative routing algorithms, such as LLPR, are superior to SPR in the context of reducing traffic blocking, implementing algorithms like LLPR is much more difficult as it requires up-to-the-minute knowledge of the network state.

### 4.3.2 Power consumption of WDM-layer equipment

Power consumption values of devices in the WDM layer, adopted from [18,40,44], are reported in Table 4.2. Looking at these values, it is evident that regenerators consume the most power, while OXCs consume the least. As the number of switched-on regenerators is dependent on the transmission distance of traffic, power consumption of regenerators can be reduced by routing traffic demands via short paths. Power consumption of the TU and OXCs can be reduced by cutting down the number of switched-on active fibers. Depending on its length, each fiber is allotted multiple ILAs. Thus, minimizing the length of switched-on active fibers can reduce power consumption of the ILAs.

Table 4.2: Power consumption of network devices

Device	Power consumption (W)	Remarks
40-channel TU (per fiber-pair)	80 [44]	1 Multiplexer or Demultiplexer, 1 Pre-/Post-Amplifier (without overhead)
ILA (bi-directional)	52 [44,269]	Amplifier only (without management)
40 Gbps Rg (per wavelength)	150 [44]	A regenerator is assumed to consume less than twice the power of a 40 Gbps transponder [26]
OXC ( $N$ degree)	$N \times 20$ W	Based on an 80-channel Wavelength Cross Connect which has $N$ bi-directional fiber ports [44]

### 4.3.3 Costs of WDM-layer equipment

Costs of network devices, which are reported in Table 4.3, can be obtained from either the many available price models in the literature [25, 125, 162, 254, 270, 271] or the prices listed by vendors [272–274]. However, large discrepancies are observed between listed equipment prices,

partly because actual prices of network devices are often kept confidential and are subjected to different discount rates. Moreover, using quoted prices of different years to make a comparison is questionable. Therefore, in this study, we utilize a normalized price model derived from the work in [162, 254, 271]. Total expenditure of a fiber deployment project is dominated by the fiber-laying cost (e.g., cost of digging, obtaining approvals). This accounts for approximately 80% of the initial investment [24, 275], while only the remaining 20% is attributed to actual fiber cost. Hence, the cost of building a backbone network is the sum of the fiber deployment cost and total device cost.

Table 4.3: Normalized price model of network equipment

Device/Activity	Normalized cost (units) [162]	Remarks
Fiber (per km)	0.0125	Dispersion compensation fibers with 1500 km optical reach
Fiber-laying (per km)	2	Cost of laying a conduit consisting of 40 fibers
40-channel TU (per fiber-pair)	7.5	Includes 1 MUX/De-Mux, 1 PrA, 1 PoA, 2 Array Waveguides
Erbium-doped ILA (bi-directional)	2.77	Each EDFA is placed 80 km apart from each other
40 Gbps Rg (per wavelength)	7.24	Regenerates wavelengths at every 2000 km
OXC ( $N$ degree)	$N \times 6$	Based on an OXC built with Wavelength Selective Switch with $N$ bi-directional fiber ports.

#### 4.4 Problem formulation

The network optimization problem has two fundamental objectives. First, to minimize cost, reducing the number of physical links, active fibers, and electronic devices is desired. Second, to reduce power consumption, active fibers are required to be switched off according to traffic variation. The network optimization problem can then be represented in the following manner.

1. **Given** the physical topology, peak traffic demands of the foreseen future, hourly traffic demands, resource capacities, device costs, and power consumption,
2. **Find** the minimum number of *conduits, active fibers, electronics, and regenerators* needed to serve *peak traffic demands of the foreseen future* such that *cost* is minimized, and
3. **Find** the minimum number of *active fibers* that needs to remain *switched-on* to serve *traffic at an arbitrary hour* such that *power consumption* is minimized;
4. **Subject to** flow conservation, wavelength continuity and resource capacity constraints, and providing protection against single link failures.

In [174], Coiro et al. modelled the power consumption minimization problem of a backbone network that is resilient against link failure. However, power consumption of regenerators are not included in the developed model. Furthermore, the formulation does not constrain a traffic demand to a single working path. The ILP formulation presented in this paper is built on the foundation laid by [174]. While preserving the constraints defined in [174], we modify the objective function and include new constraints to achieve the two objectives of this study.

#### 4.4.1 Input parameters

- $G = (V, E)$  : Graph with  $V$  set of nodes and  $E$  set of links. Let  $N = |V|$  and  $L = |E|$  be the total number of nodes and the links in the network, respectively.
- $F$  : Maximum number of fibers installed in every physical link
- $W$  : Set of wavelengths in each fiber. Let  $\Lambda = |W|$  be the maximum number of wavelengths in every fiber.
- $R$  : Line rate of every wavelength in Gbps
- $s, d$  : Indices of nodes in the topology
- $sd$  : Connection request (i.e., traffic demand) between nodes  $s$  and  $d$ . Let  $P$  denote the set of all connection requests,  $sd \in P$ .
- $t^{sd}$  : Number of wavelengths carrying traffic of connection request  $sd$
- $l_{ij}$  : Physical link connecting nodes  $i$  and  $j$

- $|l_{ij}|$  : Physical length of link  $l_{ij}$  in km
- $\phi_{ij}$  : Number of ILAs along link  $l_{ij}$ , which is equal to  $\lceil |l_{ij}|/80 \rceil$ .
- $p^{sd}$  : Feasible working path (e.g., shortest routing path) for connection request  $sd$  (i.e., all links along  $p^{sd}$  are shorter than the optical reach of a lightpath with rate  $R$ ).
- $C_c$  : Cost of laying 1 km of conduit
- $C_f$  : Cost of a fiber per 1 km
- $C_{ILA}, C_{TU}, C_{OXC}, C_{RG}$  : Costs of an ILA, TU (2 TUs serve 2 fibers. Thus, 1 TU serves a single fiber), I/O port pair of an OXC, and Rg, respectively
- $E_{ILA}, E_{TU}, E_{OXC}, E_{RG}$  : Power consumption of an ILA, TU, I/O port pair of an OXC, and Rg, respectively

#### 4.4.2 Variables

- $\zeta_{ij}$  : 1, if there is a direct physical link between nodes  $i$  and  $j$ ; else, 0
- $K_{ij}$  : Number of active fibers in link  $l_{ij}$ , ( $K_{ij} \leq F$ )
- $r^{nsd}$  : 1, if connection request  $sd$  is required to be regenerated at node  $n$  (pre-calculated) when travelling along selected path  $p^{sd}$ ; else, 0
- $W_{ijkw}^{sd}$  : 1, if wavelength  $w$  of  $k^{\text{th}}$  fiber in link  $l_{ij}$  ( $0 < k < K_{ij}$ ) is used by the working path of connection request  $sd$ ; else, 0
- $P_{ijkw}^{sd}$  : 1, if wavelength  $w$  of  $k^{\text{th}}$  fiber in link  $l_{ij}$  ( $0 < k < K_{ij}$ ) is used by the protection path of connection request  $sd$ ; else, 0
- $x_{ijk}$  : 1, if  $k^{\text{th}}$  fiber in link  $l_{ij}$  ( $0 < k < K_{ij}$ ) is used by at least one connection request; else, 0
- $W_{ij}^{sd}$  : 1, if link  $l_{ij}$  is feasible on the working path of connection request  $sd$ , i.e., link  $l_{ij}$  is shorter than the optical reach of a lightpath with rate  $R$  and  $\zeta_{ij} = 1$ ; else, 0
- $P_{ij}^{sd}$  : 1, if link  $l_{ij}$  is feasible on the protection path of connection request  $sd$ ; else, 0
- $P_{ijkw}$  : 1, if wavelength  $w$  of  $k^{\text{th}}$  fiber in link  $l_{ij}$  is used by at least one protection path; else, 0

### 4.4.3 Objectives

#### Cost minimization (considering peak traffic demands of the foreseen future)

Minimize:

$$\begin{aligned} & \overbrace{\sum_{(i,j) \in V} (C_c \cdot \zeta_{ij} \cdot |l_{ij}|)}^{\text{Conduit-laying}} + \overbrace{\sum_{(i,j) \in V} [K_{ij} \cdot \zeta_{ij} (C_f |l_{ij}| + \phi_{ij} C_{ILA} + C_{TU} + C_{OXC})]}^{\text{Fibers + ILAs + TUs + OXCs}} \\ & + \overbrace{\sum_{n \in V, sd \in P} (C_{Rg} \cdot r^{nsd} \cdot t^{sd})}^{Rgs} \end{aligned} \quad (4.1)$$

#### Power consumption minimization (at arbitrary hour $t$ )

Minimize:

$$\begin{aligned} & \overbrace{\sum_{(i,j) \in V} [K_{ij} \cdot \zeta_{ij} (\phi_{ij} E_{ILA} + E_{TU} + E_{OXC})]}^{\text{ILAs + TUs + OXCs}} + \overbrace{\sum_{n \in V, sd \in P} (E_{Rg} \cdot r^{nsd} \cdot t^{sd})}^{Rgs} \end{aligned} \quad (4.2)$$

The set of objectives defined above is subject to a set of constraints, as defined in [174]. These include the wavelength continuity constraint, flow conservation constraint, and constraints on the installed devices. A set of additional constraints are formed to ensure that the network supports shared path protection. While preserving these existing constraints, we introduce the additional constraints below.

### 4.4.4 Constraints

The working and protection paths of the same connection request are path-disjoint. Therefore, as presented in Equation 4.3, link  $l_{ij}$  cannot be shared by the working and protection paths of the same connection request  $sd$ .

$$Wl_{ij}^{sd} + Pl_{ij}^{sd} \leq 1 \quad \forall (i, j) \in V, sd \in P \quad (4.3)$$

The working path of connection request  $sd$  and the protection path of connection  $s_1 d_1$  cannot use the same wavelength in the same fiber. This condition is described in Equation 4.4.

$$Wf_{ijkw}^{sd} + Pf_{ijkw}^{s_1 d_1} \leq 1 \quad (4.4)$$

$$\forall sd \in P, s_1 d_1 \in P, (i, j) \in V, w \in W, (0 < k \leq K_{ij})$$

Equation 4.5 constrains a wavelength in a fiber to be assigned to a single working path only.

$$\sum_{sd \in P} W f_{ijkw}^{sd} \leq 1 \quad \forall (i, j) \in V, w \in W, (0 < k \leq K_{ij}) \quad (4.5)$$

If protection paths of two different connection requests share a wavelength in a fiber, their working paths have to be link-disjoint. This constraint is presented in Equation 4.6.

$$W l_{ij}^{s_1 d_1} + W l_{ij}^{s_2 d_2} + P f_{i_2 j_2 k w}^{s_1 d_1} + P f_{i_2 j_2 k w}^{s_2 d_2} \leq 3 \quad (4.6)$$

$$\forall (i, j, i_2, j_2) \in E, w \in W, (0 < k \leq K_{ij})$$

Equation 4.7 guarantees that every node  $n$  is connected to at least two other nodes.

$$\sum_j \zeta_{nj} \geq 2 \quad \forall n \in V \quad (4.7)$$

The total traffic requirement of each connection request  $sd$  has to be satisfied along both the working and protection paths. These constraints are represented in Equations 4.8, 4.9, 4.10 and 4.11 below.

$$\sum_{j \in V, w \in W, (0 < k \leq K_{sj})} R \cdot W l_{sj}^{sd} \cdot W f_{sjkw}^{sd} = t^{sd} \quad (4.8)$$

$$\sum_{i \in V, w \in W, (0 < k \leq K_{id})} R \cdot W l_{id}^{sd} \cdot W f_{idkw}^{sd} = t^{sd} \quad (4.9)$$

$$\sum_{j \in V, w \in W, (0 < k \leq K_{sj})} R \cdot P l_{sj}^{sd} \cdot P f_{sjkw}^{sd} = t^{sd} \quad (4.10)$$

$$\sum_{i \in V, w \in W, (0 < k \leq K_{id})} R \cdot P l_{id}^{sd} \cdot P f_{idkw}^{sd} = t^{sd} \quad (4.11)$$

$$\forall sd \in P$$

Equations 4.12 and 4.13 impose the wavelength continuity and routing constraints on both

the working and protection paths.

$$\sum_{i \in V, (0 < k \leq K_{in})} W f_{inkw}^{sd} - \sum_{j \in V, (0 < q \leq K_{nj})} W f_{njqw}^{sd} = \begin{cases} -1 & \text{if } n = s \\ 1 & \text{if } n = d \\ 0 & \text{if } n \neq s, d \end{cases} \quad (4.12)$$

$$\forall sd \in P, n \in V, i \neq j, w \in W$$

$$\sum_{i \in V, (0 < k \leq K_{in})} P f_{inkw}^{sd} - \sum_{j \in V, (0 < q \leq K_{nj})} P f_{njqw}^{sd} = \begin{cases} -1 & \text{if } n = s \\ 1 & \text{if } n = d \\ 0 & \text{if } n \neq s, d \end{cases} \quad (4.13)$$

$$\forall sd \in P, n \in V, i \neq j, w \in W$$

Wavelengths of the connection request  $sd$  are allowed to travel along a single working path only. Therefore, links in the selected working path carry the total traffic  $t^{sd}$  of connection request  $sd$ , while other links do not carry traffic of the same connection request  $sd$ . This condition is represented in Equation 4.14. The same condition holds true for links along the protection path and is represented in Equation 4.15.

$$R \cdot \sum_{w \in W, (0 < k \leq K_{ij})} W f_{ijkw}^{sd} = \begin{cases} t_{sd} & \text{if } W l_{ij}^{sd} = 1 \\ 0 & \text{else} \end{cases} \quad \forall sd \in P, (i, j) \in V \quad (4.14)$$

$$R \cdot \sum_{w \in W, (0 < k \leq K_{ij})} P f_{ijkw}^{sd} = \begin{cases} t_{sd} & \text{if } P l_{ij}^{sd} = 1 \\ 0 & \text{else} \end{cases} \quad \forall sd \in P, (i, j) \in V \quad (4.15)$$

Equation 4.16 determines if wavelength  $w$  of fiber  $k$  is used by the protection path of one or more connection requests.

$$P_{ijkw} = \begin{cases} 1 & \text{if } \sum_{sd} P f_{inkw}^{sd} \geq 1 \\ 0 & \text{else} \end{cases} \quad \forall (i, j) \in V, w \in W, (0 < k \leq K_{ij}) \quad (4.16)$$

Equation 4.17 guarantees that the number of wavelengths used in a fiber  $k$  does not exceed the maximum fiber capacity  $\Lambda$ .

$$\sum_{w \in W} \left( \sum_{sd \in P} (W f_{ijkw}^{sd}) + P_{ijkw} \right) \leq \Lambda \quad \forall (i, j) \in V, (0 < k \leq K_{ij}) \quad (4.17)$$

Equation 4.18 ensures that the total number of fibers in a link does not exceed the maximum link capacity  $K$ .

$$K_{ij} \leq F \quad \forall (i, j) \in V \quad (4.18)$$

To solve the presented ILP formulation, a very large number of variables has to be optimized. For example, if  $|V| = 14$  and  $|E| = 21$  (e.g., as in the NSF network) and  $F = 10$  and  $W = 100$ , then the number of  $W f_{ijkw}^{sd}$ 's is  $14 \times 13 \times 14 \times 13 \times 10 \times 100 = 33,124,000$ . Therefore, finding an optimal solution to the presented ILP formulation becomes a difficult and computationally exhaustive task. Moreover, each connection request can be routed using different routing paths. If then, for every possible  $p^{sd}$ ,  $r^{nsd}$  has to be pre-calculated. The wavelength continuity constraint increases the complexity of the problem. Due to these reasons, the presented ILP formulation falls into the category of NP-hard problems. Hence, a heuristic approach is used in this study to reduce cost and power consumption of WDM-layer devices of an OCS network.

## 4.5 Heuristic algorithms

In this study, we reduce cost by dimensioning the network using the two heuristics introduced at the start of this chapter, namely, IS and GS. The two strategies use the proposed Link-Reducing (LR) and Multi-Objective (MO) algorithms in opposing sequence. Power consumption of the backbone network is reduced using the proposed MO algorithm only.

### 4.5.1 Link-Reducing algorithm

The primary objective of the LR algorithm is to dimension the physical link topology (i.e., link/conduit layout) to reduce cost and assure network connectivity in the occurrence of single-link failure. A dimensioned network is a two-connected graph.

In the past, researchers dimensioned the physical link topology by maximizing or minimizing an objective function [64, 119, 276]. In these studies, physical links are sequentially *added to*

or removed from the topology using an iterative process. In this study, a new topology is created by sequentially removing links from either an existing topology (as used in IS) or a full-mesh topology (as used in GS), which is defined by the LR algorithm presented in Algorithm 2. This algorithm too involves an iterative process. In each iteration, a link (e.g.,  $l_{ij}$ ) that maximizes  $O_{ij}$  in Equation 4.19 is removed from the topology, and traffic is re-routed along residual links.

**Algorithm 2: Link-Reducing (LR) Algorithm**

```

input : The initial topology  $G = (V, E_{Init})$ 
output: Conduit minimized topology  $G^* = (V, E_{New})$ 

1 begin
2    $O_f = [ ]$ ; // A list to store value of  $O_{ij}$  of every link
3    $E_{Temp} = [ ]$ ; // A list to store the links that are checked
4    $\beta = 1$ ; //  $\beta$  is 1 if  $G$  is two-connected, else 0

   // Until every link is checked
5   while  $|E_{Temp}| < |E_{Init}|$  do
6     for  $l_{ij} \in E_{Init}$  do
7       if  $l_{ij} \notin E_{Temp}$  then
8         Evaluate  $O_{ij}$  in Eqn. 4.19 with link  $l_{ij}$ ;
9          $O_{ij} \rightarrow O_f$ ; // Append  $O_{ij}$  into set  $O_f$ 
10      end
11    end
12    while  $O_f$  not empty do
13      Select the largest  $O_{ij}$  in  $O_f$ ;
14      Remove the corresponding link  $l_{ij}$  in  $G$ ; // Temp. update  $G$ 
15      Re-route traffic along shortest available path;
16      if  $\beta == 1$  then
17        Remove  $l_{ij}$  from  $E_{Init}$ ;
18        Update  $G$ ; // Perm. update  $G$ 
19         $l_{ij} \rightarrow E_{Temp}$ ; // Append  $l_{ij}$  into  $E_{Temp}$ 
20        Let  $O_f = [ ]$ ;
21      else
22        Re-instate link  $l_{ij}$  in  $G$ ; // Perm. update  $G$ 
23         $l_{ij} \rightarrow E_{Temp}$ ; // Append  $l_{ij}$  into  $E_{Temp}$ 
24        Remove  $O_{ij}$  from list  $O_f$ ;
25      end
26    end
27  end
   // Let ( $G^* =$  updated  $G$ ) and ( $E_{New} =$  updated  $E_{Init}$ )
28  Return  $G^* = (V, E_{New})$ 
29 end

```

To reduce cost, the network needs to be dimensioned with the minimum number of physical links. However, if the number of physical links in the network is reduced, traffic has to travel through longer routing paths. Consequently, a larger number of active fibers and regenerators

would be required to serve connection requests which, in turn, would increase network cost. Moreover, when a link is removed, respective traffic of the removed links has to travel along residual links. It would then be difficult to remove these residual links in subsequent iterations. To reduce the burden on residual links and minimize the distance travelled by network traffic, it is preferable to remove links that cause minimal re-routing. This is achieved by maximizing  $O_{ij}$  defined in Equation 4.19.

The objective function  $O_{ij}$ , defined in Equation 4.19, consists of two terms. By maximizing  $O_{ij}$ , the LR algorithm selects the link that reduces cost and minimizes re-routing. The first term maximizes the length of the selected link, while the second term ensures that the selected link causes minimal re-routing.

$$\text{Maximize } O_{ij} = \left( \frac{|l_{ij}|}{l_{\text{MAX}}} + \frac{P_{\text{MAX}}}{P_{ij}} \right) \quad (4.19)$$

where,

$|l_{ij}|$  = Physical length of link  $l_{ij}$ .

$l_{\text{MAX}}$  = Length of the longest physical link.

$P_{ij}$  = Sum of products of traffic (measured in wavelegths)

and their respective travelling distances in the absence of link  $l_{ij}$

$P_{\text{MAX}}$  = The maximum  $P_{mn}$  among all links

#### 4.5.2 Multi-Objective algorithm

The MO algorithm is used to reduce the number of active fibers and electronic devices. Not only can this algorithm be used to reduce cost but it can also be used to reduce power consumption. First, we selectively switch off active fibers by running the MO algorithm with peak traffic demand. To reduce cost, we dimension the network by removing switched-off fibers and attached electronics. To reduce power consumption, some of the active fibers are switched off during an arbitrary hour as dictated by the MO algorithm. Given the initial parameters  $G$ ,  $F$ , and  $W$ , and traffic matrix, the MO algorithm, presented in Algorithm 3, switches off active fibers (i.e., dimensions active fibers) one after another by re-routing traffic via the primary path (shortest path) or an alternative path (i.e., working path) along residual active fibers. To provide

resilience against single-link failure, primary and working paths are protected by link-disjoint backup paths.

In past studies, a number of sorting-based algorithms were developed to selectively switch off active fibers. In these algorithms, fibers are sorted according to a specific criterion, after which active fibers are switched off one after another. The sorting criteria used in these algorithms are:

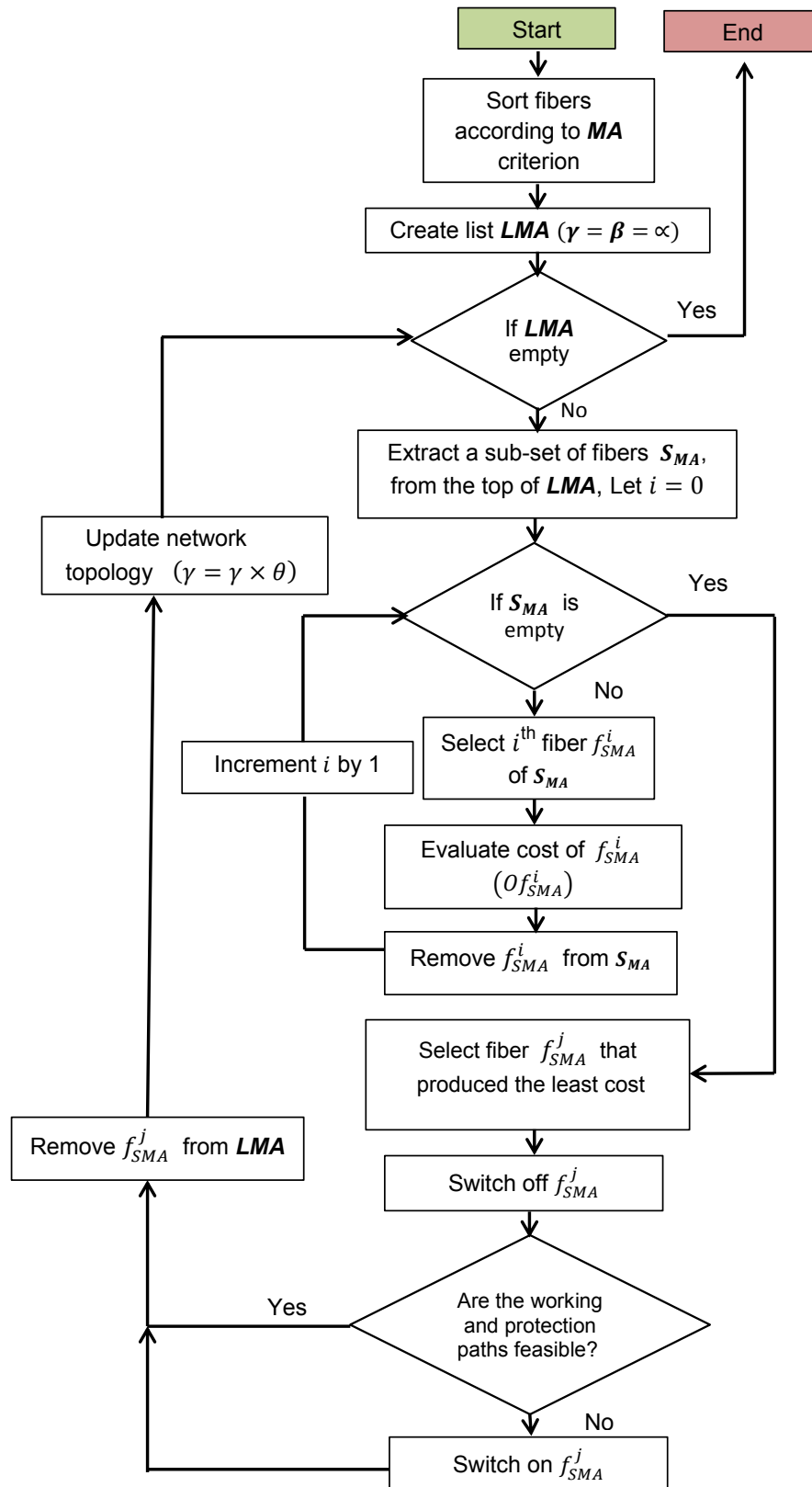
- *Least utilized fiber (LF)* [171,174]: fibers are sorted in increasing order of their utilization.
- *Most amplifiers (MA)* [171,174]: fibers are sorted in decreasing order of the number of ILAs along them which is proportional to the actual physical length.
- *Disjoint-path Power Savings Factor (DPSF)* [174]: fibers are sorted in descending order of the difference between the number of ILAs along the switched-off fiber prior to de-activation and the number of ILAs along the fibers of the updated backup path of the affected traffic after de-activation.

The three sorting-criteria-based algorithms each involve three stages. First, the algorithm sorts fibers in the current topology according to the selected sorting criterion. Second, a fiber is selected from the sorted list and is *temporarily switched off*. Third, using the selected RWA scheme, the algorithm checks if viable working and back-up paths exist for lightpaths of every traffic demand. If working and backup paths are found and wavelengths are available in the residual fibers, the selected fiber is *permanently switched off*. Else, the temporarily switched-off fiber is switched back on. These three steps are repeated until all fibers in the list are duly inspected. Lastly, the remaining fibers in the network are noted and relevant measurements are extracted.

Similar to these three stages of the above sorting-criteria-based algorithms, the MO algorithm proposed in this study involves three stages, namely, fiber sorting, fiber selection, and RWA.

- **Fiber sorting:** At the start of each iteration, active fibers in the network are sorted and listed according to the MA criterion. The list is named LMA. The MA criterion-based algorithm is helpful in selecting and switching off 'long fibers' (i.e., fibers containing a large number of ILAs). However, as shown in [174], the MA criterion-based algorithm switches off long fibers without affording any consideration to the amount of traffic they

Algorithm 3: Flow diagram of the MO algorithm



carry. When a fiber is switched off, its traffic has to travel through residual fibers. Consequently, if long fibers that accommodate a large amount of traffic are switched off in the first few iterations of the algorithm, it becomes difficult to switch off additional fibers as they would need to remain active to accommodate the network traffic. To overcome these drawbacks of the MA criterion-based algorithm, we employ the following multi-objective link-selection approach.

- **Fiber selection:** Starting from the longest fiber, a sub-set of fibers ( $S_{MA}$ ) having  $|S_{MA}|$  number of fibers is extracted from the list LMA. These extracted fibers in set  $S_{MA}$  are numbered and identified as  $f_{SMA}^1, f_{SMA}^2, \dots, f_{SMA}^n$ . The value of the objective function ( $O f_{SMA}^i$ ), defined in Equation 4.20, is evaluated for every fiber  $f_{SMA}^i \in S_{MA}$ . The fiber ( $f_{SMA}^j$ ) that produces the **least cost** is then selected to be switched off.

When switching off a particular fiber, it is advantageous if doing so would only pose a minimum burden on the remaining fibers. As fewer wavelengths can be easily accommodated along the remaining fibers, fibers that are less utilized less are first selected to be switched off. To reduce cost and power consumption, it is also necessary to switch off *long fibers*. Thus, when selecting a fiber to be switched off, it is essential to consider both physical length and fiber utilization. Taking these two factors into account, we propose the normalized objective function in Equation 4.20. By minimizing this objective, we select and switch off fibers from the list  $S_{MA}$  that contain more ILAs but carry less traffic.

$$O f_{SMA}^j = \left( \frac{a_{ILA}^{Max}}{\beta \times a_{ILA}^j} + \frac{\gamma \times n_{Lpaths}^j}{n_{Lpaths}^{Max}} \right) \quad (4.20)$$

, where

$a_{ILA}^{Max}$  = Number of ILAs along the longest fiber

$a_{ILA}^j$  = Number of ILAs along fiber  $f_{SMA}^j$

$n_{WL}^{Max}$  = Number of wavelengths along the most used fiber

$n_{WL}^j$  = Number of wavelengths through fiber  $f_{SMA}^j$

At the beginning of each iteration, the weights  $\beta$  and  $\gamma$  are adjusted accordingly. To

maximize power reduction, we first remove long fibers that carry fewer wavelengths.  $\beta$  and  $\gamma$  are assigned weights ( $\beta = \gamma = \alpha$ ) that give equal priority to physical length (i.e., the number of ILAs) and fiber utilization. As the algorithm progresses, it becomes difficult to remove additional fibers as residual fibers possess only limited capacity. Therefore, when evaluating the objective function in Equation 4.20, greater priority is given to fiber utilization than to the number of ILAs as the algorithm progress. Thus,  $\gamma$  is gradually incremented by a factor of  $\theta$  ( $\gamma_{\text{next}} = \gamma_{\text{previous}} \times \theta$ ) as shown in the flow diagram in Figure 3. This enables the algorithm to switch off long fibers without disrupting traffic flows. When assessing fiber utilization, traffic flows on both working and back-up paths are considered.

- **Routing and wavelength assignment (RWA):** We temporarily switch off the selected fiber  $f_{SMA}^j$ . If RWA is able to route all traffic demands via primary or working paths and protected by back-up paths, then the selected fiber ( $f_{SMA}^j$ ) is permanently switched off. Else, the selected fiber ( $f_{SMA}^j$ ) is switched back on. Next, fiber  $f_{SMA}^j$  is removed from the list LMA, the network is updated, and the algorithm is repeated with the residual fibers in the list.

### 4.5.3 Long Fiber Removal algorithm

The LFR algorithm is an extension of the MO algorithm. After optimizing the active fibers using the MO algorithm, LFR is adopted to switch off additional *long fibers*. The steps involved in the LFR algorithm are summarized below.

**Step 1:** Sort the residual fibers in the network according to the MA criterion. Denote this list as

$$\text{LMA}_2; (\text{LMA}_2 = [f_{\text{LMA}}^1, f_{\text{LMA}}^2, \dots, f_{\text{LMA}}^n]).$$

**Step 1.1:** Select the first fiber (e.g.,  $f_{\text{LMA}}^1$ ) of list  $\text{LMA}_2$ .

**Step 2:** Sort and list the physical links in decreasing order of their utilization. Denote this list

$$\text{LINKS}; (\text{LINKS} = [l_{ij}, \dots, l_{in}, \dots, l_{n-1,n}]).$$

**Step 2.1:** Starting from the most-utilized link in LINKS, extract a sub-set of links and append to list  $S_1$ ; ( $S_1 \subset \text{LINKS}$ ,  $|\text{LINKS}| \geq |S_1|$ ).

**Step 3:** Select the first link in list  $S_1$  (e.g., link  $l_{ij}$ ) and check if the physical length of the selected link (e.g.,  $|l_{ij}|$ ) is shorter than the length of the fiber (e.g.,  $|f_{\text{LMA}}^1|$ ).

**If true and list  $S_1$  is not empty :** temporarily switch off  $f_{LMA}^1$  and temporarily switch on an *additional fiber*,  $f_{ij}$ , in link  $l_{ij}$ . Proceed to **Step 4**.

**If false and list  $S_1$  is not empty :** remove link  $l_{ij}$  from list  $S_1$ , and repeat **Step 3**.

**If false and list  $S_1$  is empty :** proceed to **Step 6**.

**Step 4:** Check if all connection requests can be accommodated via working and backup paths.

**If successful:** then permanently switch off  $f_{LMA}^1$  and proceed to **Step 5**.

**Else:**

- $f_{ij}$  on link  $l_{ij}$  is switched off
- fiber  $f_{LMA}^1$  is switched on again
- link  $l_{ij}$  is removed from set  $S_1$
- proceed to **Step 3**.

**Step 5:** Update the number of switched-on fibers in the network and reset lists  $LMA_2$ , LINKS, and  $S_1$ . Repeat the entire process from **Step 1** until  $LMA_2$  is empty.

**Step 6:** Remove fiber  $f_{LMA}^1$  from  $LMA_2$ . Proceed to **Step 1.1** and repeat the process until  $LMA_2$  is empty.

#### 4.5.4 Incremental and Greenfield heuristic strategies

To reduce cost, physical links, active fibers, and electronics of the network need to be dimensioned appropriately. While the developed ILP formulation reduces cost by optimizing Equation 4.1, the proposed IS and GS heuristics reduce cost by performing two tasks using the LR and MO algorithms described above:

1. Task A: Dimensioning physical links.
2. Task B: Dimensioning active fibers and electronics (e.g., TUs, amplifiers, regenerators, etc.).

The GS heuristic performs Task A first and then performs Task B. By taking into account predicted peak traffic demands, to perform Task A, GS removes links successively from a fully-connected (full-mesh) physical topology ( $G$ ) using the LR algorithm. After dimensioning the

physical link topology, to perform Task B, GS applies the MO algorithm to switch off fibers. Switched-off fibers are removed from their respective link.

The IS heuristic performs task B first and then performs task A. By taking into account predicted peak traffic demands and the existing physical link topology  $G$ , to perform Task B, IS switches off redundant fibers using the MO algorithm and removes them from their respective link. After reducing the number of active fibers, IS performs task A using the LR algorithm. Links are selected and removed from the network in succession while maintaining network connectivity and resilience against link failures as well as accommodating all peak traffic demands.

## 4.6 Reducing deployment cost or CAPEX

Using simulation-based experiments, in this section, we assess the deployment cost (i.e., CAPEX) of a backbone network dimensioned separately with IS and GS heuristics. Additionally, we evaluate the average traffic transmission distance in IS- and GS-optimized networks.

### 4.6.1 Experiment environment

Simulation-based experiments are performed on the node set of the NSF network comprising 14 core nodes, located in different cities in USA, and 21 physical links [277,278]. Before dimensioning the network with either GS or IS, every physical link is assigned 6 active fibers ( $F = 6$ ). The CAPEX of this non-dimensioned NSF network is found to be equal to 35,256 units using Equation 4.1, the price model in Table 4.3 and parameter values from [277,278]. With IS, the initial network topology mimics the non-dimensioned network with 21 physical links. With GS, the initial network topology mimics a fully-connected topology consisting of 182 links.

Using IS and GS, the initial physical topology is dimensioned to serve projected peak traffic demands. Cisco predicts the total peak traffic of USA to be equal to 11 Tbps (28 Exabytes per month). This projected total peak traffic is distributed among core nodes by scaling the traffic matrix reported in [259]. SPR and FF wavelength assignment scheme are used to route traffic and assign wavelengths, respectively. Equations 4.1 and 4.2 are used to calculate cost and power consumption of the dimensioned networks, respectively.

An optical fiber can carry between 20 to 160 wavelengths ( $W = 20, 40, \dots, 160$ ). Therefore, experiments are repeated with different  $W$ . Figure 4.2 depicts the CAPEX or deployment cost

of the networks dimensioned with IS and GS for different values of  $W$ . Figure 4.3 shows the number of physical links and active fibers in the networks dimensioned with IS and GS. Total length of the links and active fibers is depicted in Figure 4.4. Lastly, power consumption and average transmission distance of the dimensioned networks are depicted in Figure 4.6 and Figure 4.5, respectively.

#### 4.6.2 CAPEX minimization

The plotted graph in Figure 4.2 shows that the network dimensioned with either GS or IS incurs a smaller CAPEX than the non-dimensioned NSF network. At all  $W$ , CAPEX of both dimensioned networks is less than 35,256 units of CAPEX of the non-dimensioned network. It is also evident that the network dimensioned with GS costs less than the network dimensioned with IS. Recall that total cost is determined by the sum of costs of physical links, active fibers, and devices attached to these fibers (e.g., TUs, OXC ports). However, deployment cost is dominated by the conduit-laying cost [24, 256].

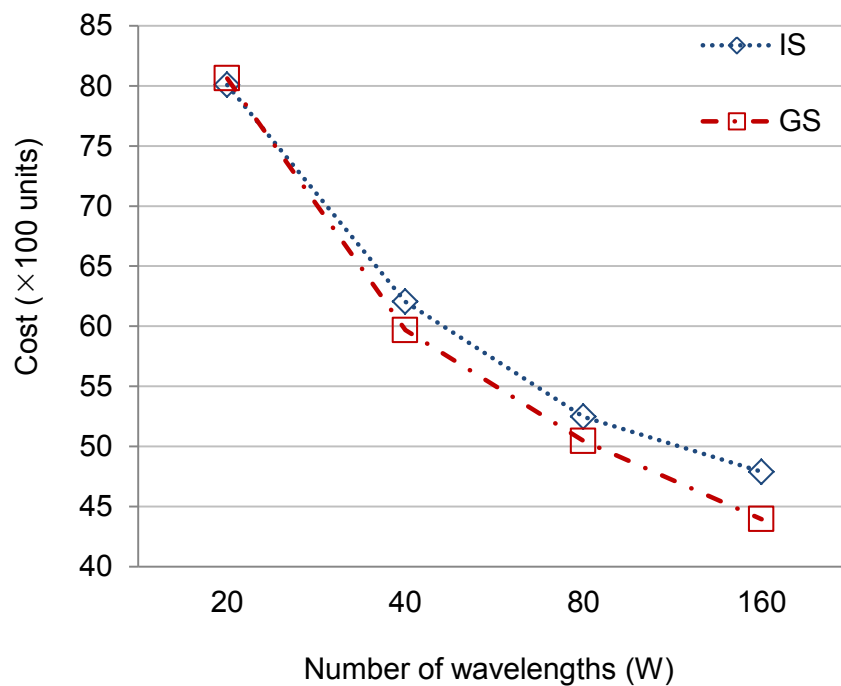


Figure 4.2: CAPEX against increasing  $W$

As depicted in Figure 4.3, the network dimensioned with GS provisions fewer physical links than the network dimensioned with IS. The difference in the number of physical links between the two dimensioned networks increases as  $W$  increases. Starting from a full-mesh topology

(182 links), GS reduces the number of physical links from 19 to 13 as  $W$  is increased from 20 to 160. As the number of physical links reduces, their total length decreases from 21,000 km to 13,500 km in the GS-dimensioned network, as shown in Figure 4.4. However, in the network dimensioned with IS, the number of physical links and their total length remain constant at 21 and 24000 km, respectively, at every value of  $W$ . It is then reasonable to argue that performing Task B prior to Task A (as the IS heuristic does) detracts from the utility of Task A.

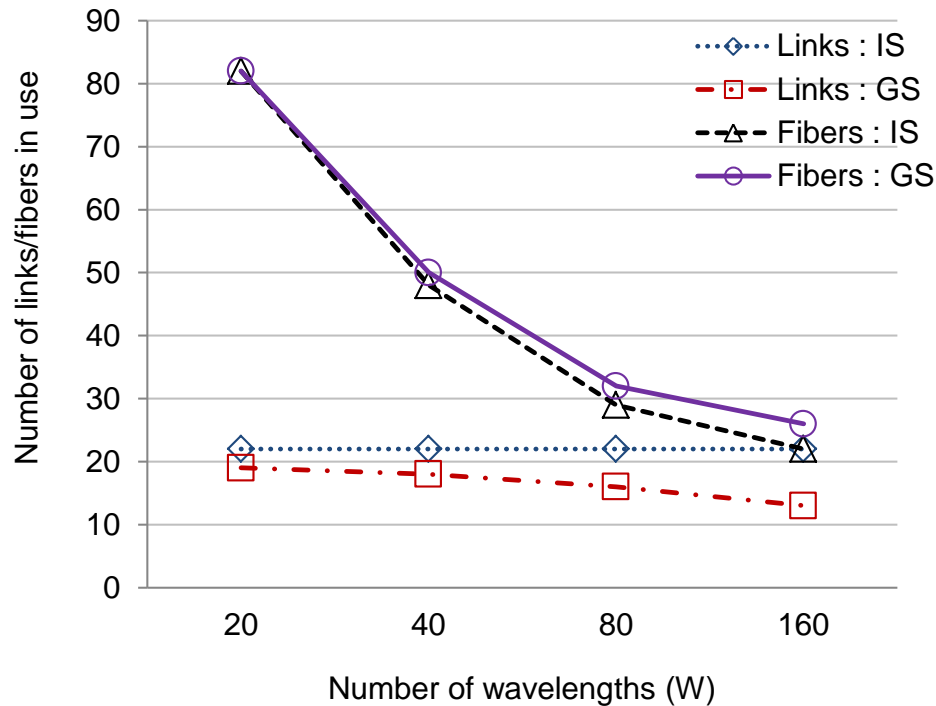


Figure 4.3: Number of fibers/links against increasing  $W$ .

As shown in Figure 4.3, the network dimensioned with GS employs more active fibers than the network dimensioned with IS. However, the GS-dimensioned network possess fewer physical links and, thus, has limited node-connectivity. As a result, the remaining physical links in the GS dimensioned network are required to carry more active fibers to accommodate peak traffic demand. On the other hand, the IS-dimensioned network can serve traffic using fewer active fibers due to high node-connectivity. Thus, TUs, PrAs/PoAs, and OXCs port cost more in the network dimensioned with GS than with IS.

The cost of ILAs is determined by the length of active fibers. Although the network dimensioned with IS uses fewer active fibers, in Figure 4.4, we observe only a marginal difference in the total length of active fibers between the networks dimensioned with IS and GS.

The number of regenerators (Rgs) used by each network is governed by the distance trav-

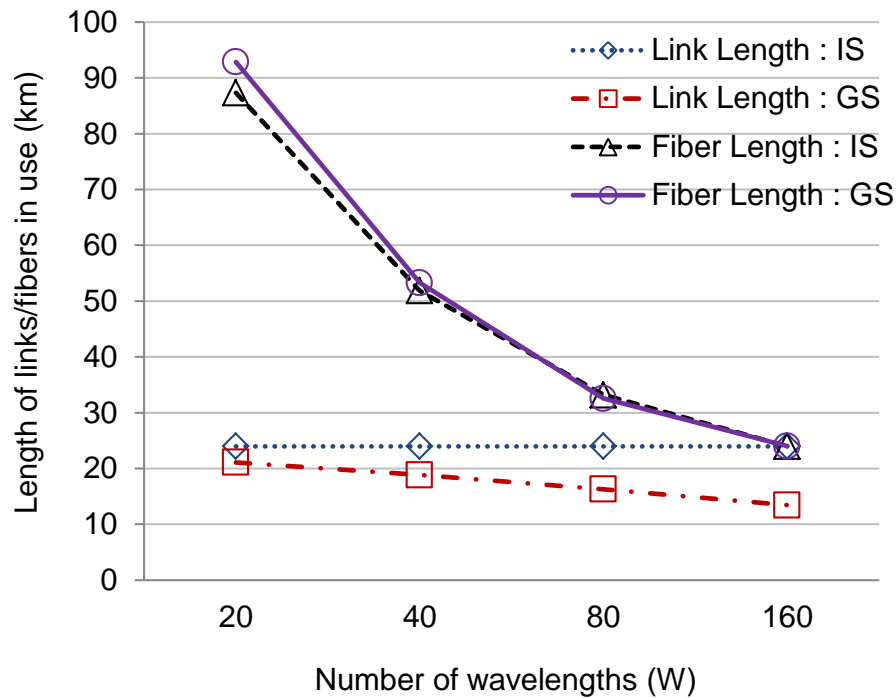


Figure 4.4: Total length of the fibers/links against increasing  $W$ .

elled by traffic. As observed in Figure 4.5, when the network is dimensioned with GS, lightpaths travel through a higher number of core node hops than with IS. A higher hop count indirectly refers to a longer travelling distance of lightpaths. As a result of this increased hop count, lightpaths are regenerated more often when the network is dimensioned with GS than with IS. Thus, regenerators cost more in the network dimensioned with GS.

Based on the above discussion, fibers, PrAs/PoAs, TUs, OXCs, and Rgs cost less in the network dimensioned with IS. However, a significant difference in the costs of ILAs between the two networks is not observed. Physical links cost less in the network dimensioned with GS. As physical links dominate deployment cost, the network dimensioned with GS costs less than the IS-dimensioned network in terms of CAPEX.

#### 4.6.2.1 Power consumption

Figure 4.6 depicts power consumed by the networks dimensioned with IS and GS for different values of  $W$ . It is observed that power consumption decreases as  $W$  increases. At all  $W$  values, the network dimensioned with IS consumes less power than the network dimensioned with GS. The IS-dimensioned network employs fewer active fibers and, consequently, amplifiers, TUs, and OXCs consume less power. Furthermore, as previously highlighted, when the network is

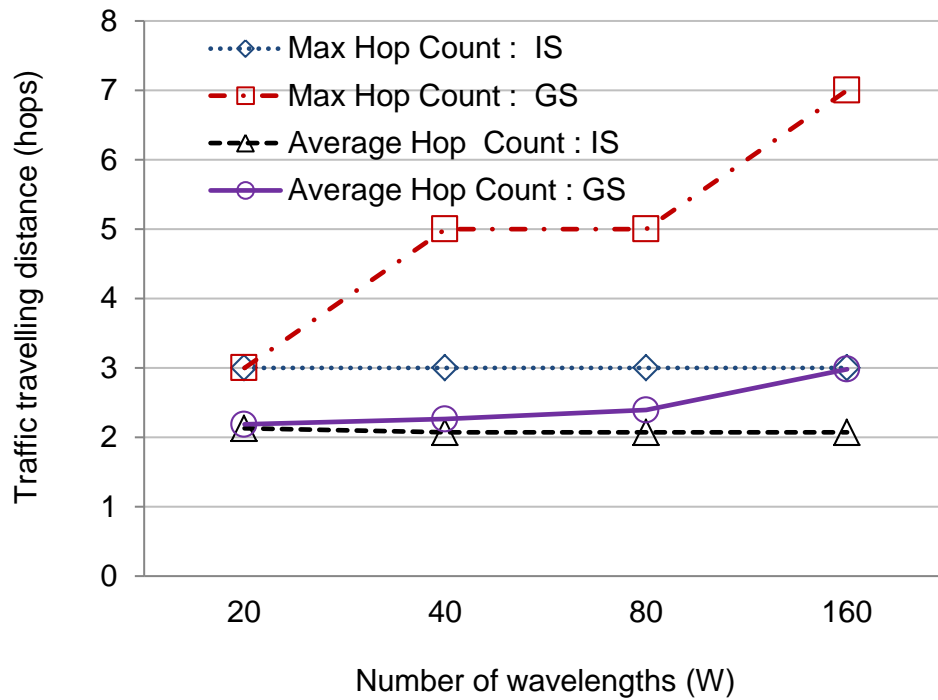


Figure 4.5: Number of hops travelled by traffic demands against increasing  $W$ .

dimensioned with IS, lightpaths travel through fewer hops, which suggest a shorter travelling distance. Therefore, regenerators consume less power in the IS-dimensioned network.

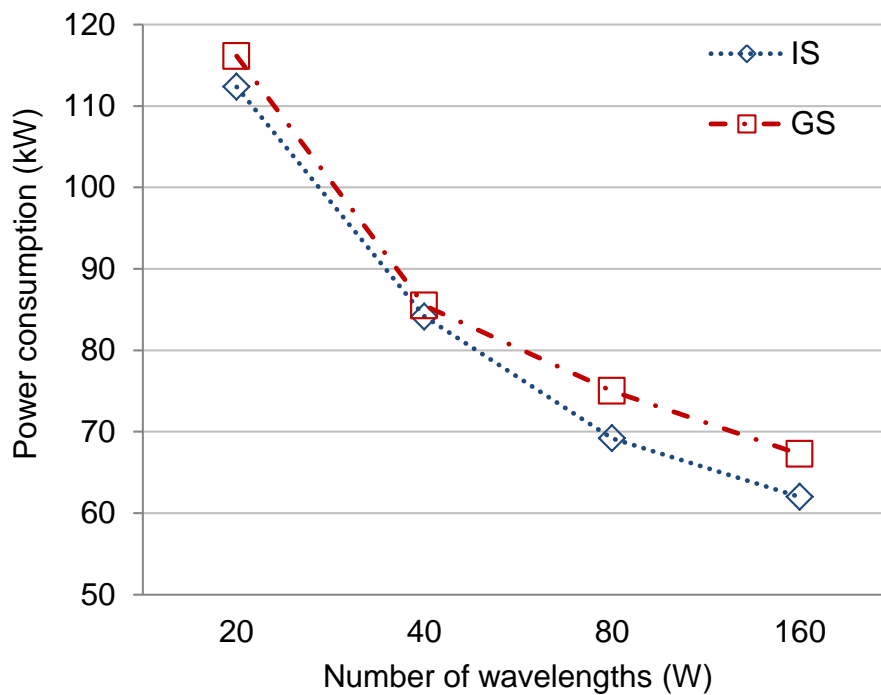


Figure 4.6: Power consumption against increasing  $W$ .

#### 4.6.2.2 Transmission distance

To reduce transmission delay and signal degradation, that occur due to induced cross talk on pass-through lightpaths in OXCs, traffic has to be routed via a minimum number of intermediate core nodes. Figure 4.5 shows the *average* and the *maximum* number of hops travelled by lightpaths when the network is dimensioned with IS and GS. As a result of reduced network connectivity between core nodes, lightpaths travel via an increased number of hops in the network dimensioned with GS. Consequently, when  $W$  is 160, certain lightpaths incur extensive signal degradation as they travel through 7 hops. On the other hand, when the network is dimensioned with IS, lightpaths travel through the minimum number of hops at all  $W$  values. Therefore, between GS and IS, the network dimensioned with IS reduces transmission distance the most.

#### 4.6.2.3 Comparison of cost, power consumption and delay

The outcomes of the above analysis are summarised in Table 4.4. In this table, we compare the performance of the networks dimensioned with IS and GS in terms of cost, power consumption and transmission distance. While  $\uparrow$  indicates that the considered heuristic consumes/costs *more* than the other,  $\downarrow$  indicates that it consumes/costs *less*. Essentially, our results show that if CAPEX is to be minimized, the network should be dimensioned with the GS heuristic. However, to reduce power consumption, transmission delay, and signal degradation, the network should be dimensioned with IS. Since the cost of electricity is rising, dimensioning the network using IS is likely to provide long-term cost benefits (OPEX savings) that would surpass initial CAPEX savings attained by dimensioning the network using GS. Therefore, based on our results, we are compelled to select the IS heuristic over the GS heuristic.

Table 4.4: A simple comparison of IS and GS heuristics

Strategy	Cost (arrow) / Power (arrow)					Trans. delay
	Total	Conduits	TUs	OXCs	Rgs	
Incremental (IS)	$\uparrow / \downarrow$	$\uparrow / \text{NA}$	$\downarrow / \downarrow$	$\downarrow / \downarrow$	$\downarrow / \downarrow$	$\downarrow$
Greenfield (GS)	$\downarrow / \uparrow$	$\downarrow / \text{NA}$	$\uparrow / \uparrow$	$\uparrow / \uparrow$	$\uparrow / \uparrow$	$\uparrow$

Note: Trans. delay represents transmission delay

## 4.7 Reducing power consumption during low-load periods

Statistics show that network traffic experiences significant fluctuations during the course of the day. During peak hours (e.g., day time), the network is loaded with relatively high volumes of traffic in comparison to off-peak hours (e.g., early morning). Power consumption can be reduced during off-peak hours (i.e., low-load periods) by selectively switching off active fibers and their equipment using the proposed the MO algorithm. To assess our algorithm's capability in switching off active fibers, we first compare MO with the near-optimal results reported in [252,260]. We then demonstrate that MO saves more power than available LF, MA, and DPSF criteria-based algorithms.

### 4.7.1 Comparison of MO algorithm with near-optimal results

In [252, 260], the authors used ILP-based optimization techniques to minimize the number of active fibers needed to serve network traffic. By optimizing the developed ILP formulations, the authors produced near-optimal (NO) results. To compare MO and NO in [252, 260], a similar experiment is performed on a modified NSF network (14 core nodes and 44 uni-directional links). The experiment is performed using a realistic traffic matrix comprising 360 unidirectional traffic demands and using different values for  $W$  [259]. The results obtained using the proposed MO algorithm are reported in Table 4.5. These results are comparable with the NO results reported in [252, 260] and other relevant work [259, 261]. Average percentage differences ( $\Delta$ ) between the NO results of prior studies and the MO results of the current study are 4% and 6% for unprotected and shared-protected networks, respectively. Despite allowing traffic demands to arrive in an arbitrary order, and restraining each of them to a single working path, the proposed MO algorithm also produces near-optimal results.

### 4.7.2 Comparison of MO algorithm with other criteria-based algorithms

During low-traffic-load periods, power consumption can be reduced by selectively switching off active fibers. To increase power savings, it is desirable to switch off long fibers, equipped with a higher number of amplifiers, and allow traffic to travel a shorter distance, which then uses a smaller number of regenerators and OXC ports. In past studies, MA, LF, and DPSF criteria-based algorithms are used to selectively switch off fibers and reduce power consump-

Table 4.5: Comparison of results with MO and near-optimal (NO) results in [252, 259, 260]

$W$	Unprotected			Shared-protected		
	NO	MO	$\Delta\%$	NO	MO	$\Delta\%$
8	106	104	1.9	161	177	9.9
16	58	58	0	95	97	2.1
32	35	33	5.7	55	57	3.6
64	24	22	8.3	38	41	7.9

tion. To demonstrate that our proposed MO algorithm offers higher power savings than these existing algorithms, we perform an experiment on the NSF network consisting of 14 core nodes and 21 bi-directional links. Each link is initially provisioned with 6 active optical fibers and  $F$  is assigned the value 40. Thus, a total of 126 fibers with an accumulated length of 136,254 km is equipped with the necessary electronics. Each fiber is allowed to carry a maximum of 40 wavelengths ( $W = 40$ ) at a maximum bit-rate of 40 Gbps. Important parameters  $\alpha$ ,  $\beta$ ,  $\gamma$ ,  $|S_{MA}|$ , and  $S_1$  are assigned the values 1, 1, 1.1, 20, and 5, respectively.

Traffic between node pairs is represented using the gravity model described in [279]. The network is first dimensioned with IS to support peak traffic of 25 Tbps. Total network traffic during low-load periods (i.e., off-peak hours) is defined as a percentage (e.g., 20%, 40%, 60%, and 80%) of peak traffic. These percentages represent hourly traffic variations reported in [165]. Every traffic demand is served with an integer multiple of a 40 Gbps wavelength.

The MA, LF, DPSF, and MO heuristic algorithms are evaluated in terms of the number of switched-on or active fibers remaining in the network (Figure 4.7) and their total length (Figure 4.8), the number of regenerators used (Figure 4.9), increase in hop count, and power consumption (Figure 4.12).

#### 4.7.2.1 Switching off active fibers

To reduce power consumption of TUs and OXCs, the number of active fibers needs to be minimized. In the non-optimized network, a total of 126 active fibers remain switched on during both peak and low-load traffic periods.

From Figure 4.7, it is evident that the MA, LF, DPSF, and MO algorithms perform exceptionally well in switching off active fibers according to traffic variations. However, slight dif-

ferences are noted among them. Particularly, during-low load traffic periods (e.g. 20%, 40%, 60%), the MO algorithm switches off approximately 8%-10% more fibers compared to other algorithms. On average, a network optimized with the MO algorithm uses 66% less active fibers than a non-optimized network. This is closely followed by the LF and DPSF algorithms which offer a reduction in active fibers of 65% and 64%, respectively. The MA criteria-based algorithm offers the least reduction in fibers. By taking into account fiber utilization and intelligently increasing the value assigned to parameter  $\gamma$  as the algorithm progresses, the MO algorithm switches off a higher number of active fibers without over-burdening other fibers. On the other hand, the MA criterion-based algorithm switches off long fibers without considering fiber utilization and, therefore, overwhelms the capacity of remaining fibers.

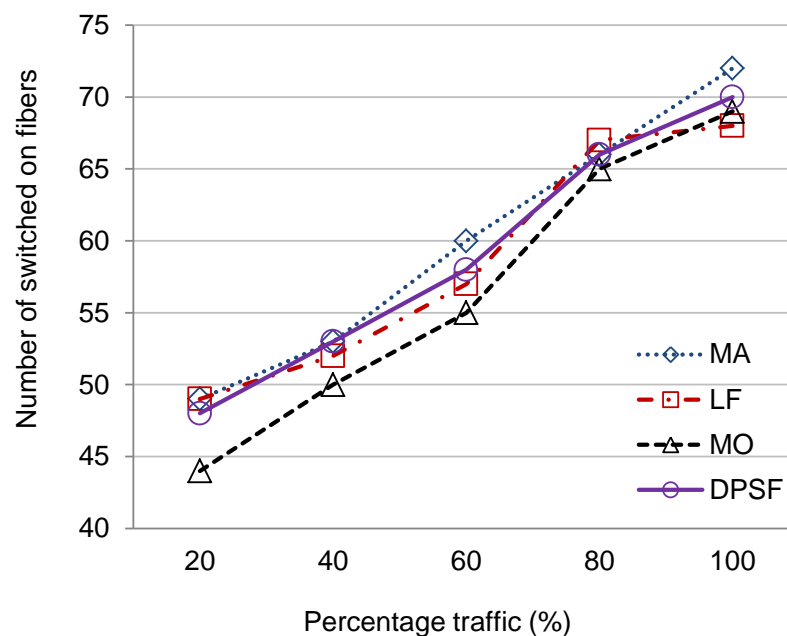


Figure 4.7: The number of switched-on fibers remaining against traffic variations

#### 4.7.2.2 Reducing the length of active fibers

Next, in Figure 4.8, we evaluate fiber length reduction. To reduce power consumption of ILAs, it is crucial to reduce the length of active fibers that are left switched on. From Figure 4.8, we understand that MO, DPSE, and MA, which take into account fiber length, outperform LF in the context of reducing length of active fibers. When network traffic is low, the proposed MO algorithm reduces the length of active fibers by 7-10% over other algorithms. In comparison to the non-optimized network, the length of active fibers that are left switched on is reduced

by 53%, on average, when the network is optimized using the MO algorithm proposed in this study.

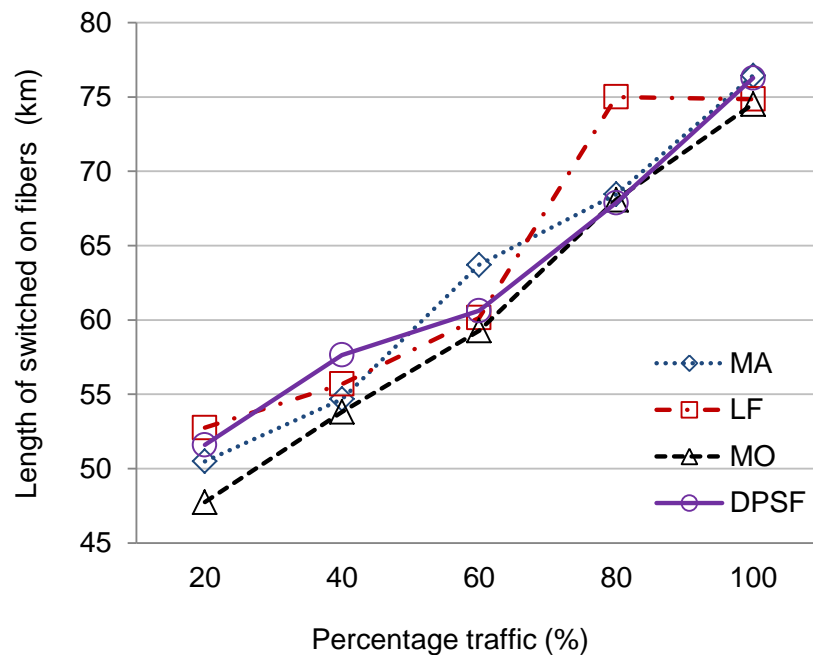


Figure 4.8: The total length of switched-on fibers remaining against traffic variations

#### 4.7.2.3 Reducing the number of regenerators used

Figure 4.9 depicts the number of regenerators used at each traffic volume by different algorithms. The use of regenerators depends on the number and travelling distance of traffic demands. As traffic volume increases, more lightpaths will require the service of regenerators. Thus, we observe an increase in the number of regenerators used at high traffic volumes.

In this study, all four algorithms route each traffic demand along the shortest available path. Regardless of network traffic volume and the algorithm used then, lightpaths travel through two physical links (two hops) on average. Therefore, a significant difference in the number of regenerators used among networks optimized with the different algorithms is not observed. Furthermore, the maximum number of hops travelled by any lightpath is found to be 3 for both non-optimized and optimized networks. Hence, no significant difference in the number of regenerators is again observed between optimized and non-optimized networks.

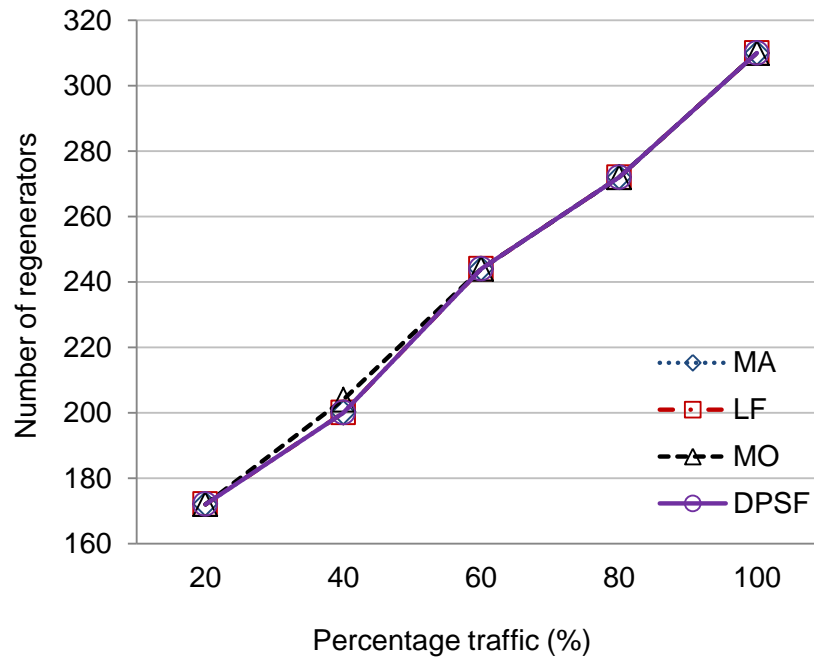


Figure 4.9: The number of regenerators used against traffic variations

#### 4.7.2.4 Reducing CAPEX

Figure 4.10 depicts the costs of individual devices as a percentage of CAPEX. Fiber-laying projects (i.e., assigning physical links) consume 87% of the CAPEX, while the remaining 13% is spent on purchasing electronic devices. The cost of electronics can be reduced by activating (i.e., equipping) fewer fibers. The number of active fibers and, thereby, the cost of attached electronics can be reduced by optimizing the network using the MA, LF, DPSF and MO algorithms considering peak traffic demand (100% traffic load).

The obtained values of normalized CAPEX for the 14-node, 21-link NSF network using the three algorithms are tabulated in Table 4.6. In comparison to the non-optimized network where each physical link is allotted 6 active fibers, the proposed MO algorithm activates less than 4 fibers in every link. As a result, MO reduces CAPEX by 4,039 units over the non-optimized network. We also observe that the network using the MO algorithm offers higher CAPEX savings in comparison to networks using the other criteria-based heuristic algorithms.

#### 4.7.2.5 Reducing daily/monthly power consumption and OPEX

Power consumed by individual devices of a network optimized with the MO algorithm at peak traffic demand is plotted as a percentage of total power in Figure 4.11. It is observed that ILAs

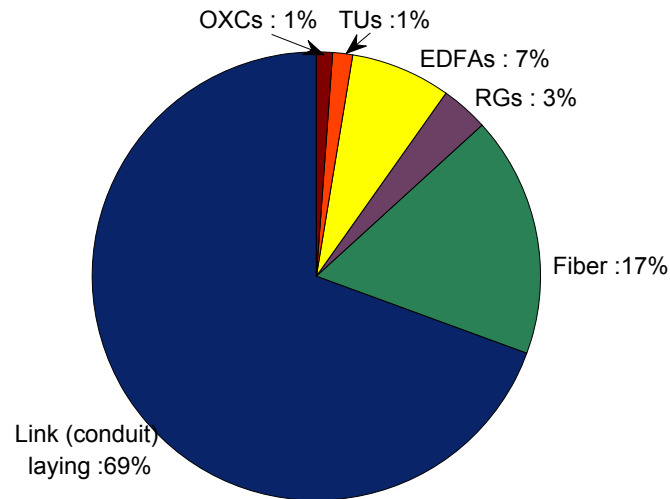


Figure 4.10: Breakdown of CAPEX

Table 4.6: Cost of a network designed to serve peak hour traffic optimized with different heuristic algorithms

Heuristic Algorithm	Cost (unit)
Non-optimized	10469
MA	6560
LF	6433
DPSF	6525
MO	6430

and regenerators consume a significant amount of power, while TUs and OXCs consume very little power.

By taking into account variations in network traffic during a 24-hour period, we may evaluate total power consumption of networks optimized with the different algorithms. Power consumed by the networks optimized with the MA, LF, DPSF, and MO algorithms, at different hours, is depicted in Figure 4.12. As expected, when network traffic increases from low-load to peak, power consumption of the networks increase. Power consumed is dependent on the increase in the number of active fibers (affecting power consumption of TUs and OXCs), length of the active fibers (affecting power consumption of ILAs), and the travelling distance of light-paths (affecting power consumption of Rgs). In comparison to the non-optimized network, the network optimized with MO consumes, on average, 1.3 MWh less power in a single day and

40 MWh less power in a whole month. According to current pricing data [280], this translates into an OPEX saving of USD 3,013 per month (at 7 Cents/kWh) in comparison to networks optimized with the other algorithms. Specifically, the network optimized with MO consumes 1.1 MWh, 1 MWh, and 0.8 MWh less power per month than those optimized with MA, LF, and DPSF, respectively.

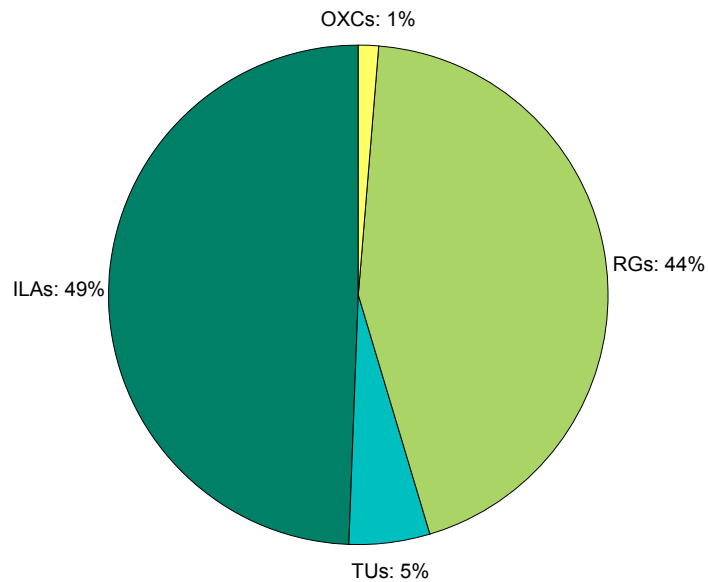


Figure 4.11: Percentage power consumption of network devices using the MO algorithm with peak-hour traffic)

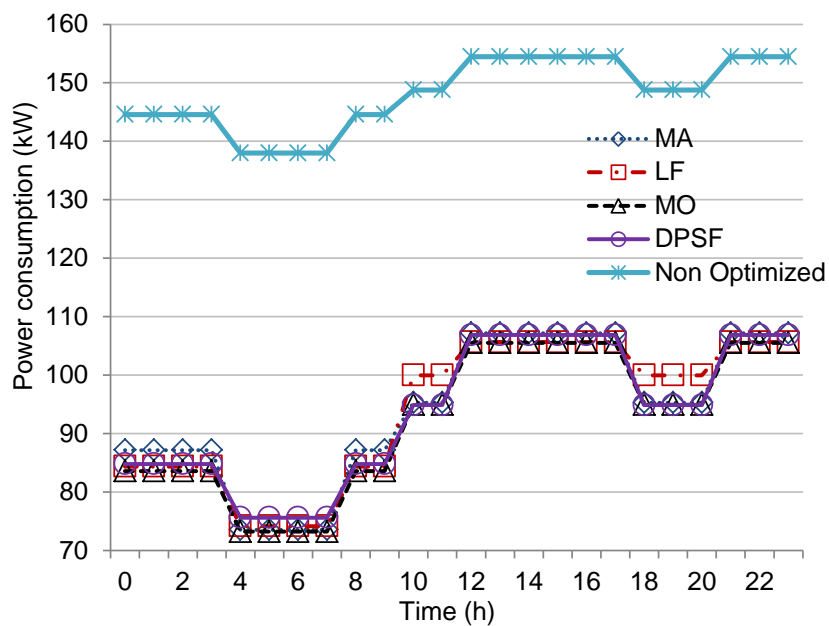


Figure 4.12: Power consumption against increasing time

## 4.8 Summary of findings

In this chapter, we attempted to minimize cost and power consumption of the WDM layer of a survivable OCS backbone network by redesigning the link topology and adopting sleep mode of operation.

We first modelled the cost and power consumption minimization problems using ILP formulation, which were then solved using proposed algorithms.

AS network cost is dominated by link-laying cost, it is essential to dimension the physical link topology using fewer links in order to reduce network cost. The cost of electronics can be reduced by activating only a few fibers in every link. Among the two proposed heuristic strategies, IS and GS, the latter reduced more physical links but provisioned more active fibers. If short-term cost benefits are desired (i.e., minimized CAPEX), the physical link topology should be dimensioned using the GS heuristic. However, if long term cost benefits are desired (i.e., minimized OPEX), the network should be dimensioned with the IS heuristic.

Network traffic varies substantially over the course of a single day. Power consumption can be reduced by selectively switching off active fibers during low-traffic-load periods. Using the MO algorithm proposed in this study and considering traffic dynamics, we selectively switch off long fibers during low-load periods and save approximately 1.3 MWh of electricity in a single day. We also show that the proposed MO algorithm outperforms existing algorithms.

The work undertaken in this chapter reduces cost and power consumption of a survivable OCS backbone network by explicitly modifying the physical topology and capacity of physical links. In the next chapter, we investigate how power consumption of a backbone network can be reduced by aggregating traffic into wavebands and using sophisticated all-optical devices.

---

# DESIGNING POWER-EFFICIENT BAND-SWITCHED OCS NETWORKS

---

## 5.1 Introduction

Traffic grooming is the process of aggregating several low-granularity traffic flows into fewer high-granularity traffic flows. As discussed in Section 2.4 of Chapter 2, traffic can be groomed at several granularities.

In an OCS network (i.e., IP-OTN), traffic between core nodes are transmitted along light-paths established in the form of wavelengths. An OCS network could also, therefore, be referred to as a Wavelength Switched Network (WSN). In a WSN, core nodes consist of core routers and OXCs. Sub-wavelength traffic arriving from the access network is groomed into wavelengths by the core routers. These wavelengths are then multiplexed into a minimum number of optical fibers using the WDM technique. At intermediate core nodes, wavelengths carrying pass-through traffic are optically switched from one fiber to another by the OXCs.

As network traffic grows beyond the zettabyte threshold [12], the number of wavelengths traversing the backbone network will rapidly increase. Consequently, OXCs with a large number of I/O ports (i.e., large-scale OXCs) will be required at core nodes to switch this growing traffic. The increasing number of I/O ports is a major contributor to the overall cost of the network [145, 146]. Furthermore, due to inherent complexity of large-scale OXCs, it is difficult to manage and control them [281]. Consequently, port capacity of OXCs presents a severe bottleneck for scaling of future WSNs. To overcome this bottleneck, a backbone network could adopt waveband grooming [145, 146] and replace OXCs with Multi-Granular Optical Cross Connects (MG-OXCs) [281]. A backbone network capable of waveband grooming is referred to as a Band Switched Network (BSN).

A BSN can be realized using MG-OXCs that have a hybrid (i.e., HOXCs), single-layer, or three-layer architecture [27]. An HOXC relies on both electronic and optical switches and, thus, involves power-hungry O-E/E-O conversions. A single-layer MG-OXC consumes fewer I/O ports than a three-layer MG-OXC [27,282], but is less flexible than the latter [27,282]. In a BSN, the design parameter of *Band Size* (BS) dictates the number of wavelengths grouped within a waveband [27]. Another design parameter, *grouping policy*, decides when and where to group and split wavebands. *Band configuration* is yet another important design parameter that is used together with a uniform BS to either minimize multiplexing/de-multiplexing of pass-through wavebands or reduce bandwidth waste in optical fibers [27,283].

In [28,156,157], BS and grouping policy are shown to have a significant impact on cost and power consumption of a BSN. The authors suggest that, to minimize power consumption, a BSN should use the Same-Ends (SE) grouping policy, instead of the Intermediate (INT) grouping policy, as well as a small BS [28,156,157]. However, in these studies, an I/O port is assumed to consume an insignificant amount of power. In turn, the reduction in the number of I/O ports achieved through waveband grooming is assumed to have a negligible impact on reducing backbone network power consumption. The authors experiment on a BSN provisioned with HOXCs instead of three-layer MG-OXCs [28,156,157]. Total electricity consumption is measured as the sum of power consumed by the O-E/E-O interfaces of the HOXCs. The power consumption of amplifiers, regenerators, and I/O ports, however, is not included in their final analysis [28,156,157].

In another important study, Naas et al., [158] indicate that BS has to be selected according to traffic volume and the number of wavebands allowed within a single fiber in order to reduce power consumption. However, the authors [158] do not justify or explain why a BSN consumes less power with a specific BS value than other values. Furthermore, in [158], power consumption of the network is measured using hypothetical values instead of actual power consumption values. To the best of our knowledge, the effect of band configuration on power consumption has also not been evaluated in previous studies.

As highlighted in Chapter 2.3, AOWCs and AORs are currently being developed in research laboratories [22]. Lab-based experiments show that AOWCs and AORs offer similar, at times better, performance to electronic devices [22,85–88]. In [114–117], researchers developed multi-wavelength All-Optical Regenerators (mAORs), which can simultaneously regenerate multiple wavelengths that have an *identical line rate* (e.g.,  $8 \times 10$  Gbps,  $4 \times 40$  Gbps, and  $4 \times 10$  Gbps).

Based on these developments, in the future, MG-OXC's can be equipped with AOWCs and AORs [29,282] to minimize O-E/E-O conversions, thereby reducing power consumption. Furthermore, MG-OXC's could utilize mAORs to circumvent the need for frequent de-multiplexing of wavebands [237,238] that impedes the reduction of I/O ports of a BSN. While several studies assess the impact of AOWCs on reducing port cost of MG-OXC's [29,282], to the best of our knowledge, no study thus far has examined *power consumption* of a BSN employing *three-layered MG-OXC's equipped with AOWCs and AORs*.

We identify the following critical gaps in existing research on power consumption of backbone networks.

1. To date, no prior study has accounted for the power consumption of I/O ports of MG-OXC's.
2. Power consumption of BSNs which employ three-layer MG-OXC's equipped with advanced all-optical devices has not been evaluated in the past.
3. Researchers claim that selection of either grouping policy (SE or INT) results in a trade-off between minimizing cost and reducing power consumption [156,157]. Yet, the above claim has not been verified in BSNs which use three-layer MG-OXC's equipped with advanced all-optical devices.
4. Conclusions drawn in previous studies are based on experiments performed on a single network, using a single traffic distribution model [156,157], and often using hypothetical power consumption values [158].
5. The potential impact of band configuration on power consumption has not been analyzed in previous studies.

To address the above gaps identified in the literature, in this chapter, we carry out a comprehensive investigation of power consumption of a BSN that employs three-layer MG-OXC's equipped with AOWCs and AORs. We evaluate the power consumption of different-sized BSNs using different traffic models and with different traffic volumes. The effects of *grouping policy*, *band size*, and *band configuration* on power consumption is closely analyzed. Power consumed by the BSN is also compared with power consumed by a WSN. We perform three main tasks in this chapter, which form the contributions of this chapter. They are:

1. Modelling the power consumption minimization problem of a BSN that employs three-layer MG-OXCs equipped with advanced all-optical devices.
2. Developing a novel heuristic algorithm to tackle the power consumption minimization problem.
3. Quantifying the reduction in power consumption of a BSN over a WSN and assessing the impact of each design parameter on overall power consumption.

By carrying out the above tasks, this chapter provides solution(s) to research problem 3:

- How can waveband grooming effectively incorporate the advanced features of MG-OXCs and all-optical technologies to minimize power consumption of an OCS network?

## 5.2 Design parameters: Grouping policy, band size and band configuration

Existing waveband grouping policies can be categorized as Same-Ends (SE) and Intermediate (INT) grouping policies [27]. SE groups wavelengths travelling between identical source and destination nodes into *end-to-end waveband(s)*. End-to-end wavebands do not multiplex or demultiplex at intermediate core nodes. INT groups wavelengths that travel along a common path via identical links, regardless of their source and destination nodes, into *sub-path waveband(s)*. As a sub-path waveband can be formed at either a source or an intermediate node, it can be demultiplexed and grouped into a different waveband at an intermediate node.

Waveband size BS dictates the number of wavelengths allowed within a single waveband. According to [27], a BSN can use either uniform or non-uniform band sizes. If every waveband carries an identical number of wavelengths, the corresponding BSN is called a uniform BSN. If otherwise, it is referred to as a non-uniform BSN. While non-uniform BSNs show higher wavelength utilization and reduced de-multiplexing, MG-OXCs of these networks require additional hardware support [27]. Hence, uniform BSNs are considered much simpler to implement in comparison to non-uniform BSNs [284]. Considering these factors, in this study, we investigate the power consumption of a uniform BSN [284].

Waveband configuration is another parameter that is used when designing a uniform BSN. An example, derived from the work of [27,283] and depicted in Figure 5.1, provides a simple comparison between two band configurations. In this example, the source node  $a$  transmits

traffic via lightpaths occupying 2, 3, and 1 wavelengths to nodes  $b$ ,  $c$ , and  $d$ , respectively. A single optical fiber provides physical connectivity among the nodes. Every wavelength originates at node  $a$  and passes through node  $n$ . Let us assume that traffic is served using a uniform BSN with a BS of 2. A uniform BSN can group wavelengths according to two different band configurations. If the *first configuration* (C1) is used, the set of wavelengths is grouped into three wavebands, as shown in Figure 5.1. The third waveband carries traffic between both node pairs  $(a, c)$  and  $(a, d)$ , as  $BS = 2$ , and has to be de-multiplexed at node  $n$ . However, if the *second configuration* (C2) is used, traffic between node pairs  $(a, c)$  and  $(a, d)$  are grouped separately into two partially-filled wavebands (the third and fourth wavebands in Figure 5.1), respectively. Consequently, C2 uses fewer I/O ports than C1 at node  $n$  as demultiplexing is not needed. However, as the third and fourth wavebands are only partially-filled, C2 reduces bandwidth utilization and increases fiber use.

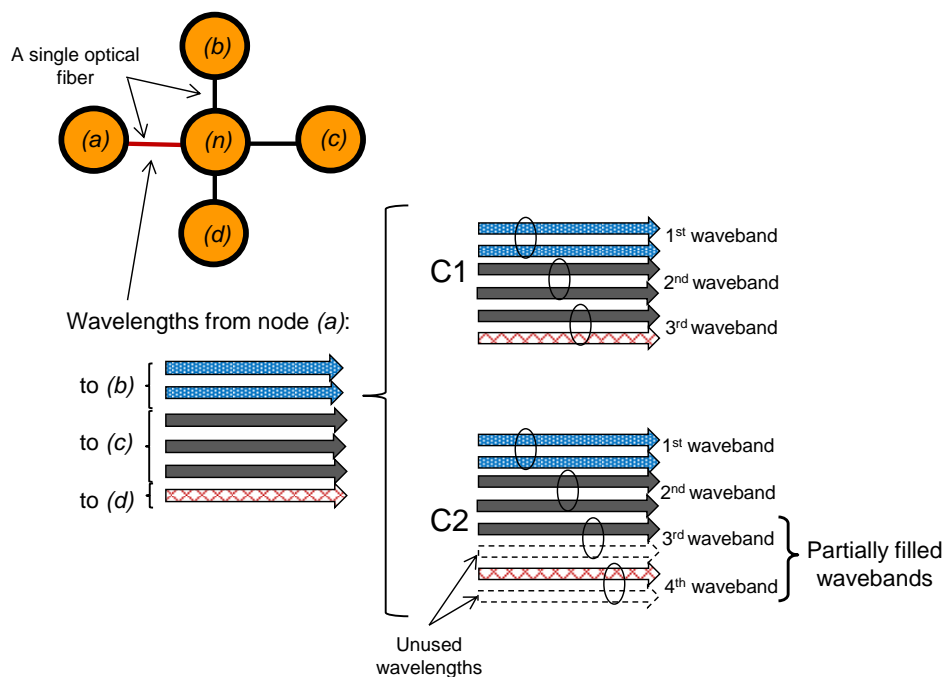


Figure 5.1: Comparison of C1 and C2 configurations with a uniform BS of 2

### 5.3 Network model

Section 5.3.1 explains the architecture of a three-layer MG-OXC equipped with all-optical devices. The relevant power consumption model is then presented in Section 5.3.2.

### 5.3.1 Node architecture

The general architecture of a backbone network was depicted in Figure 2.1. This could be transformed into a BSN by replacing OXCs with MG-OXCs.

The architecture of a three-layer MG-OXC [27] is depicted in Figure 5.2. A three-layer MG-OXC comprises three switching layers, namely, Wavelength Cross-Connect (WXC), Band Cross-Connect (BXC), and Fiber Cross-Connect (FXC). Local add traffic is added via wavelength/band/fiber add-ports ( $W_{add}/B_{add}/F_{add}$ ) to the respective cross-connect of the MG-OXC. Similarly, traffic arriving at the destination core node (also known as *local drop traffic*) is dropped through wavelength/waveband/fiber drop-ports ( $W_{drop}/B_{drop}/F_{drop}$ ) of the MG-OXC. Pass-through traffic travels through the WXC, BXC, and FXC at wavelength (referred to as a pass-through wavelength), waveband (referred to as a pass-through waveband), and fiber (referred to as a pass-through fiber) granularities, respectively.

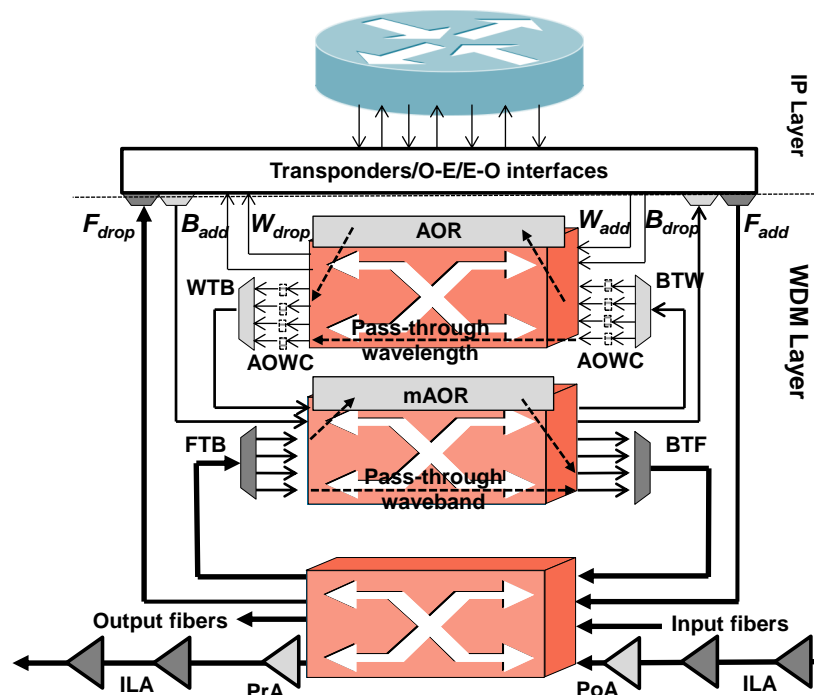


Figure 5.2: The architecture of a three-layer MG-OXC containing AOWCs and AORs

An incoming fiber or waveband consisting of both local and pass-through traffic is decomposed into lower granularities by Fiber-to-Band (FTB) and Band-to-Wavelength (BTW) demultiplexers, respectively. Lower granularity traffic is multiplexed into higher granularities by Wavelength-to-Band (WTB) and Band-to-Fiber (BTF) multiplexers. The hierarchical structure of the three-layer MG-OXC imposes the following constraints on traversing traffic:

- Traffic entering the MG-OXC via input fibers cannot be switched by the WXC, unless they travel through the FTB, BXC, and BTW in sequence.
- Traffic that is switched by the WXC has to travel through the WTB, BXC, and BTF in sequence before arriving at the FXC.

To minimize multiplexing and de-multiplexing and reduce I/O port consumption, MG-OXCs have to switch traffic at the highest possible granularity [144].

In Figure 5.2, the three-layer MG-OXC is assigned with AOWCs and AORs. Researchers believe that AOWCs and AORs are superior to electronic devices as they possess the ability to convert and regenerate multiple wavelengths simultaneously [22, 114, 161]. As such, to minimize intra-MG-OXC switching and multiplexing/de-multiplexing, the BXC layer could be equipped with advanced *multi-wavelength* AOWCs and AORs. However, MG-OXCs can also be realized using readily-available *single-wavelength* AOWCs by appropriately assigning wavelengths to lightpaths [30]. Therefore, in the depicted three-layer MG-OXC architecture in Figure 5.2, the WXC is equipped with dedicated single-wavelength AOWCs, while the WXC and BXC layers are equipped with a set of shared single-wavelength and multi-wavelength AORs, respectively.

### 5.3.2 Modelling power consumption

In the network architecture presented in Figure 2.1, traffic is added to and dropped from the WDM layer of the backbone network at wavelength granularity via O-E/E-O interfaces (i.e., transponders) [53]. Pass-through traffic is converted, regenerated, and switched by translucent OXCs of intermediate nodes. Thus, core routers only process local-add and local-drop traffic. This process remains the same even if OXCs are replaced with MG-OXCs, effectively transforming the WSN to a BSN. However, replacing OXCs with MG-OXCs does not affect the power consumption of core routers and transponders because the amount of traffic added to or dropped from the network is still the same [53]. Therefore, core routers and transponders are omitted from the developed power consumption model, which then represents power consumption of the WDM layer of the BSN.

Switching layers of the MG-OXC in Figure 5.2 are constructed of Micro-Electro-Mechanical Systems (MEMS)-based switches. Each switching layer is equipped with PrAs/PoAs, add/drop multiplexers, and modules for termination of the OSC [113, 162]. Power consump-

tion of a switching layer is dependent on the number of I/O ports [101, 163] or the number of wavelengths supported by them [18, 44]. According to [28, 101], an I/O port consumes approximately 7 W of power. Although power consumption of a single I/O port is relatively small in comparison to other devices, when combined, they draw a vast amount of electricity as a large number of I/O ports are used to switch high volumes of traffic.

Since an AOR regenerates a single wavelength, total power consumed by AORs is proportional to the number of wavelengths regenerated at every core node. Power consumption of AORs is derived from the work of [46–48]. A multi-wavelength AOR (mAOR) performs the task of several AORs within an integrated device, using a single cooling system, chassis, and power supply [161]. Therefore, a single mAOR is expected to consume less power than multiple AORs.

An AOWC consumes only a trace amount of power ( $\approx 0.7\text{-}2$  W) [51, 52]. Furthermore, by appropriately assigning wavelengths, the use of AOWCs can be minimized. Therefore, power consumption of AOWCs is not included in the developed power consumption model. WTB and BTF multiplexers and FTB and BTW de-multiplexers are considered to be passive devices, which do not consume electricity [174]. Power consumption of PrAs and PoAs is proportional to the number of fibers carrying traffic (i.e., active fibers) [18]. Power consumption of ILAs depend on the length of active fibers and the distance between two ILAs [18].

Equation 5.1 combines the aforementioned relationships to produce the power consumption model of the WDM layer of a BSN ( $P_{\text{WDM}}$ ) consisting of  $V$  set of nodes and  $E$  set of links [18].

$$P_{\text{WDM}} = \underbrace{n_{\text{p}}\Gamma}_{\text{I/O ports}} + \underbrace{n_{\text{wr}}\Psi + n_{\text{br}}(\Psi \cdot \text{BS} \cdot \nabla\%)}_{\text{Regenerators}} + \underbrace{2 \cdot n_{\text{f}}\Theta + n_{\text{ILA}}\Pi}_{\text{Amplifiers}} \quad (5.1)$$

Notations  $n_{\text{p}}$ ,  $n_{\text{wr}}$ ,  $n_{\text{br}}$ ,  $n_{\text{f}}$ , and  $n_{\text{ILA}}$  represent the total number of I/O ports, AORs, mAORs, fibers, and ILAs used by the BSN accommodating a given traffic volume. The respective numbers are found using Equations 5.2, 5.3, 5.4, 5.5, and 5.6. In Equation 5.1, notations  $\Gamma$  and  $\Psi$  denote power consumption of an I/O port and an mAOR, respectively. Power consumption of regenerators is calculated by summing two terms. The first term calculates power consumed by AORs and the second term calculates power consumed by mAORs. In this work, an mAOR

is assumed to be capable of regenerating BS number of wavelengths simultaneously (1 waveband), and consumes  $\nabla\%$  less power than BS number of AORs. Thus,  $n_{br}$  is multiplied by  $(\Psi \cdot BS \cdot \nabla\%)$ . While  $\Theta$  represents power consumption of a PrA or a PoA,  $\Pi$  denotes the power consumption of an ILA. As every fiber is assigned with a PoA and a PrA,  $\Theta$  is multiplied by 2 for every fiber.

$$n_p = \sum_{\forall n \in V} \{WXC^n + BXC^n + FXC^n\} \quad (5.2)$$

Equation 5.2 determines  $n_p$ . The terms  $WXC^n$ ,  $BXC^n$ , and  $FXC^n$  denote the number of ports used at the respective switching layers of node  $n$ .

$$n_{wr} = \sum_{\forall n \in V} \lambda^n \quad (5.3)$$

$$n_{br} = \sum_{\forall n \in V} \rho^n \quad (5.4)$$

Equations 5.3 and 5.4 determine  $n_{wr}$  and  $n_{br}$ . In these equations,  $\lambda^n$  and  $\rho^n$  denote the number of AORs and mAORs used at node  $n$ , respectively.

$$n_f = \sum_{\forall l_{ij} \in E} \chi_f \quad (5.5)$$

$$n_{ILAs} = \sum_{\forall l_{ij} \in E} \chi_f \cdot \left\lceil \frac{|l_{ij}|}{d_{ILA}} \right\rceil \quad (5.6)$$

Numbers  $n_f$  and  $n_{ILAs}$  are found using Equations 5.5 and 5.6, respectively. Notation  $\chi_f$  represents the number of active fibers in link  $l_{ij}$  that physically connects node pair  $(i, j)$ . The length of the link  $l_{ij}$  is equivalent to  $|l_{ij}|$ . Notation  $d_{ILA}$  denotes the distance between two ILAs.

## 5.4 Problem framework

According to Equation 5.1, power consumption of the WDM layer of a BSN can be minimized by jointly reducing power consumption of I/O ports, regenerators, and amplifiers. To reduce power consumption of I/O ports and regenerators, it is necessary to switch and regenerate pass-through traffic directly at waveband granularity. This can be achieved by tightly group-

ing wavelengths into wavebands. Power consumption of the amplifiers can be minimized by appropriately assigning wavelengths and wavebands to reduce bandwidth waste. The power consumption minimization problem of a BSN can then be represented using the input parameters, constraints, and objective function presented in the following sub-sections.

#### 5.4.1 Input parameters

- $G = (V, E)$  : Graph with  $V$  set of nodes and  $E$  set of links
- $l_{ij}$  : Physical link connecting node  $i$  to node  $j$
- $|l_{ij}|$  : Physical length of link  $l_{ij}$  in km
- $T$  :  $|V| \times |V|$  traffic matrix
- $P$  : Set of node pairs with non-negative traffic between them
- $sd$  : Connection request (i.e., traffic demand) between nodes  $s$  and  $d$ .
- $t^{sd}$  : Number of wavelengths carrying traffic between node pair  $(s, d)$
- $p^{sd}$  : A feasible routing path for node pair  $(s, d)$  among many available paths (i.e., the length of link  $l_{ij}$  on  $p^{sd}$  is  $\leq$  optical reach of every lightpath).
- $h^{sd}$  : Set of nodes along path  $p^{sd}$  (excluding nodes  $s$  and  $d$ )
- $\phi_{ij}^{sd}$  : 1, if link  $l_{ij}$  is feasible on path  $p^{sd}$  (i.e., the shortest path from node  $i$  to  $j$  is  $\leq$  optical reach of the lightpath); else, 0.
- $\Upsilon$  : Power consumption of a transponder
- $\Psi$  : Power consumption of an AOR
- $\Omega$  : Power consumption of an mAOR ( $\Omega = (\Psi \cdot \text{BS} \cdot \nabla\%)$ )
- $\Gamma$  : Power consumption of an I/O port of the WXC/BXC/FXC layers
- $\Pi$  : Power consumption of an ILA
- $\Theta$  : Power consumption of a PrA/PoA
- $d_{\text{ILA}}$  : Distance between two amplifiers

- $\phi^{ij}$  : Number of amplifiers on a fiber in link  $l_{ij}$  (which is equal to  $\lceil |l_{ij}|/d_{ILA} \rceil$ )
- $F$  : Maximum number of fibers per link
- BS : Number of wavelengths per waveband (i.e., band size)
- $B$  : Number of wavebands per fiber
- $F_c$  : Maximum capacity of a fiber, defined in terms of traffic volume

#### 5.4.2 Notations

- $I^n$  : Set of input fibers to node  $n$  excluding the input fibers from local transponders
- $A^n$  : Set of input fibers from transponders carrying local traffic
- $O^n$  : Set of output fibers from node  $n$  excluding the output fibers to local transponders
- $D^n$  : Set of output fibers to local transponders carrying local traffic
- $IA^n$  : Total input fibers to node  $n$  (i.e.,  $I^n + A^n$ )
- $OD^n$  : Total output fibers from node  $n$  (i.e.,  $O^n + D^n$ )
- $I_f^{nm}$  : Input fiber  $f$  to node  $n$  connected from node  $m$
- $O_f^{nm}$  : Output fiber  $f$  from node  $n$  connected to node  $m$
- $w_b$  : Set of wavelengths in band  $b$ .
- $b_i$  : Set of wavebands in fiber  $i$ .
- $F_{ij}$  : Number of fibers used in link  $l_{ij}$
- $\lambda^n$  : Number of AORs used in the WXC layer of node  $n$
- $\rho^n$  : Number of mAORs used in the BXC layer of node  $n$
- $WXC^n, BXC^n, FXC^n$  : Number of I/O ports used in the WXC, BXC, and FXC layers of node  $n$ , respectively

### 5.4.3 Variables

- $t_{ijfw}^{sd}$  : 1, if wavelength  $w$  of node pair  $(s, d)$  is routed on fiber  $f$  in link  $l_{ij}$  (i.e.,  $\phi_{ij}^{sd} = 1$ ) on path  $p^{sd}$ ; else, 0.
- $r_w^{nsd}$  : 1, if wavelength  $w$  of node pair  $(s, d)$  is required to be regenerated at node  $n$  on path  $p^{sd}$ ; else, 0. These are pre-calculated based on the assigned line rate for every node pair  $(s, d) \in P$  at all nodes  $n \in V$ .
- $\theta_{ijb}^f$  : 1, if a non-empty waveband  $b$  travels through fiber  $f$  of link  $l_{ij}$ ; else, 0.
- $V_{iow}^{nsd}$  : 1, if node  $n$  serves traffic of node pair  $(s, d)$  on wavelength  $w$  travelling along  $p^{sd}$  from incoming fiber  $i$  to outgoing fiber  $o$ ; else, 0.
- $W_{iow}^n$  : 1, if node  $n$  adds/passes through/drops wavelength  $w$  at the WXC layer from incoming fiber  $i$  to outgoing fiber  $o$ ; else, 0.
- $B_{iob}^n$  : 1, if node  $n$  adds/passes through/drops waveband  $b$  at the BXC layer from incoming fiber  $i$  to outgoing fiber  $o$ ; else, 0.
- $F_{io}^n$  : 1, if node  $n$  adds/passes through/drops fiber  $i$  to outgoing fiber  $o$  at the FXC layer; else, 0.
- $FTB_i^n$  : 1, if input fiber  $i$  needs to be demultiplexed at node  $n$  ( $i \in I_n$ ); else, 0.
- $BTF_o^n$  : 1, if a waveband needs to be multiplexed into output fiber  $o$  at node  $n$  ( $o \in O_n$ ); else, 0.
- $BTW_{ib}^n$  : 1, if at node  $n$ , waveband  $b$  on input fiber  $i$  needs to be demultiplexed into wavelengths ( $i \in I_n$ ); else, 0.
- $WTB_{ob}^n$  : 1, if at node  $n$ , a wavelength needs to be multiplexed into waveband  $b$  of output fiber  $o$  at node  $n$  ( $o \in O_n$ ); else, 0.

### 5.4.4 Objective

The primary objective of the work undertaken in this chapter is to jointly reduce power consumption of I/O ports, regenerators, and fiber amplifiers. Following the notations defined

above, the objective can be represented in Equation 5.7 in the following manner.

$$\begin{aligned}
 \text{Minimize} \quad & \overbrace{2.\Gamma. \sum_n (WXC^n + BXC^n + FXC^n)}^{\text{Term 1: I/O ports}} \\
 & + \overbrace{\sum_n (\Psi.\lambda^n + \Omega.\rho^n)}^{\text{Term 2: Regenerators}} + \overbrace{\sum_{l_{ij}} F_{ij}(\Theta + \Pi.\phi_{ij})}^{\text{Term 3: Amplifiers}}
 \end{aligned} \tag{5.7}$$

Considering the symmetry of the MG-OXC, we assume that the number of input ports is equivalent to the number of output ports [146]. Thus, Term 1 includes a factor of 2. Term 2 calculates the power consumed by AORs and mAORs at every node  $n \in V$ . Term 3 calculates the power consumed by amplifiers on active fibers along every link  $l_{ij} \in E$ .

## 5.4.5 Constraints

### 5.4.5.1 Set of general constraints

As reported in [145, 146], the set of constraints on traffic flows, wavelength capacity, and wavelength continuity can be derived from the constraints of traditional RWA ILP formulations. Equation 5.8 ensures that a lightpath of node pair  $(s, d)$  cannot be added to or dropped from any other node except nodes  $s$  and  $d$ , respectively. Equations 5.9 and 5.10 guarantee that total  $t^{sd}$  is added to and dropped from nodes  $s$  and  $d$ , respectively. Equations 5.11 and 5.12 present the wavelength capacity constraints of every fiber. In this study, we assume that the WXC layer on every node is provisioned with dedicated AOWCs. Therefore, the wavelength continuity constraint is applied to traffic traversing the BXC (as in Equation 5.13) and FXC layers (as in Equation 5.14) only.

$$\sum_{i \in A^n, o \in O^n} V_{iow}^{nsd} = \sum_{i \in I^n, o \in D^n} V_{iow}^{nsd} = 0 \quad n \neq s, n \neq d, \forall w \quad (5.8)$$

$$\sum_{w, i \in A^n, o \in O^n} V_{iow}^{nsd} = t^{sd} \quad n = s, \forall w \quad (5.9)$$

$$\sum_{w, i \in I^n, o \in D^n} V_{iow}^{nsd} = t^{sd} \quad n = d, \forall w \quad (5.10)$$

$$\sum_{sd, i \in IA^n} V_{iow}^{nsd} \leq 1 \quad o \in O^n, \forall w \quad (5.11)$$

$$\sum_{sd, o \in OD^n} V_{iow}^{nsd} \leq 1 \quad i \in I^n, \forall w \quad (5.12)$$

$$\begin{aligned} \sum_{b \in b_i, i \in IA^m, o \in O_f^{mn}} V_{iow}^{msd} \cdot B_{iob}^m - \sum_{b \in b_i, o \in OD^n, i \in I_f^{nm}} V_{iow}^{nsd} \cdot B_{iob}^n \\ = 0 \quad \forall m, n, sd, w, f \end{aligned} \quad (5.13)$$

$$\begin{aligned} \sum_{i \in IA^m, o \in O_f^{mn}} V_{iow}^{msd} \cdot F_{io}^m - \sum_{o \in OD^n, i \in I_f^{nm}} V_{iow}^{nsd} \cdot F_{io}^m \\ = 0 \quad \forall m, n, sd, w, f \end{aligned} \quad (5.14)$$

#### 5.4.5.2 Constraints on regenerators

Equations 5.15 and 5.16 guarantee that the lightpaths of node pair  $(s, d)$  can only be regenerated at intermediate nodes on path  $p^{sd}$ . Equation 5.17 determines the number lightpaths regenerated at the WXC layer of node  $n$ . Equation 5.18 determines the usage of mAORs at the BXC layer of node  $n$ . Equation 5.19 ensures that regeneration of lightpaths of all node pairs is accounted for at node  $n$ .

$$r_w^{ssd} = 0 \quad \forall sd, w \quad (5.15)$$

$$r_w^{dss} = 0 \quad \forall sd, w \quad (5.16)$$

$$\rho^n \geq \sum_{i \in I^n, o \in O^n} \left[ \frac{\sum_{w \in w_b, sd} (r_w^{nsd} \cdot V_{iow}^{nsd} \cdot B_{iob}^n)}{\text{BS}} \right] \quad \forall n \quad (5.17)$$

$$\lambda^n \geq \sum_{i \in I^n, o \in O^n, w, sd} (r_w^{nsd} \cdot V_{iow}^{nsd} \cdot W_{iow}^n) \quad \forall n \quad (5.18)$$

$$(\text{BS} \cdot \rho^n) + \lambda^n \geq \sum_{sd, w} r_w^{nsd} \quad \forall n \quad (5.19)$$

### 5.4.5.3 Constraints on fibers

Equation 5.20 ensures that a fiber  $f$  of link  $l_{ij}$  does not exceed the maximum capacity of a fiber ( $F_c$ ). A fully- or partially-filled waveband  $b$  consumes  $k \cdot \text{BS}$  Gbps of fiber capacity, assuming that a wavelength travels at a line rate of  $k$  Gbps. Equation 5.21 determines the number of fibers used to carry wavebands in link  $l_{ij}$ . Equation 5.22 guarantees that the number of active fibers in link  $l_{ij}$  does not exceed the threshold  $F$ .

$$0 \leq F_c - \sum_{b \in b_f} (k \cdot \text{BS} \cdot \theta_{ijb}^f) \quad \forall f, l_{ij} \quad (5.20)$$

$$F_{ij} = \sum_{f \in [0, 1, \dots, F-1]} \left[ \sum_{b \in b_f} (k \cdot \text{BS} \cdot \theta_{ijb}^f) / F_c \right] \quad \forall l_{ij} \quad (5.21)$$

$$F_{ij} \leq F \quad \forall l_{ij} \quad (5.22)$$

### 5.4.5.4 Constraints on waveband switching

For waveband switching, the following additional constraints are required. Equations 5.23 to 5.27 ensure that (1) exactly 1 I/O port of each of the FXC, BXC, and WXC layers is used when a wavelength  $w$  of node pair  $(s, d)$  in band  $b$  is switched from incoming fiber  $i \in I^n$  to outgoing fiber  $o \in O^n$ ; (2) exactly 1  $F_{add}$ ,  $B_{add}$ , and  $W_{add}$  port will be used when a lightpath of node pair  $(s, d)$  is added from incoming fiber  $i \in A^n$  to outgoing fiber  $o \in O^n$ ; (3) exactly 1  $F_{drop}$ ,  $B_{drop}$ , and  $W_{drop}$  port will be used when a lightpath of node pair  $(s, d)$  is dropped from incoming fiber  $i \in I^n$  to outgoing fiber  $o \in D^n$ .

$$\begin{aligned} 1 &\geq F_{io}^n + B_{iob}^n + W_{iow}^n \\ &\geq \sum_{sd} V_{iow}^{nsd} \quad \forall w \in w_b, b \in b_i, i \in IA^n, o \in OD^n \end{aligned} \quad (5.23)$$

$$1 \geq F_{io}^n + \sum_{sd, o_1 \neq o} V_{io_1w}^{nsd} \quad \forall w, i \in IA^n, o \in OD^n \quad (5.24)$$

$$1 \geq F_{io}^n + \sum_{sd, i_1 \neq i} V_{i_1ow}^{nsd} \quad \forall w, i \in IA^n, o \in OD^n \quad (5.25)$$

$$1 \geq B_{iob}^n + \sum_{sd, o_1 \neq o} V_{io_1w}^{nsd} \quad \forall w \in w_b, i \in IA^n, o \in OD^n \quad (5.26)$$

$$1 \geq B_{iob}^n + \sum_{sd, i_1 \neq i} V_{i_1ow}^{nsd} \quad \forall w \in w_b, i \in IA^n, o \in OD^n \quad (5.27)$$

In addition, the constraint in Equation 5.28 ensures that a wavelength added/switched via the WXC layer travels through WTB and then BTF multiplexers before leaving node  $n$  via fiber  $o$ . Similarly, Equation 5.29 guarantees that a wavelength dropped/switched at the WXC layer of node  $n$  has to come through an FTB demultiplexer and then a BTW demultiplexer.

$$1 \geq BTF_o^n \geq WTB_{ob}^n \geq W_{iow}^n \quad \forall w \in w_b, o \in O^n, i \in IA^n \quad (5.28)$$

$$1 \geq FTB_i^n \geq BTW_{ib}^n \geq W_{iow}^n \quad \forall w \in w_b, o \in OD^n, i \in I^n \quad (5.29)$$

$$BTF_o^n \geq B_{iob}^n \quad \forall b \in b_i, o \in O^n, i \in IA^n \quad (5.30)$$

$$FTB_i^n \geq B_{iob}^n \quad \forall b \in b_i, o \in OD^n, i \in I^n \quad (5.31)$$

Equation 5.30 ensures that an added/passed-through waveband travels through the BTF multiplexer before leaving node  $n$  on output fiber  $o \in O^n$ . On the same note, Equation 5.31 constrains a dropped/passed-through waveband  $b$ , coming from the fiber  $i \in I^n$ , to travel through an FTB de-multiplexer before entering the BXC layer.

#### 5.4.5.5 Port numbers

The following set of equations determines the number of input ports at each switching layer of node  $n$ . Equation 5.32 determines the number of input ports of the WXC layer of node  $n$ , which includes the locally added/passed-through/dropped lightpaths. In Equation 5.33, the number of input ports is found by summing the added/passed-through/dropped wavebands and the wavebands coming from or going to WTB and BTW, respectively. Finally, the total number of input ports of the FXC layer is denoted by Equation 5.34, which takes into account added/passed-through/dropped and multiplexed/de-multiplexed fibers of node  $n$ .

$$WXC^n = \sum_{i \in IA^n, o \in OD^n, w} W_{iow}^n \quad \forall n \quad (5.32)$$

$$\begin{aligned} BXC^n &= \sum_{i \in IA^n, o \in OD^n, bo \in O^n, b} B_{iob}^n \sum WTB_{ob}^n \\ &+ \sum_{i \in I^n, b} BTW_{ib}^n \quad \forall n \end{aligned} \quad (5.33)$$

$$\begin{aligned} FXC^n &= \sum_{i \in IA^n, o \in OD^n} F_{io}^n + \sum_{o \in O^n} BTF_o^n \\ &+ \sum_{i \in I^n} FTB_i^n \quad \forall n \end{aligned} \quad (5.34)$$

Most researchers agree that solving ILP formulations becomes unmanageable as the size of the problem grows [30, 144, 146]. As explained in Section 4.4, the complexity of the ILP formulation is amplified by the stringent wavelength continuity constraint. Additional constraints pertaining to the different switching layers of MG-OXCs add extra complexity. Hence, heuristic algorithms are developed in this chapter to provide a practical solution to research problem 3.

#### 5.4.6 Existing heuristics

Balanced-Path routing with Heavy-Traffic first (BPHT) heuristic algorithm, proposed in [145, 146] is considered one of the most effective heuristics in optimizing an BSN. The BPHT algorithm has three stages and uses the INT grouping policy. In Stage 1, routing paths are assigned to every connection request using the Balanced-Path (BP) routing algorithm. Wavelengths are assigned to sorted connection requests (i.e., traffic demands) in Stage 2. In Stage 3, wavelengths are grouped into wavebands using the INT grouping policy.

Based on the foundation of the BPHT algorithm, Wang et al. [144] proposed the Hierarchical Waveband Assignment (HWA) algorithm. HWA accommodates fiber-tier traffic, band-tier traffic, and wavelength-tier traffic, in sequence. Results obtained show that a BSN optimized with HWA consumes fewer I/O ports than BPHT in both uniform and random traffic environments. However, neither the BPHT algorithm nor the HWA algorithm takes advantage of wavelength converters. The BPHT algorithm does not allow an assigned wavelength to be changed at a later stage. Accordingly, a wavelength that cannot be grouped with adjacent wavelengths cannot also be grouped with other wavelengths to form a waveband.

Graph-based heuristics are developed in [29, 30, 126, 153, 154, 157] to form wavebands in BSNs provisioned with the wavelength conversion capability. The Waveband Assignment with Path Graph (WAPG) heuristic, proposed in [29, 30], jointly minimizes traffic blocking probability and uses wavelength converters in a BSN serving dynamic traffic demands. Algorithms developed in [126, 153, 154, 157] can only be applied to BSNs employing HOXCs.

### 5.5 Balanced-Path Light-Splitting algorithm

To reduce power consumption of a BSN that employs three-layer MG-OXCs equipped with all-optical devices, we develop the BPLS algorithm in this study. The proposed algorithm in-

volve two stages. In Stage 1, routing paths are assigned to every connection request using the existing Balanced-Path (BP) routing algorithm. In Stage 2, connection requests are assigned wavelengths and grouped into wavebands. Given the initial network topology  $G$  and relevant design parameters, the proposed BPLS algorithm is expected to appropriately assign wavebands, thereby reducing the number of I/O ports, regenerators, and amplifiers used by the BSN. Each stage of the BPLS heuristic algorithm is explained below.

### 5.5.1 Stage 1: Balanced-Path routing

By routing traffic via shorter paths, the use of regenerators and amplifiers can be reduced. However, routing paths have to be carefully selected to ensure that links are not overwhelmed by traffic and that traffic is balanced across available links, or a failed link could disturb many traffic demands. Thus, routing paths are assigned in the following manner:

1. Find  $K$  short paths for every node pair  $(s, d)$  and sort them in ascending order of their respective hop count as  $p_1^{sd}, p_2^{sd}, p_K^{sd}$ . Let the number of hops along the shortest path be  $H^{sd}$ .
2. Let load on every link,  $l_{ab}$ , be measured as the number of lightpaths travelling through it. Let ML define the maximum link load among all links.
3. For the node pair with the largest  $H^{sd}$ , determine the shortest path from the sorted list  $p_1^{sd}, p_2^{sd}, p_K^{sd}$  which minimizes ML the most. If two or more paths (e.g.,  $p_1^{sd}$  and  $p_2^{sd}$ ) produce the same minimum ML, select the shortest path among them.
4. Repeat step 3 for every node pair until each is assigned a path.

### 5.5.2 Stage 2: Light-Splitting wavelength/waveband assignment

The BPLS algorithm assigns wavelengths and wavebands using Algorithms 4 and 5 proposed in this section. First, two virtual copies of the initial topology  $G$  is created, which are named the Lightpath Layer ( $LL$ ) and the Waveband Layer ( $WL$ ). Figure 5.3(i) shows the initial topology  $G$ . In the virtual topologies  $LL$  and  $WL$  (Figures 5.3(ii) - (iv)), node  $V_x$  represents a physical node  $x \in V$ . In the considered example, traffic flows from node  $s$  to nodes  $d$  and  $g$ .

Next, Algorithm 4 is adopted to create virtual lightpaths in topology  $LL$ . In  $LL$ , traffic between every node pair is represented using an end-to-end lightpath(s). For example, as shown in Figure 5.3(ii), in  $LL$ , the traffic between the node pairs  $(s, d)$  and  $(s, g)$  is accommodated via

virtual lightpaths  $\Lambda^{sd}$  and  $\Lambda^{sg}$ , respectively, along the pre-defined paths  $p^{sd}$  and  $p^{sg}$  found in Stage 1. Every node  $V_x \in LL$  possesses the wavelength conversion capability. Thus, an end-to-end lightpath,  $\Lambda^{sd}$ , that is assigned between a node pair  $(s, d)$  and traverses multiple nodes can be split into two or more lightpaths at any intermediate node (e.g., nodes  $V_f, V_g$ ). For example, lightpath  $\Lambda^{sd}$  can be split at node  $V_g$  into lightpaths  $\Lambda^{sg}$  and  $\Lambda^{gd}$ . After assigning virtual light-

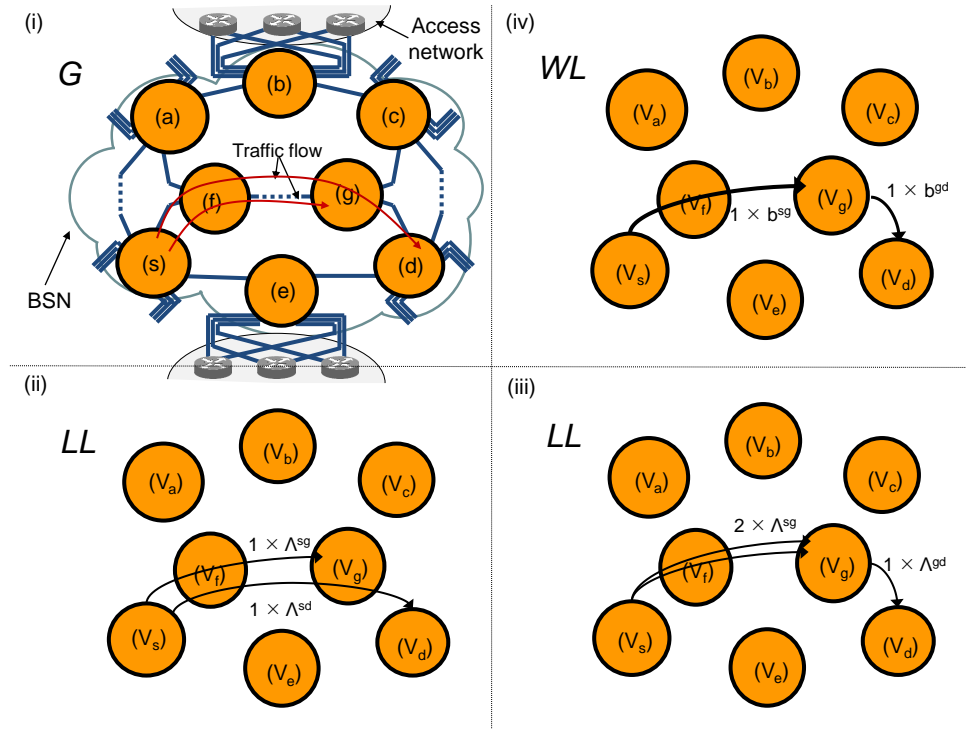


Figure 5.3: Representation of (i) the initial topology  $G$ , (ii) initial virtual topology  $LL$ , (iii) updated  $LL$ , and (iv) updated  $WL$

**Algorithm 4:** Assign virtual lightpaths for every node pair  $(s, d)$  in  $LL$

```

input : Virtual topology  $LL$ , traffic matrix, pre-determined routing paths
output: Updated  $LL$  assigned with end-to-end lightpaths

1 begin
2   for every node pair  $(s, d)$  do
3     while  $t^{sd}$  not empty do
4       Add a logical lightpath,  $\Lambda^{sd}$ , between nodes  $V_s$  and  $V_d$  along route
5          $p^{sd}$ ;
6         Update  $LL$ ;
7          $t^{sd} - = 1$ 
8     end
9   end

```

paths in  $LL$ , Algorithm 5 is adopted to assign wavelengths and group them into wavebands in

virtual topology  $WL$ . Every waveband has a uniform band size of BS. Therefore, if a waveband is partially-filled, the bandwidth of certain wavelengths is wasted [285].

In Algorithm 5, the variable  $b$  (initialized to be 0) is the index of the respective waveband from which the search starts for an available or unused waveband. Each waveband is formed by grouping adjacent wavelengths. For example, a waveband connecting nodes  $s$  and  $g$  are assigned adjacent wavelengths  $\lambda_i, \lambda_{i+1}, \dots, \lambda_{i+BS-1}$  in sequence. Let nodes within a selected route  $p^{sd}$  be denoted as  $s, s+1, s+2, \dots, d-2, d-1, d$ . Lightpaths that travel through nodes  $V_f$  and  $V_g$  along path  $p^{fg}$  in  $LL$  (e.g.,  $\Lambda^{sd}, \Lambda^{sg}$ ) are appended to list  $L^{fg}$ . A waveband assigned between nodes  $V_s$  and  $V_d$  in  $WL$  is denoted using notation  $b^{sd}$ . If the INT grouping policy is selected, Algorithm 5 involves 6 steps which are presented below. However, if the SE grouping policy is selected, Steps 4 and 5 are omitted.

1. Initialize an empty list  $SList$ . Sort node pairs in descending order of  $H^{sd}$  and append to list  $SList$ .
2. If two or more node pairs have identical  $H^{sd}$ , sort them in descending order of their respective  $t^{sd}$ .
3. Starting with the first node pair  $(s, d)$  in  $SList$ , use Algorithm 5 to create wavebands between node pair  $(s, d)$  along path  $p^{sd}$ .
4. Use Algorithm 5 to create wavebands between source node  $s$  and every other node along path  $p^{sd}$ , starting with node pair  $(s, d-1)$ , node pair  $(s, d-2), \dots$ , until node pair  $(s, s+2)$ .
5. Remove node pair  $(s, d)$  from  $SList$ . Repeat steps 3 and 4 with the remaining node pairs in  $SList$ .
6. Let the residual lightpaths in  $LL$  travel through each WXC along their designated routing path via single-hop wavebands.

The objective of Algorithm 5 is to group a maximum number of lightpaths in  $LL$  into wavebands with a minimum hop distance of two. Step 1 sorts node pairs according to hop distance along their designated routing path. Traffic between node pairs that travel a higher number of hops are fed first into Algorithm 5 to establish long wavebands. Step 2 is initiated to break ties between node pairs that travel an equal distance (i.e., an equal number of hops). Traffic

between a selected node pair  $(s, d)$  is first grouped into an end-to-end waveband(s) in Step 3. In Step 4, lightpaths that cannot be grouped into end-to-end wavebands are split and merged with other lightpaths of different node pairs into sub-path wavebands that terminate close to the destination node  $d$ . The  $LL$  topology is updated accordingly as shown in Figure 5.3(iii), and  $\Lambda^{sd}$  is grouped with  $\Lambda^{sg}$  into waveband  $b^{sg}$  as depicted in the  $WL$  topology in Figure 5.3(iv). After repeating Steps 3 and 4 with every node pair, the remaining lightpath(s) (e.g.,  $\Lambda^{gd}$ ) is aggregated into a single-hop, partially-filled waveband(s) (e.g.,  $b^{gd}$ ) in Step 6.

The BPLS algorithm can be explained using a simple example depicted in Figure 5.4. Figure 5.4(a) shows the  $LL$  and  $WL$  virtual topologies of a small-scale backbone network  $G$ . Assume that each link contains 4 fibers ( $F = 4$ ), each fiber has the capacity to carry 10 wavebands ( $B = 10$ ), and BS takes the value of 3. Traffic between node pairs  $(1, 5)$ ,  $(1, 4)$ ,  $(1, 3)$ ,  $(2, 5)$ ,  $(3, 5)$ , and  $(6, 4)$  is assumed to occupy 1, 1, 1, 1, 2, and 2 wavelengths, respectively. After determining the path of each traffic demand in Stage 1, Algorithm 4 assigns end-to-end lightpaths in  $LL$ . Note that each lightpath in  $LL$  represents traffic carried by a single wavelength. The node pairs are sorted and appended to  $SList$  in the order  $(1, 5)$ ,  $(6, 4)$ ,  $(2, 5)$ ,  $(1, 4)$ ,  $(1, 3)$ , and  $(3, 5)$  in Steps 1 and 2 of Algorithm 5.

In Step 3, the first node pair  $(1, 5)$  is selected from  $SList$  and evaluated using Algorithm 5. Since  $|L^{15}|$  is equal to 1, a waveband cannot be assigned between the node pair  $(1, 5)$ . Therefore, we move to Step 4, where the lightpaths  $\Lambda^{15}$ ,  $\Lambda^{14}$ , and  $\Lambda^{13}$  of list  $L^{13}$  are split and aggregated into a sub-path waveband. These lightpaths are removed from  $LL$  and waveband  $b^{13}$  is assigned between node pair  $(1, 3)$  in  $WL$ . New lightpaths  $\Lambda^{35}$  and  $\Lambda^{34}$  are added to  $LL$  as shown in Figure 5.4(b).

Next, the node pair  $(6, 4)$  is selected from  $SList$ . Since  $|L^{64}|$  and  $|L^{63}| < BS$ , a waveband cannot be assigned in Steps 3 and 4, respectively. Therefore, no change is made to  $LL$  and  $WL$ . The BPLS algorithm next selects node pair  $(2, 5)$  from  $SList$ . A sub-path waveband  $b^{24}$  is assigned in  $WL$  in Step 4 between node pair  $(2, 4)$  by aggregating  $2 \times \Lambda^{64}$  and  $1 \times \Lambda^{25}$  at node 2. This is accomplished by splitting lightpaths  $2 \times \Lambda^{64}$  at node 2 and lightpath  $\Lambda^{25}$  at node 4. New lightpaths,  $2 \times \Lambda^{64}$  and  $\Lambda^{45}$ , are added to  $LL$ .  $LL$  and  $WL$  are updated accordingly as illustrated in Figure 5.4(c). Since lightpaths do not exist between node pairs  $(1, 4)$  and  $(1, 3)$  in the updated  $LL$ , these node pairs are ignored. The final node pair  $(3, 5)$  is next selected by the BPLS algorithm. Since  $|L^{35}| = 3$ , a waveband is assigned, and  $LL$  and  $WL$  are updated as shown in Figure 5.4(d).

**Algorithm 5:** Assign wavebands between node pair  $(s, d)$ 

```

input :  $G, LL, WL, L^{sd}$ 
output: Updated  $LL, WL$ 

1 begin
2   while  $|L^{sd}| \geq BS$  do
3     Find a free band  $m$  starting with  $b$  along path  $p^{sd}$ ;
4     Initialize an empty list  $S^{sd}$ ;
5     if band  $m$  exists then
6       Starting with lightpaths sourced at node  $s$  (if available), extract
7       BS lightpaths from  $L^{sd}$  and append to  $S^{sd}$ ;
8       for every lightpath  $\Lambda^{qr}$  in  $S^{sd}$  do
9         if  $q == s$  and  $r == d$  then /* Same source same
10          destination */
11           Remove  $\Lambda^{qr}$  from  $LL$ ;
12         else if  $q! = s$  and  $r == d$  then /* Different source
13          same destination */
14           Split  $\Lambda^{qr}$  at node  $V_s$ ;
15           Remove  $\Lambda^{qr}$  from  $LL$ ;
16           Add  $\Lambda^{qs}$  and  $\Lambda^{sd}$  to  $LL$ ;
17           Replace  $\Lambda^{qr}$  with  $\Lambda^{sd}$  in  $S^{sd}$ ;
18         else if  $q == s$  and  $r! = d$  then /* Same source
19          different destination */
20           Split  $\Lambda^{qr}$  at node  $V_d$ ;
21           Remove  $\Lambda^{qr}$  from  $LL$ ;
22           Add  $\Lambda^{qd}$  and  $\Lambda^{dr}$  to  $LL$ ;
23           Replace  $\Lambda^{qr}$  with  $\Lambda^{sd}$  in  $S^{sd}$ ;
24         else if  $q! = s$  and  $r! = d$  then /* Different source
25          different destination */
26           Split  $\Lambda^{qr}$  at nodes  $V_s$  &  $V_d$ ;
27           Remove  $\Lambda^{qr}$  from  $LL$ ;
28           Add  $\Lambda^{qs}, \Lambda^{sd}$  &  $\Lambda^{dr}$  to  $LL$ ;
29           Replace  $\Lambda^{qr}$  with  $\Lambda^{sd}$  in  $S^{sd}$ ;
30       end
31       Group lightpaths in  $S^{sd}$  into band  $m$ ;
32       Add waveband  $m$  across nodes  $V_s$  and  $V_d$  in  $WL$  on route  $p^{sd}$ ;
33        $b = (m + 1) \% B$ ; /* Next band in the same fiber or
34       first band in next fiber */
35       Update  $LL$  and  $L^{sd}$ ;
36       Aggregate lightpaths in  $S^{sd}$  into waveband  $m$ ;
37       Add waveband  $m$  across nodes  $V_s$  and  $V_d$  in  $WL$  on path  $p^{sd}$ ;
38        $b = (m + 1) \% B$ ;
39       Update  $LL$  and  $L^{sd}$ ;
40     else
41       Increase  $F$  by 1 on links across path  $p^{sd}$  and go to While;
42     end
43   end
44 end

```

Since traffic is only added at nodes 1 and 6, traffic enters directly through FXC ports at these two nodes. Similarly, as node 5 only serves drop traffic, it does not require the service of the WXC and BXC layers.

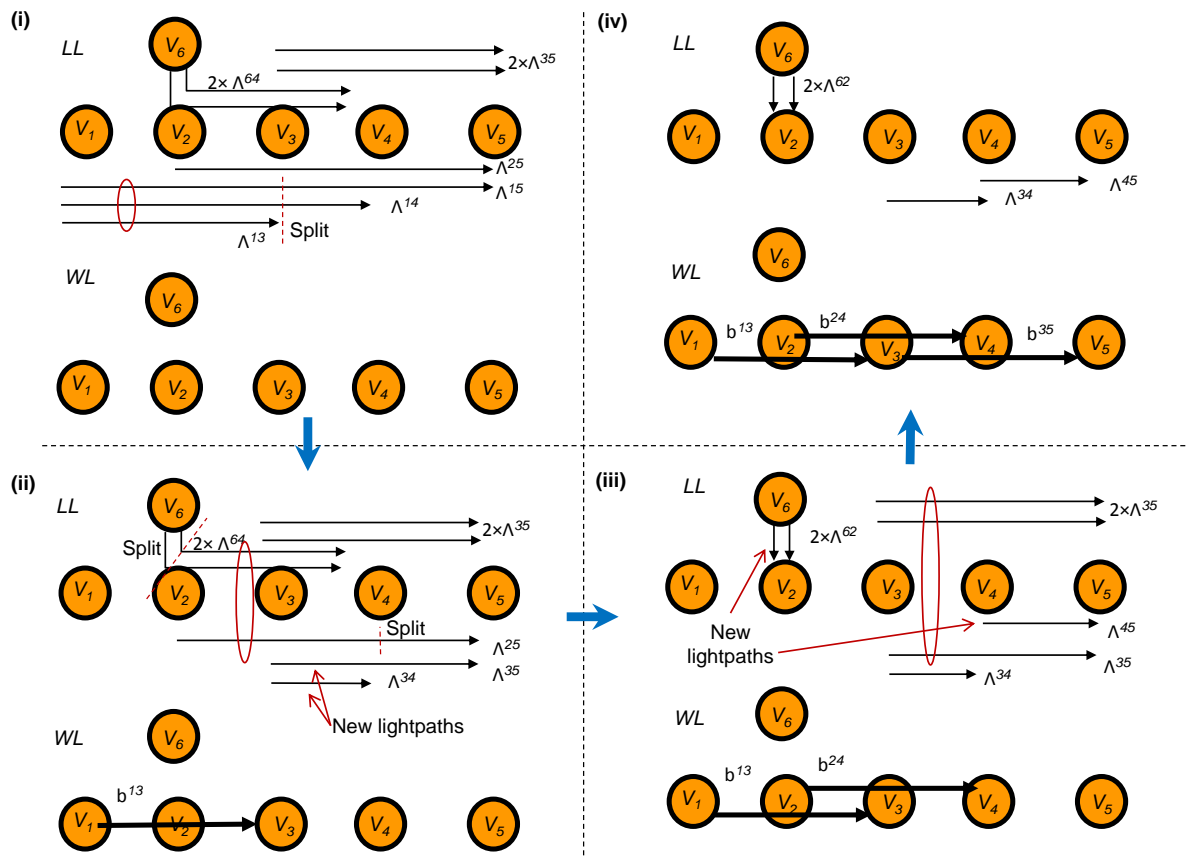


Figure 5.4: An illustrative example of waveband assignment using Algorithms 4 and 5

## 5.6 Evaluation of results

In this section, we compare power consumption of a BSN that employs advanced MG-OXCs with a WSN. Specifically, we analyse how design parameters, namely, BS, grouping policy, and band configuration affect power consumption of a BSN. To provide a general yet accurate analysis, the experiment is repeated on different-sized networks at different traffic volumes using different traffic distribution models.

Results are evaluated as a ratio of power consumption of BSN to WSN, as defined in Equation 5.35. It is desired that the BSN consumes less power than the WSN and, hence,  $Rt$  is

expected be small.

$$R_t = \frac{\text{Power consumed by the BSN}}{\text{Power consumed by the WSN}} \quad (5.35)$$

### 5.6.1 Experiment procedure

First, we analyze the impact of *BS* and *grouping policy* on power consumption. This first set of experiments is performed using C1 band configuration. The effects of C1 and C2 band configurations on power consumption are evaluated and compared separately at a later stage.

An experiment evaluates  $R_t$  for every possible combination of BS and grouping policy. The different combinations are shown in Figure 5.5. For simplicity's sake, a single combination of BS and grouping policy is denoted using the notation 'BG'. Every experiment is repeated (1) on different-sized networks, namely, the NSF (14 nodes and 21 links) and EON (28 nodes and 41 links) networks [277,278], (2) using separately two traffic distribution models, namely, uniform and gravity, (3) at different traffic volumes.

The experiments provide results in the form of number of I/O ports, regenerators, and amplifiers. By substituting these results into Equation 5.1, power consumption of a BSN can be found. Equation 5.35 is then used to calculate  $R_t$ . Results of the experiments are tabulated in Table 5.1 for every network, traffic volume, and traffic distribution model. For example, test result  $TS_{SE2}^{NU3}$  in Table 5.1 presents results obtained for the combination of SE grouping policy and BS of 2 (i.e., BG is *SE-BS2*) for the NSF network, using a uniform traffic model where traffic between every node pair is served using 3 wavelengths. Similarly,  $TS_{INT8}^{EG12}$  denotes results obtained when BG is *INT-BS8*, the test network is EON, and 12 wavelengths of traffic are distributed, on average, between all node pairs, using the gravity traffic distribution model.

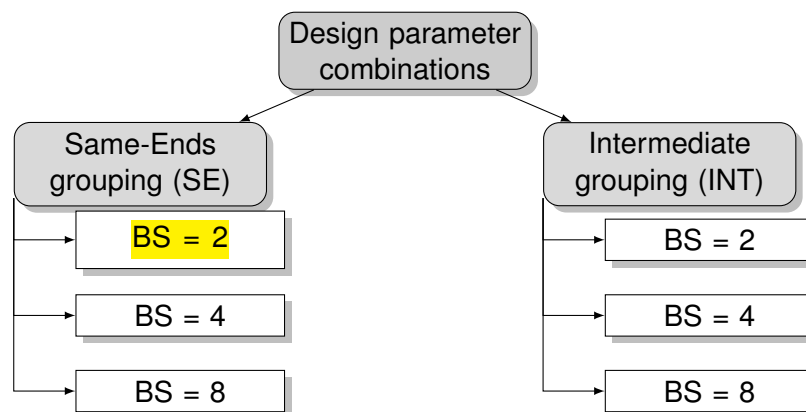


Figure 5.5: Different combinations of design parameters with BG = *SE-BS2* highlighted

Table 5.1: Testing every BG in Figure 5.5 with different networks, traffic models, and traffic volumes

		Traffic volume (Avg. no. of wavelengths)				
		3	...	12		
Network	NSFnet	$TS_{SE2}^{NU3}, TS_{INT2}^{NU3}, \dots$	...	...	Uniform	Traffic model
		...	...	...	Gravity	
	EON	...	...	...	Uniform	
		...	...	$TS_{SE2}^{EG12}, \dots, TS_{INT8}^{EG12}$	Gravity	

### 5.6.2 Input parameters

In this thesis, the number of fibers in a link ( $F$ ) and the number of wavelengths in a fiber ( $W$ ) are assigned values of 4 and 256, respectively. These values were selected based on the work of Saleh et al., [53], recent findings in [203], and the following rationale. According to Infinera [203], in the near future, an optical fiber would be capable of transporting 1.6 Tbps to 8 Tbps traffic in one direction. When fibers possess such high capacities, Saleh et al., [53] suggest that the total traffic of a link could be accommodated using just a single fiber. However, to overcome capacity bottlenecks of the future, it is preferable to equip every link with at least two fibers [53]. To provide resilience against fiber failures, every fiber could then be complimented with an additional backup fiber. This strategy would then increase the number of fibers in a link to a minimum of 4. If each fiber accommodates 2.6 Tbps (a value between 1.6 Tbps and 8 Tbps) of traffic, then a total of 256 wavelengths of 10 Gbps could be transported along a single fiber.

Power consumption of network devices is reported in Table 5.2. Discrepancies are observed in the reported power consumption of the same device in different studies. In [101, 163], the authors report that an OXC consisting of 1000 I/O ports consumes 8 kW of power (8 W per I/O port), while the authors of another study [28] report that an optical I/O port consumes 6 W of power. Taking note of these differences, in this study, an I/O port is assumed to consume 7 W of power (a value between 6 and 8). Power consumption of a single-wavelength AOR and amplifiers is derived from the work of [46–48] and [18, 44], respectively. Taking a conservative approach, an mAOR that can simultaneously regenerate BS number of wavelengths is assumed

to consume 25% less power than the product of BS and total power consumption of AORs. Thus, in Equation 5.1, notation  $\nabla$  is assigned a value of 25.

Table 5.2: Power consumption of network devices

Device	Notation	Capacity	Power consumption
I/O port	$\Gamma$	Per port (inclusive of PrAs/PoAs, add/drop multiplexers, modules for termination of the OSC, and control circuitry)	$\approx 7$ W [28,101]
AOR	$\Psi$	Per wavelength	50 W [46–48]
PrA/PoA	$P_{PrA}, P_{PoA}$	Per fiber	30 W [18,44]
ILA	$P_{ILA}$	Per fiber, at every 80 km	25 W [18,44]

### 5.6.3 General trend

Figures 5.6 and 5.7 depict  $Rt$  obtained for every combination (BG) of BS and grouping policy on the NSF network at different traffic volumes (measured in terms of the average number of wavelengths between a node pair) distributed using the uniform and gravity models, respectively. Similarly, Figures 5.8 and 5.9 depict  $Rt$  for every BG on the EON at different traffic volumes distributed using the uniform and gravity models, respectively. In Figures 5.6 to 5.9, the following general trends are observed.

Regardless of network type (NSF or EON) and traffic model (uniform or gravity),  $Rt$  for every BG declines as traffic volume increases. However, the rate of reduction in  $Rt$  for every BG decreases as traffic volume increases. Steep fluctuations are observed in Figures 5.6 and 5.8 when traffic is uniformly distributed.

The plotted results in Figures 5.6 to 5.9 show that the BSN consumes 40%-80% less power than the WSN when the network is loaded with a high traffic volume. Translating these  $Rt$  ratios into actual power savings, the BSN reduces power consumption by a maximum of 177 kW and 323 kW over the WSN when traffic is distributed in the NSF network using uniform

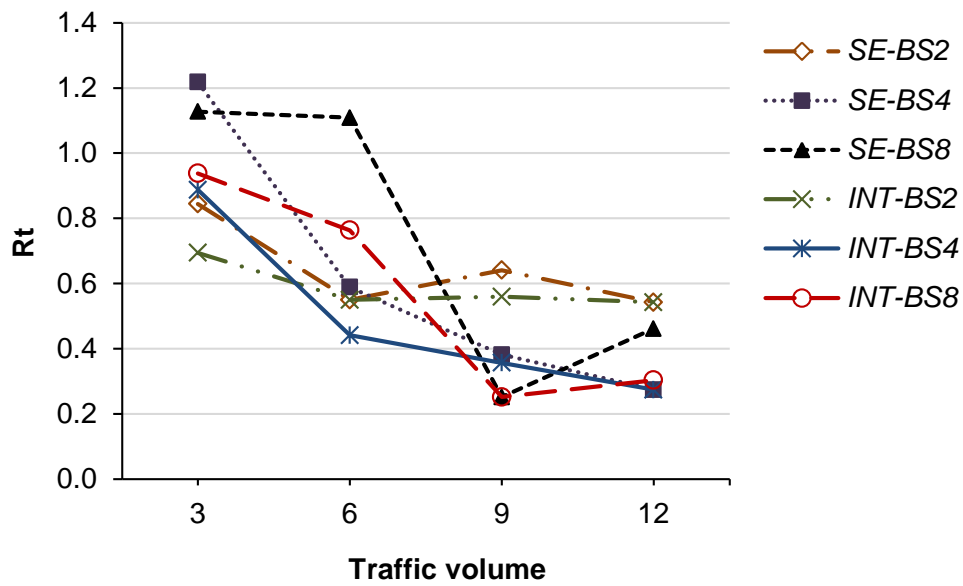


Figure 5.6:  $Rt$ , obtained for different combinations of band size and grouping policy (i.e., BG) on the NSF network with a **uniform** traffic model, plotted against increasing traffic volume

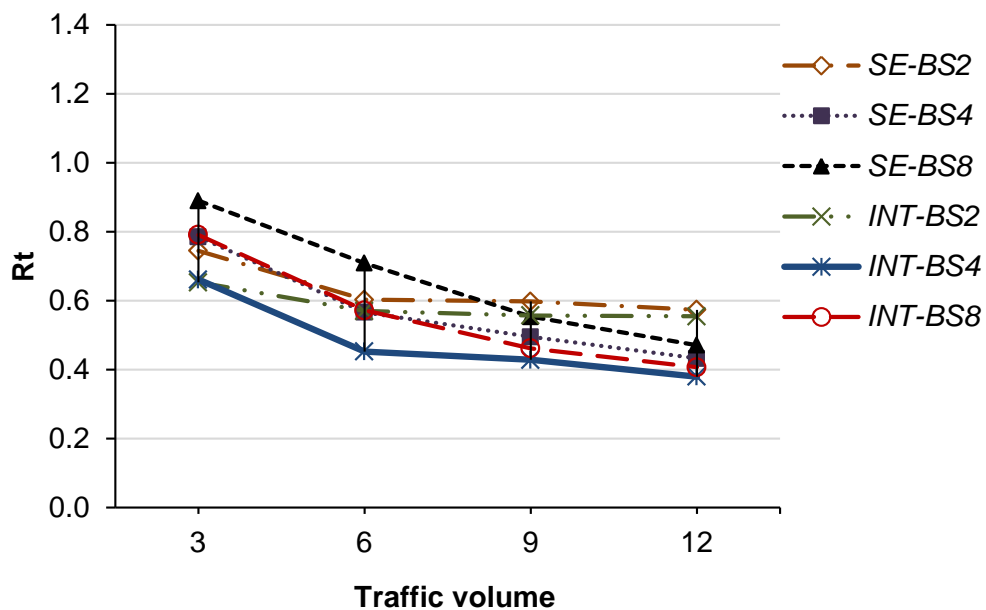


Figure 5.7:  $Rt$ , obtained for different BG on the NSF network with a **gravity** traffic model, plotted against increasing traffic volume

and gravity traffic models, respectively. Similarly, the BSN consumes 802 kW and 606 kW less power than the WSN, when tested on the EON using uniform and gravity traffic models, respectively.

In general, the plotted results in Figures 5.6 to 5.9 indicate that different combinations of BS

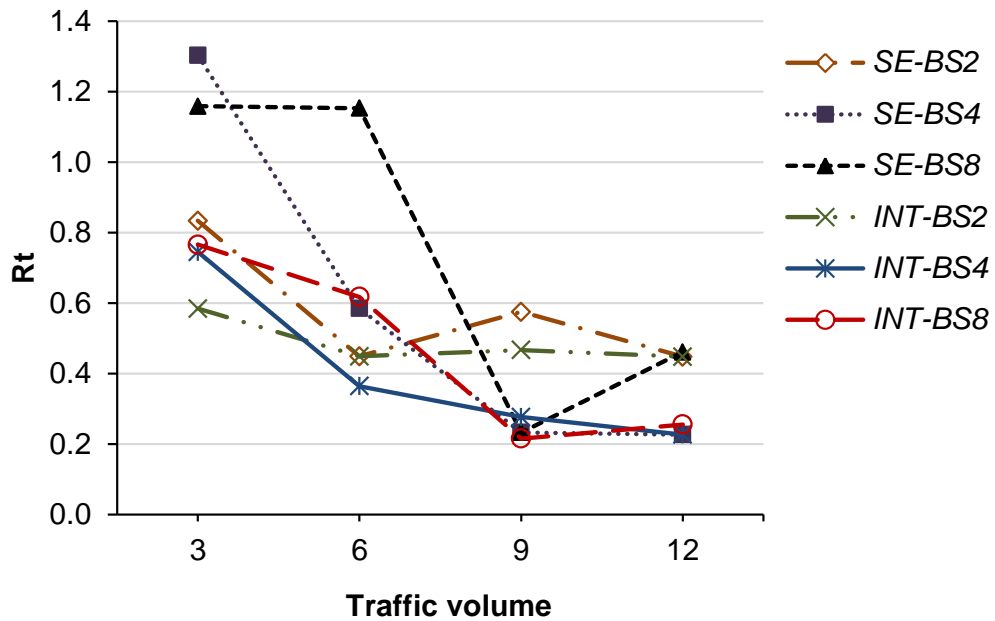


Figure 5.8:  $R_t$ , obtained for different BG on the EON network with a **uniform** traffic model, plotted against increasing traffic volume

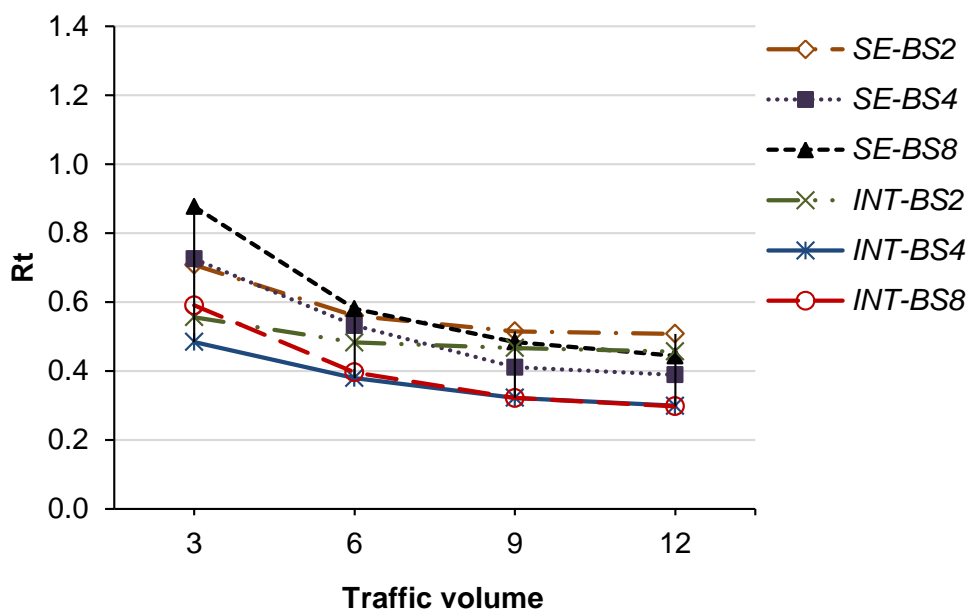


Figure 5.9:  $R_t$ , obtained for different BG on the EON network with a **gravity** traffic model, plotted against increasing traffic volume

and BG produce dissimilar  $R_t$  (the ratio of power consumption of BSN over a WSN). BS and BG are two critical design parameters that determine how efficiently wavebands can be formed and how far a waveband can travel before being de-multiplexed into individual wavelengths.

With certain combinations of BS and BG, BSNs consume significantly less power (lower  $R_t$ ) over WSN. This indicates that BS and BG have an impact on power consumption of a BSN. The following sections explain the effect of BS and BG, individually, on power consumption of a BSN. As will be explained in these sections, BS has to be selected according to actual traffic demand to increase end-to-end waveband forming and avoid single-hop wavebands. Similarly, grouping policy (i.e., BG) has to be selected accordingly to let wavebands travel a longer distance without the need for excessive multiplexing and de-multiplexing. The results indicate that, by appropriately selecting BS and grouping policy, power consumption of a BSN can be significantly reduced over a WSN.

#### 5.6.4 Impact of BG on different-sized networks

Figures 5.10 and 5.11 depict  $R_t$  averaged over the entire range of traffic volumes distributed using uniform and gravity models, respectively.  $R_t$  in Figures 5.10 and 5.11 is plotted against the respective BG for both NSF and EON networks, respectively. Both figures show that the NSF and EON networks exhibit a similar trend. With either network, peaks and troughs are observed when BG is *SE-BS8* and *INT-BS4*, respectively. The BSNs provide less power savings when SE is used instead of the INT grouping policy.

While these similarities are observed, average  $R_t$  differs between the NSF and EON networks for identical BGs. Between the NSF and EON networks, the latter produces higher power savings (lower average  $R_t$ ) for every BG. Differences in average  $R_t$  between the two networks is much clearer with the INT grouping policy. Based on these observations, we deduce that the BSN provides higher power savings in EON than in the NSF network. The  $R_t$  of EON also appears to be slightly more sensitive to BG (plotted results show greater variation) in comparison to that of the NSF network.

The difference in power savings of the EON and NSF networks could be attributed to network size. The EON accommodates more core nodes than the NSF network. In backbone networks containing a large number of core nodes (i.e., a large network like EON), lightpaths travel, on average, a much longer distance than in networks with fewer core nodes. For example, in [277,278], average hop distance in the EON and NSF networks is reported to be 3.56 and 2.14, respectively. As the average hop distance in EON is larger, traffic has to pass through a higher number of intermediate OXCs. Then, if WSN is used in the EON, the network will consume a substantial amount of power due to the excessive use of I/O ports and AORs. On

the other hand, if wavelengths in the EON are aggregated into wavebands using BSN, traffic in EON could be switched using fewer I/O ports and regenerated using fewer mAORs, thus providing more power savings over WSN. However, in the NSF network, as the average hop distance is smaller compared to EON, using BSN would not provide as significant a power saving as in the larger network of EON. Therefore, the larger the network, BSN is able to provide greater power savings.

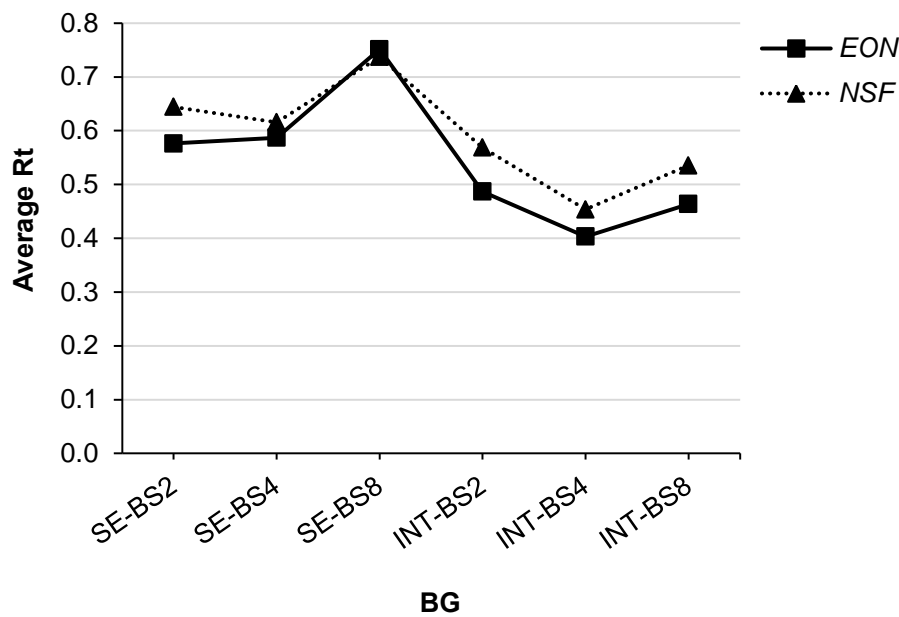


Figure 5.10:  $R_t$ , averaged over the range of traffic volumes distributed using the **uniform** traffic model, plotted against every BG on the NSF and EON networks

### 5.6.5 Impact of BG on different traffic models

In this section, we examine the impact of BG on power consumption of a BSN whose traffic is distributed using different traffic models.

Averaged  $R_t$  varies between 0.4 and 0.75 in Figure 5.10 and between 0.4 and 0.6 in Figure 5.11. The variation in  $R_t$ , across the range of BG, fluctuates more when traffic is distributed using the uniform rather than gravity traffic model. Hence, power consumption of the BSN is more sensitive to BG when a uniform traffic model is used.

If uniform traffic distribution models are used, traffic between every node pair is assigned an equal number of wavelengths. At high traffic volumes, a large number of wavelengths carry traffic between node pairs that are situated farther apart. If these wavelengths cannot be

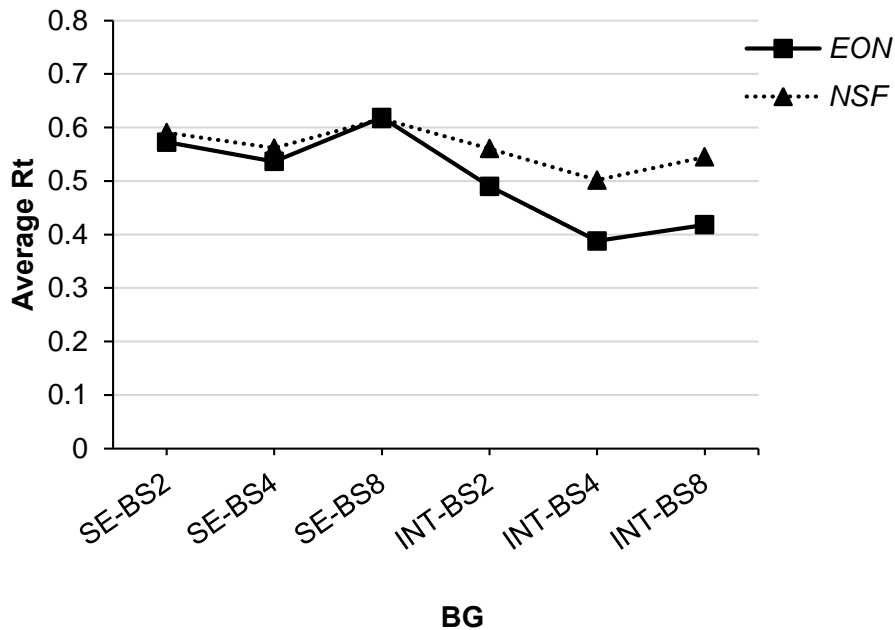


Figure 5.11:  $Rt$ , averaged over the range of traffic volumes distributed using the **gravity** traffic model, plotted against every BG in the EON and NSF networks

grouped into end-to-end wavebands, the SE grouping policy would result in increased power consumption due to excessive I/O port use at intermediate nodes. However, if the INT grouping policy is used, wavelengths would be efficiently grouped into sub-path wavebands. Consequently, INT would offer more power savings over SE, especially at high traffic volumes, when the uniform traffic distribution model is used.

In contrast, if the gravity traffic distribution model is used, nodes situated in close proximity to each other are assigned heavy traffic (more wavelengths), and nodes situated farther apart are assigned light traffic (fewer wavelengths). As a result, even at high traffic volumes, heavy traffic has to only travel through a smaller number of intermediate core nodes. Unlike with a uniform traffic model, the INT grouping policy is then unable to provide a significant reduction in the use of I/O ports and AORs over SE. This explains why average  $Rt$  shows reduced variation across BG when the gravity traffic model is used in Figure 5.11.

### 5.6.6 Effect of grouping policy

We now examine the impact of waveband grouping policy on the power consumption of a BSN network.

By observing the plotted results in Figures 5.6 to 5.9, it is evident that the BSN optimized

with the INT grouping policy consumes less power than when optimized with SE. To provide a more accurate comparison, we depict  $R_t$  of the NSF network optimized with SE and INT grouping policies, when  $BS = 4$ , using the uniform and gravity traffic models in Figures 5.12 and 5.13, respectively. By plotting the graphs for a single band size these two figures, we are able to isolate the effect of waveband grouping policy and, in turn, enable a clearer comparison of the networks optimized with the two grouping policies.

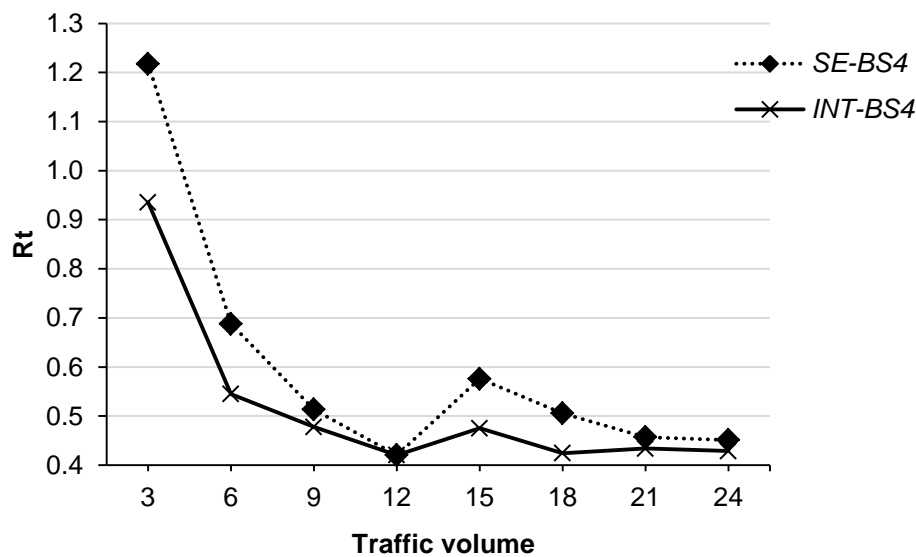


Figure 5.12:  $R_t$  of combinations *SE-BS4* and *INT-BS4* plotted against increasing traffic volumes on the NSF network using the **uniform** traffic model

In Figure 5.12, when a uniform traffic model is used, SE and INT grouping policies produce identical or near-identical  $R_t$  values at certain traffic volumes. For example, when traffic volume is 12 and 24, the  $R_t$  of *SE-BS4* and *INT-BS4* coincide, because traffic volumes are integer multiples of the band size, ( $BS = 4$ ). When traffic volume is an integer multiple of the band size, every traffic demand can be accommodated using only end-to-end wavebands with either SE or INT grouping policy. Although not shown in Figure 5.12, similar to the outcome at traffic volumes of 12 and 24, the  $R_t$  values of *SE-BS4* and *INT-BS4* can be expected to coincide at traffic volumes 4, 8, 16, and 20 as they are integer multiples of the band size, ( $BS=4$ ).

In both Figures 5.12 and 5.13, it is observed that the difference in  $R_t$  between SE and INT grouping policies narrows as the traffic volume increases. For example, in Figure 5.13, when traffic volume is 3, the difference of  $R_t$  between SE and INT is approximately 0.1, which then reduces to 0.03 as traffic volume increases to 24. A similar shrinking pattern is observed in Fig-

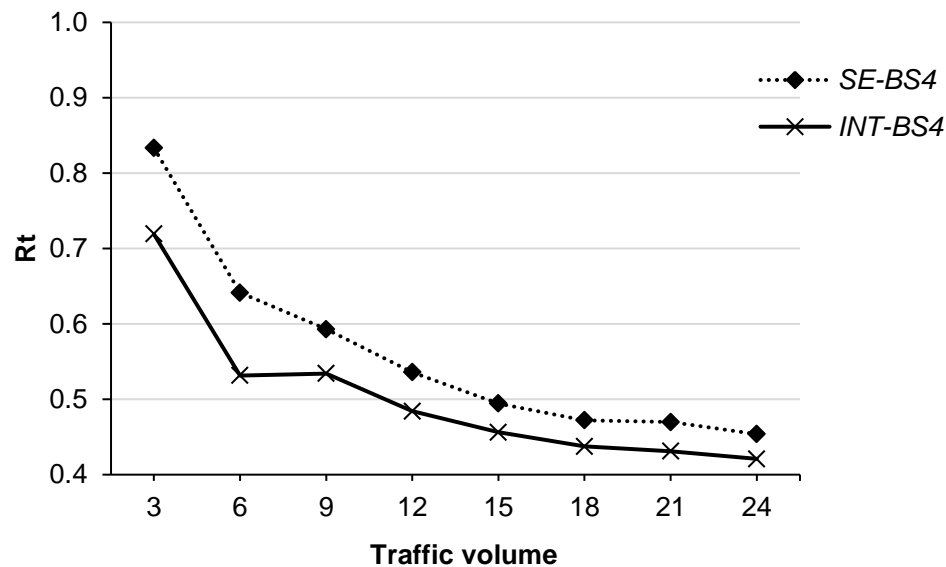


Figure 5.13:  $R_t$  of combinations *SE-BS2* and *INT-BS2* plotted against increasing traffic volumes on the NSF network using the **gravity** traffic model

ure 5.12. The reason for the decreasing gap in  $R_t$  between the two grouping policies, as traffic volume increases, can be explained using Figure 5.14. This figure plots power consumption of the individual network devices in the NSF network using SE and INT grouping policies and a uniform traffic distribution model. Note that power consumption of amplifiers is not depicted in Figure 5.14 due to a lack of observable difference between the grouping policies.

In Figure 5.14, it is observed that devices consume less power when the INT grouping policy is used. Since INT encourages wavebands to be assigned between both end-to-end and intermediate nodes, most traffic passes through the BXC of each intermediate node directly, without entering the WXC. This not only minimizes multiplexing, de-multiplexing, and wavelength conversion, but also allows wavebands to be regenerated using mAORs instead of multiple AORs. As a result, WXC and T-AOR (i.e., sum of AORs and mAORs) consume 5 kW and 10 kW less power, on average, with INT than with SE. However, the difference in power consumption between INT and SE for BXC, FXC, and AOWCs is insignificant.

At low traffic volumes, BXC, WXC, and T-AOR are the dominant power-consuming devices, irrespective of the grouping policy used. However, as these devices consume less power with INT than SE at both high and low traffic volumes, the difference in power consumption between INT and SE is significant for these devices. Compared to high traffic volumes, at low traffic volumes, this difference is more significant relative to total power consumption when SE

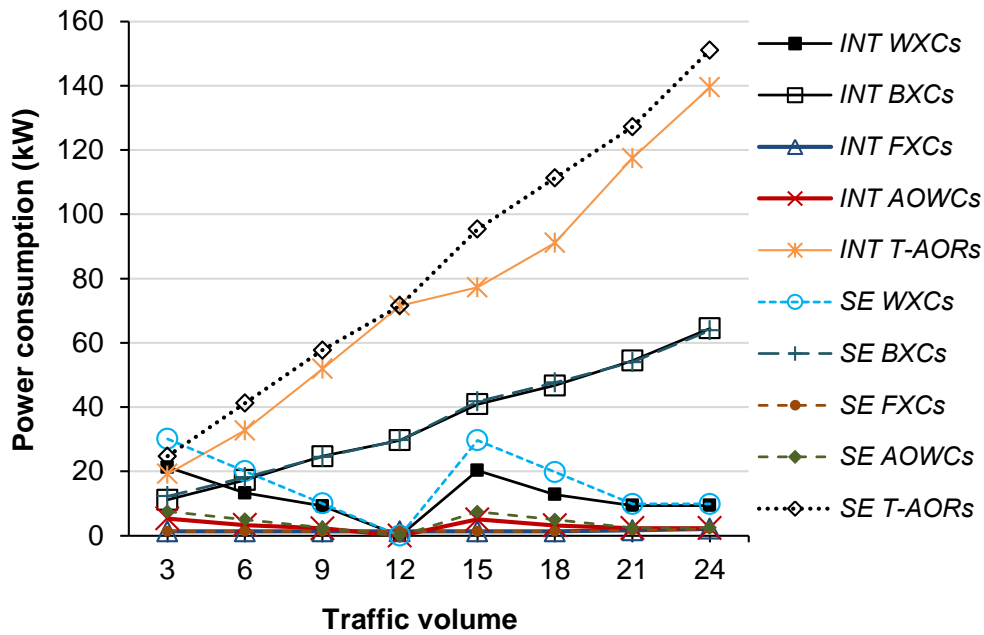


Figure 5.14: Device power consumption plotted against increasing traffic volume for each grouping policy on the NSF network, using a **uniform** traffic model

is used.

The difference in power consumption between the SE and INT grouping policies is also dependent on BS. The graphs in Figures 5.10, and 5.11 show that, regardless of the network and traffic distribution model used, INT is more power-efficient than SE, particularly when BS is large (e.g., BS = 8). When BS is small (e.g., BS = 2), the difference in power consumption between the two policies is relatively small. With a small BS, most traffic is grouped into end-to-end wavebands. Thus, INT can only provide marginal savings of I/O ports in the WXC layers in comparison to SE. On the other hand, when BS is large and traffic volume is not equal to an integer multiple of BS, a considerable number of wavelengths cannot be grouped into end-to-end wavebands. By grouping these wavelengths into sub-path wavebands, INT can significantly reduce the use of I/O ports and AORs at the WXC layers significantly when BS is large. Thus, the difference between power savings of INT and SE grouping policies widens with larger BS.

Based on our results and discussion, we conclude that the INT grouping policy consumes less power than the SE grouping policy with any network, traffic model, and band size at most traffic volumes.

### 5.6.7 Effect of band size

We now assess the impact of BS on power consumption. Figure 5.15 plots  $R_t$  for *INT-BS2*, *INT-BS4*, and *INT-BS8* against uniformly distributed traffic in the NSF network. In Figure 5.16,  $R_t$  for *SEBS2*, *SE-BS4*, and *SE-BS8* is plotted against increasing traffic volumes distributed using the gravity model in the NSF network. In each of these figures, the network, grouping policy, and traffic model are kept constant to isolate the impact of band size on power consumption.

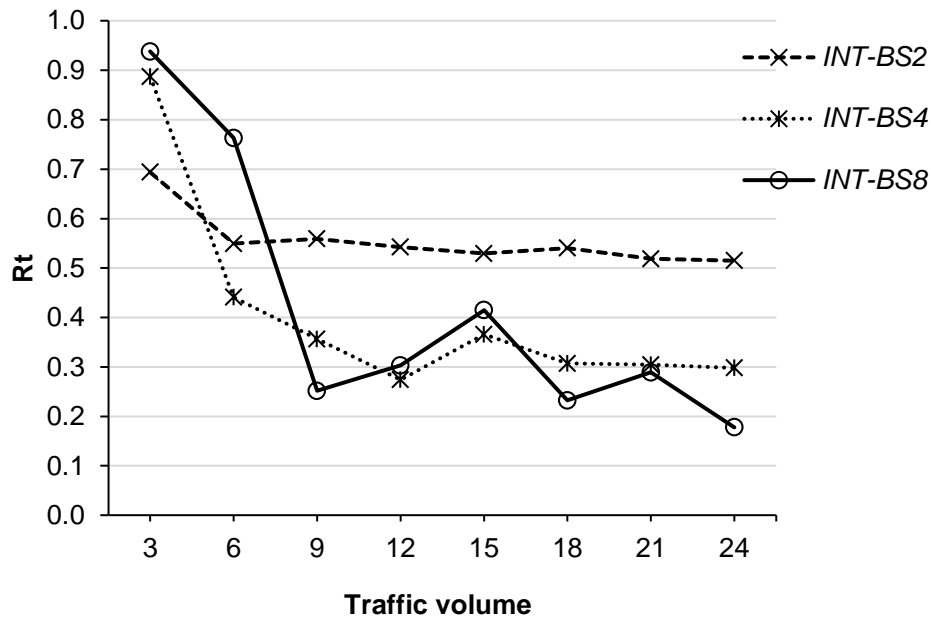


Figure 5.15: Power savings of a BSN using the INT grouping policy with respect to *different BS* and a **uniform** traffic model on the NSF network

In Figure 5.15 and, to a lesser extent, in Figure 5.16, a sharp decline is observed in the plotted lines when traffic increases from low to moderate volumes. For example,  $R_t$  of *INT-BS4* drops from 0.9 to 0.42 as traffic volume increases from 3 to 6. Recall that traffic volume is the average number of wavelengths assigned between every node pair. When traffic volume is smaller than BS, most traffic passes through the WXC layer of intermediate nodes as end-to-end wavebands cannot be assigned. For example, for *INT-BS4*, end-to-end wavebands cannot be assigned when traffic volume is less than 4. When traffic volume exceeds BS, a large percentage of traffic is accommodated via end-to-end wavebands. As a result, when traffic increases from 3 to 6 (exceeds 4), a rapid decline in  $R_t$  is observed for *INT-BS4* as a result of the reduction in use of I/O ports and AORs at intermediate nodes.

In Figures 5.15 and 5.16, when traffic volume is at its lowest at 3,  $R_t$  of *INT-BS2* and *SE-BS2*,

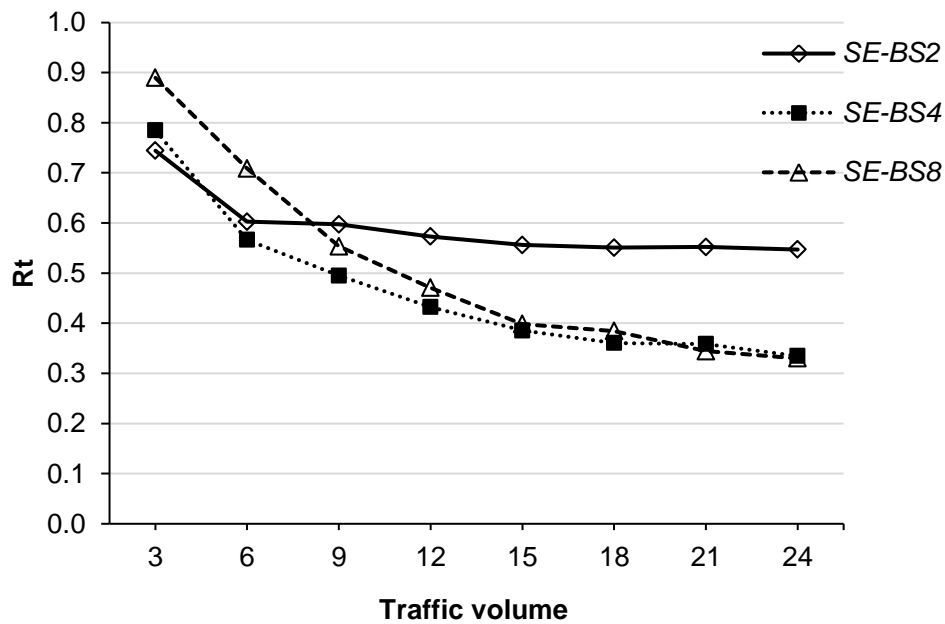


Figure 5.16: Power savings of a BSN using the **SE** grouping policy with respect to *different BS* and a **gravity** traffic model on the **NSF** network

respectively, is smaller than that of other combinations. Contrarily, at peak traffic volume, the smallest  $R_t$  is obtained for *INT-BS8* and *SE-BS8*. We could then argue that, to reduce power consumption, a small BS should be chosen when the network is serving low traffic volumes and a large BS when the network is serving peak traffic volumes.

By selecting a small BS (e.g.,  $BS = 2$ ), most traffic can be grouped into end-to-end wavebands and can, thus, be served using fewer I/O ports and AORs. As a result, especially when traffic volume is low,  $R_t$  of *INT-BS2* and *SE-BS2* is significantly smaller than that of other combinations. However, if a large band size is selected (e.g.,  $BS = 8$ ), end-to-end wavebands cannot be assigned with low traffic volumes. A large percentage of traffic would then traverse the BXC and WXC layers of intermediate nodes, consuming more I/O ports. As a result,  $R_t$  of *INT-BS8* and *SE-BS8* is larger than the  $R_t$  for other combinations when traffic volume is low.

At high traffic volumes, a large percentage of traffic can be accommodated via end-to-end wavebands with both small and large BS. A small BS produces a large number of end-to-end wavebands at high traffic volumes. These wavebands would consume a significant number of I/O ports at the BXC layers of the intermediate nodes. Conversely, if a large BS is selected, at high traffic volumes, traffic can be served using a smaller number of wavebands, thus using fewer I/O ports at the BXC layers. Therefore, when the BSN is serving high traffic volumes,

the smallest  $Rt$  is obtained for combinations with a large BS (e.g., *INT-BS8* and *SE-BS8*).

### 5.6.8 Effect of band configurations

As described in Section 5.2, a uniform BSN could be implemented with either C1 or C2 configurations. While C1 increases fiber and wavelength utilization, C2 reduces multiplexing and de-multiplexing at intermediate nodes. We now analyze the power consumption of BSNs implemented with these configurations.

When C1 is selected, wavelengths that cannot be grouped into a waveband, with a minimum hop distance of two, pass through WXC's and are regenerated by AORs at intermediate nodes. On the other hand, if C2 is selected, residual wavelengths are grouped into partially-filled wavebands. These partially filled wavebands pass through BXC's and are regenerated by mAORs at intermediate nodes. Recall that, in Section 5.3.2, power consumption of an mAOR is assumed to be a function of BS. Therefore, regardless of waveband utilization (fully or partially-filled), an mAOR is considered to consume a constant amount of power.

To compare the two configurations, simulations are performed on the NSF network. As projected in [12], the total IP traffic in North America will reach 28 exabytes per month (11 Tbps) by the year 2016 and will continue to grow at 22% every year. Using these predicted values, the Internet traffic in North America is estimated to grow from 5 Tbps to approximately 20 Tbps between the years 2012 and 2020. Therefore, total network traffic is varied between 5 Tbps and 20 Tbps and is distributed among the nodes using the gravity traffic model.

Every BG is separately tested with C1 and C2 configurations. When wavebands are assigned in the BSN with the C2 configuration, Step 6 of the BPLS algorithm is replaced with the following step:

6. Identify the residual lightpaths in  $LL$  that cannot be grouped into wavebands with a minimum distance of two hops. Group these lightpaths into partially-filled end-to-end wavebands.

The obtained results are plotted in Figures 5.17, 5.18, and 5.19 that illustrate, for every BG, total power consumption of the MG-OXC's and amplifiers, power consumption of the MG-OXC's only, and power consumption of the amplifiers only, respectively. Power consumption of the MG-OXC's is calculated as the sum of power consumed by the I/O ports of the three layers and AORs. Power consumption of the amplifiers is measured as the total power consumed by PrAs,

PoAs, and ILAs. Results shown in Figure 5.17 indicate that, with C1 band configuration, MG-

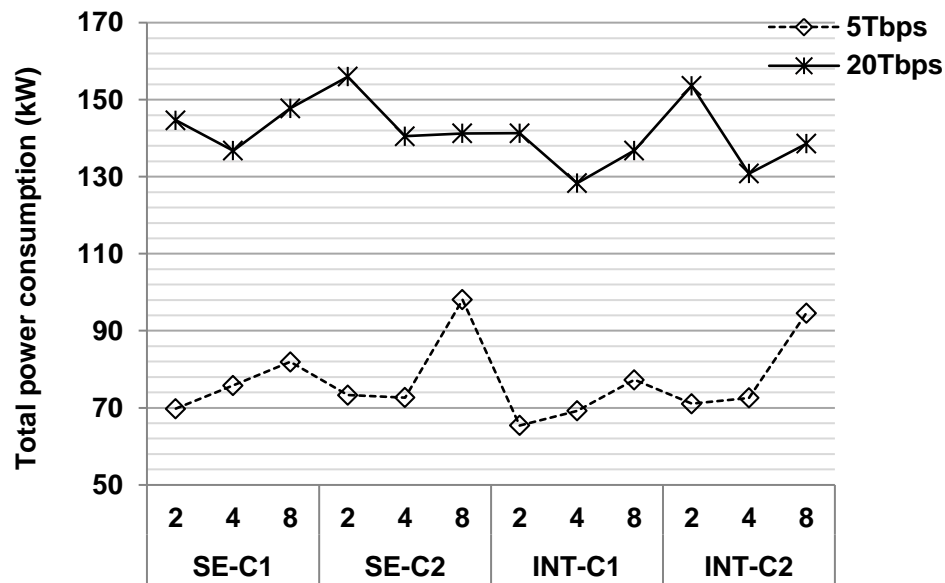


Figure 5.17: Total power consumption of the MG-OXCs and amplifiers, using SE and INT grouping policies with C1 and C2 configurations, plotted against three band sizes

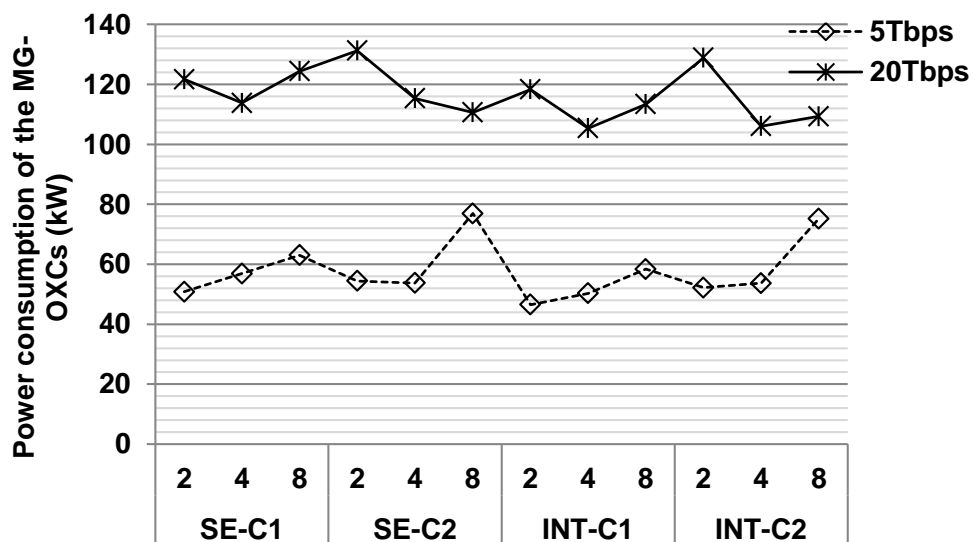


Figure 5.18: Power consumption of the MG-OXCs, using SE and INT grouping policies with C1 and C2 configurations, plotted against three band sizes

OXC and amplifiers combined consume less power with either grouping policy at most band sizes. The only two occasions where total power consumption with C2 is marginally less than with C1 are when the SE grouping policy is paired with BS = 4 and BS = 8 for 5 Tbps and 20 Tbps

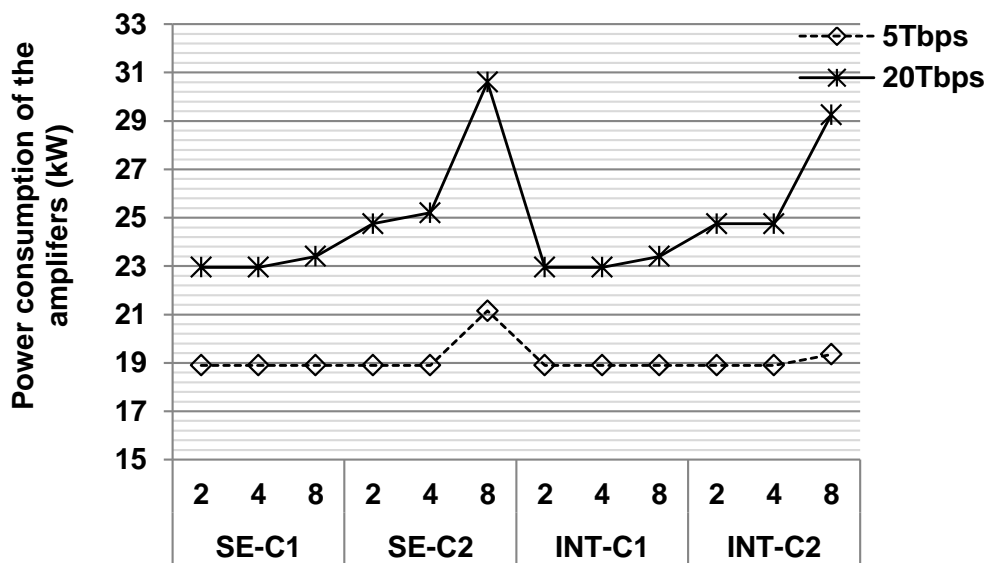


Figure 5.19: Power consumption of the amplifiers, using SE and INT grouping policies with C1 and C2 configurations, plotted against three band sizes

network traffic, respectively. As expected, between the two grouping policies, INT consumes less power with either configuration and every BS than SE. A similar result is observed in power consumption of the MG-OXCs alone, where the MG-OXCs consume less power with C1 configuration than C2 in most occasions. With respect to the power consumption of the amplifiers alone, we can clearly see that amplifiers consume more power with C2 configuration, particularly with a large BS of 8.

To obtain a more detailed analysis of power consumption of the two band configurations, we refer to Figure 5.20, which illustrates the power consumption of the amplifiers and individual devices of the MG-OXCs when C1 and C2 are used with the *INT-BS4* combination. The results indicate that the WXCs and AOWCs consume less power with C2 (denoted as *INT-C2-BS8*) as a result of reduced multiplexing and de-multiplexing. However, since most partially-filled wavebands are regenerated by mAORs that consume more power than a single AOR, total regenerators used (denoted by T-AOR in Figure 5.20 which is the sum of mAORs and AORs) consume more power when C2 configuration is used instead of C1. Furthermore, due to reduced fiber and wavelength utilization, C2 uses more fibers which, in turn, increases amplifier power consumption, albeit insignificantly.

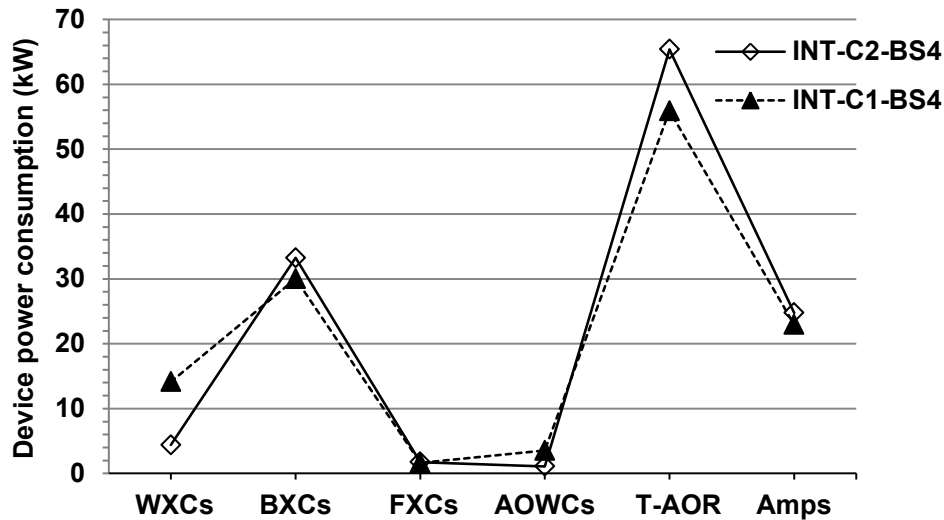


Figure 5.20: Power consumed by amplifiers and the individual devices of MG-OXCs, using C1 and C2 configurations with INT grouping policy and BS = 4, when total network traffic is 25 Tbps.

## 5.7 Summary of findings

In this chapter, we analyzed how advanced features of three-layer MG-OXCs and waveband grooming can be efficiently used to reduce power consumption of an OCS backbone network. Specifically, we investigated how design parameters can be adjusted to maximize power savings under different network environments.

In previous studies, MG-OXCs are not considered to be equipped with all-optical devices and I/O ports of the cross-connects are assumed to consume an insignificant amount of power. Thus, most researchers argue that waveband grooming has a negligible impact on power consumption. However, our analysis shows that by appropriately selecting design parameters, namely, grouping policy, band size, and band configuration, power consumption of a BSN can be reduced by hundreds of kilo-watts, at certain traffic volumes, over traditional WSNs. Therefore, waveband grooming will play an important role in reducing power consumption of optical backbone networks in the future.

In summary, a BSN offers higher power savings than a WSN when the network size is large. The INT grouping policy consumes less power than the SE grouping policy regardless of network size, traffic distribution, and waveband configuration. The difference in power consumption between the two grouping policies becomes significant when traffic is evenly distributed among node pairs. However, if traffic between every node pair is an integer multiple

of the band size, both grouping policies consume an identical amount of electricity. Between uniform and gravity traffic distribution models, a BSN shows increased sensitivity to grouping policy and band size when the gravity model is used to distribute traffic.

The results of this study also show that, to reduce power consumption, a small band size should be selected when the network is loaded with less traffic. On other hand, when network traffic is high, power savings can be maximized by selecting a large band size. Therefore, band size needs to be tuned to match traffic dynamics. Between the two band configurations, the first configuration (i.e., C1) increases fiber utilization and, thereby, reduces power consumption over the second configuration (i.e., C2).

In the next chapter, we investigate how waveband grooming can be combined with load-adaptive operation approaches to further increase power savings in an OCS backbone network.

---

# MLR-BASED BAND SWITCHED OCS

## NETWORKS

---

### 6.1 Introduction

By allowing multiple wavelengths to traverse a core node as a waveband, waveband grooming reduces consumption of I/O ports in Band Switched Networks (BSNs) [27]. As discussed in the previous chapter, core nodes of a BSN are provisioned with three-layer MG-OXC. To minimize O-E/E-O conversions and, thereby, reduce power consumption, it is envisioned that future MG-OXCs will be equipped with AOWCs [85,286] and AORs [22,116,164].

Mixed/Multi-Line Rate (MLR), a technique classified under the approach of load-adaptive approaches in Section 2.6, shows superior results in reducing power consumption of backbone networks [26,205]. A backbone network that adopts MLR is referred to as an MLR-based network. Reported power consumption values of network devices in [44] reveal that high-capacity/rate devices consume less power per bit of transmitted traffic and, thus, offer a ‘volume discount’ on power [5,59]. By exploiting this volume discount, an MLR-based network assigns higher line rates to connection requests (i.e., traffic demands) that require more bandwidth. Similarly, connection requests that demand less bandwidth are served using low-capacity/rate devices. In comparison to a backbone network that utilizes a Single Line Rate (SLR), that is referred to as an SLR-based network, transponders in an MLR-based network consume less power. However, optical reach (i.e., transmission reach) of a lightpath is reduced in an MLR-based network due to non-linear effects (e.g., cross-phase modulation) induced among co-propagating wavelengths at different line rates. Consequently, regenerators consume more power in an MLR-based network than in an SLR-based network [26]. To jointly minimize cost and power consumption, a backbone network could combine MLR and waveband grooming

techniques to effectively form an MLR-based BSN (MBSN). In this chapter, we address the power consumption minimization problem of an MBSN to solve research problem 4:

- How can waveband grooming and MLR be combined to reduce power consumption of an OCS backbone network?

While *cost* of MLR-based networks, BSNs, and MBSNs is individually examined in several studies [237,238,287], no prior study to the best of our knowledge investigates power consumption of an MBSN. In this chapter, we evaluate power consumption of an MBSN. Key differences between this study and relevant past work will be discussed in detail in Section 6.2. To make our findings valid in the future, we examine an MBSN that employs core nodes consisting of three-layer MG-OXCs equipped with AOWCs and AORs. The power consumption minimization problem of the MBSN is modelled as an ILP formulation, and solutions to this problem are found using path, rate, and wavelength/waveband assignment heuristics proposed in this study. Power consumption of the MBSN is compared against SLR-based and MLR-based traditional Wavelength Switched Networks (WSNs/MWSNs) and SLR-based BSNs (SBSNs).

The remainder of this chapter is organized in the following sequence. First, we provide a review of related literature in Section 6.2. In Section 6.3, we provide an overview of the backbone network and MG-OXC architecture and highlight the differences in SLR/MLR-based WSNs/BSNs. The power consumption minimization problem is mathematically modelled in Section 6.4. Section 6.5 presents the proposed path, rate, and wavelength/waveband assignment schemes. Results obtained through simulation-based experiments are reported in Section 6.6. Lastly, Section 6.7 presents a summary of the findings.

## 6.2 Overview of related work

This section presents an overview the relevant literature on BSNs, MLR techniques, and the development of all-optical technologies, and identifies gaps in the existing literature.

In Chapter 5, we highlighted that many researchers [156,157] believe waveband grooming to have an insignificant impact on reducing power consumption of backbone networks, because I/O ports of an MG-OXC are assumed to consume a negligible amount of electricity. As a result, these researchers fail to quantify actual power savings from waveband grooming. However, Murakami et al. [101] and Hou et al. [28] report that an I/O port consumes approximately 7 W of power, which cannot be considered as negligible.

Hou et al. [156] and Wang et al. [157] explored power consumption of an SBSN where core nodes consist of HOXCs rather than transparent three-layer MG-OXCs. Power consumption of MWSNs has also been previously explored by [39] and [26]. However, research to date on MBSNs is sparse and what few studies exist focus on the *cost* of such networks [237, 238, 288]. For example, Ferdousi et al. show that an MBSN costs less than an MWSN at various traffic volumes. They also report that the MBSN incurs a lower cost than 10 Gbps, 40 Gbps, and 100 Gbps SBSNs. In another study, Varma et al. [288] investigate how regenerator site selection affects cost of I/O ports, transponders, and regenerators of an MBSN.

According to Ferdousi et al. [237, 238], and Varma et al. [288], it is challenging to group a set of wavelengths with dissimilar line rates into a waveband, as they do not possess the same transmission reach. Such a waveband needs to be demultiplexed at an intermediate core node and its constituents have to be regenerated by single-wavelength regenerators provisioned at the WXC layer of the MG-OXC. As a result, the waveband can pass through the BXC layers of only a few intermediate nodes, which is detrimental to reducing the number of I/O ports.

However, future MG-OXCs are likely to be equipped with more advanced all-optical converters and regenerators (AOWCs and AORs) [29, 282], as these devices are progressing towards commercial realization [22, 85–88]. Furthermore, the authors of [114–117] use a single device to simultaneously regenerate multiple wavelengths having an *identical line rate* (e.g.,  $8 \times 10$  Gbps,  $4 \times 40$  Gbps, and  $4 \times 10$  Gbps). Therefore, MG-OXCs could also be equipped with a multi-wavelength AOR (mAOR). MG-OXCs equipped with mAORs would circumvent the need for multiplexing/de-multiplexing of wavebands and O-E/E-O conversions, thereby reducing power consumption.

Based on the above review, we are able to identify important research gaps. No study, thus far, has attempted to investigate power consumption of MBSNs. Despite the developments being made in all-optical wavelength conversion and regeneration technologies, in most studies, wavelength conversion and regeneration are performed by power-hungry electronic devices. However, the use of AOWCs and AORs evades the need for electrical processing, thereby reducing power consumption. The use of mAORs can further reduce power consumption as it replaces multiple AORs. To fill these voids in current research and to take advantage of recent developments in all-optical technologies, in this chapter, we evaluate power consumption of an MBSN that employs three-layer MG-OXCs equipped with AOWCs, AORs, and mAORs.

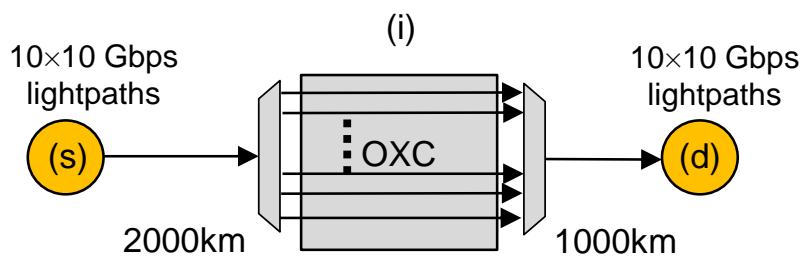
### 6.3 Network models

In this study, we consider the power consumption minimization problem of a BSN which contains core nodes consisting of three-layer MG-OXC equipped with AOWCs, AORs, and mAORs.

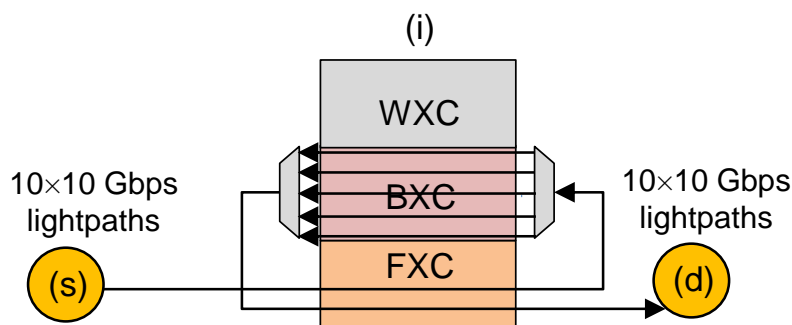
The architecture, functionality, and hierarchical traffic flow of a three-layer MG-OXC were explained in Chapter 5. In this study, we assume that every waveband complies with a *uniform* band size and that each can carry wavelengths of an *identical line rate*. Wavebands are formed using the *INT grouping policy*. Furthermore, lightpaths are tightly aggregated into wavebands according to the first band configuration (C1), described in [27] and evaluated in Chapter 5, to minimize fiber bandwidth wastage.

The differences among SWSN, SBSN, MWSN, and MBSN can be explained using the illustrative examples in Figure 6.1 and 6.2. Figures 6.1a, 6.1b, 6.2a, and 6.2b figures depict how 100 Gbps of traffic that travels 3000 km from node  $s$  to  $i$  is handled by the OXC/MG-OXC of node  $i$  in a SWSN, MWSN, SBSN, and MBSN, respectively. While SLR-based networks (i.e., SWSN, SBSN) are only allowed to utilize a 10 Gbps line rate, the MLR-based networks (i.e., MWSN and MBSN) are allotted with line rates of 10 Gbps and 40 Gbps. The 10 Gbps lightpath in the SLR-based networks has a maximum optical reach of 3,000 km [288]. In the MLR-based networks, the 10 Gbps and 40 Gbps lightpaths are assumed to have a maximum optical reach of 3,000 km and 2,000 km, respectively [289, 290]. In Figures 6.1a and 6.1b, twenty 10 Gbps transponders are used to add and drop traffic at nodes  $s$  and  $d$ . On the other hand, in Figures 6.2a and 6.2b four 40 Gbps transponders and four 10 Gbps transponders are used to add and drop traffic. Due to the increased optical reach of 10 Gbps SLR and MLR lightpaths, in Figures 6.1a to 6.2b, the 10 Gbps lightpaths do not involve regenerators. The two 40 Gbps lightpaths in Figure 6.2a are regenerated using two AORs. On the other hand, in Figure 6.2b, the two 40 Gbps lightpaths are grouped within a single waveband ( $BS = 2$ ) and regenerated by a single mAOR.

Let us now evaluate the power consumption of node  $i$  in each network. Assume that a 10 Gbps transponder consumes 1 unit of power. According to [44], a 40 Gbps and a 100 Gbps transponder consume twice and thrice the amount of power of a 10 Gbps transponder, respectively. A 10 Gbps, 40 Gbps, and 100 Gbps AOR are assumed to consume 2, 4, and 6 units of power, respectively. Power consumption of an mAOR cannot be found in public records



(a) SLR-based WSN (SWSN)

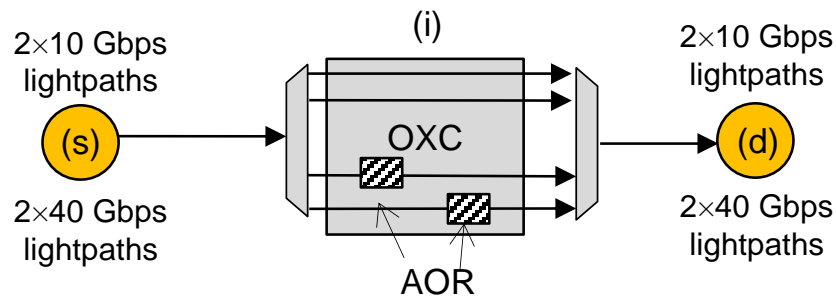


(b) SLR-based BSN (SBSN)

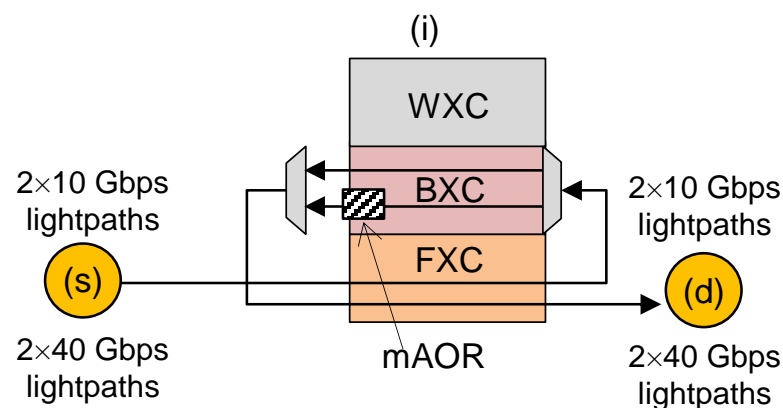
Figure 6.1: Serving two connection requests  $(s_1, d)$  and  $(s_2, d)$  in an SLR-based WSN/BSN

even with our best search efforts. An mAOR regenerates multiple wavelengths in a single package that shares the same chassis and cooling system. It could therefore be expected to consume less power than multiple AORs which each use a chassis and cooling system [161]. Thus, we assume an mAOR serving  $X$  wavelengths with an identical line rate to consume 50% less electricity than the combined power consumption of  $X$  number of AORs with the same line rate. An AOWC consumes only between 1 and 2 W of power while delivering 100-160 Gbps of throughput [51,52]. Thus, a dedicated wavelength converter located at the WXC layer consumes only 0.03 units of power, which is considered as negligible. By taking into account the data presented in [28, 101], we assume that an optical switch port consumes 0.15 unit of power ( $\approx 7$  W). Power consumption of amplifiers in all four SLR/MLR-based WSN/BSNs is identical because traffic travels the same distance via a single fiber. Therefore, amplifier power consumption is not considered in this study.

Under these assumptions, node  $i$  of SWSN, SBSN, MWSN, and MBSN networks consumes



(a) MLR-based WSN (MWSN)



(b) MLR-based BSN (MBSN)

Figure 6.2: Serving two connection requests  $(s_1, d)$  and  $(s_2, d)$  in an MLR-based WSN/BSN

23, 22.1, 21.2, and 17.2 units of power, respectively. Although node  $i$  consumes a similar number of I/O ports in MWSN (Figure 6.2a) and MBSN (Figure 6.2b), the MBSN consumes less electricity than MWSN as a single mAOR draws less power than two AORs.

## 6.4 Problem framework

To reduce power consumption of an MBSN, power consumption of transponders, regenerators, optical switch ports, and amplifiers is required to be jointly minimized. As a dedicated AOWC consumes only a trace amount of power [51, 52], AOWCs are not included in the power consumption minimization problem. To reduce power consumption of transponders, an MBSN needs to accommodate traffic by assigning appropriate line rates. Power consumption of optical switch ports and regenerators can be reduced by grouping wavelengths into wavebands.

Furthermore, wavebands should be intelligently assigned to reduce bandwidth waste and minimize the use of partially-filled wavebands, which would reduce fiber use. Considering these aspects, we model the power consumption minimization problem of an MBSN in the following sections.

#### 6.4.1 Input parameters

- $G = (V, E)$  : Graph with  $V$  set of nodes and  $E$  set of links
- $l_{ij}$  : Physical link connecting node  $i$  to  $j$
- $|l_{ij}|$  : Physical length of link  $l_{ij}$  in km
- $T : |V| \times |V|$  traffic matrix
- $P$  : Set of node pairs with non-negative traffic between them
- $sd$  : Connection request (i.e., traffic demand) between nodes  $s$  and  $d$ . Let  $P$  denote the set of all connection requests,  $sd \in P$ .
- $t^{sd}$  : Traffic between node pair  $(s, d)$  measured in Gbps
- LR : Set of supported line rates (e.g., 10 Gbps, 40 Gbps, 100 Gbps)
- $p^{sd}$  : A feasible routing path for node pair  $(s, d)$  among many available paths (i.e., the length of link  $l_{ij}$  on  $p^{sd}$  is  $\leq$  optical reach of every  $k \in$  LR rate lightpath)
- $h^{sd}$  : Set of nodes along path  $p^{sd}$  (excluding nodes  $s$  and  $d$ )
- $\phi_{ij}^{sd}$  : 1, if link  $l_{ij}$  is feasible on path  $p^{sd}$  at rate  $k \in LR$  (i.e., the shortest path from node  $i$  to  $j$  is  $\leq$  optical reach of a  $k$ -rate lightpath); else, 0.
- $\Upsilon_k$  : Power consumption of a  $k$ -rate transponder
- $\Psi_k$  : Power consumption of a  $k$ -rate AOR
- $\Omega_k$  : Power consumption of a  $k$ -rate mAOR
- $\Gamma$  : Power consumption of an I/O port of the WXC/BXC/FXC layers
- $\Pi$  : Power consumption of an ILA
- $\Theta$  : Power consumption of a PrA/PoA

- $d_{\text{ILA}}$  : Distance between two amplifiers
- $\phi^{ij}$  : Number of amplifiers on a fiber in link  $l_{ij}$  (which is equal to  $\lceil |l_{ij}|/d_{\text{ILA}} \rceil$ )
- $F$  : Maximum number of fibers per link
- BS : Number of wavelengths per waveband (i.e., waveband size)
- $B_k$  : Number of wavebands with rate  $k$  per fiber
- $F_c$  : Maximum capacity of a fiber, defined in traffic volume

#### 6.4.2 Notations

- $I^n$  : Set of input fibers to node  $n$  excluding input fibers from local transponders
- $A^n$  : Set of input fibers to node  $n$  from transponders carrying local add traffic
- $O^n$  : Set of output fibers from node  $n$  excluding output fibers to local transponders carrying local drop traffic
- $D^n$  : Set of output fibers from node  $n$  to local transponders carrying local traffic
- $IA^n$  : Total input fibers to node  $n$  (i.e.,  $I^n + A^n$ )
- $OD^n$  : Total output fibers from node  $n$  (i.e.,  $O^n + D^n$ )
- $I_f^{nm}$  : Input fiber  $f$  to node  $n$  connected from node  $m$
- $O_f^{nm}$  : Output fiber  $f$  from node  $n$  connected to node  $m$
- $w_{bk}$  : Set of wavelengths in band  $b$  that has rate  $k$
- $b_i$  : Set of wavebands in fiber  $i$
- $F_{ij}$  : Number of fibers used in link  $l_{ij}$
- $\lambda_k^n$  : Number of  $k$ -rate AORs used in the WXC layer of node  $n$ .
- $\rho_k^n$  : Number of  $k$  rate mAORs used in the BXC layer of node  $n$ .
- $WXC^n, BXC^n, FXC^n$  : Number of I/O ports used in the WXC, BXC, and FXC layers of node  $n$ , respectively.

### 6.4.3 ILP variables

- $t_{ijfwk}^{sd}$ : 1, if wavelength  $w$  of node pair  $(s, d)$  is routed on fiber  $f$  in link  $l_{ij}$  (i.e.,  $\phi_{ij}^{sd} = 1$ ) on path  $p^{sd}$  at rate  $k$ ; else, 0.
- $r_{wk}^{nsd}$ : 1, if wavelength  $w$  at rate  $k$  of node pair  $(s, d)$  is required to be regenerated at node  $n$  on path  $p^{sd}$ ; else, 0. These are pre-calculated for each line rate  $k$  for every node pair  $(s, d) \in P$  at all nodes  $n \in V$ .
- $\theta_{ijbk}^f$ : 1, if a non-empty waveband  $b$  of rate  $k$  travels through fiber  $f$  of link  $l_{ij}$ ; else, 0.
- $V_{iowk}^{nsd}$ : 1, if node  $n$  serves traffic of node pair  $(s, d)$  on wavelength  $w$  travelling along path  $p^{sd}$  at line rate  $k$  from incoming fiber  $i$  to outgoing fiber  $o$ ; else, 0.
- $W_{iowk}^n$ : 1, if wavelength  $w$  with rate  $k$  is added/passed through/dropped at the WXC layer at node  $n$  from incoming fiber  $i$  to outgoing fiber  $o$ ; else, 0.
- $B_{iobk}^n$ : 1, if waveband  $b$  with rate  $k$  is added/passed through/dropped at the BXC layer at node  $n$  from incoming fiber  $i$  to outgoing fiber  $o$ ; else, 0.
- $F_{io}^n$ : 1, if fiber  $i$  is added/passed through/dropped to outgoing fiber  $o$  at the FXC layer at node  $n$ ; else, 0.
- $FTB_i^n$ : 1, if input fiber  $i$  needs to be demultiplexed at node  $n$  ( $i \in I^n$ ); else, 0.
- $BTF_o^n$ : 1, if a waveband needs to be multiplexed into output fiber  $o$  at node  $n$  ( $o \in O^n$ ); else, 0.
- $BTW_{ibk}^n$ : 1, if waveband  $b$  with rate  $k$  on input fiber  $i$  needs to be demultiplexed into wavelengths at node  $n$  ( $i \in I^n$ ); else, 0.
- $WTB_{obk}^n$ : 1, if a wavelength with rate  $k$  on output fiber  $o$  needs to be multiplexed into waveband  $b$  with rate  $k$  at node  $n$  ( $o \in O^n$ ); else, 0.

### 6.4.4 Objective

The primary objective of the work presented in this chapter is to jointly reduce power consumption of I/O ports, transponders, regenerators, and fiber amplifiers. Following the nota-

tions defined above, the objective can be represented in Equation 6.1 in the following manner:

$$\begin{aligned}
 \text{Minimize} \quad & \overbrace{2\Gamma \cdot \sum_n (WXC^n + BXC^n + FXC^n)}^{\text{Term 1: I/O ports}} + \overbrace{\sum_{sd,j,f,w,k} 2 \cdot \Upsilon_k \cdot t_{sjfwk}^{sd}}^{\text{Term 2: Transponders}} \\
 & + \overbrace{\sum_{n,k} (\Psi_k \cdot \lambda_k^n + \Omega_k \cdot \rho_k^n)}^{\text{Term 3: Regenerators}} + \overbrace{\sum_{l_{ij}} F_{ij}(\Theta + \Pi \cdot \phi_{ij})}^{\text{Term 4: Amplifiers}}
 \end{aligned} \tag{6.1}$$

Due to the symmetry of MG-OXCs, we assume that the number of input ports is equivalent to that of output ports [146]. Thus, Term 1 includes a factor of 2. Term 2 calculates power consumed by transponders that add and drop wavelengths of every node pair  $(s, d)$ . Wavelength  $w$  carrying traffic of node pair  $(s, d)$  and travelling through link  $l_{sj}$  along path  $p^{sd}$  is added and dropped via 2 transponders. Thus, Term 2 includes a factor of 2. Term 3 measures power consumed by AORs and mAORs of rate  $\forall k \in \text{LR}$  at every node  $n \in V$ . Finally, Term 4 calculates power consumed by amplifiers on fibers along every link  $l_{ij} \in E$ .

## 6.4.5 Constraints

### 6.4.5.1 Set of general constraints

As reported in [145, 146], the set of constraints on traffic flows, wavelength capacity, and wavelength continuity can be derived from the constraints of traditional RWA ILP formulations. Equation 6.2 ensures that a lightpath of node pair  $(s, d)$  cannot be added to or dropped from any other node except nodes  $s$  and  $d$ , respectively. Equations 6.3 and 6.4 guarantee that total  $t^{sd}$  is added to and dropped from nodes  $s$  and  $d$ , respectively. Equations 6.5 and 6.6 present the wavelength capacity constraints of every fiber. In this study, we assume that the WXC layer on every node is provisioned with dedicated AOWCs. Therefore, the wavelength continuity constraint is applied to traffic traversing the BXC (as in Equation 6.7) and FXC layers (as in

Equation 6.8) only.

$$\sum_{i \in A^n, o \in O^n, k} V_{iowk}^{nsd} = \sum_{i \in I^n, o \in D^n, k} V_{iowk}^{nsd} = 0 \quad n \neq s, n \neq d, \forall w \quad (6.2)$$

$$\sum_{w, k, i \in A^n, o \in O^n} k \cdot V_{iowk}^{nsd} = t^{sd} \quad n = s \quad (6.3)$$

$$\sum_{w, k, i \in I^n, o \in D^n} k \cdot V_{iowk}^{nsd} = t^{sd} \quad n = d \quad (6.4)$$

$$\sum_{sd, k, i \in IA^n} V_{iowk}^{nsd} \leq 1 \quad o \in O^n, \forall w \quad (6.5)$$

$$\sum_{sd, k, o \in OD^n} V_{iowk}^{nsd} \leq 1 \quad i \in I^n, \forall w \quad (6.6)$$

$$\begin{aligned} \sum_{k, b \in b_i, i \in IA^m, o \in O_f^{mn}} V_{iowk}^{msd} \cdot B_{iobk}^m - \sum_{k, b \in b_i, o \in OD^n, i \in I_f^{nm}} V_{iowk}^{nsd} \cdot B_{iobk}^n \\ = 0 \quad \forall m, n, sd, w, f \end{aligned} \quad (6.7)$$

$$\begin{aligned} \sum_{k, i \in IA^m, o \in O_f^{mn}} V_{iowk}^{msd} \cdot F_{io}^m - \sum_{k, o \in OD^n, i \in I_f^{nm}} V_{iowk}^{nsd} \cdot F_{io}^m \\ = 0 \quad \forall m, n, sd, w, f \end{aligned} \quad (6.8)$$

#### 6.4.5.2 Constraints on regenerators

Equations 6.9 and 6.10 ensure that the lightpaths of node pair  $(s, d)$  can only be regenerated at intermediate nodes on path  $p^{sd}$ . Equation 6.11 determines the number of lightpaths regenerated at the WXC layer of node  $n$ . Equation 6.12 determines the usage of mAORs at the BXC layer of node  $n$ . Based on the existing literature [115–117], an mAOR is assumed to be capable of regenerating BS number of wavelengths with an *identical line rate*. Equation 6.13 ensures that regeneration of lightpaths of all node pairs is accounted for at node  $n$ .

$$r_{wk}^{ssd} = 0 \quad \forall sd, w, k \quad (6.9)$$

$$r_{wk}^{dss} = 0 \quad \forall sd, w, k \quad (6.10)$$

$$\rho_k^n \geq \sum_{i \in I^n, o \in O^n, b \in b_i} \left[ \frac{\sum_{w \in w_{bk}, sd} (r_{wk}^{nsd} \cdot V_{iowk}^{nsd} \cdot B_{iobk}^n)}{\text{BS}} \right] \quad \forall n \quad (6.11)$$

$$\lambda_k^n \geq \sum_{i \in I^n, o \in O^n, w, k, sd} r_{wk}^{nsd} \cdot V_{iowk}^{nsd} \cdot W_{iowk}^n \quad \forall n \quad (6.12)$$

$$\text{BS} \cdot \rho_k^n + \lambda_k^n \geq \sum_{sd, w, k} r_{wk}^{nsd} \quad \forall n \quad (6.13)$$

### 6.4.5.3 Constraints on fibers

Equation 6.14 ensures that fiber  $f$  of link  $l_{ij}$  does not exceed the maximum capacity of a fiber ( $F_c$ ). A fully or partially-filled waveband  $b$  at rate  $k$  consumes  $k \cdot \text{BS}$  Gbps of fiber capacity. Equation 6.15 determines the number of fibers used to carry wavebands in link  $l_{ij}$ . Equation 6.16 guarantees that the number of active fibers in link  $l_{ij}$  does not exceed the threshold  $F$ .

$$0 \leq F_c - \sum_{k,b \in b_f} k \cdot \text{BS} \cdot \theta_{ijbk}^f \quad \forall f \in [0, 1, \dots, F-1] \in \forall l_{ij} \quad (6.14)$$

$$F_{ij} = \sum_{f \in [0, 1, \dots, F-1]} \left[ \sum_{k,b \in b_f} \frac{(k \cdot \text{BS} \cdot \theta_{ijbk}^f)}{F_c} \right] \quad \forall l_{ij} \quad (6.15)$$

$$F_{ij} \leq F \quad \forall l_{ij} \quad (6.16)$$

### 6.4.5.4 Constraints on waveband switching

For waveband switching, the following additional constraints are required. Equations 6.17 - 6.21 ensure that (1) exactly 1 I/O port of each of the FXC, BXC, and WXC layers is used when a  $k$ -rate wavelength  $w$  of node pair  $(s, d)$  in band  $b$  is switched from incoming fiber  $i \in I^n$  to outgoing fiber  $o \in O^n$ , (2) exactly 1  $F_{add}$ ,  $B_{add}$ , and  $W_{add}$  port will be used when a lightpath of node pair  $(s, d)$  is added from incoming fiber  $i \in A^n$  to outgoing fiber  $o \in O^n$ ; (3) exactly 1  $F_{drop}$ ,  $B_{drop}$ , and  $W_{drop}$  port will be used when a lightpath of node pair  $(s, d)$  is dropped from incoming fiber  $i \in I^n$  to outgoing fiber  $o \in D^n$ .

$$\begin{aligned} 1 &\geq F_{io}^n + B_{iobk}^n + W_{iowk}^n \\ &\geq \sum_{sd} V_{iowk}^{nsd} \quad \forall w \in w_{bk}, b \in b_i, i \in IA^n, o \in OD^n \end{aligned} \quad (6.17)$$

$$1 \geq F_{io}^n + \sum_{sd, o_1 \neq o} V_{io_1wk}^{nsd} \quad \forall w, k, i \in IA^n, o \in OD^n \quad (6.18)$$

$$1 \geq F_{io}^n + \sum_{sd, i_1 \neq i} V_{i_1owk}^{nsd} \quad \forall w, k, i \in IA^n, o \in OD^n \quad (6.19)$$

$$1 \geq B_{iobk}^n + \sum_{sd, o_1 \neq o} V_{io_1wk}^{nsd} \quad \forall w \in w_{bk}, k, i \in IA^n, o \in OD^n \quad (6.20)$$

$$1 \geq B_{iobk}^n + \sum_{sd, i_1 \neq i} V_{i_1owk}^{nsd} \quad \forall w \in w_{bk}, k, i \in IA^n, o \in OD^n \quad (6.21)$$

In addition, the constraint in Equation 6.22 ensures that a  $k$ -rate wavelength added/switched via the WXC layer travels through WTB and BTF multiplexers, in sequence,

before leaving node  $n$  via fiber  $o$ . Similarly, Equation 6.23 guarantees that a  $k$ -rate wavelength dropped/switched at the WXC layer of node  $n$  has to travel through FTB and BTW demultiplexers, in sequence.

$$1 \geq BTF_o^n \geq WTB_{obk}^n \geq W_{iowk}^n \quad \forall w \in w_{bk}, o \in O^n, i \in IA^n \quad (6.22)$$

$$1 \geq FTB_i^n \geq BTW_{ibk}^n \geq W_{iowk}^n \quad \forall w \in w_{bk}, o \in OD^n, i \in I^n \quad (6.23)$$

$$BTF_o^n \geq B_{iobk}^n \quad \forall k, b \in b_i, o \in O^n, i \in IA^n \quad (6.24)$$

$$FTB_i^n \geq B_{iobk}^n \quad \forall k, b \in b_i, o \in OD^n, i \in I^n \quad (6.25)$$

Equation 6.24 ensures that an added/passed-through waveband travels through the BTF multiplexer before leaving node  $n$  on output fiber  $o \in O^n$ . On the same note, equation 6.25 constrains a dropped/passed-through waveband  $b$ , coming from the fiber  $i \in I^n$ , to travel through the FTB demultiplexer before entering the BXC layer.

#### 6.4.5.5 Port numbers

The following set of equations determines the number of input ports at each switching layer of node  $n$ . Equation 6.26 determines the number of input ports of the WXC layer of node  $n$ , which includes locally added/passed-through/dropped lightpaths. In Equation 6.27, the number of input ports is found by summing the added/passed-through/dropped wavebands and the number of wavebands coming from or going to WTB and BTW, respectively. Finally, the total number of input ports of the FXC layer is denoted by Equation 6.28, which takes into account added/passed-through/dropped and multiplexed/demultiplexed fibers of node  $n$ .

$$WXC^n = \sum_{i \in IA^n, o \in OD^n, w, k} W_{iowk}^n \quad \forall n \quad (6.26)$$

$$\begin{aligned} BXC^n = & \sum_{i \in IA^n, o \in OD^n, b, k} B_{iobk}^n \sum_{o \in O^n, b, k} WTB_{obk}^n \\ & + \sum_{i \in I^n, b, k} BTW_{ibk}^n \quad \forall n \end{aligned} \quad (6.27)$$

$$\begin{aligned} FXC^n = & \sum_{i \in IA^n, o \in OD^n} F_{io}^n + \sum_{o \in O^n} BTF_o^n \\ & + \sum_{i \in I^n} FTB_i^n \quad \forall n \end{aligned} \quad (6.28)$$

## 6.5 Heuristic Approaches

As previously explained in Section 4.4, solving an ILP formulation becomes unmanageable and infeasible for large-scale networks as it has to deal with a substantial number of variables. Constraints pertaining to wavelength continuity, line rate, and hierarchical switching layers add extra complexity by increasing the number of variables in MLR-based BSNs. Therefore, while the ILP formulation presented above can be solved for small networks that consist of a few core nodes with each fiber carrying a few wavelengths [146], for large-scale backbone networks, it is more feasible to develop efficient heuristics.

In the present section, we describe the heuristic algorithms developed to reduce power consumption of an MBSN. Transponder power consumption can be reduced by appropriately assigning line rates. Power consumption of I/O ports can be reduced by grouping several wavelengths and switching them as a waveband. Regenerator power consumption can be minimized by using an mAOR instead of many single AORs. By grouping wavebands using a *uniform* band size and the *first configuration* (C1) presented in [27], bandwidth waste can be marginalized and amplifier power consumption can thus be reduced.

Extending the work of [237, 238], three heuristic algorithms are developed in this chapter. Each algorithm involves three stages. In Stage 1, the routing path for each traffic demand is determined. In Stage 2, line rates are assigned to traffic demands using one of the proposed algorithms. In the third and final stage, wavelengths with identical line rates are grouped into wavebands using the INT grouping policy as dictated by the proposed Lightpath Splitting (LS) algorithm.

### 6.5.1 Notations

The notations used in subsequent sections are described below.

- $t^{sd}$  : Traffic demand between node pair  $(s, d)$  measured in Gbps
- $m_{10}, m_{40}, m_{100}$  : Maximum optical reach of a 10 Gbps, 40 Gbps, and 100 Gbps lightpath, respectively, when MLR is used
- $s_{10}, s_{40}, s_{100}$  : Maximum optical reach of a 10 Gbps, 40 Gbps, and 100 Gbps lightpath, respectively, when SLR is used

- $n_k^{sd}$  : Number of times a lightpath is regenerated when travelling between node pair  $(s, d)$  at line rate  $k$  along path  $p^{sd}$
- $\Lambda^{sd}$  : Set of all possible rate assignment choices for traffic  $t^{sd}$
- $\Lambda_i^{sd}$  : The  $i^{\text{th}}$  rate assignment choice in  $\Lambda^{sd}$
- $\Lambda_{ik}^{sd}$  : Number of lightpaths at rate  $k$  in  $\Lambda_i^{sd}$
- $\Lambda_k^{sd}$  : Established lightpath between node pair  $(s, d)$  at rate  $k$
- $L_{sd}^k$  : List of lightpaths established between node pair  $(s, d)$  at rate  $k$ , e.g.,  $L_{sd}^k = [\Lambda_k^{sd}, \Lambda_k^{sd}, \dots, \Lambda_k^{sd}]$
- $L_{sd}$  : A set that carries every list  $L_{sd}^k$  ( $\forall k \in \text{LR}$ ), e.g.,  $L_{sd} = [L_{sd}^k, L_{sd}^{k_2}, L_{sd}^{k_3}]$
- $b_k^{sdi}$  :  $i^{\text{th}}$  indexed waveband between node pair  $(s, d)$  with rate  $k$
- $\Upsilon_k$  : Power consumption of a transponder with rate  $k$
- $\Psi_k$  : Power consumption of an AOR with rate  $k$

### 6.5.2 Stage 1: Path selection using Balanced-Path routing

Introduced in this thesis in Section 5.5, the routing path for each connection request (i.e., traffic demand) is found using the balanced-path (BP) routing scheme presented in [145, 146]. The steps involved in assigning routes to each node pair are stated below.

1. Find  $K$  short paths for every node pair  $(s, d)$  and sort them in ascending order of their respective hop count as  $p_1^{sd}, p_2^{sd}, p_K^{sd}$ . Let the number of hops along the shortest path be  $H^{sd}$ .
2. Let the traffic load on every link,  $l_{ab}$ , be measured as the number of lightpaths travelling through it. Let ML define the maximum link load among all links.
3. For the node pair with the largest  $H^{sd}$ , determine the shortest path from the sorted list  $p_1^{sd}, p_2^{sd}, p_K^{sd}$  which minimizes ML the most. If two or more paths (e.g.,  $p_1^{sd}$  and  $p_2^{sd}$ ) produce the same minimum ML, select the shortest path among them.
4. Repeat step 3 for every node pair until each is assigned a path.

### 6.5.3 Stage 2: Line rate assignment

Every traffic demand  $t^{sd}$  is served using lightpaths of different line rates. For example,  $t^{sd}$  carrying 50 Gbps traffic can be accommodated via five 10 Gbps lightpaths, a single 40 Gbps and a single 10 Gbps lightpath, or a single 100 Gbps lightpath. These three rate assignment choices are represented as  $\Lambda_1^{sd}, \Lambda_2^{sd}, \Lambda_3^{sd}$  and are included in  $\Lambda^{sd}$ . For the  $i^{\text{th}}$  rate assignment choice ( $\Lambda_i^{sd} \in \Lambda^{sd}$ ), the following holds true;

$$\{t^{sd} \leq \sum_{k \in \text{LR}} k \cdot \Lambda_{ik}^{sd}\}. \quad (6.29)$$

Power consumption of the transponders and regenerators is dependent on the rate assignment choice. The sum of power consumption of the transponders and regenerators for the  $i^{\text{th}}$  rate assignment choice of  $t^{sd}$  is represented by the function  $E_i^{sd}$ , where

$$E_i^{sd} = \sum_{k \in \text{LR}} (\Upsilon_k \cdot \Lambda_{ik}^{sd} + \Psi_k \cdot n_k^{sd} \cdot \Lambda_{ik}^{sd}). \quad (6.30)$$

#### 6.5.3.1 Minimize transponder and regenerator power consumption using MTR

The objective of the MTR heuristic is to jointly minimize power consumption of the transponders and regenerators. To achieve this objective, among the many available rate assignment choices for traffic demand  $t^{sd}$ , the MTR heuristic selects the  $i^{\text{th}}$  rate assignment choice (e.g.,  $\Lambda_i^{sd}$ ) which produces the minimum value for Equation 6.30.

The MTR heuristic can be explained using a simple example. Assume that 30 Gbps traffic is transmitted from nodes  $s$  to  $d$  along path  $p^{sd}$  via two intermediate nodes, as depicted in Figure 6.3. Based on findings in [287, 288],  $m_{10}$ ,  $m_{40}$ , and  $m_{100}$  are assigned the values of 3,000, 2,000, and 1,000 km, respectively. Let  $s_{10}$ ,  $s_{40}$ , and  $s_{100}$  be equal to 3,000, 3,000, and 4,000 km, respectively [289, 290]. Traffic demand  $t^{sd}$  could be served using three rate assignment choices, which are  $\Lambda_1^{sd} : 3 \times 10$  Gbps,  $\Lambda_2^{sd} : 1 \times 40$  Gbps, and  $\Lambda_3^{sd} : 1 \times 100$  Gbps as shown in Figure 6.3.

If  $\Lambda_1^{sd}$  is chosen, lightpaths do not have to be regenerated. On the other hand, if either  $\Lambda_2^{sd}$  or  $\Lambda_3^{sd}$  is chosen, lightpaths are regenerated at one intermediate node or both intermediate nodes, respectively (see Figure 6.3). Using relative power consumption (units) of transponders and regenerators at different line rates, the three rate assignment choices produce 3 ( $E_1^{sd} = (1 \times 3) + (0)$ ), 6 ( $E_2^{sd} = (2 \times 1) + (4 \times 1 \times 1)$ ), and 15 ( $E_3^{sd} = (3 \times 1) + (6 \times 2 \times 1)$ ) units when evaluated using Equation 6.30. Since  $\Lambda_1^{sd}$  produces the smallest value, the MTR

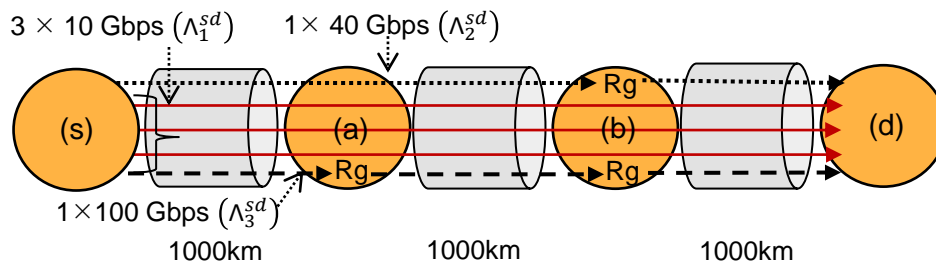


Figure 6.3: Three rate assignment choices for  $t^{sd}$  of 30 Gbps

heuristic accommodates  $t^{sd}$  using three 10 Gbps lightpaths.

### 6.5.3.2 Minimize transponder power consumption using MT

Taking full advantage of the offered volume discount on power consumption by high-capacity transponders, the MT heuristic selects the rate assignment choice that minimizes the first term in Equation 6.30. Using the previous example, the three rate assignment choices,  $\Lambda_1^{sd}$ ,  $\Lambda_2^{sd}$ , and  $\Lambda_3^{sd}$ , then produce the values 3, 2, and 3, respectively. Based on these results,  $\Lambda_2^{sd}$  is chosen by the MT heuristic.

### 6.5.3.3 Combining MTR and SLR using HMTR

The HMTR is a hybrid of the MTR heuristic. Although a 100 Gbps transponder offers the highest volume discount on power, a 100 Gbps lightpath in an MLR-based network has a limited optical reach, requiring more regeneration. To jointly minimize power consumption of transponders and regenerators, the MTR heuristic assigns 100 Gbps line rates to lightpaths that only travel a short distance. As reported in [26], when traffic connections demand high bandwidth (in excess of 100 Gbps), serving traffic using 100 Gbps SLR instead of MLR leads to reduced power consumption.

The HMTR heuristic effectively combines the advantages of both MLR and SLR approaches. It allows traffic connections to be assigned multiple line rates. While 10 Gbps and 40 Gbps lightpaths travel along the same the fiber(s) in every physical link, the HMTR heuristic forces 100 Gbps lightpaths to travel through dedicated fiber(s) as a single line rate. As a result, 100 Gbps lightpaths encounter less signal degradation and, thus, require minimum regeneration. However, the HMTR heuristic elevates fiber use as dedicated fiber(s) only carry the 100 Gbps lightpaths. The HMTR heuristic can be explained using the illustrative example in Figure 6.4.

In this example,  $t^{sd}$  is assumed to be equal to 150 Gbps. The HMTR heuristic accommodates  $t^{sd}$  using a single 10 Gbps, a single 40 Gbps, and single 100 Gbps lightpath, as depicted in Figure 6.4. The 40 Gbps lightpath travelling along path  $p^{sd}$  will undergo regeneration at one intermediate node, while the 10 Gbps and 100 Gbps lightpaths do not undergo regeneration.

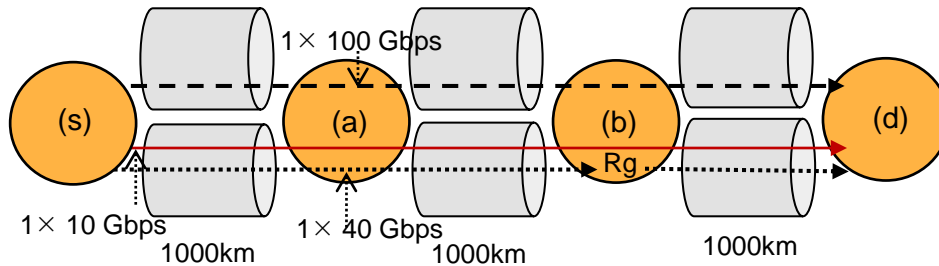


Figure 6.4: Assignment of rates for  $t^{sd}$  of 150 Gbps using the HMTR algorithm

As with the MTR algorithm, HMTR assigns line rates to  $t^{sd}$  by minimizing the cost function defined in Equation 6.30. Prior to assigning multiple line rates, the value of  $m_{100}$  is replaced with the value of  $s_{100}$ , while values of  $m_{10}$  and  $m_{40}$  remain intact. The respective  $n_k^{sd}$  values are then found using these adjusted values. The MG-OXC(s) will multiplex the 10 Gbps and 40 Gbps lightpaths into a shared fiber(s), while the 100 Gbps lightpath(s) is multiplexed into a separate fiber of the same output link.

#### 6.5.4 Stage 3: Wavelength and waveband assignment using Lightpath Splitting

After paths and line rates are assigned to every traffic demand  $t^{sd}$  in Stages 1 and 2, wavelengths and wavebands are assigned using the Lightpaths Splitting (LS) Algorithm that comprises Algorithms 6 and 7. These are slight modifications of Algorithms 4 and 5 developed in Chapter 5.

First, two virtual copies of the initial topology  $G$  is created, which are named the *Lightpath Layer (LL)* and the *Waveband Layer (WL)*. Figure 6.5(i) shows an example of an actual network. In virtual topologies  $LL$  and  $WL$ , node  $V_x$  represents a physical node  $x \in V$ . In the considered example, traffic flows from node  $s$  to nodes  $d$  and  $g$ .

Next, Algorithm 6 is used to create virtual lightpaths in topology  $LL$ . In  $LL$ , traffic between every node pair is represented using an end-to-end lightpath(s). Lightpaths are established using wavelengths travelling at specific line rates determined by the rate assignment choice in Stage 2. For example, as shown in Figure 6.5(ii), in  $LL$ , traffic between node pairs  $(s, d)$  and

$(s, g)$  is accommodated via lightpaths  $1 \times \Lambda_k^{sd}$  and  $2 \times \Lambda_{k_2}^{sd}$ , and  $1 \times \Lambda_k^{sg}$ , respectively. These lightpaths travel along pre-defined paths  $p^{sd}$  and  $p^{sg}$ , respectively, which are found in Stage 1. Every node  $V_x \in LL$  possesses wavelength conversion capability. Thus, an end-to-end lightpath (e.g.,  $\Lambda_k^{sd}$ ) can be split into two or more lightpaths at any intermediate node (e.g.,  $V_f$  and  $V_g$ ). For example, lightpath  $\Lambda_k^{sd}$  can be split at node  $V_g$  to create lightpaths  $\Lambda_k^{sg}$  and  $\Lambda_k^{gd}$ .

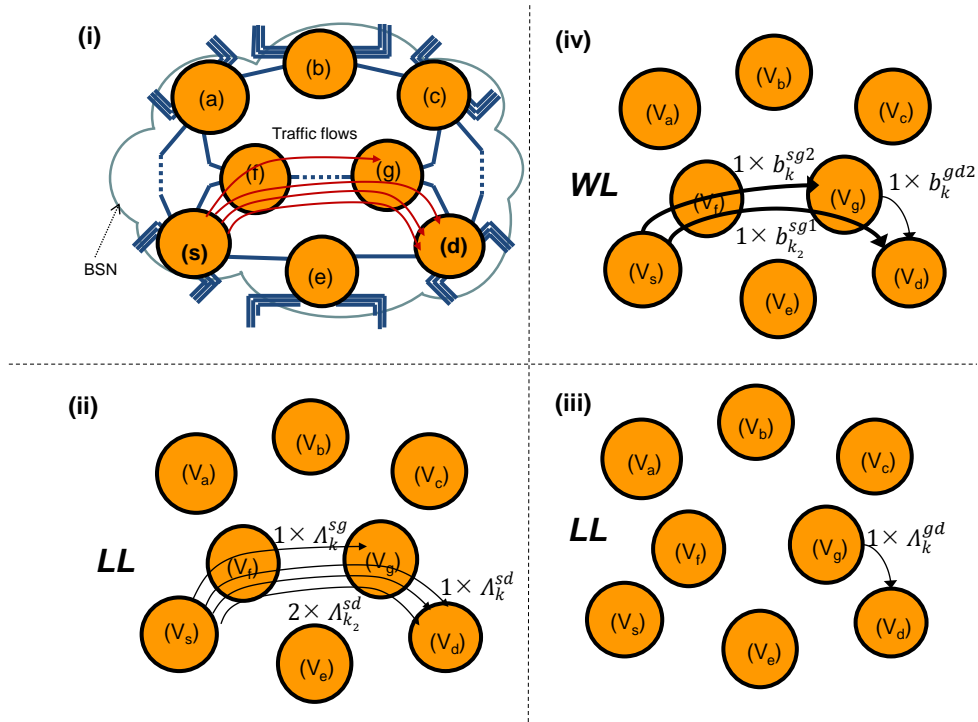


Figure 6.5: Representation of (i) the actual topology  $G$ , (ii) initial  $LL$ , (iii) updated  $LL$ , and (iv)  $WL$

After end-to-end lightpaths are established in  $LL$ , Algorithm 7 is adopted to assign wavelengths and form wavebands and generate the  $WL$  virtual topology. A waveband is formed by grouping adjacent wavelengths with identical line rates. The  $n^{\text{th}}$  indexed waveband  $b_k^{sgn}$  between nodes  $s$  and  $g$  is formed by grouping  $2 \times \Lambda_k^{sg}$  which are assigned adjacent wavelengths  $\lambda_i$  and  $\lambda_{i+BS-1}$ , respectively. Every waveband has a uniform band size (BS) and, thus, carries a fixed number of wavelengths. If a waveband is partially-filled (i.e., only a fraction of BS wavelengths carry traffic), bandwidth is wasted [285]. To provide port savings, a waveband has to travel a minimum of two hops (via an intermediate node) before de-multiplexing.

In Algorithm 7, the variable  $b$  (initialized to be 0) is the index of the respective waveband from which the search starts for an available or unused waveband. Nodes within the selected path  $p^{sd}$  are represented as  $s, s+1, s+2, \dots, d-2, d-1, d$ . In the  $LL$  virtual topology, lightpaths

**Algorithm 6:** Assign virtual lightpaths between every node pair  $(s, d)$  in  $LL$

```

input : The virtual topology  $LL$ , selected rate assignment choice (e.g.,
 $\Lambda_i^{sd}$ ) for every node pair (from Stage 2), pre-determined routing
paths (from Stage 1)
output: Updated  $LL$  with end-to-end lightpaths

1 begin
2   for every node pair  $(s, d)$  do
3     for every  $k$  in  $LR$  do
4       for every  $k$ -rate lightpath in  $\Lambda_i^{sd}$  do
5         Add a logical lightpath  $\Lambda_k^{sd}$  between nodes  $V_s$  and  $V_d$ 
6         along path  $p^{sd}$  at rate  $k$ ;
7         Update  $LL$ ;
8         Remove the  $k$ -rate lightpath from  $\Lambda_i^{sd}$ 
9       end
10    end
11 end

```

that travel through nodes  $V_f$  and  $V_g$  along path  $p^{fg}$  at rate  $k$  (e.g.,  $2 \times \Lambda_k^{sg}$ ) are appended to list  $L_k^{fg}$ , while the lightpath travelling at rate  $k_2$  (e.g.,  $\Lambda_{k_2}^{sd}$ ) is appended to list  $L_{k_2}^{fg}$ . Lists  $L_k^{fg}$  and  $L_{k_2}^{fg}$  are then appended to set  $L^{fg}$ . As wavebands are grouped using the INT grouping policy, Algorithm 7 involves the following 7 steps.

1. Initialize an empty list  $SList$ . Sort node pairs in descending order of  $H^{sd}$  and append to list  $SList$ .
2. If two or more node pairs have identical  $H^{sd}$ , sort them in descending order of their respective number of lightpaths of different line rates.
3. Starting with the first node pair  $(s, d)$  in  $SList$ , use Algorithm 7 to create wavebands between node pair  $(s, d)$  along path  $p^{sd}$ .
4. Update every  $L^{sd}$  ( $\forall (s, d) \in V$ ) according to the current status of  $LL$ .
5. Use Algorithm 7 to create wavebands between source node  $s$  and every other node along path  $p^{sd}$  starting with node pair  $(s, d - 1)$ ,  $(s, d - 2)$  and so on until node pair  $(s, s + 2)$ . Repeat Step 4.
6. Repeat Steps 3-5 with the remaining node pairs in  $SList$ .
7. Let the residual lightpaths in  $LL$  travel through each WXC along their designated routing path.

**Algorithm 7:** Assign wavebands between node pair  $(s, d)$  in  $WL$ 

```

input :  $G, LL, WL, L^{sd}$ 
output: Updated  $LL, WL$ 

1 begin
2   for every list in set  $L_{sd}$  do
3     while  $|L_k^{sd}| \geq BS$  do
4       Find a free band  $m$  starting with  $b$  along path  $p^{sd}$ ;
5       Initialize an empty list  $S^{sd}$ ;
6       if band  $m$  exists then
7         Starting with lightpaths sourced at  $s$  (if available), extract BS
8         lightpaths from  $L_k^{sd}$  and append to  $S^{sd}$ ;
9         for every lightpath  $\Lambda_k^{qr}$  in  $S^{sd}$  do
10          if  $q == s$  and  $r == d$  then           // Same source same
11          destination
12            Remove  $\Lambda_k^{qr}$  from  $LL$ ;
13          else if  $q != s$  and  $r == d$  then       // Different source
14          same destination
15            Split  $\Lambda_k^{qr}$  at node  $V_s$ ;
16            Remove  $\Lambda_k^{qr}$  from  $LL$ ;
17            Add  $\Lambda_k^{qs}$  and  $\Lambda_k^{sr}$  to  $LL$ ;
18            Replace  $\Lambda_k^{qr}$  with  $\Lambda_k^{sd}$  in  $S^{sd}$ ;
19          else if  $q == s$  and  $r != d$  then       // Same source
20          different destination
21            Split  $\Lambda_k^{qr}$  at node  $V_d$ ;
22            Remove  $\Lambda_k^{qr}$  from  $LL$ ;
23            Add  $\Lambda_k^{qd}$  and  $\Lambda_k^{dr}$  to  $LL$ ;
24            Replace  $\Lambda_k^{qr}$  with  $\Lambda_k^{qd}$  in  $S^{sd}$ ;
25          else if  $q != s$  and  $r != d$  then       // Different source
26          different destination
27            Split  $\Lambda_k^{qr}$  at nodes  $V_s$  &  $V_d$ ;
28            Remove  $\Lambda_k^{qr}$  from  $LL$ ;
29            Add  $\Lambda_k^{qs}, \Lambda_k^{sd},$  &  $\Lambda_k^{dr}$  to  $LL$ ;
30            Replace  $\Lambda_k^{qr}$  with  $\Lambda_k^{sd}$  in  $S^{sd}$ ;
31          end
32          Group lightpaths in  $S^{sd}$  and create waveband  $b_k^{sdm}$ ;
33          Add waveband  $b_k^{sdm}$  across nodes  $s$  and  $d$  in  $WL$  on path  $p^{sd}$ ;
34          Update  $b$ ;
35          Update  $LL$  and  $L^{sd}$ ;
36        else
37          Increase  $F$  by 1 on links across path  $p^{sd}$  and go to while
38        end
39      end
40    end
41  end

```

Algorithm 7 can be explained using the illustrated example in Figure 6.5. Assume that BS is assigned the value 2.  $SList = [(s,d), (s,g)]$  is created in Step 1. In Step 3, node pair  $(s, d)$  is fed into Algorithm 7. An end-to-end waveband  $(b_{k_2}^{sg1})$  is created by grouping  $2 \times \Lambda_k^{sd}$  in  $WL$ . In Step 5, node pair  $(s, g)$  (i.e.,  $(s, d - 1)$ ) is fed into Algorithm 7. As  $\Lambda_k^{sd}$  and  $\Lambda_k^{sg}$  share a common path, a waveband  $b_k^{sg2}$  is created between node pair  $(s, g)$  in the  $WL$  topology, as shown in Figure 6.5(iv). A lightpath is added across node pair  $(g, d)$  in the updated  $LL$  (Figure 6.5(iii)). Step 6 is ignored as  $SList$  is empty. Lastly, in Step 7, lightpath  $\Lambda_k^{gd}$  is accommodated via partially-filled, single-hop waveband  $b_k^{gd2}$ .

Note that if  $|LR|$  is equivalent to one, the heuristics described in this section could be used to assign wavelengths and wavebands in an SLR-based BSN. On the other hand, if the FXC and BXC layers, and corresponding I/O ports and mAORs, are to be removed or eliminated, the  $LS$  algorithm described here can also be used to assign wavelengths in SLR/MLR-based WSNs.

## 6.6 Evaluation of results

Using simulation-based experiments, we assess the power consumption of an MLR-based BSN with each rate assignment heuristic (i.e., MTR, MT, and HMTR). MLR-based BSNs (i.e., MB-SNs) are compared with SLR-based BSNs, and SLR-based and MLR-based WSNs (i.e., SBSNs, SWSNs, and MBSNs). The experiments are performed on the 14-node and 21-link NSF network [277] and repeated with increasing traffic volumes ranging from 5 Tbps to 35 Tbps. Network traffic is uniformly distributed among all node pairs. MLR-based networks are allowed to serve traffic using 10 Gbps, 40 Gbps, and 100 Gbps line rates. The optical reach of 10 Gbps, 40 Gbps, and 100 Gbps lightpaths is assumed to be 3,000 km, 2,000 km, and 1,000 km, respectively [288]. In SLR-based networks, the maximum optical reach of a 10 Gbps, 40 Gbps, and 100 Gbps lightpath is assumed to be 3,000 km, 3,000 km, and 4,000 km, respectively [289, 290]. The tests are performed with a *uniform* BS of 4. Based on [203], an optical fiber is assumed to have a maximum bandwidth of 8 Tbps ( $F_c = 8$  Tbps). The relevant power consumption values of network devices are reported in Table 6.1.

In subsequent sections, we study the power consumption of optical switching ports (i.e., I/O ports), transponders (Tran.), all-optical wavelength converters (AOWCs) and regenerators (AORs), and amplifiers (PrA/PoA, ILA). We then analyse and compare total power consumption between SLR/MLR-based WSNs and BSNs.

Table 6.1: Rated power consumption of WDM-layer devices

Device	Capacity	Power consumption
I/O port	Per port (inclusive of pre/post amplifiers, add/drop multiplexers, modules for termination of the OSC, and control circuitry)	$\approx 7$ W [28,101]
Tran.	10 Gbps	50W [44]
	40 Gbps	100 W [44]
	100 Gbps	150 W [44]
AOWC	Per wavelength	2 W [51,52]
AOR	10 Gbps/per wavelength	50 W (approx.) [46,47]
	40 Gbps	100 W (approx.)
	100 Gbps	150 W (approx.)
PrA/PoA	Per fiber	30 W [18,44]
ILA	Every 80 km, per fiber	25 W [18,44]

The results from this series of experiments are presented in Figures 6.6 to 6.12. WSNs utilizing 10 Gbps, 40 Gbps, and 100 Gbps single line rates are denoted as SLR10-WSN, SLR40-WSN, and SLR100-WSN, respectively. Similarly, BSNs utilizing 10 Gbps, 40 Gbps, and 100 Gbps line rates are denoted as SLR10-BSN, SLR40-BSN, and SLR100-BSN, respectively. As line rates are assigned in the MLR-based WSN using only the MTR heuristic, the MLR-based WSN is denoted as MLR-WSN-MTR. The MLR-based BSNs tested with all rate assignment heuristics (MTR, MT, and HMTR), are classified as MLR-BSN-MTR, MLR-BSN-MT, and MLR-BSN-HMTR, respectively.

### 6.6.1 Power consumption of transponders

Figure 6.6 depicts the power consumption of transponders at every traffic volume for each test network. Table 6.2 reports the percentage reduction in power consumption of individual devices in each network, relative to the network with the highest power consumption for the respective device.

Traffic is added to and dropped from the OXC/MG-OXC at wavelength granularity [53]. Thus, between SLR-based WSNs and BSNs, at each line rate of 10 Gbps, 40 Gbps, and 100 Gbps, transponders consume an identical amount of power. Among the three line rates in SLR-based networks in general, transponders of the 10 Gbps SLR-based WSN/BSN consume the most power at all traffic volumes, as they offer the least volume discount on power consumption.

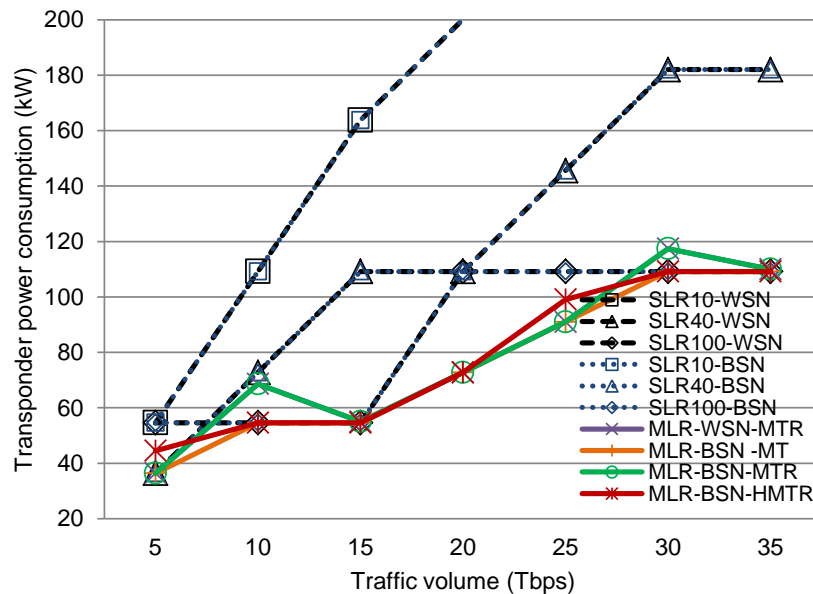


Figure 6.6: Power consumption of transponders at every traffic volume (Tbps) in all test networks

Therefore, the number of 10 Gbps transponders increases rapidly as network traffic grows. Transponder power consumption of 40 Gbps and 100 Gbps SLR-based networks shows a step-wise increment. On average, transponders of 100 Gbps SLR-based networks consume the least power among available single line rates. The only exception is when traffic volume is very low at 5 Tbps, at which point 100 Gbps transponders remain heavily under-utilized.

Between SLR-based and MLR-based networks, generally, transponders of the latter consume less power. However, exceptions are found at 10 Tbps and 30 Tbps, where transponders of 100 Gbps SLR-based networks consume less power than MLR-WSN-MTR and MLR-BSN-MTR.

Among the MTR, MT, and HMTR rate assignment heuristics, transponders of the MLR-BSN-MT consume the least amount of power at every traffic volume. As MT assigns different line rates to minimize transponder power consumption, it outperforms MTR and HMTR in terms of reducing transponder power consumption. MTR and HMTR, on the other hand, provide a balance between transponder and regenerator power consumption. At certain traffic volumes, to minimize regenerator power consumption, traffic is served using transponders that offer a reduced volume discount.

According to Table 6.2, MLR-BSN-MT offers the largest reduction in transponder power consumption of 63.57% over SLR10-WSN where transponders consume the highest power.

Table 6.2: Percentage reduction in power consumption (%) of devices in each network, averaged over the considered traffic range, relative to highest power consumption

Net. type	I/O.	Tran.	Amp.	Rg.	Tot.
SLR10-WSN	Highest	Highest	30.0	57.1	Highest
SLR40-WSN	70.7	42.5	30.0	75.1	48.5
SLR100-WSN	85.5	58.7	30.0	94.6	65.0
SLR10-BSN	68.3	0	30.0	76.0	22.6
SLR40-BSN	83.1	42.5	30.0	82.8	53.1
SLR100-BSN	85.7	58.7	30.0	94.6	65.1
MLR-WSN-MTR	83.1	62.1	30.0	Highest	54.4
MLR-BSN-MTR	82.3	62.1	30.0	18.4	56.5
MLR-BSN-MT	84.5	63.7	30.0	18.4	56.8
MLR-BSN-HMTR	84.7	62.6	Highest	94.4	64.8

MLR-BSN-HMTR provides the second best power savings of 62.64% over SLR10-WSN.

### 6.6.2 Power consumption of regenerators

Figure 6.7 plots power consumed by regenerators at every traffic volume in all test networks. At first glance, it is evident that regenerators of most MLR-based networks (with the exception of MLR-BSN-HMTR) consume more power than the regenerators of SLR-based networks. Among the 10 Gbps, 40 Gbps, and 100 Gbps SLR-based networks, regenerators consumes the least amount of power when the selected single line rate is 100 Gbps. A 100 Gbps line rate has a massive advantage over 10 Gbps and 40 Gbps single line rates due to its increased optical reach, thus needing minimum regeneration.

As MG-OXCs are provisioned with mAORs in BSNs, generally, regenerators of these networks (e.g., SLR40-BSN, MLR-BSN-MTR) consume less power than those of WSNs (e.g., SLR40-WSN, MLR-WSN-MTR). The difference in power consumption increases as traffic volume grows. At high traffic volumes, a higher percentage of regenerated traffic passes through the MG-OXCs as wavebands and, thus, mAORs are able to offer increased power savings over AORs.

Comparing MLR-based networks and SLR-based networks, regenerators of MLR-based networks consume more power than the latter as a result of the reduced optical reach of high-

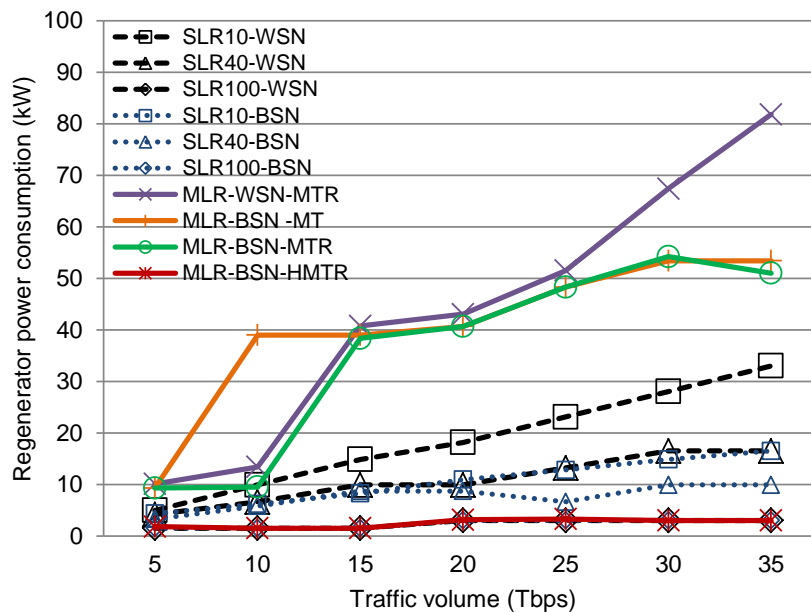


Figure 6.7: Power consumption of regenerators at every traffic volume (Tbps) in all test networks

rate lightpaths in MLR. Recall that in Chapter 2 and at the start of this chapter, we explained that the optical reach of lightpaths is lower in MLR-based networks than in SLR-based networks due to non-linear effects induced among co-propagating wavelengths at different line rates [26].

In Figure 6.7, a sudden hike in the graphs of MLR-BSN-MT is observed between traffic volumes of 5 Tbps and 10 Tbps. A similar hike is observed between 10 Tbps and 15 Tbps traffic volumes in the plotted results of MLR-BSN-MTR and MLR-WSN-MTR. This phenomenon occurs when these MLR-based networks begin to use 100 Gbps line rates as traffic increases across the respective range. 100 Gbps lightpaths have reduced optical reach in MLR-based networks, thus elevating the power consumption of regenerators.

Interestingly, the regenerators of MLR-BSN-HMTR consume a small amount of power. In this network, 100 Gbps lightpaths travel along dedicated optical fibers and possess increased optical reach. Thus, among the MLR-based networks with the three proposed rate assignment heuristics, MLR-BSN-HMTR minimizes regenerator power consumption the most.

As tabulated in Table 6.2, regenerators, on average, consume 94.64% less power in SLR100-based WSNs and BSNs than the MLR-WSN-MTR network where regenerators consume the most power. The next highest power savings of 94.41% is offered by MLR-BSN-HMTR.

### 6.6.3 Power consumption of amplifiers

Figure 6.8 depicts the power consumption of amplifiers of the test networks at every traffic volume. Recall that the maximum bandwidth of an optical fiber is assumed to be equal to 8 Tbps in this study [203]. Based on this assumption, an optical fiber can carry a maximum of  $800 \times 10$  Gbps,  $200 \times 40$  Gbps, or  $8 \times 100$  Gbps wavelengths. Since fibers have high bandwidth, traffic can be often served using a single optical fiber. Bandwidth is efficiently utilized in optical fibers as OXCs and MG-OXCs are assumed to be capable of converting wavelengths.

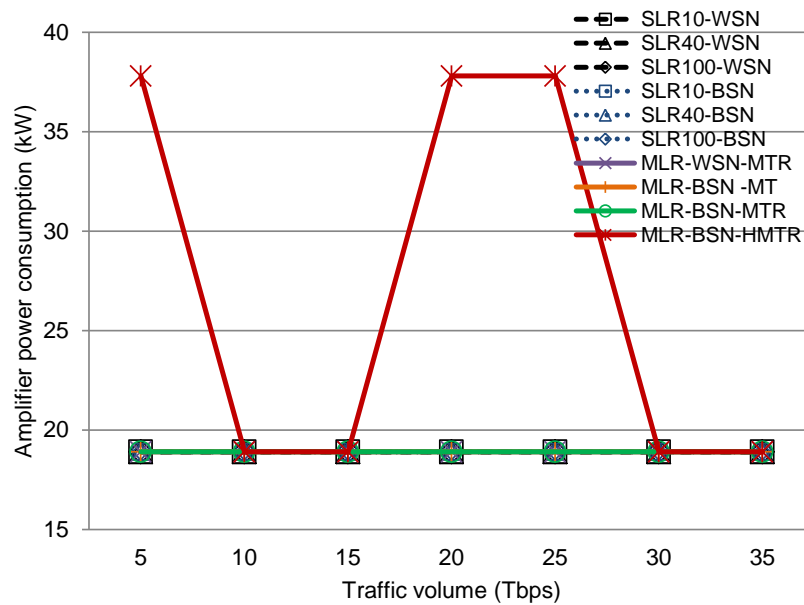


Figure 6.8: Power consumption of optical amplifiers at every traffic volume (Tbps) in all test networks

Consequently, all SLR-based and MLR-based networks, with the only exception of MLR-BSN-HMTR, use the same number of optical fibers and amplifiers that consume identical amounts of power in each network. This is depicted in Figure 6.8 by the horizontal line (all networks except MLR-BSN-HMTR are overlapping) across the considered range of traffic volume. Amplifier power consumption also does not differ between wavelength-switched (i.e., WSN) and waveband-switched (i.e., BSN) networks.

In MLR-BSN-HMTR, 100 Gbps lightpaths use dedicated fibers. When 100 Gbps line rates are used in tandem with 10 Gbps and 40 Gbps line rates in this network, traffic will travel through two separate fibers. Therefore, at certain traffic volumes, amplifiers consume more power in MLR-BSN-HMTR. On average, amplifiers consume 30% more power in MLR-BSN-HMTR than in other networks.

### 6.6.4 Power consumption of optical switch ports

Power consumption of optical switching ports is proportional to the number of I/O ports consumed at the OXCs and MG-OXCs of respective WSNs and BSNs.

Figure 6.9 shows the port consumption of SLR-based networks for every traffic volume. It is evident that the 10 Gbps SLR-based network consumes more ports than other networks with single line rates, while the 100 Gbps SLR-based network consumes the smallest number of ports. Between the 10 Gbps SLR-based WSN and BSN, the latter consumes less ports. Between the 40 Gbps SLR-based WSN and BSN, the latter once again consumes much fewer ports than the WSN at high traffic volumes. However, the difference in the number of ports used between WSN and BSN is minimal when the line rate is 100 Gbps.

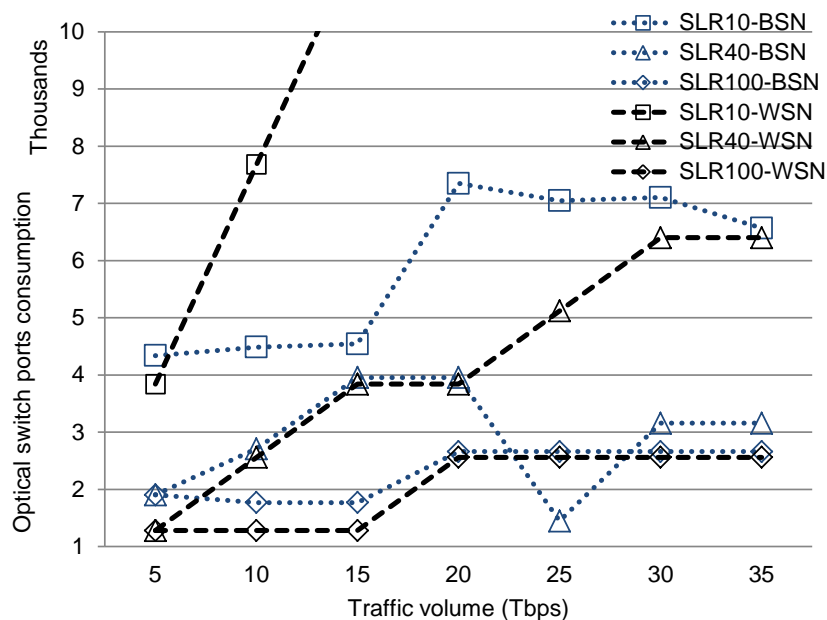


Figure 6.9: Number of optical switch ports consumed by SLR-based networks at every traffic volume (Tbps)

When SLR-based networks use a fast line rate (e.g., 100 Gbps), traffic is served using fewer lightpaths, which makes it difficult to form end-to-end wavebands. A considerable number of lightpaths then travel through the WXC layer of intermediate nodes. Hence, SLR100-BSN is unable to reduce port consumption over SLR100-WSN.

Nevertheless, at very high traffic volumes (i.e., when a large number of lightpaths are established) in SLR-based networks, the ratio of end-to-end wavebands to the number of lightpaths traversing the WXC layer increases. Resultantly, SLR100-BSN will match the port consumption of SLR100-WSN as traffic increases (not shown in the graph). At even higher traffic volumes,

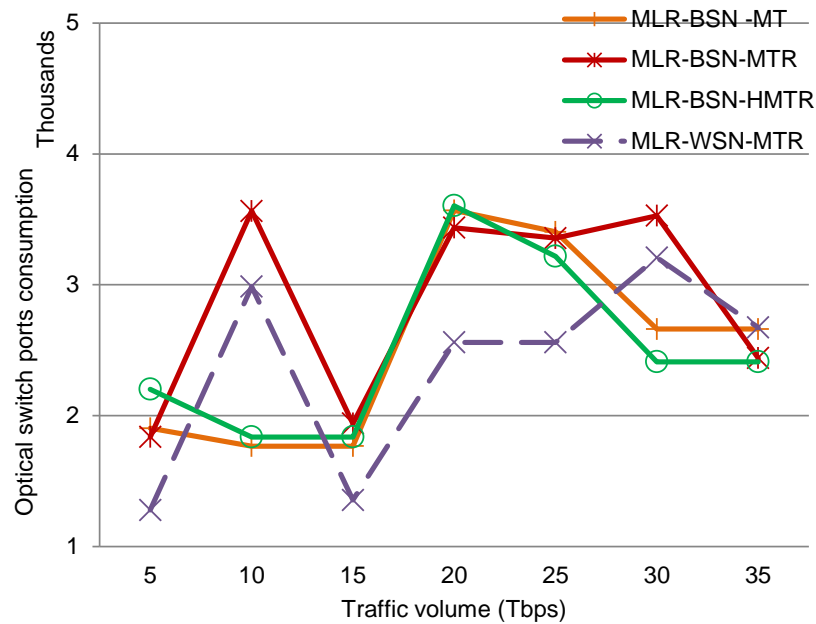


Figure 6.10: Number of optical switch ports consumed by MLR-based networks at every traffic volume (Tbps)

we could then expect SLR100-BSN to consume less ports than SLR100-WSN.

Figure 6.10 shows the port consumption of MLR-based networks. By comparing the plots of Figures 6.9 and 6.10, we argue that, on average, MLR-based networks consume less ports than SLR-based networks. As shown in Figure 6.10, among the MLR-based networks, MLR-WSN-MTR consumes the least number of ports compared to the three BSN networks. This is because, in MLR-based networks, wavelengths have dissimilar line rates, making it difficult to group them into wavebands. Recall that a waveband is formed by aggregating wavelengths with an identical line rate.

Figure 6.11 depicts total power consumption of the optical switching ports and dedicated AOWCs combined. Since the BPLS algorithm minimizes the use of wavelength converters, less power is consumed by wavelength converters in BSNs. Compared to the 10 Gbps and 40 Gbps SLR-based networks, the MLR-based networks generally consume less power, except at the traffic volume of 25 Tbps.

As reported in Table 6.2, average power consumption of I/O ports is highest for SLR10-WSN. I/O ports consume approximately 85.5% less power in SLR100-BSN and SLR100-WSN networks than in SLR10-WSN. I/O ports of the proposed MLR-BSN-HMTR comes only second in terms of achieving high power savings, consuming 84.73% lesser power than SLR10-WSN.

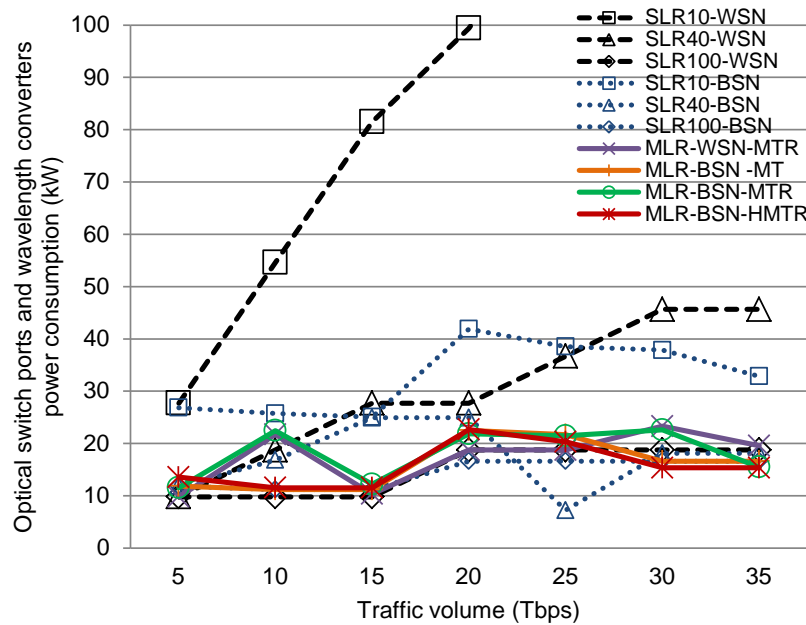


Figure 6.11: Combined power consumption of *optical switch ports* and *wavelength converters* at every traffic volume (Tbps) in all test networks

### 6.6.5 Total power consumption

Figure 6.12 shows the overall power consumption of the WDM layer of all test networks at every traffic volume. It is clearly visible that 10 Gbps SLR-based WSN and BSN consume the most power, which is primarily attributed to high power consumption of 10 Gbps transponders. The 40 Gbps SLR-based WSN and BSN consume more power than both 100 Gbps SLR-based and MLR-based networks. On average, SLR100-BSN and SLR100-WSN consume 65% less power than the power-hungry SLR10-WSN (see Table 6.2).

The MLR-based BSNs consume less power than the MLR-based WSN at high traffic volumes, primarily due to lower regenerator power consumption. Analyzing these results, it becomes evident that waveband grooming could be jointly utilized with MLR to reduce power consumption when a network is loaded with a high traffic volume.

Despite consuming less power than 10 Gbps and 40 Gbps SLR-based networks and MLR-based WSN (i.e., MLR-WSN-MTR), MLR-BSN-MT/MTR consume more power than 100 Gbps SLR-based networks. Among the three MLR-based BSNs, MLR-BSN-HMTR consumes the least power and provides 64.78% and 17% power savings over SLR10-WSN and SLR40-WSN, respectively (see Table 6.2).

At most traffic volumes, power consumption of MLR-BSN-HMTR is comparable to that of the 100 Gbps SLR-based WSN and BSN. However, due to additional fiber use, MLR-BSN-

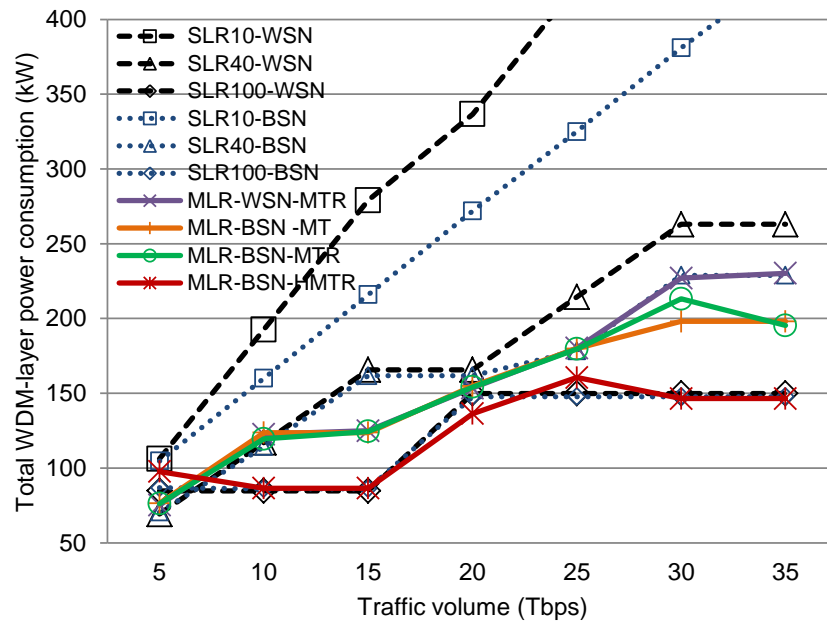


Figure 6.12: Total power consumption of the WDM-layer devices of all test networks at every traffic volume (Tbps)

HMTR consumes marginally more power than 100 Gbps SLR-based networks at 5 Tbps and 25 Tbps traffic volumes.

## 6.7 Summary of findings

This chapter investigated the power consumption minimization problem of a backbone network that jointly uses MLR with waveband grooming, referred to as an MLR-based band switched network (MBSN). This problem was modelled using an ILP formulation. Three heuristics, namely, MTR, MT, and HMTR, were then developed to assign line rates to light-paths. Using the proposed LS algorithm, wavelengths and wavebands were assigned to light-paths of different line rates. Using simulation-based experiments, we analyzed power consumption of the MBSN and compared it to the amount of power consumed by SLR-based WSN/BSN and MLR-based WSN.

The results obtained in this study indicate that 10 Gbps and 40 Gbps SLR-based band switched networks (i.e., SBSNs) consume less power than 10 Gbps and 40 Gbps SLR-based wavelength switched networks (i.e., SWSNs), respectively. The difference in power consumption between SBSNs and SWSNs increases as traffic volume grows. When SLR is 100 Gbps, however, the SBSN consumes more power than the SWSN at low traffic volumes. It is ob-

---

served that BSNs find it more difficult to reduce I/O port consumption than WSNs especially when lightpaths are assigned very high line rates (e.g., 100 Gbps) or multiple line rates.

MLR-based BSN (i.e., MBSNs) consume less power than 10 Gbps and 40 Gbps SWSNs and SBSNs. However, as a result of the reduced optical reach of 100 Gbps lightpaths in MLR-based networks, MBSN very closely offers the second best power savings after 100 Gbps SWSN and SBSN.

Among the three rate assignments heuristics, the HMTR reduces the most power. Its key drawback, however, is its use of additional optical fibers. HMTR combined with MLR and BSN (i.e., MLR-BSN-HMTR) offers comparable power consumption results to that of 100 Gbps SWSN and SBSN at most traffic volumes.

Although 100 Gbps SWSN and SBSN do offer significant power savings, they incur a large deployment cost due to the use of expensive transponders [39]. Moreover, if 100 Gbps SWSN/SBSN is used in networks with heterogeneous traffic demands, it could result in reduced bandwidth utilization [26]. Therefore, based on the results of this study and limitations of the different networks, we argue that legacy 10 Gbps and 40 Gbps SLR-based networks should be replaced with MLR-based BSNs employing state-of-the-art three-layer MG-OXCs that are equipped with all-optical converters and regenerators to reduce power consumption of OCS backbone networks.

Thus far, this thesis has focused on the power consumption minimization problem of OCS networks. The work undertaken in the preceding and present chapters shows that power consumption of an OCS network can be reduced by adopting a range of solutions from the four power consumption reduction approaches identified. In the next chapter, we move along the evolution of optical backbone networks to investigate how power consumption can be minimized in the next stage of Optical Burst Switching (OBS) backbone networks.

---

# SLEEP-MODE-ENABLED OBS NETWORKS

---

## 7.1 Introduction

The evolution cycle of backbone networks presented in Figure 1.2 in Chapter 1.1 shows that backbone networks are expected to progress from optical circuit switched (OCS) to burst switched (OBS) networks. Key differences between PtP-WDM, OCS, and OBS networks are discussed in Section 2.3. At present, a limited amount of research exists on minimizing power consumption of OBS networks. These studies show significant power savings from adopting the sleep mode of operation technique in OBS networks. Developments in this line of research and key findings are discussed in Section 2.3 and Section 2.5. In this chapter, we intend to reduce power consumption of a sleep-mode-enabled OBS network by proposing a novel burst assembly algorithm. Using this proposed algorithm, we assess how much more power can be saved in an OBS network in order to provide solution(s) to research problem 5:

- How much more power can be minimized in an OBS network by using sleep mode of operation?

In an OBS network, core nodes consist of burst switches (BuS). In this chapter, a BuS is referred to as an OBS router. As depicted in Figure 7.1, an OBS router situated at the source or destination core nodes (i.e., network edge) is specifically referred to as a burst assembly router or edge router [194], while those located in the intermediate core nodes are referred to as OBS core routers. A core node could possess the functionalities of both a burst assembly router and an OBS core router if it is serving both local and pass-through traffic. As shown in Figure 7.2, the burst assembly routers aggregate local IP traffic into data bursts. A data burst is released when the Threshold Releasing Criterion (TRC) is satisfied. At an intermediate OBS core router, data bursts carrying pass-through traffic are switched between input/output links by optical

devices.

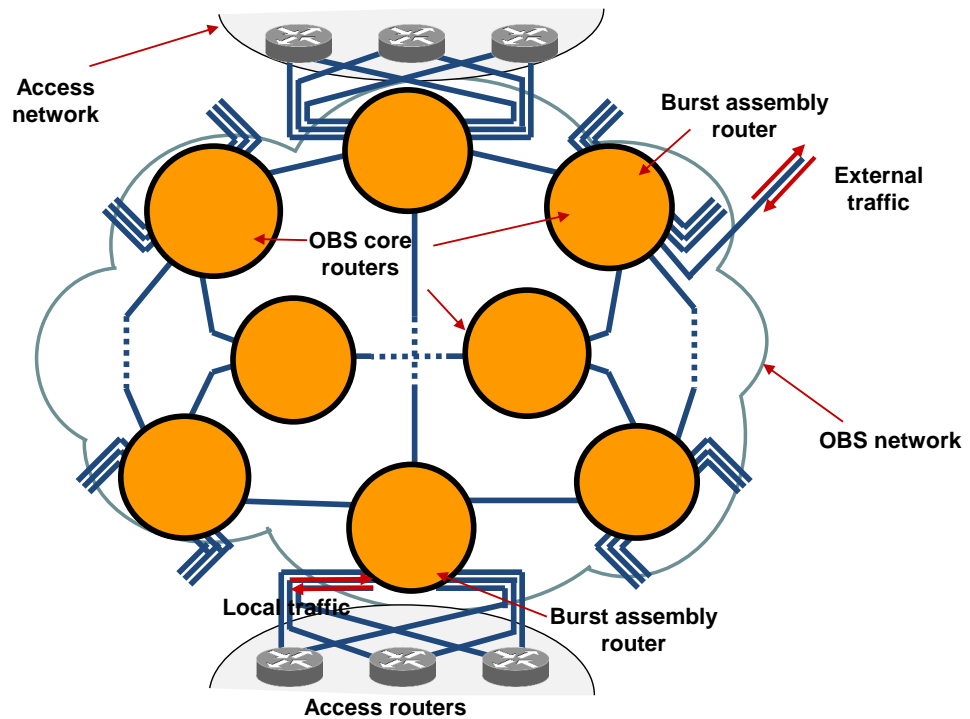


Figure 7.1: The fundamental architecture of an OBS network

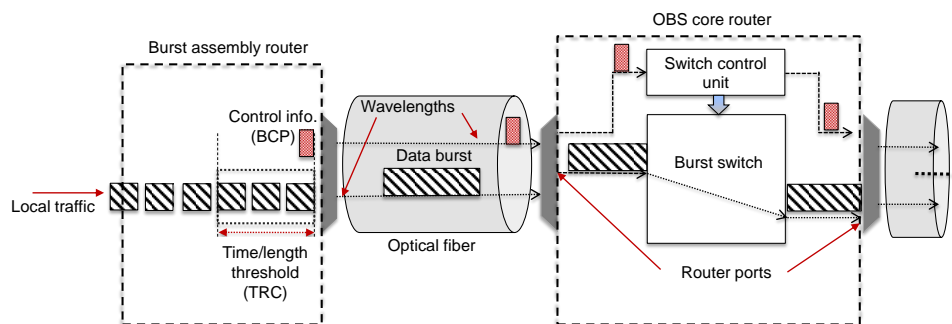


Figure 7.2: Key devices and operations of a burst assembly router and an OBS core router

In a PtP-WDM network, the ‘header’ (that carries control information) and the ‘payload’ (that carries actual data) are transmitted together as a single IP packet. However, as shown in Figure 7.2, in an OBS network, the Burst Control Packet (BCP) (that carries control information) and the data burst (that comprises multiple IP packets) are transmitted separately at consecutive time intervals along different wavelengths [291]. Since a BCP is significantly smaller than a data burst [292], it is processed at intermediate core nodes by electronics that operate at a slow speed.

Recent research efforts show that power consumption of an OBS network can be considerably reduced by adopting the sleep mode of operation [195, 196, 199, 293, 294]. Such networks are often referred to as sleep-mode-enabled OBS networks. According to [195, 199, 293, 294], network devices of a sleep-mode-enabled OBS network operate in three different states, namely, *active*, *sleep*, and *transition* states. The power consumption of a network device that serves two data bursts is illustrated in Figure 7.3. Total power consumed by a network device is considered to be proportional to the duration the device remains in each state [199]. A device consumes the most power when operating in *active state*, and the least power when operating in *sleep state*. A device moves between sleep and active states via *wake* and *sleep transition states*.

As described in Section 2.5, it is important that network devices sleep for longer durations and be switched on for shorter durations in order to reduce their power consumption. As a considerable amount of power is consumed by devices when they transition from one operating state to another, it is critical to reduce these transitions in order to minimize power consumption [196].

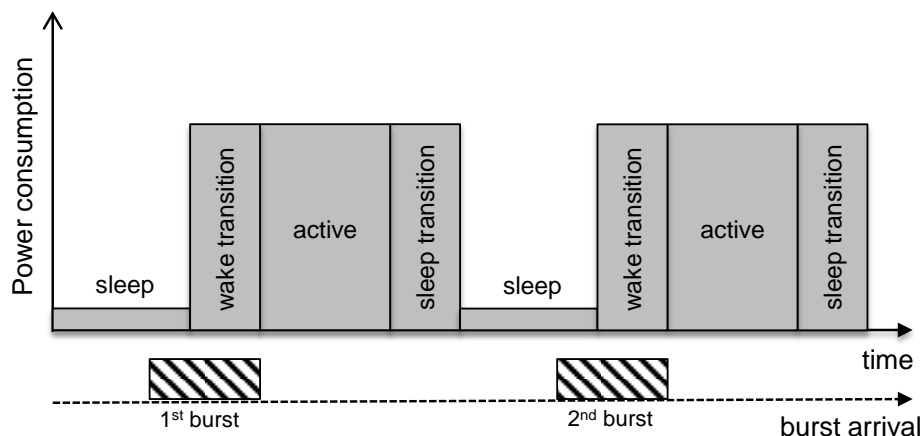


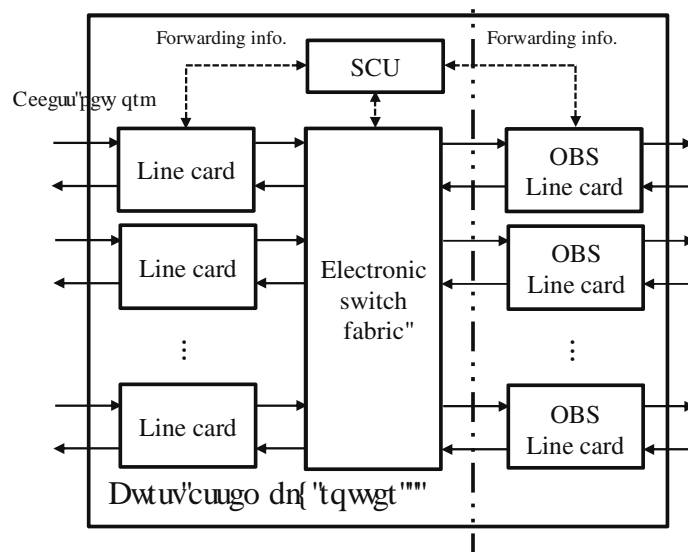
Figure 7.3: Power consumption at different operating states of a device in a sleep-mode-enabled OBS network

## 7.2 Network model

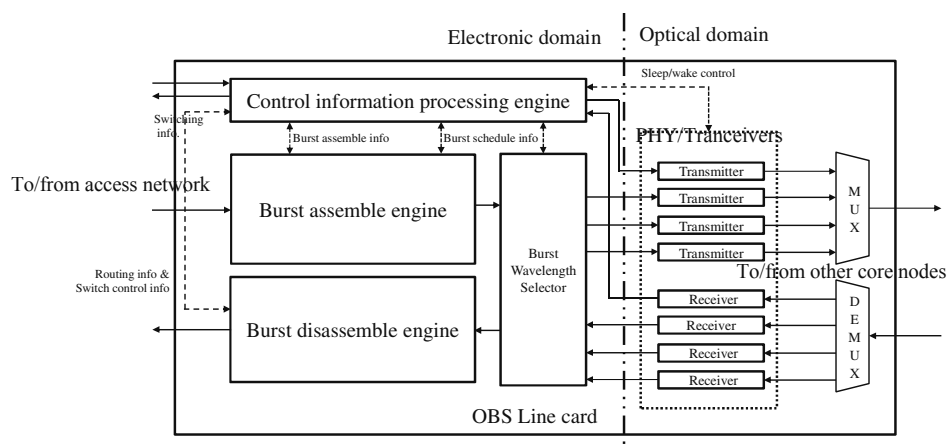
This section describes the network devices, their respective power consumption, and operations of a sleep-mode-enabled OBS network.

### 7.2.1 Burst assembly router

Figure 7.4a depicts the architecture of a sleep-mode-enabled burst assembly router [194]. The burst assembly router consists of line cards, an electronic switch fabric (i.e., Electronic Cross Connect EXC), a Switch Control Unit (SCU), and OBS line cards. The line cards work as the interface between the burst assembly router and the access network. Local traffic is *added to* or *dropped from* the backbone network via these line cards. The EXC, which is controlled by the SCU, provides the connection between line cards and OBS line cards. The OBS line cards assemble, disassemble, transmit, and receive data bursts.



(a) Block diagram of a burst assembly router [194]



(b) Block diagram of an OBS line card [194]

Figure 7.4: The architecture of an OBS burst assembly router [194]

As depicted in Figure 7.4b, an OBS line card consists of a control unit, burst assemble/disassemble engine, burst wavelength selector, and physical layer (PHY) transceivers. The

control unit retrieves information from incoming BCPs and generates outgoing BCPs. Incoming bursts that carry drop traffic are de-aggregated into IP traffic by the burst disassemble engine. Local add traffic is buffered in destination-based queues by the burst assemble engine. When a queue reaches the releasing threshold (also referred to as the burst threshold), aggregated traffic is released in the form of a data burst. The burst wavelength selector assigns a specific wavelength to the data burst. The PHY transceivers transmit outgoing bursts to, and receives incoming bursts from, the optical fibers. To reduce power consumption, a sleep/wake controller, integrated within the control unit of an OBS line card, forces the PHY transceivers to operate in sleep state while bursts are being generated.

If the releasing threshold is small, bursts are generated at a high frequency. To serve these data bursts, the PHY transceivers would have to frequently change between active and sleep operating states. On the other hand, if the releasing threshold is large, the PHY transceivers could operate in sleep state for longer durations and incur limited state transitions. In order to reduce power consumption then, it is preferable to increase the size of the releasing threshold [196].

### 7.2.2 OBS core router

Figure 7.5 portrays the basic architecture of an OBS core router. An OBS core router consists of an SCU and a Switch Block (SB). The SB contains an optical burst switch and Data Transmission Units (DTUs) integrated within the line cards. The DTU of a line card comprises a PHY transceiver and a fabric interface. While the PHY transceiver of the line card receives and transmits bursts, the fabric interface connects the line card ports and optical switch fabric. The sleep/wake controller, housed within the SCU, determines the burst arrival time and changes the operating states of the modules accordingly. To reduce power consumption, the PHY transceivers and the fabric interface operate in sleep state until a burst arrives at the DTU of the line card. The optical burst switch, BCP switch, and routing engine remain active unless all line cards are operating in sleep state.

Tables 7.1 and 7.2 report the power consumption values of these constituent devices of the burst assembly router and the OBS core router, respectively, which are extracted from [120, 194]. In [120, 194], power consumption of the OBS network devices is estimated using values available for conventional core routers (e.g., Cisco CRS-1) [14,93] and modules [295]. According to the power consumption values reported in [120, 194], if total power consumed by the Cisco

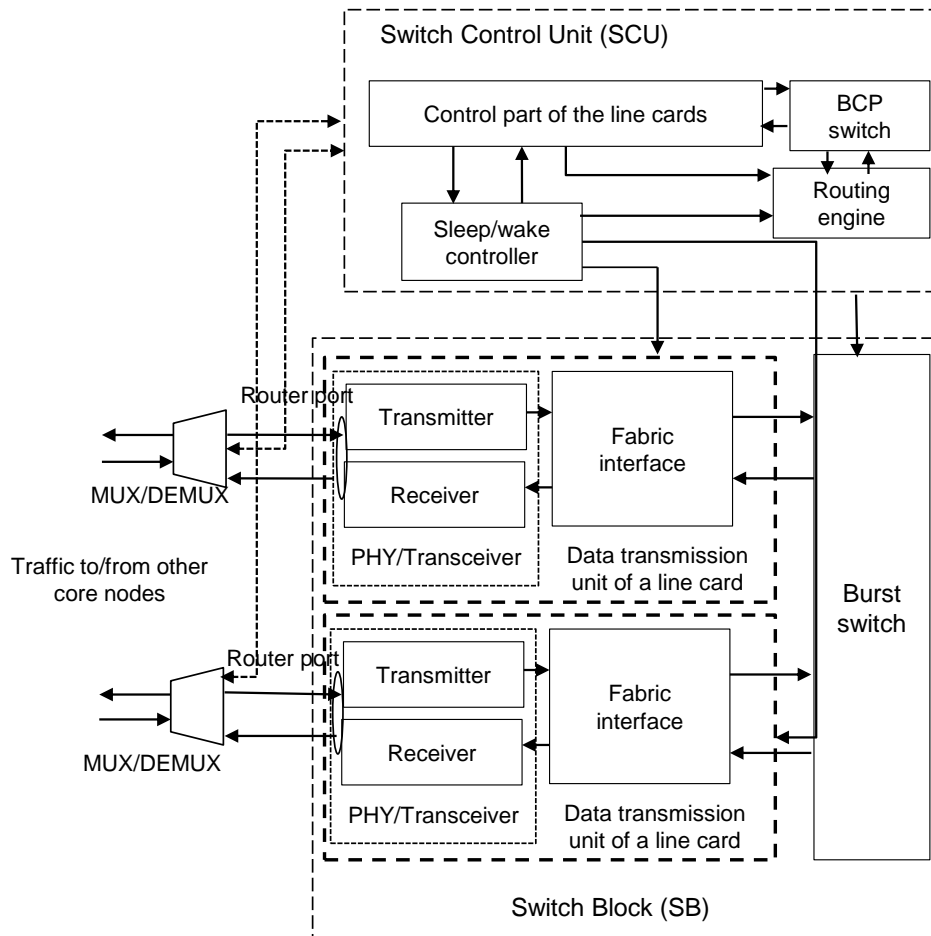


Figure 7.5: Block diagram of an OBS core router [120]

CRS-1 4-slot core router is 100%, then total power consumed by the sleep-mode-enabled burst assembly router is 130.6%. The values reported in Table 7.1 in this study then represent power consumption of the individual devices of the burst assembly router as a percentage of its total power consumption. Similarly, based on values reported in [120,194], if total power consumed by the Cisco CRS-1 4-slot core router with 4 line cards is 211.2% (the baseline Cisco CRS-1 4-slot core router with 1 line card is 100%), then total power consumed by the sleep-mode-enabled OBS core router with 4 active line cards is 268.8%. Therefore, Table 7.2 presents power consumption of the individual devices of the OBS core router as a percentage of its total power consumption.

As previously explained, the sleep/wake controller changes the operating state of the PHY transceivers (in the burst assembly routers) and DTUs (of line cards in the OBS core routers) according to burst arrival frequency. In [296], the single-shelf Cisco CRS-1 4-slot router is reported to have a switch capacity of 320 Gbps [93] and consume 4 kW of power. Power consumption

of a PHY transceiver would then be equal to 60 W according to 7.1. The DTU of a line card (referred to as an interface module) is reported to consume 150 W of power in [295] and [44].

Table 7.1: Power consumption of the devices in a burst assembly router as a percentage of its total power consumption [93]

Block	Module	Power (%)
OBS line card	Control unit	38.5
	Burst assemble engine	6.2
	Burst disassemble engine	7.9
	Wavelength selector	12.8
	PHY transceiver (40 Gbps)	1.5
SCU	Routing engine	39.4
	Switch controller	0.4
EXC (320 Gbps)		23.9
Total (Burst assembly router)		130.6
<i>Total (Cisco CRS-1 4-slot core router)</i>		<i>100</i>

### 7.2.3 Operation of a sleep-mode-enabled OBS network

The general operation of a sleep-mode-enabled OBS network is explained using Figure 7.6. Assume that the access network of node  $a$  is transmitting data to core nodes  $c$  and  $d$ . The burst assembly router of node  $a$  categorizes incoming traffic from the access network according to the destination and temporarily stores them in the respective queues of the burst assemble engines. Each queue is initiated when time (denoted by  $t$ ) is equal to 0 (i.e.,  $t = 0$ ). When a queue reaches the TRC, it releases a burst with length  $BL$  which is transmitted by the PHY transceiver. The bursts that carry traffic from node  $a$  to nodes  $c$  and  $d$  are denoted as  $b_{ac}$  and  $b_{ad}$ , respectively. The respective burst control packets are denoted as  $BCP_{ac}$  and  $BCP_{ad}$ . A BCP is released  $t_i$  seconds prior to releasing the respective data burst. Depending on the local data arrival rate and TRC, the respective queues take  $tQ_{ac}$  and  $tQ_{ad}$  seconds to generate  $b_{ac}$  and  $b_{ad}$ , respectively. Assume that to transmit a bit of traffic from nodes  $a$  to  $b$ ,  $b$  to  $c$ , and  $c$  to  $d$ , a total

Table 7.2: Power consumption of the devices in an OBS core router with 4 line cards as a percentage of its total power consumption [93]

Block	Module	Power (%)
SCU		215.6
Switch block	Data transmission unit (DTU)	30
	Optical switch fabric	19.4
Sleep wake controller		3.7
Total (OBS core router with 4 line cards)		268.7
<i>Total (Cisco CRS-1 4-slot core router with 4 line cards)</i>		<i>211.2</i>

of  $t_{ab}$ ,  $t_{bc}$ , and  $t_{cd}$  seconds are taken. Also assume that each node takes  $t_p$  seconds to examine, process, and switch a BCP. The control information is used to configure the DTUs of the OBS core routers to receive and transmit data bursts. Notations  $t_{wt}$  and  $t_{st}$  denote the time taken to awaken and sleep a PHY transceiver and a DTU. The amount of time taken to switch a data burst with length  $BL$  by the PHY transceiver and DTU during the active state is equal to  $t_a$  seconds, as defined in Equation 7.1. Time  $t_a$  depends on the switching speed ( $\Phi$ ) of the router port and  $BL$ .  $BL$  is considered to be identical to length-based TRC, as defined in Equation 7.2. If we assume that resources are configured using Just-Enough-Time (JET) one-way reservation protocol [297],  $b_{ac}$  and  $b_{ad}$  would arrive at node  $b$  after  $(tQ_{ac} + t_a + t_{ab})$  and  $(tQ_{ad} + t_a + t_{ab})$  seconds on two different wavelengths.

$$t_a \propto \frac{BL}{\Phi} \quad (7.1)$$

$$BL = \text{TRC} \quad (7.2)$$

In this example, bursts only carry pass-through traffic at node  $b$ . Therefore,  $BCP_{ac}$ ,  $b_{ac}$ ,  $BCP_{ad}$ , and  $b_{ad}$  are forwarded to node  $c$ . While  $b_{ac}$  is disassembled at node  $c$ ,  $BCP_{ad}$  and  $b_{ad}$  are forwarded to node  $d$ . At source node  $a$  and intermediate node  $b$ ,  $b_{ac}$  and  $b_{ad}$  arrive at overlapping time periods. However,  $b_{ac}$  and  $b_{ad}$  are switched separately and are thus handled individually by two PHY transceivers in node  $a$  and two DTUs at node  $b$ .

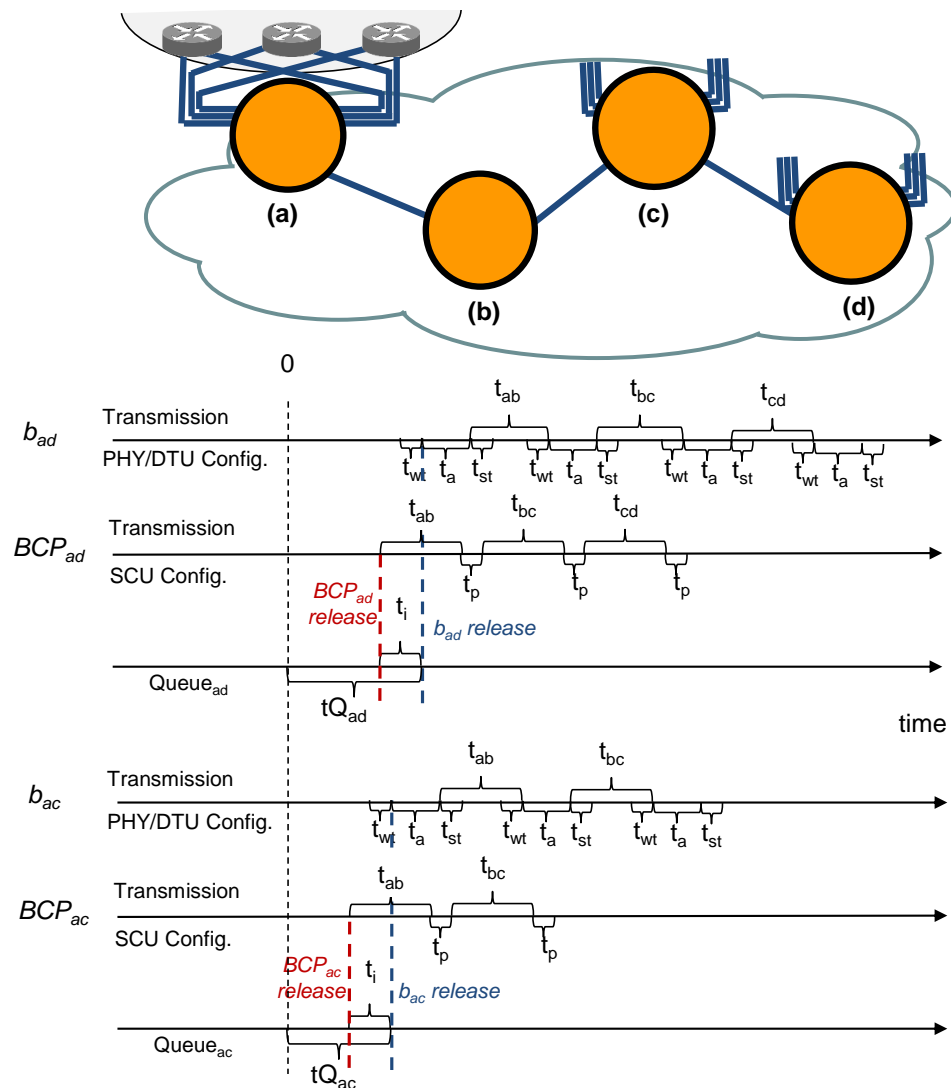


Figure 7.6: A simple example of a sleep-mode-enabled OBS network

#### 7.2.4 Power consumption model

As previously highlighted in this chapter, a burst assembly router and an OBS core router consist of line cards, with each containing a single or multiple router ports [93]. Each router port transmits and receives bursts through the PHY transceiver that operates in different states. In this study, we investigate power consumption of the OBS routers (both burst assembly and core routers) employing line cards that receive and transmit bursts through a single OC-768 (40 Gbps) router port [93]. When a router port is idle, the DTU and the PHY transceiver will operate in sleep state. In the remainder of this chapter, the term ‘router port’ is herein used to refer to the PHY transceiver of the burst assembly router and the DTU of the OBS core router.

Total power consumption of a sleep-mode-enabled burst assembly/core router for a period of  $T$  seconds is dependent on the amount of time that the router ports operate in each different

state [170,199]. Assuming that a router port of node  $q$  consumes  $P^a$ ,  $P^s$ , and  $P^t$  power as it spends a total of  $T_q^a$ ,  $T_q^s$ , and  $T_q^t$  seconds in active, sleep, and transition states, respectively, total power consumption of the router ports of node  $q$  ( $P_q^T$ ) can be represented using Equation 7.3 below. Note that  $P_q^T$  essentially represent energy consumption of the router ports of node  $q$ , which is measured using units Watt Seconds (Ws) or Joules (J).

$$P_q^T = P^a \times T_q^a + P^s \times T_q^s + P^t \times T_q^t \quad (7.3)$$

The corresponding values of  $T_q^a$ ,  $T_q^s$ , and  $T_q^t$  for a period of  $T$  seconds are approximated using the three equations below.

$$T_q^a = \left( \begin{array}{c} \text{locally assembled bursts} \\ \frac{R_{ql} \cdot T}{BL} \\ \text{pass-through bursts} \\ \frac{R_{qp} \cdot T}{BL} \end{array} \right) t_a \quad (7.4)$$

$$T_q^t = \left( \frac{R_{ql} \cdot T}{BL} + \frac{R_{qp} \cdot T}{BL} \right) t_t \quad (7.5)$$

$$T_q^s = T - (T_q^a - T_q^t) \quad (7.6)$$

Total time spent in the active state  $T_q^a$  is the product of the number of bursts switched by the router ports of node  $q$  and the time taken to switch a single burst  $t_a$  (that is defined in Equation 7.1). The number of bursts served by the router ports of node  $q$  depends on traffic arrival rates ( $R_{ql}$  and  $R_{qp}$ ) and  $BL$ . The router ports of node  $q$  serve data bursts which carry local traffic sourced at node  $q$  and travelling to other nodes, as well as pass-through traffic that traverses node  $q$ .  $R_{ql}$  denotes the arrival rate of local traffic and  $R_{qp}$  represent the arrival rate of pass-through traffic.

As depicted in Figure 7.6, the active state of a router port is always preceded and followed by a transition state. The total transition time, represented by notation  $T_q^t$  in Equation 7.5, is the product of the number of bursts switched by the router ports of node  $q$  and the sum ( $t_t$ ) of wake transition ( $t_{wt}$ ) and sleep transition times ( $t_{st}$ ) of each burst. According to [294],  $t_{wt}$  and  $t_{st}$  take fixed values.

Looking at Equations 7.1 to 7.6, it is observed that increasing TRC would increase the  $BL$ , resulting in traffic being accommodated by a smaller number of bursts. However, if  $BL$  increases,  $t_a$  would also increase. Therefore, despite reducing the number of bursts, increasing TRC would not impact  $T_q^a$ . However, as  $t_t$  remains fixed, increasing TRC would result in a

reduced total transition time  $T_q^t$ . Consequently, according to Equation 7.7, total energy consumption of the router ports of node  $q$  will reduce TRC.

Total energy consumed by the router ports of an OBS network ( $E_{\text{tot}}$ ) comprising  $V$  set of core nodes can then be modelled in Equation 7.7 as:

$$E_{\text{tot}} = \sum_{\forall q \in V} P_q^T \quad (7.7)$$

### 7.3 Problem definition

The goal of this chapter is to reduce power consumption of the router ports of a sleep-mode-enabled OBS network. If the TRC is small, burst assembly routers will generate bursts at a high frequency. Then, to serve these data bursts, the router ports (i.e., PHY transceivers and DTU) will rapidly oscillate between different operating states. On the other hand, if the TRC is large, fewer bursts are generated and router ports would undergo fewer state transitions. As a considerable amount of power is consumed when a device transits between different states, a large TRC is preferred over a small TRC to reduce power consumption of a sleep-mode-enabled OBS network [196]. However, a large TRC could degrade QoS by causing excessive queuing delay (i.e., the time taken to generate a burst) and lengthening the time between bursts arriving at destination nodes [199]. Taking these points into consideration, the power consumption minimization problem can be described using the following input parameters, assumptions, and goals.

#### 7.3.1 Input parameters

- The physical topology  $G = (V, E)$  consists of  $V$  set of core nodes and  $E$  set of physical links.
- Each core node has  $L$  number of line cards and each line card supports a single router port that has a maximum operation speed of  $O$ .
- Each physical link carries  $F$  number of fibers and every fiber can accommodate a maximum of  $W$  wavelengths. The maximum capacity of each wavelength is  $C$ .
- $R^{sd}$  is the arrival rate of traffic between node pair  $(s, d)$ .

### 7.3.2 Assumptions

- The traffic arrival rate does not change during the optimization process. Thus,  $R^{sd}$  for the node pair  $(s, d)$  remains constant.
- The wavelength assigned to a data burst cannot be changed at any intermediate node. Thus, the wavelength continuity constraint applies to every data burst.
- A router port cannot serve two or more data bursts at the same time period. Thus, burst overlapping does not occur at any given router port.
- Prior to the arrival of a data burst, the router port is awakened and reserved by the SCU based on the information carried by the respective BCP which precedes the data burst. Thus, data bursts do not encounter any additional delay as they travel through intermediate core nodes.
- If network resources do not have enough capacity to accommodate traffic,  $W$ ,  $L$ , and  $F$  can be increased accordingly. Thus, burst dropping is minimized.
- An active operating state of a router port is always preceded and followed by wake transition and sleep transition states, forming a single cycle. A router port can serve two or more data bursts within a single cycle only if bursts arrive back-to-back without any delay or overlapping.

### 7.3.3 Goals

- To reduce power consumption of the router ports in all core nodes of a sleep-mode-enabled OBS backbone network, which can be achieved by minimizing Equation 7.4.
- To satisfy QoS constraints by ensuring that the queuing delay does not exceed the maximum tolerance.

## 7.4 Methodology

We achieve the above goals using two separate strategies. First, we reduce the number of generated data bursts by increasing the TRC. Appropriate measures are taken to ensure acceptable queuing delay. Next, we propose a novel scheme which allows multiple bursts to be served as

a single entity and, in turn, reduce power consumption of a sleep-mode-enabled OBS network by minimizing state transitions of network devices.

#### 7.4.1 Strategy 1: Increase the Threshold Releasing Criterion

An OBS network can use time-based or length-based TRCs [197]. If a time-based TRC is used, a data burst is released from its respective queue after a specific time period. A timer is activated when a queue starts receiving traffic from its access network. The data within the queue is aggregated into a burst and released when the timer reaches the pre-defined value. The main advantage of a time-based TRC is that bursts are spaced at equal intervals, which minimizes the incurred delay between consecutive bursts. However, a time-based TRC is oblivious to the data arrival rate. Thus, if traffic arrives at a slow rate, a time-based TRC will generate multiple data bursts, each carrying a negligible amount of data. Nevertheless, as bursts are released at equal intervals, the router ports would still undergo the same number of transitions.

A length-based TRC releases a data burst when traffic in the queue reaches a pre-determined data length. The main advantage of the length-based TRC is that it generates equal-sized data bursts. The length of every data burst,  $BL$ , would then be equal. A length-based TRC is unlikely to release small-sized bursts and, thus, transitions between states are minimized. However, if data from the access network arrives at a slow rate, and if the length-based TRC is large, it could lead to significant queueing delay. Therefore, to reduce the number of transitions and delay, the length-based TRC has to be appropriately adjusted.

Using a simulation-based experiment, we seek to identify the best length-based TRC that provides the optimum balance between reducing power consumption and reducing queueing delay at different data arrival rates. The experiment is performed on a burst assembly router that receives IP traffic from the access network and transmits to other core nodes via router ports as shown in Figure 7.1. During each simulation, traffic from the access network arrives at the burst assembly router at a constant rate. The burst assembly router is provisioned with four OBS line cards, with each line card containing a single OC-768 router port. Incoming traffic is queued and converted into bursts by the burst assemble engines. These bursts are then transmitted by the PHY transceivers of the router ports. In each simulation, total power consumption of a sleep-mode-enabled burst assembly router is calculated for a time period of 1 second ( $T = 1$ ). The respective values used in the simulations are reported in Table 7.3. Total power consumption of the router ports for each arrival rate and TRC (measured in terms

of  $BL$ ), is plotted in Figure 7.7. Figure 7.8 depicts the queueing delay incurred with different combinations of traffic arrival rates and burst sizes.

Table 7.3: Values assigned to the parameters

Parameter	Value
$t_t(t_{wt} + t_{st})$	$\approx 10\mu s$ [294]
$T$	1s
$\Phi$	40 Gbps
$P^a, P^t$	150 W [93]
$P^i$	$0.1 \times P_a$ [195]

When traffic arrives at a rate of 100 Mbps or slower, the plotted results in Figure 7.7 show that router ports consume a negligible amount of power regardless of the burst threshold (i.e., TRC). As discussed in Section 7.2.4, the number of bursts generated is closely related to traffic arrival rate. If traffic arrives at a faster rate, a higher number of bursts is generated which, in turn, increases state transitions of burst assembly routers. As the data arrival rate increases beyond 1 Gbps, it is observed that the TRC has a significant impact on power consumption of the router ports. According to Figure 7.7, a TRC of 1 Mb substantially reduces power consumption at data arrival rate above 1 Gbps. However, only a trace amount of improvement is observed when the TRC is increased to over 1 Mb.

To maintain adequate QoS, queueing delay has to be restricted to a few tenths of a millisecond [298, 299]. Among the tested TRCs, 100 kb and 1 Mb TRCs are able to maintain an acceptable queueing delay (below 1 ms) for all traffic arrival rates.

The results of this study shows that, to provide balanced results of reducing power consumption and mitigating the negative impact on queueing delay, TRC of 1 Mb needs to be chosen over 100 kb, 10 Mb, and 100 Mb TRCs. Although the experiment only reports the reduction in power consumption of a burst assembly router, OBS core routers could also benefit by increased TRC as they too will then be required to only serve fewer data bursts.

#### 7.4.2 Strategy 2: Concatenate multiple bursts into a single burst

To minimize state transitions and reduce power consumption, traffic can be served using fewer bursts by appropriately adjusting the length-based TRC. However, if traffic arrives at a slow

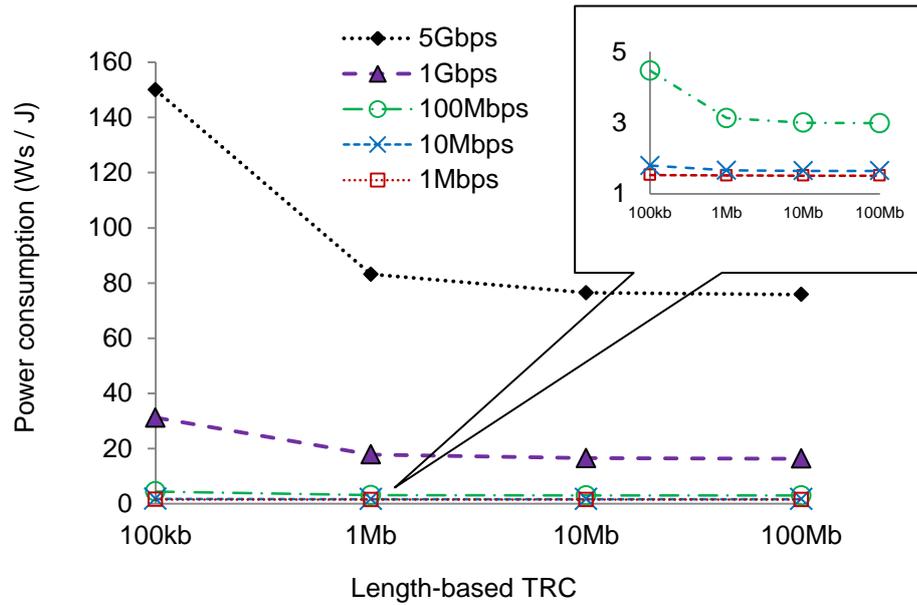


Figure 7.7: Relationship between power consumption, TRC, and traffic arrival rate

rate, a large TRC may cause excessive queueing delay. To counter this problem, we propose a novel scheme that serves multiple bursts as one burst to reduce the number of state transitions and, thereby, reduce power consumption.

In traditional OBS networks, a burst assembly router uses a Destination-Based (DEB) burst assembly scheme that aggregates traffic destined to a single destination into individual bursts. These bursts are required to travel through intermediate OBS core routers before arriving at the destination node. Bursts are individually switched by the router ports of these core routers.

Figure 7.9 portrays a segment of a traditional OBS network, where the access network of node  $s$  transmits traffic to nodes  $d_1$  and  $d_2$  at rates  $R^{sd_1}$  and  $R^{sd_2}$ , respectively. Bursts generated by the DEB burst assembly scheme at node  $s$ , within a period of  $t$  seconds, travel independently via core nodes  $b$  and  $c$  to their respective destinations. Since traffic arrival rates  $R^{sd_1}$  and  $R^{sd_2}$  are dissimilar ( $R^{sd_1}$  is faster than  $R^{sd_2}$ ), bursts are released at different time intervals. Consequently, the respective queues  $Q_{sd_1}$  and  $Q_{sd_2}$  take  $tQ_{sd_1}$  and  $tQ_{sd_2}$  time, respectively, to achieve the TRC. The respective data bursts  $b_{ad_1}$  and  $b_{ad_2}$  are served using two router ports (e.g.  $RP_1$  and  $RP_2$ ) at every core node.

Note that if a queue fails to achieve the releasing threshold within a pre-defined maximum time period (e.g.,  $tQ_{sd_1}^*$ ), the data within the queue is aggregated and transmitted as a partially-filled data burst  $b_{ad_1}^*$ .

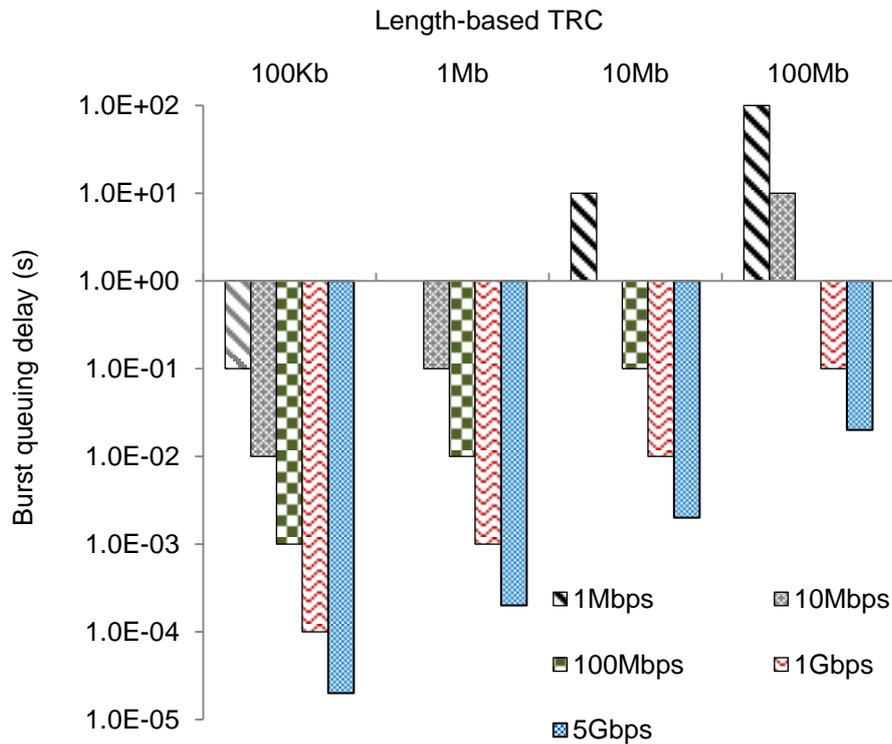


Figure 7.8: Relationship between queuing delay, TRC, and traffic arrival rate

#### 7.4.2.1 Destination- and Path-based Segmentation burst assembly scheme

The Destination- and Path-based Segmentation (DPS) burst assembly scheme, proposed in this study, identifies and concatenates multiple bursts that travel along a common path into a single 'Burst-of-Bursts' (BoB). The BoB is switched using a single router port, thereby reducing the operating state transitions of router ports. Unlike in a traditional OBS network (using the DEB scheme) where a single burst is served in a single cycle, in an OBS network employing the DPS burst assembly scheme, a router port could serve multiple bursts in a single cycle. Indirectly, the DPS scheme would then increase the burst size and assist in reducing state transitions.

It is important to note that, before concatenating bursts of two different traffic streams, the DPS scheme considers the traffic arrival rates, the number of core nodes traversed in the common sub-path, and the number of core nodes traversed by traffic beyond the common sub-path.

The operation of the DPS burst assembly scheme can be explained using the illustrative Figure 7.10. As in Figure 7.9, core node  $s$  transmits traffic to nodes  $d_1$  and  $d_2$  at rates  $R^{sd_1}$  and  $R^{sd_2}$ , respectively. Since  $R^{sd_1}$  is faster than  $R^{sd_2}$ , queue  $Q_{sd_1}$  achieves the releasing threshold prior to queue  $Q_{sd_2}$ . Thus,  $tQ_{sd_1}$  is smaller than  $tQ_{sd_2}$ . After evaluating the condition in Equation 7.8

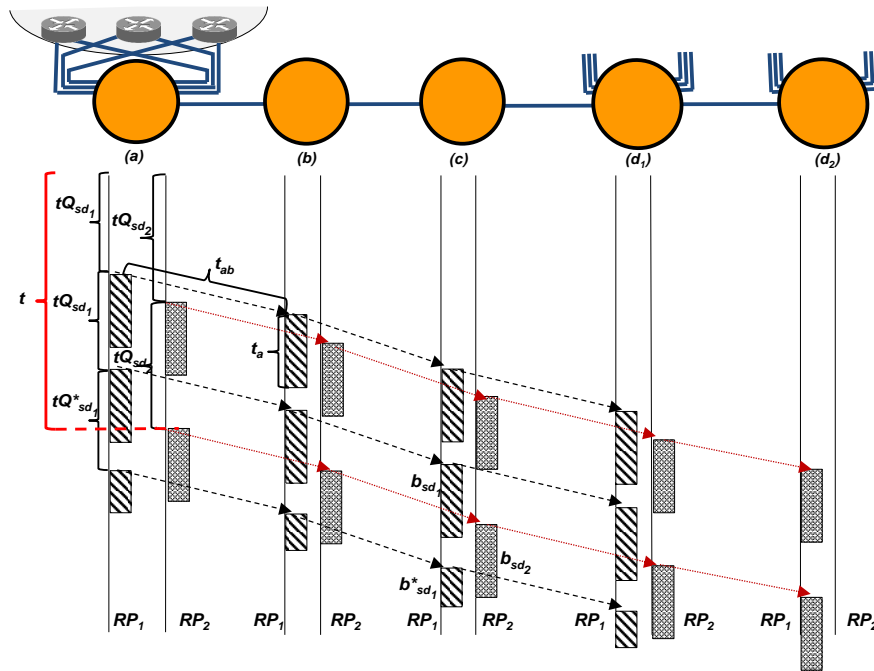


Figure 7.9: An example of a *traditional* OBS network which accommodates traffic between node pairs  $(s, d_1)$  and  $(s, d_2)$  that arrives at a rate of  $R^{sd_1}$  and  $R^{sd_2}$ , respectively, using the **DEB burst assembly scheme**

below, the DPS burst assembly scheme concatenates burst  $b_{sd_1}$  with the partially-filled burst  $b_{sd_2}$  (within  $tQ_{sd_2}^*$  seconds,  $tQ_{sd_2} > tQ_{sd_2}^*$ ) and produces a single BoB that is large in size. Since the BoB is released at the faster traffic arrival rate  $R^{sd_1}$ , the incurred queuing delay is minimized for both traffic streams. The BoB, in turn, travels through intermediate core nodes  $b$  and  $c$  as a single entity. Hence, the proposed DPS burst assembly scheme minimizes the number of state transitions of router ports  $RP_1$  and  $RP_2$  at intermediate nodes  $b$  and  $c$ , thereby reducing power consumption of the router ports of the OBS network. However, a slight increase in the number state transitions is experienced at node  $d_2$  since the BoB carries only fragments of  $b_{sd_2}$ . When the BoB arrives at node  $d_1$ , it is segmented [300,301] into multiple bursts, which are switched to the respective core nodes via corresponding router ports.

#### 7.4.2.2 Testing the condition

The condition in Equation 7.8 ensures that bursts can only be combined if it reduces the number of transitions within the period of  $T$  seconds. If this condition is not satisfied, the bursts are switched independently as in a traditional OBS network. Notations  $n$ ,  $n_{d_1}$ , and  $n_{d_2}$  denote the number of nodes along the common sub-path for the BoB, the remaining distance to node  $d_1$ , and the remaining distance to node  $d_2$ , respectively.

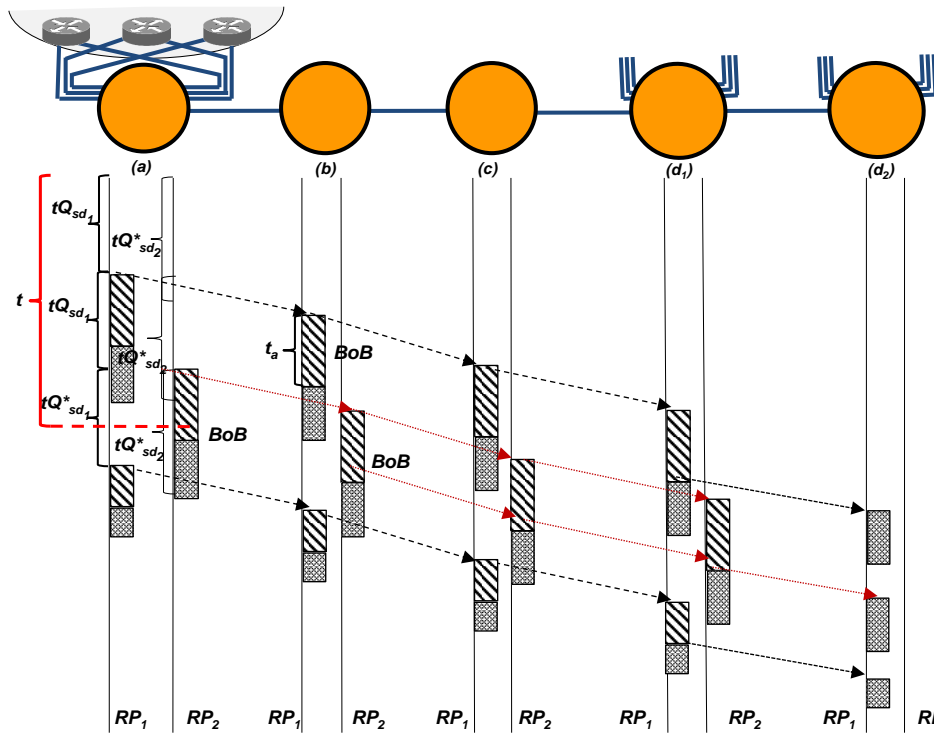


Figure 7.10: An example of an OBS network which accommodates traffic between node pairs  $(s, d_1)$  and  $(s, d_2)$  that arrives at a rate of  $R^{sd_1}$  and  $R^{sd_2}$ , respectively, using the **DPS burst assembly scheme**

Assume that in Figure 7.10,  $R_{sd_1}$ ,  $R_{sd_2}$ ,  $n$ ,  $n_{d_1}$ , and  $n_{d_2}$  are equal to 4.5 Gbps, 5 Gbps, 3, 0, and 1, respectively. Let the length-based TRC equal 100 kb. Effectively,  $BL$  would take the value 100 kb as well. Each intermediate OBS core router is allotted four line cards. Each line card has a single router port that operates at a maximum speed of 20 Gbps. The combined switching capacity of an OBS core router is then equal to 80 Gbps.  $t_{wt}$  and  $t_{st}$  are assigned fixed values of  $4.48 \mu s$  and  $2.88 \mu s$  [294]. We assume that a router port consumes equal amounts of power when operating in active and transition states. In [295] and [44], it is reported that each interface module of a line card consumes 150 W of power. In this study, each line card has a single router port which is connected to the DTU and PHY transceiver. Thus,  $P_a$  and  $P_t$  are each assumed to consume 150 W of power [93]. According to [195], a device operating in sleep state consumes  $0.1 \times P_a$  of power. Prior to concatenating bursts, the condition in Equation 7.8 is calculated in Equation 7.9 with these aforementioned values.

$$\underbrace{\frac{R^{sd_1} \cdot T}{TRC} (n + n_{d_1} + n_{d_2})}_{\text{Transitions with DPS}} < \underbrace{\frac{R^{sd_1} \cdot T}{TRC} (n + n_{d_1}) + \frac{R^{sd_2} \cdot T}{TRC} (n + n_{d_2})}_{\text{Transitions with DEB}} \quad (7.8)$$

Since  $R^{sd_1}$  is faster than  $R^{sd_2}$ , a BoB is generated at every  $\frac{100 \text{ kb}}{5 \text{ Gbps}} = 20 \mu s$ . If  $T$  is assumed to be 1 second, the condition 7.8 holds true, as can be seen in Equation 7.9 below.

$$\frac{5 \text{ Gbps} \cdot 1s}{100 \text{ kb}} (3 + 0 + 1) < \frac{5 \text{ Gbps} \cdot 1s}{100 \text{ kb}} (3 + 0) + \frac{4.5 \text{ Gbps} \cdot 1s}{100 \text{ kb}} (3 + 1) \quad (7.9)$$

## 7.5 Evaluation of results

To validate the superiority of the DPS burst assembly scheme, a simulation-based experiment is performed on a large-scale backbone network. The topology is generated by randomly placing 100 core nodes in different cities in Europe and connecting them through a two-connected physical links graph. Each physical link is initially provisioned with a single optical fiber that supports 80 wavelengths. By adjusting the node connectivity, it is guaranteed that traffic between nodes travels through 10 intermediate core nodes, on average, before arriving at the destination nodes along the shortest available path [8]. Each core node transmits traffic at different rates to other core nodes within the simulation period of  $T$  seconds. The maximum and minimum data arrival rates of traffic streams at each test instance is reported in Table 7.4. Bursts are generated with a length-based TRC which is varied between values 1 Mb and 100 kb, as shown in Table 7.4. Routing and wavelength assignment are performed using the SPR algorithm and FF wavelength assignment scheme, respectively. The power consumption values and sleep/wake transition times considered for these experiments are reported in Table 7.3. Burst assembly routers and OBS core routers are provisioned with four line cards, with each consisting of a single OC-768 router port. When the condition in Equation 7.8 is satisfied, bursts are concatenated; else, they are served independently. Simulations experiments for all test instances are run for 10 seconds each (i.e.,  $T = 10$ ).

Figure 7.11 shows the total energy consumption of the router ports for each test instance in Table 7.4. It is observed that the DPS burst assembly scheme has a positive impact on reducing power consumption over traditional OBS networks employing the DEB burst assembly scheme. The DPS scheme reduces energy consumption by a maximum of 1.1 kW at test instance 6. On average, the DPS burst assembly scheme reduces energy consumption by 0.48 kW at every test instance.

Figure 7.12 depicts the average burst queuing delay at each test instance. It is observed that the average queuing delay remains below 1 ms. Therefore, it is reasonable to argue that the

Table 7.4: Max. and Min. traffic arrival rates and burst threshold of the test network

Test instance	Data rate		Burst threshold	Avg. burst queueing delay
	Maximum	Minimum		
1	5 Gbps	5 Gbps	1 Mb	0.32 ms
2	5 Gbps	5 Gbps	100 kb	0.02 ms
3	5 Gbps	4.5 Gbps	1 Mb	0.27 ms
4	5 Gbps	4.5 Gbps	100 kb	0.02 ms
5	5 Gbps	500 Mbps	100 kb	0.02 ms
6	5 Gbps	500 Mbps	100 kb	0.02 ms

DPS burst assembly scheme does not drastically increase queueing delay while attempting to minimize the number of transition states.

Contrary to the encouraging results obtained for large-scale networks, the experiments indicate that the proposed DPS scheme has a limited impact on reducing power consumption when tested on networks with fewer core nodes (i.e., small-scale networks). We also observe that the number of core node hops shared by a BoB ( $n$ ) and the number of hops travelled by the bursts after segmenting ( $n_{d_1}$  and  $n_{d_2}$ ) have a strong impact on the feasibility of the DPS scheme. For example, if  $n$  is small and  $n_{d_1}$  and  $n_{d_2}$  are much larger, the condition in Equation 7.8 would not be satisfied and then the DPS scheme would not be applicable. Therefore, when the network consists of fewer core nodes (e.g., the NSF network),  $n$  is relatively small and bursts cannot be concatenated using the DPS scheme. Thus, the proposed DPS burst assembly scheme is more suited for networks with a large number of core nodes and physical links.

## 7.6 Summary of findings

In this chapter, we sought to address the power consumption minimization problem of a sleep-mode-enabled OBS network.

Sleep-mode-enabled OBS networks have garnered considerable interest in recent years. Novel node architectures and burst assembly/release algorithms have been proposed by many researchers to increase power savings of these networks. To increase power savings, the modules of core nodes have to undergo fewer operating state transitions, and to maintain QoS,

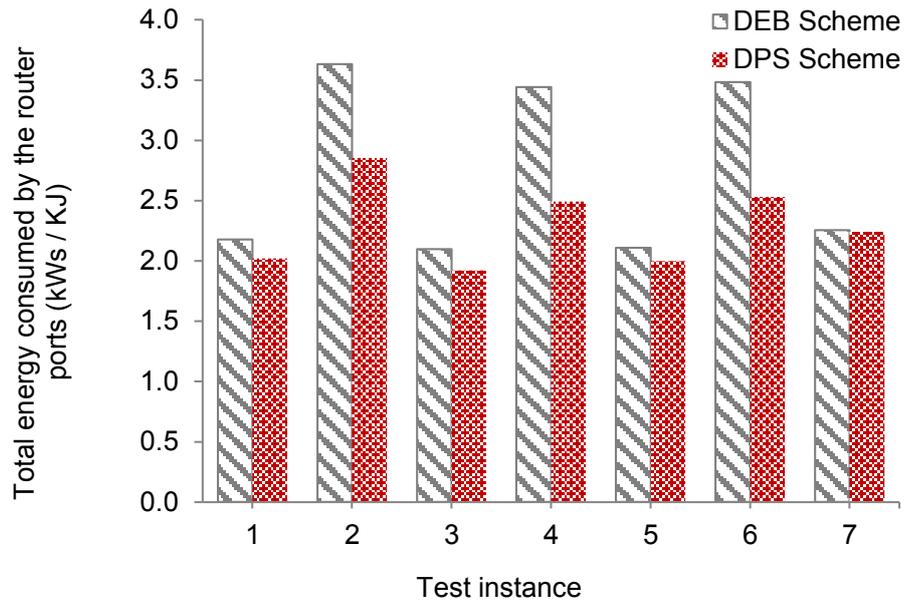


Figure 7.11: Power consumption of the router ports at every test instance when bursts are generated with the DEB and DPS schemes

burst queuing delay needs to be reduced.

In this chapter, we were able to identify the appropriate length-based TRC that could provide the best balance between reducing power consumption and maintaining an acceptable burst queuing delay. Our results show that this optimal value for length-based TRC should be 1 Mb.

We also proposed a novel DPS burst assembly scheme that reduces power consumption by intelligently releasing data bursts. To reduce power consumption, data bursts that travel via a common set of core nodes are concatenated into a single Burst-of-Burst (BoB). Preliminary results show that our proposed DPS burst assembly scheme reduces power consumption by 0.5 kW, on average, in comparison to traditional OBS backbone networks that use the DEB burst assembly scheme. As this work is only preliminary, future research could extend this work by experimenting on different networks using different traffic arrival rates.

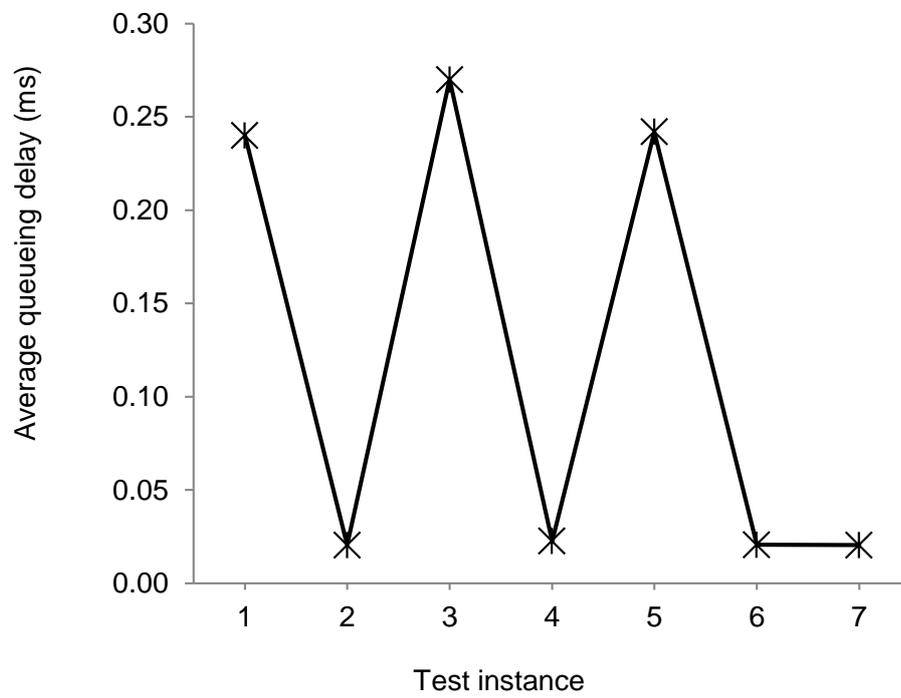


Figure 7.12: Average burst queueing delay at every test instance

---

# CONCLUSION

---

## 8.1 Looking back

Rising global electricity consumption and depleting fossil fuels that is the primary energy source for electricity are recognized as serious economic and environmental concerns. One of the significant ongoing discussions on reducing global electricity consumption is power consumption of the Internet. The current study was motivated by the consensus among researchers that power consumption of the Internet's backbone network will surpass that of its access network in the near future as network traffic triples. The central question in this thesis asks how the increasing power consumption problem of the Internet's backbone network can be solved.

Existing backbone networks are PtP-WDM networks that primarily use electronic devices and technologies such as electronic core routers. However, limitations of these electronic devices and technologies, such as the large amount of electricity consumed and heat dissipated as well as limited switching capacity, makes it difficult to serve increasing future traffic demands with PtP-WDM networks. As a result, these networks are gradually evolving into optical backbone networks, with OCS networks being the closest stage in the evolution of backbone networks. This thesis thus set out to analyze the power consumption of OCS backbone networks and identify solutions to reduce power consumption of these optical networks.

The existing literature was comprehensively analyzed to identify available solutions and determine if these solutions could be improved and/or if novel methods could be developed to reduce power consumption. Numerous solutions have been developed by researchers to tackle the power consumption issue of backbone networks. Based on observed similarities among these reviewed solutions, we were able to identify four main approaches used by researchers to reduce power consumption. We named these approaches as network redesign,

traffic engineering, power-aware networking, and load-adaptive operation.

Using the network redesign approach, power consumption is sought to be reduced by re-designing core nodes that is a main constituent device of the backbone network. Optical devices such as OXCs are gradually being introduced into core nodes to replace electronic core routers and transform PtP-WDM networks to OCS networks due to the inability to further increase power efficiency of electronic devices. However, completely replacing electronic devices with optical ones is not beneficial due to limitations in the optical buffering, processing and switching technologies of optical core nodes.

We found that solutions relying on hybrid technology, such as hybrid core nodes (i.e., HCNs) consisting of both electronic core routers and OXCs, reduce power consumption by negating the need for O-E/E-O conversions. Nevertheless, core routers are both expensive and power-hungry and, therefore, it is desirable to minimize the use of these devices in HCNs. However, there has been little discussion in the literature that indicates if all core nodes need to be equipped and how they can be equipped with core routers. This knowledge gap prompted us to define the first research problem in this thesis.

- How can core nodes be selectively equipped with core routers to minimize power consumption of an OCS backbone network?

Optimizing the physical topology of a backbone network is another network redesign solution that can be used to reduce power consumption. Laying physical links underground incurs a large CAPEX attributed to labour cost and over-provisioning physical links with a large number of active optical fibers leads to unnecessary power consumption during low traffic periods. Therefore, it is desirable to reduce the number of links and active fibers to reduce both cost and power consumption of a backbone network.

However, much of the research to date examine reduction of *either* cost *or* power consumption. To reduce cost, on one hand, network redesign approach (reducing the number of links) is used. To reduce power consumption, on the other hand, power-aware networking approach (switching off active fibers) is used. What is not yet clear is how much cost *and* power consumption can be reduced by using either method. Furthermore, these solutions have only been applied to non-survivable backbone networks, and very little is thus known about survivable networks, although survivability is an important QoS constraint. Additionally, link-laying cost which is the dominant contributor to CAPEX has not been accounted for in the studies that examined cost reduction. These limitations led to the formulation of the second research problem

in this thesis.

- How much electricity and cost can be reduced in an OCS network by appropriately configuring physical links?

Waveband grooming is a traffic engineering solution that is effectively used with the aim of reducing the number of optical switching ports of OXCs to reduce cost and overcome scalability limitations. However, many researchers subscribe to the belief that it has a minimal impact on reducing power consumption, because I/O ports are assumed to consume a negligible amount of power. However, recent evidence suggests that an I/O port of an OXC consumes 8 W of power which in truth is not negligible. Therefore, it is still important to examine power consumption of a backbone network that is capable of waveband grooming (i.e., BSN).

Most studies on power consumption of BSNs consider core node architectures with hybrid OXCs (HOXCs) and single-layer MG-OXCs only. However, power consumed by three-layer MG-OXCs that involve less O-E/E-O conversions than HOXCs and offer more flexibility in reconfiguration than single-layer MG-OXCs have received limited attention. Furthermore, as advanced AOWCs and AORs will soon reach commercial realization, they could be used to improve port savings of MG-OXCs. Yet, the reduction in power consumption that can be attained by using these advanced optical technologies in the three-layer MG-OXCs of BSNs is unknown. Lack of knowledge on this issue motivated the third research problem in this thesis.

- How can waveband grooming effectively incorporate the advanced features of MG-OXCs and all-optical technologies to minimize power consumption of an OCS network?

While waveband grooming is a traffic engineering solution that can be used to reduce power consumption of OXCs/MG-OXCs, MLR is a solution of the load-adaptive operation approach that reduces power consumption of transponders. A few studies have combined waveband grooming and MLR to examine how network *cost* can be reduced in an MLR-based BSN. However, no research was found that investigates how *power consumption* can be minimized in an MLR-based BSN. There are also currently no developed methods to implement an MLR-based BSN using advanced MG-OXCs.

Although transponders consume less power in MLR-based networks, these networks cannot necessarily be assumed to consume less power, because regenerators consume higher power due to the reduced transmission reach of lightpaths in MLR-based networks. Therefore, it becomes important to examine how waveband grooming and MLR can be combined to

reduce power consumption of an OCS network by maximizing power consumption reduction of transponders without greatly elevating regenerator power consumption. This research need gave rise to the fourth research problem in this thesis.

- How can waveband grooming and MLR be combined to reduce power consumption of an OCS network?

While the above research problems focused our research efforts on the power consumption issue of OCS networks, we also considered possible solutions that could be adopted to reduce power consumption of OBS networks that is the next stage in the evolution of backbone networks. OBS is a network (core node) redesign solution as its core node architecture differs from that of traditional PtP-WDM and OCS networks.

Recent studies have shown that using the power-aware networking solution of sleep mode of operation in OBS networks can offer significant power savings. From these studies, it is understood that power consumption can be further reduced by minimizing the number of operating state transitions of network devices in a sleep-mode-enabled OBS network. As research on sleep-mode-enabled OBS networks are still in early stages, more work needs to be done on reducing their power consumption. This knowledge gap in research spurred the fifth and final research problem in this thesis.

- How much more power can be minimized in an OBS network by using the sleep mode of operation?

Given the initial topology and traffic matrix, each research question attempted to determine how devices of core nodes and/or links could be optimized to reduce power consumption. These optimizations take the form of reducing the number of devices, modifying technology, modules, capacity, or speed of devices, and/or changing the operating states of devices/modules. In the following sections, we present a brief overview of the general process that was undertaken to solve each research problem. Key findings from solving each research problem are then summarized, followed by a discussion of future work.

## 8.2 General approach

In this thesis, five stages were involved in solving each research problem stated above. These stages included:

1. Defining the network architecture
2. Developing the power consumption model
3. Defining the problem
4. Solving the problem using heuristics
5. Evaluating the results

*Defining the network architecture:* The fundamental network architecture of the backbone network, explained using Figure 1.1 in Chapter 1, remained consistent across all research problems, although specific values for certain constituent devices of core nodes and links differed in some research problems. While most research problems dealt with a homogeneous backbone network consisting of identical core nodes (i.e., all core nodes are hybrid core nodes consisting of a core router and a OXC), research problem 1 dealt with a heterogeneous backbone network consisting of either hybrid core nodes or core nodes containing only OXCs.

*Developing the power consumption model:* Total power consumption of the backbone network was determined by the sum of power consumed by core nodes and links. Power consumption of a core node or a link was equivalent to total electricity consumed by their constituent devices. Power consumption of a device was modelled in two different ways. The first modelling scheme used in solving research problem 1 differed from that used to solve the remaining research problems. This modelling scheme considered power consumption of a network device to be equivalent to the product of *device utilization* and *power consumption of the device at its maximum capacity*, assuming that network devices satisfy much-needed power-load proportionality. In all other research problems, the second modelling scheme was used, which assumed that power consumption of a network device was equivalent to the sum of electricity drawn by all active modules of the respective device.

*Defining the problem:* Given the initial network topology and traffic matrix, the primary objective of each research problem was to reduce power consumption by optimizing devices of the core nodes and/or links. The objective of every research problem was defined using the respective power consumption model and represented as an ILP formulation. Research problems 1 and 4 investigated the problem of reducing power consumption of both IP- and WDM-layer devices of the backbone network. Research problems 2 and 3 addressed the power consumption minimization issue of WDM-layer devices only, while research problem Robs

addressed the power consumption minimization issue of IP-layer devices only. In addition to reducing power consumption, research problems 2, 4, and 5 also accounted for certain QoS constraints such as ensuring network survivability, reducing cost, and reducing transmission distance and delay.

*Solving the problem using heuristics:* Network optimization problems are generally categorized as NP-hard problems. As shown in Chapter 4, certain variables (e.g., wavelength continuity constraint) may have hundreds of thousands of instances, which leads to increased complexity. Due to high complexity, solving the defined problem for large-scale networks is not trivial. Optimum results may only then be attained for small-scale networks. Therefore, in this thesis, heuristic-based algorithms were used to solve the research problems.

After determining the initial parameters and the expected final result, an objective function(s) was defined. The objective was then achieved by minimizing or maximizing the developed objective function(s) using the proposed heuristic algorithms. Although the steps in the proposed algorithms vary across research problem, every algorithm routed and assigned wavelengths using the SPR algorithm and FF wavelength assignment scheme, respectively.

*Evaluating the results:* The proposed algorithms were evaluated by running simulation-based algorithms on randomly-generated or real-life networks. The relevant traffic matrix was generated by using different traffic distribution models or using reported actual traffic statistics. Results obtained for each research problem were evaluated by comparing them to existing solutions and/or benchmarked results.

Key differences in the network architecture, power consumption model, problem definition, heuristics proposed, and obtained results among the five research problems are summarized in Table 8.1.

## **8.3 Summary of key findings**

### **8.3.1 Sparse grooming in OCS networks**

Power consumption of an OCS backbone network was first reduced by selectively transforming all-optical core nodes to grooming nodes. Specifically, by placing core routers at a few selected core nodes, power consumption of links and core nodes was jointly reduced. The following conclusions are drawn from this study on sparse grooming, which solve the first research problem on how core nodes should be selectively equipped with core routers to minimize power

Table 8.1: Key differences across research problems

Parameter	Problem 1	Problem 2	Problem 3	Problem 4	Problem 5
Network	OCS	OCS	OCS	OCS	OBS
Node type	Hybrid & All-optical	Hybrid	Hybrid	Hybrid	OBS router
Pwr. Model	1*	2*	2	2	2
Layer	IP & WDM	WDM	WDM	IP & WDM	IP
Minimize	Power	Power & Cost <sup>◇</sup>	Power & Cost <sup>†</sup>	Power & Cost <sup>†</sup>	Power
QoS	-	Two connected topology, survivable network	Reduce transmission distance	Reduce transmission distance	Reduce burst queueing delay
Heuristic	Greedy	MO	BPLS	MT, MTR, HMTR	DPS
Wavelength conversion	Not allowed	Not allowed	Allowed	Allowed	Not allowed
Exprm. Network	Australian	NSF	NSF & EON	NSF	Random
Traf. Model	Gravity	Statistical	Uniform & Gravity	Uniform	Controlled Random

consumption:

1. A backbone network with full grooming capability consumes a significant amount of power.
2. To reduce power consumption, a core router should only be placed at:
  - core nodes which handle large amounts of sub-wavelength traffic, and
  - core nodes that are placed farther from other nodes.

The above conclusions were derived using a power-load proportional model, a static traffic matrix generated using a gravity traffic distribution model, and by running experiments on the Australian network.

### 8.3.2 Traffic-dependent link optimization

Next, we reduced power consumption and cost by optimizing the physical link topology using physical topology redesign and power-aware networking approaches. The following conclusion are drawn from this research on physical link optimization, which solve the second research problem on how much electricity and cost can be reduced by configuring physical links:

1. Deployment cost of a backbone network can be reduced by appropriately assigning physical links.
2. The physical link topology can be dimensioned using the proposed IS or GS schemes.
3. As a large proportion of CAPEX is made up of link-laying cost, CAPEX can be minimized the most by using the GS scheme as it reduces more physical links than the IS scheme.
  - CAPEX of the OCS network optimized with the GS scheme is reduced by approximately 77% to 87% compared to a non-optimized network.
4. Power consumption can be reduced by dimensioning the network using the IS scheme and allowing devices to sleep during low-load traffic periods using the proposed MO algorithm.
  - Power consumption of the OCS network optimized with the MO algorithm reduces power consumption, on average, by 1.3 MWh in a day and 40 MWh in a month.

### 8.3.3 Designing power-efficient band-switched OCS networks

Then, power consumption of a BSN was reduced by appropriately selecting three design parameters - band size, grouping policy, and band configuration - according to different network environments (i.e., different-sized networks, different traffic volumes, and different traffic distribution models). The following conclusions are drawn from this study on BSNs employing three-layer MG-OXCs provisioned with all-optical devices, which solve the third research problem on how waveband grooming can incorporate advanced MG-OXCs and all-optical technologies to minimize power consumption:

1. A BSN consumes less power than a WSN, especially when network traffic is high and when traffic is distributed using the gravity traffic distribution model.
2. If design parameters are not adjusted appropriately, a BSN may consume more power than a WSN due to stringent hierarchical traffic flow constraints of three-layer MG-OXCs.
3. Regardless of the size of the network and traffic distribution model, our research shows that power consumption can be reduced by using the following design parameters:
  - Assign a small band size when network traffic is low,
  - Assign a large band size when network traffic is high,
  - Group wavelengths using the INT grouping policy that allows wavebands to be regrouped at intermediate nodes, and
  - Group wavebands with C1 band configuration that increases bandwidth utilization, instead of C2 band configuration that reduces demultiplexing at intermediate nodes.

### 8.3.4 MLR-based band-switched OCS networks

Waveband grooming was combined with MLR to further reduce power consumption of an OCS network. The main findings of this study on MLR-based BSNs are summarized below, which solve the fourth research problem on how MLR can be used with waveband grooming to minimize power consumption:

1. MLR-based BSN consumes less power than SLR-based networks that use 10 or 40 Gbps line rates.

2. When traffic is assigned line rates with the proposed HMTR scheme, an MLR-based BSN consumes approximately the same amount of power as 100 Gbps SLR-based networks that consume the least power but are more expensive.
3. While transponders consume less power, regenerators consume more power in MLR-based networks in comparison to SLR-based networks.
4. Legacy 10 and 40 Gbps SLR-based networks should be replaced with HMTR-optimized MLR-based BSNs employing three-layer MG-OXC equipped with all-optical converters and regenerators.

### 8.3.5 Sleep-mode-enabled OBS networks

Power consumption of a sleep-mode-enabled OBS network was reduced by switching individual modules of burst assembly routers and OBS core routers into sleep state. The following conclusions are drawn from this study on sleep-mode-enabled OBS networks, which solve the fifth research problem on how much more power can be minimized in an OBS network by using sleep mode of operation:

1. Power consumption can be drastically reduced by transporting traffic using large-sized bursts.
2. Although large-sized bursts result in reduced power consumption, they also increase the burst assembly time, thus causing increased queueing delay.
  - To keep queueing delay below 1 ms while reducing power consumption, burst length is increased to 1 Mb.
3. By concatenating multiple bursts into a single 'Burst-of-Bursts', the proposed DPS scheme reduces power consumption by 0.48 kW on average for all tested burst lengths and data arrival rates compared to OBS networks using the existing DEB scheme.

## 8.4 Expected future work

### 8.4.1 Sparse grooming in OCS networks

To provide better insight into the power-saving abilities of sparse grooming, the research undertaken in this study can be extended by considering the second power consumption model,

where power consumption of network devices is considered to be equivalent to the sum of power consumed by individual active modules.

It is important to bear in mind that the proposed algorithm was tested with a small-sized network with a set of pre-defined  $k$  and  $k_a$  values. Our findings could therefore be strengthened by performing more experiments in the future on different-sized networks, such as the NSF network and EON, using actual traffic statistics. Furthermore, to prevent our algorithm from becoming perplexed at a local optimum, methods such as Simulated Annealing could be used to improve our developed algorithm.

Furthermore, this study only utilized the DB or end-to-end wavelength grooming scheme. Therefore, to increase bandwidth utilization, the proposed sparse grooming technique can be combined with the MHB grooming scheme. In addition, instead of using core routers with a single capacity, core nodes of a sparse groomed network can be equipped with core routers of different capacities to increase power savings.

#### **8.4.2 Traffic-dependent link optimization**

The physical link topology in this research was dimensioned to reduce cost and power consumption. However, the study did not take into account geographical constraints which could impact the feasibility of the dimensioned network. Hence, this research could be extended by including geographical constraints in the optimization problem.

Furthermore, the dimensioned network is only resilient against single-link failures. However, in the occurrence of natural or man-made disasters, two or more links can fail. A network would then need to be dimensioned to be resilient against multiple link failures, which serves as an interesting future direction for this research.

#### **8.4.3 Designing power-efficient band-switched OCS networks**

In this study, the WXC layer of the MG-OXCs and OXCs were assumed to be provisioned with wavelength converters. Given this assumption, results indicated that a BSN consumes less power. However, if MG-OXCs are not allowed to use wavelength converters, the proposed BPLS algorithm will need to be modified accordingly. Then, whether a BSN employing three-layer MG-OXCs would still consume less power and ports than a WSN is an interesting question that can be explored in the future.

Previously, the impact of design parameters on power consumption was examined for BSNs

employing hybrid MG-OXCs. This research evaluated the impact of design parameters on power consumption of a BSN employing advanced three-layer MG-OXCs. It would then be interesting to identify how these design parameters would affect power consumption of a BSN employing single-layer MG-OXCs, thereby enabling a comparison of the three MG-OXC architectures in terms of power savings.

The study could also be extended to analyze the effect of design parameters on power consumption of a BSN under dynamic traffic demands.

Based on prior assumptions and work of scholars, this study similarly assumed that an mAOR consumes less power than many single-wavelength AORs. However, actual power consumption of an mAOR is yet to be made publicly available. When actual power consumption of mAORs becomes readily available, this experiment should be repeated to ensure validity of the obtained results and derived conclusions.

#### **8.4.4 MLR-based band-switched OCS networks**

This research undertaken on MLR-based BSNs can be extended by experimenting with dynamic traffic demands and using different traffic distribution models. Cost savings of the proposed MBSN can also be compared against SLR-based networks.

To allow wavelengths of a waveband to be served using a single mAOR, a waveband in this research was only allowed to carry wavelengths of identical line rates. This makes it difficult to form wavebands when wavelengths are assigned multiple line rates. As a result, a large number of wavelengths had to travel via single-hop wavebands and traverse the WXC layer of intermediate nodes. Therefore, future research could analyze power consumption of MLR-based BSNs when wavebands are allowed to carry wavelengths of different line rates.

Furthermore, power consumption of AOWCs and AORs of different line rates were approximated using available data. When actual power consumption values of these devices become available, the experiments carried out in this study can be repeated to ensure that our results remain valid.

#### **8.4.5 Sleep-mode-enabled OBS networks**

Current research on sleep-mode-enabled networks is still at an early stage. Hence, we believe that there is more opportunity for further exploration and extension in this novel area. In this study, experiments were only performed on a randomly-generated network with a random-

dynamic traffic matrix. Future experiments could be performed on real-life networks using actual traffic statistics.

---

# Bibliography

---

- [1] U.S. Energy Information Administration, "International energy outlook 2013," Tech. Rep., 2013. [Online]. Available: <http://citeseerx.ist.psu.edu/viewdoc/download?doi=10.1.1.369.6789&rep=rep1&type=pdf>
- [2] S. Lambert, W. Van Heddeghem, W. Vereecken, B. Lannoo, and M. Pickavet, "Worldwide electricity consumption of communication networks," *Optics Express*, vol. 20, no. 26, pp. B513–B524, 2012.
- [3] The Cliamte Group, "SMART 2020: enabling the low carbon economy in the information age," Tech. Rep., 2008. [Online]. Available: [http://www.smart2020.org/\\_/files/02\\_Smart2020Report.pdf](http://www.smart2020.org/_/files/02_Smart2020Report.pdf)
- [4] J. Glanz, "Power, pollution and the Internet," 2012. [Online]. Available: <http://www.nytimes.com/2012/09/23/technology/data-centers-waste-vast-amounts-of-energy-belying-industry-image.html?pagewanted=1&r=2&>
- [5] M. Xia, M. Tornatore, Y. Zhang, P. Chowdhury, C. C. U. Martel, and B. Mukherjee, "Green provisioning for optical WDM networks," *IEEE Journal of Selected Topics in Quantum Electronics*, vol. 17, no. 99, pp. 437–445, 2011.
- [6] U.S. Energy Information Administration, "International carbon dioxide emissions and carbon intensity," 2006. [Online]. Available: <http://www.eia.gov/emeu/international/carbondioxide.html>
- [7] D. Clark and M. Berners-Lee, "What's the carbon footprint of the Internet," 2010. [Online]. Available: <http://www.theguardian.com/environment/2010/aug/12/carbon-footprint-internet>
- [8] J. Baliga, R. Ayre, K. Hinton, W. V. Sorin, and R. S. Tucker, "Energy consumption in optical IP networks," *Journal of Lightwave Technology*, vol. 27, no. 13, pp. 2391–2403, 2009.
- [9] R. Tucker, R. Parthiban, J. Baliga, K. Hinton, R. Ayre, and W. Sorin, "Evolution of WDM optical IP networks: a cost and energy perspective," *Journal of Lightwave Technology*, vol. 27, no. 3, pp. 243–252, 2009.
- [10] A. Dwivedi and R. Wagner, "Traffic model for USA long-distance optical network," in *Optical Fiber Communication Conference (OFC)*, New York, USA, 2000, pp. 156–158.
- [11] R. Parthiban, "Modeling and analysis of optical backbone networks," Ph.D. dissertation, Dept. Elect. and Electro. Eng., University of Melbourne., Melbourne., VIC., 2004.

- 
- [12] Cisco, "Cisco visual networking index: forecast and methodology, 2012-2017," Tech. Rep., 2013. [Online]. Available: [http://www.cisco.com/en/US/solutions/collateral/ns341/ns525/ns537/ns705/ns827/white\\_paper\\_c11-481360.pdf](http://www.cisco.com/en/US/solutions/collateral/ns341/ns525/ns537/ns705/ns827/white_paper_c11-481360.pdf)
- [13] J. Baliga, K. Hinton, and R. S. Tucker, "Energy consumption of the internet," in *Joint International Conference on Optical Internet and 32nd Australian Conference on Optical Fiber Technology (COIN-ACOFT)*, Sydney, Australia, 2007, pp. 1–3.
- [14] S. Aleksic, "Analysis of power consumption in future high-capacity network nodes," *Journal of Optical Communications and Networking*, vol. 1, no. 3, pp. 245–257, 2009.
- [15] S. Aleksic, "Power consumption issues in future high-performance switches and routers," in *10th Anniversary International Conference on Transparent Optical Networks*, Athens, Greece, 2008, pp. 194–198.
- [16] R. S. Tucker, "Green optical communications ? part II : energy limitations in networks," *IEEE Journal of Selected Topics in Quantum Electronics*, vol. 17, no. 2, pp. 261–274, 2011.
- [17] R. S. Tucker, "Green optical Ccommunications?part I: energy limitations in transport," *IEEE Journal of Selected Topics in Quantum Electronics*, no. 99, pp. 1–16, 2010.
- [18] W. Van Heddeghem, F. Idzikowski, W. Vereecken, D. Colle, M. Pickavet, and P. Demeester, "Power consumption modeling in optical multilayer networks," *Photonic Network Communications*, vol. 24, no. 2, pp. 86–102, 2012.
- [19] L. Barroso and U. Holzle, "The case of energy-proportional computing," *IEEE Computer*, vol. 40, no. 12, pp. 33–37, 2007.
- [20] P. Mahadevan, P. Sharma, S. Banerjee, and P. Ranganathan, "Energy aware network operations," in *IEEE INFOCOM Workshops 2009*, Rio de Janeiro, Brazil, 2009, pp. 1–6.
- [21] D. Blumenthal, B. Olsson, and G. Rossi, "All-optical label swapping networks and technologies," *Journal of Lightwave Technology*, vol. 18, no. 12, pp. 2058–2075, 2000.
- [22] E. Ciaramella, "Wavelength conversion and all-optical regeneration: achievements and open issues," *Journal of Lightwave Technology*, vol. 30, no. 4, pp. 572–582, 2012.
- [23] F. Idzikowski, L. Chiaraviglio, and F. Portoso, "Optimal design of green multi-layer core networks," in *3rd International Conference on Future Energy Systems*, Madrid, Spain, 2012, pp. 1–9.
- [24] L. Benjamin and S. Meinrath, "Building a 21st century broadband superhighway," 2009. [Online]. Available: [http://www.newamerica.net/publications/policy/building\\_21st\\_century\\_broadband\\_superhighway](http://www.newamerica.net/publications/policy/building_21st_century_broadband_superhighway)
- [25] P. Ferreira, W. Lehr, and L. McKnight, "Optical networks and the future of broadband services," *Technological Forecasting and Social Change*, vol. 69, no. 7, pp. 741–758, 2002.
- [26] P. Chowdhury, M. Tornatore, A. Nag, E. Ip, T. Wang, and B. Mukherjee, "On the design of energy-efficient Mixed-Line-Rate (MLR) optical networks," *Journal of Lightwave Technology*, vol. 30, no. 1, pp. 130–139, 2012.
- [27] Y. Wang and X. Cao, "Multi-granular optical switching: A classified overview for the past and future," *IEEE Communications Surveys & Tutorials*, vol. 14, no. 3, pp. 698–713, 2012.
- [28] W. Hou and L. Guo, "Robust and integrated grooming for power-and port-cost-efficient design in IP over WDM networks," *Journal of Lightwave Technology*, vol. 29, no. 20, pp. 3035–3047, 2011.

- 
- [29] X. Cao, V. Anand, and C. Qiao, "Framework for waveband switching in multigranular optical networks: part II—wavelength/waveband conversion and survivability [Invited]," *Journal of Optical Networking*, vol. 6, no. 1, pp. 48–62, 2007.
- [30] X. Cao, V. Anand, and C. Qiao, "Waveband switching for dynamic traffic demands in multigranular optical networks," *IEEE/ACM Transactions on Networking (TON)*, vol. 15, no. 5, pp. 957–968, 2007.
- [31] L. McLauchlan and M. Mehrubeoglu, "A survey of green energy technology and policy," in *IEEE Green Technologies Conference*, Grapevine, TX, USA, 2010, pp. 1–6.
- [32] United Nations, "Kyoto protocol." [Online]. Available: <http://unfccc.int/kyoto-protocol/items/3145.php>
- [33] M. Kakemizu and A. Chugo, "Approaches to green networks," *FUJITSU Science Technical Journal*, vol. 46, no. 4, pp. 398–403, 2009.
- [34] Y. Zhang, P. Chowdhury, M. Tornatore, and B. Mukherjee, "Energy efficiency in telecom optical networks," *IEEE Communications Surveys & Tutorials*, vol. 12, no. 4, pp. 441–458, 2010.
- [35] R. Bolla, R. Bruschi, F. Davoli, and S. Member, "Energy efficiency in the future internet : a survey of existing approaches and trends in energy-aware fixed network infrastructures," *IEEE Communications Surveys & Tutorials*, vol. 13, no. 2, pp. 223–244, 2011.
- [36] A. P. Bianzino, C. Chaudet, D. Rossi, and J.-L. Rougier, "A survey of green networking research," *IEEE Communications Surveys & Tutorials*, vol. 14, no. 1, pp. 3–20, 2012.
- [37] W. V. Heddeghem, B. Lannoo, D. Colle, M. Pickavet, and F. Idzikowski, "Power consumption evaluation of circuit-switched versus packet-switched optical backbone networks," in *Green Communications (GreenCom)*, Piscataway, NJ, USA, 2013, pp. 56–63.
- [38] D. Kilper, G. Atkinson, S. Korotky, S. Goyal, P. Vetter, D. Suvakovic, and O. Blume, "Power trends in communication networks," *IEEE Selected Topics in Quantum Electronics*, vol. 17, no. 2, pp. 275–284, 2011.
- [39] A. Nag, M. Tornatore, and B. Mukherjee, "Optical network design with mixed line rates and multiple modulation formats," *Journal of Lightwave Technology*, vol. 28, no. 4, pp. 466–475, 2009.
- [40] F. Idzikowski, "Power consumption of network elements in IP over WDM networks," Tech. Rep., 2009. [Online]. Available: [http://www.tkn.tu-berlin.de/fileadmin/fg112/Papers/powerNumbers\\_final.pdf](http://www.tkn.tu-berlin.de/fileadmin/fg112/Papers/powerNumbers_final.pdf)
- [41] Cisco, "10-Gbps multirate transponder card for the Cisco ONS 15454 multiservice transport platform," Tech. Rep., 2006. [Online]. Available: [http://www.cisco.com/en/US/prod/collateral/optical/ps5724/ps2006/ps5320/product\\_data\\_sheet0900aecd80121bf7.html](http://www.cisco.com/en/US/prod/collateral/optical/ps5724/ps2006/ps5320/product_data_sheet0900aecd80121bf7.html)
- [42] Cisco, "Cisco CRS 16-slot single-shelf system," 2012. [Online]. Available: [http://www.cisco.com/en/US/prod/collateral/routers/ps5763/CRS-3.16-Slot\\_DS.pdf](http://www.cisco.com/en/US/prod/collateral/routers/ps5763/CRS-3.16-Slot_DS.pdf)
- [43] Juniper Networks, "T series core routers," 2012. [Online]. Available: <http://www.juniper.net/us/en/products-services/routing/t-tx-series/>
- [44] W. Van Heddeghem and F. Idzikowski, "Equipment power consumption in optical multilayer networks - source data," Tech. Rep., 2012. [Online]. Available: <http://www.springerlink.com/index/10.1007/s11107-011-0370-7>

- [45] P. Chowdhury, A. Nag, and M. Tornatore, "Mixed-Line-Rate (MLR) optical network design considering heterogeneous fiber dispersion maps," in *IEEE 37th European Conference and Exhibition on Optical Communications (ECOC)*, Geneva, Switzerland, 2011, pp. 1–3.
- [46] R. Salem, M. Foster, A. C. Turner, D. F. Geraghty, M. Lipson, and A. L. Gaeta, "All-optical regeneration on a silicon chip," *Optics Express*, vol. 15, no. 12, pp. 7802–7809, 2007.
- [47] V. Taeed, M. Shokooh-Saremi, L. Fu, I. Littler, D. Moss, M. Rochette, B. Eggleton, Y. Ruan, and B. Luther-Davies, "Self-phase modulation-based integrated optical regeneration in chalcogenide waveguides," *Selected Topics in Quantum Electronics*, vol. 12, no. 3, pp. 360–370, 2006.
- [48] M. Rochette, G. Taeed, V. D. Moss, L. Fu, M. Shokooh-Saremi, I. Littler, Y. Ruan, B. Davies, and B. Eggleton, "Integrated all-optical regenerator in chalcogenide glass," in *31st European Conference on Optical Communications*, London, UK, 2005, pp. 407–408 (vol 3).
- [49] C. Stamatidis, K. Vyrsokinos, L. Stampoulidis, A. Maziotis, Z. Sheng, D. Van Thourhout, J. Bolten, M. Karl, T. Wahlbrink, and H. Avramopoulos, "All-optical wavelength conversion at 160Gb/s using an SOA and a 3rd order SOI nanowire periodic filter," in *IEEE Photonic Society's 23rd Annual Meeting*, Denver, CO, USA, 2010, pp. 268–269.
- [50] R. S. Tucker, "Scalability and energy consumption of optical and electronic packet switching," *Journal of Lightwave Technology*, vol. 29, no. 16, pp. 2410–2421, 2011.
- [51] L. Stampoulidis, E. Kehayas, K. Vyrsokinos, L. Zimmermann, F. Gomez-Agis, J. Kreissl, L. Moerl, and G. Preve, "Silicon nanophotonic chips enable greener and faster telecommunications networks," pp. 1–3, 2010. [Online]. Available: <http://spie.org/x39548.xml?highlight=x2400>
- [52] K. Vyrsokinos, L. Stampoulidis, F. Gomez-Agis, K. Voigt, L. Zimmermann, T. Wahlbrink, Z. Sheng, D. V. Thourhout, and H. J. S. Dorren, "Ultra-high speed, all-optical wavelength converters using single SOA and SOI photonic integrated circuits," in *IEEE Photonics Society Winter Topicals Meeting Series (WTM)*, Majorca, Spain, 2010, pp. 113–114.
- [53] A. A. M. Saleh, J. J. M. Simmons, and S. Member, "Evolution toward the next-generation core optical network," *Journal of Lightwave Technology*, vol. 24, no. 9, pp. 3303–3321, 2006.
- [54] R. S. Tucker, "Will optical replace electronic packet switching?" 2007. [Online]. Available: <http://www.spie.org/x14157.xml>
- [55] K. Hinton, J. Baliga, R. Ayre, and R. S. Tucker, "The future internet - an energy consumption perspective," in *IEEE 14th OptoElectronics and Communications Conference*, Sapporo, Japan, 2009, pp. 1–2.
- [56] R. S. Tucker, "The role of optics and electronics in high-capacity routers," *Journal of Lightwave Technology*, vol. 24, no. 12, pp. 4655–4673, 2006.
- [57] R. S. Tucker, K. Hinton, and G. Raskutti, "Energy consumption limits in high-speed optical and electronic signal processing," *Electronics Letters*, vol. 43, no. 17, pp. 906–908, 2007.
- [58] R. S. Tucker, "Optical packet-switched WDM networks: a cost and energy perspective," in *Optical Fiber Communication/National Fiber Optic Engineers Conference (OFC/NFOEC)*, San Diego, CA, USA, 2008, pp. 1–25.
- [59] A. Nag, M. Tornatore, and B. Mukherjee, "Energy-efficient and cost-efficient capacity upgrade in mixed-line-rate optical networks," *Journal of Optical Communications and Networking*, vol. 4, no. 12, pp. 1018–1025, 2012.

- 
- [60] R. Xin, G. Rouskas, and H. Perros, "On the physical and logical topology design of large-scale optical networks," *Journal of Lightwave Technology*, vol. 21, no. 4, pp. 904–915, 2003.
- [61] C. Guan and V. Chan, "Efficient physical topologies for regular WDM networks," in *Optical Fiber Communication Conference (OFC)*, Los Angeles, CA, USA, 2004, TuH1 (1–3).
- [62] D. A. R. Chaves, E. A. Barboza, C. J. A. Bastos-Filho, and J. F. Martins-Filho, "A multi-objective approach to design all-optical and translucent optical networks considering CapEx and QoT," in *14th International Conference on Transparent Optical Networks (ICTON)*, Coventry, UK, 2012, pp. 1–4.
- [63] R. Ramaswami and K. K. Sivarajan, "Design of logical topologies for wavelength-routed optical networks," *IEEE Journal on Selected Areas in Communications*, vol. 14, no. 5, pp. 840–851, 1996.
- [64] M. Xuezhou, K. Sangmin, K. Harfoush, X. Ma, and S. Kim, "Towards realistic physical topology models for internet backbone networks," in *6th International Symposium on High Capacity Optical Networks and Enabling Technologies (HONET)*, Alexandria, Egypt, 2009, pp. 36–42.
- [65] D. Neilson, "Photonics for switching and routing," *IEEE Selected Topics in Quantum Electronics*, vol. 12, no. 4, pp. 669–678, 2006.
- [66] G. Moore, "Cramming more components onto integrated circuits," *IEEE Solid State Circuits Newsletter*, vol. 86, no. 1, pp. 82–85, 1998.
- [67] ITRS, "International technology roadmap for semiconductors." [Online]. Available: <http://www.itrs.net/>
- [68] R. S. Tucker, "Optical packet switching: a reality check," *Optical Switching and Networking*, vol. 5, no. 1, pp. 2–9, 2008.
- [69] B. Krzanich, "Mobilizing Intel," in *Intel Developer Forum*, San Francisco, CA, USA, 2013, p. Key note.
- [70] S. J. B. Yoo, "Energy efficiency in the future internet: the role of optical packet switching and optical-label switching," *IEEE Selected Topics in Quantum Electronics*, vol. 17, no. 2, pp. 1–13, 2011.
- [71] M. Law and R. Colwell, "The chip design game at the end of Moore's law," in *Hot Chips*, Paris, France, 2013, p. Key Note.
- [72] A. Manocha, "Foundry driven innovation in the mobility era," in *SEMICON West 2013*, San Francisco, CA, USA, 2013, p. Key note.
- [73] T. Stern, G. Ellinas, and K. Bala, *Multiwavelength optical networks: architectures, design, and control*, Melbourne, Australia, Cambridge Univ. Press, 2008.
- [74] S. J. B. Yoo, "Optical packet and burst switching technologies for the future photonic Internet," *Journal of Lightwave Technology*, vol. 24, no. 12, pp. 4468–4492, 2006.
- [75] S. J. B. Yoo, "Optical label switching technology and energy-efficient future networks," in *International Conference on Photonics in Switching*, Pisa, Italy, 2009, pp. 1–2.
- [76] E. Burmeister, D. Blumenthal, and J. Bowers, "A comparison of optical buffering technologies," *Optical Switching and Networking*, vol. 5, no. 1, pp. 10–18, 2008.

- [77] R. Tucker and C. Chang-Hasnain, "Slow-light optical buffers: capabilities and fundamental limitations," *Journal of Lightwave Technology*, vol. 23, no. 12, pp. 4046–4066, 2005.
- [78] G. Appenzeller, I. Keslassy, and N. McKeown, "Sizing router buffers," in *Conference on Applications, Technologies, Architectures, and Protocols for Computer Communications*, Portland, OR, 2004, pp. 281–292.
- [79] H. Yang and S. Yoo, "All-optical variable buffering strategies and switch fabric architectures for future all-optical data routers," *Journal of Lightwave Technology*, vol. 23, no. 10, pp. 3321–3330, 2005.
- [80] H. Yang, V. Akella, N. Chuah, and J. Yoo, "Scheduling optical packets in wavelength, time, and space domains for all-optical packet switching routers," in *IEEE International Conference on Communications*, Piscataway, NJ, USA, 2005, pp. 1836–1842.
- [81] S. Danielsen, C. Joergensen, B. Mikkelsen, and K. Stubkjaer, "Analysis of a WDM packet switch with improved performance under bursty traffic conditions due to tuneable wavelength converters," *Journal of Lightwave Technology*, vol. 16, no. 5, pp. 729–735, 1998.
- [82] S. Danielsen, C. Joergensen, B. Mikkelsen, and K. Stubkjaer, "Optical packet switched network layer without optical buffers," *IEEE Photonics Technology Letters*, vol. 10, no. 6, pp. 896–898, 1998.
- [83] V. Eramo and M. Listanti, "Power consumption in bufferless optical packet switches in SOA technology," *Journal of Optical Communications and Networking*, vol. 1, no. 3, pp. B15–B29, 2009.
- [84] I. Szczesniak, B. Mukherjee, and T. Czacho?wski, "Approximate analytical performance evaluation of synchronous bufferless optical packet-switched networks," *IEEE Journal of Optical Communications and Networking*, vol. 3, no. 10, pp. 806–815, 2011.
- [85] N. Yan, H. Jung, I. Monroy, and T. Koonen, "All-optical multi-wavelength conversion with negative power penalty by a commercial SOA-MZI for WDM wavelength multicast," in *Optical Fiber Communication and the National Fiber Optic Engineers Conference (OFC/NFOEC)*, Anaheim, CA, USA, 2007, pp. 1–3.
- [86] C. Politi, C. Matrakidis, and A. Stavdas, "Optical Wavelength and waveband converters," in *IEEE International Conference on Transparent Optical Networks*, Nottingham, England, 2006, pp. 179–182.
- [87] N. Chi, L. Xu, K. S. Berg, T. Tökle, and P. Jeppesen, "All-optical wavelength conversion and multichannel 2R regeneration based on highly nonlinear dispersion-imbalanced loop mirror," *IEEE Photonics Technology Letters*, vol. 14, no. 11, pp. 1581–1583, 2002.
- [88] H. Chung, R. Inohara, K. Nishimura, and M. Usami, "All-optical multi-wavelength conversion of 10 Gbit/s NRZ/RZ signals based on SOA-MZI for WDM multicasting," *Electronics Letters*, vol. 41, no. 7, pp. 432–433, 2005.
- [89] National Inst. of Adv. Indust. Sci. and Tech, "Vertically integrated center for technologies of optical routing towards ideal energy saving," Tech. Rep., 2008. [Online]. Available: <http://www.aist.go.jp/aist-j/press.release/pr2008/pr20081001/pr20081001.html>
- [90] S. Peng, K. Hinton, J. Baliga, R. Tucker, Z. Li, A. Xu, P. Shuping, and L. Zhengbin, "Burst switching for energy efficiency in optical networks," in *Optical Fiber Communication/National Fiber Optic Engineers Conference (OFC/NFOEC)*, San Diego, CA, USA, 2010, pp. 1–3.

- 
- [91] F. Musumeci, M. Tornatore, G. Fontana, M. Riunno, S. Bregni, and A. Pattavina, "Energy-efficiency of all-optical transport through time driven switching," *IET Optoelectronics*, vol. 6, no. 4, pp. 173–182, 2012.
- [92] F. Musumeci, F. Vismara, V. Grkovic, M. Tornatore, and A. Pattavina, "On the energy efficiency of optical transport with time driven switching," in *IEEE International Conference on Communications (ICC)*, Kyoto, Japan, 2011, pp. 1–5.
- [93] Cisco, "Cisco CRS-1 carrier routing system," 2011. [Online]. Available: <http://www.cisco.com/en/US/products/ps5763/index.html>
- [94] R. S. Tucker, "Optical packet switching meets mythbusters," in *Optical Fiber Communication Conference/National Fiber Optic Engineers Conference 2011*, Washington, D.C., USA, 2011, p. OTuG4.
- [95] E. Bonetto, D. Cuda, G. A. G. Castillo, and F. Neri, "The role of arrayed waveguide gratings in energy-efficient optical switching architectures," in *Optical Fiber Communication/National Fiber Optic Engineers Conference (OFC/NFOEC)*, San Diego, CA, USA, 2010, pp. 10–12.
- [96] E. Bonetto, L. Chiaraviglio, D. Cuda, G. A. G. Castillo, F. Neri, P. Torino, C. Duca, and D. Abruzzi, "Optical technologies can improve the energy efficiency of networks," in *35th European Conference on Optical Communication (ECOC)*, Vienna, Austria, 2009, pp. 1–4.
- [97] S. Aleksić, "Electrical power consumption of large electronic and optical switching fabrics," in *IEEE Photonics Society Winter Topicals Meeting Series*, Majorca, Spain, 2010, pp. 95–96.
- [98] S. Aleksić and N. Fehratovic, "Requirements and limitations of optical interconnects for high-capacity network elements," in *12th International Conference on Transparent Optical Networks (ICTON)*, Munich, Germany, 2010, pp. 1–4.
- [99] P. Pavon-marino and F. Neri, "On the myths of optical burst switching," *IEEE Transactions on Communications*, vol. 59, no. 9, pp. 2574–2584, 2011.
- [100] M. Yano, F. Yamagishi, and T. Tsuda, "Optical MEMS for photonic switching-compact and stable optical crossconnect switches for simple, fast, and flexible wavelength applications in recent photonic networks," *IEEE Journal of Selected Topics in Quantum Electronics*, vol. 11, no. 2, pp. 383–394, 2005.
- [101] M. Murakami, "Analyzing power consumption in optical cross-connect equipment for future large-capacity optical networks," *Journal of Networks*, vol. 5, no. 11, pp. 1254–1259, 2010.
- [102] H. Takenouchi, R. Urata, and T. Nakahara, "First demonstration of a prototype hybrid optoelectronic router," in *5th European Conference on Optical Communication ECOC*, Vienna, Austria, 2009, pp. 2–3.
- [103] R. Takahashi, R. Urata, H. Takenouchi, and T. Nakahara, "Hybrid optoelectronic router for asynchronous optical packets," in *International Conference on Photonic Switching*, Pisa, Italy, 2009, pp. 1–2.
- [104] C. Xin, C. Qiao, Y. Ye, and S. Dixit, "A hybrid optical switching approach," in *IEEE Global Telecommunications Conference (GLOBECOM)*, San Francisco, USA, 2003, pp. 3808–3812.

- 
- [105] E. Wong and M. Zukerman, "Analysis of an optical hybrid switch," *IEEE Communications Letters*, vol. 10, no. 2, pp. 108–110, 2006.
- [106] S. Aleksii, M. Fiorani, and M. Casoni, "Energy efficiency of hybrid optical switching," in *14th International Conference on Transparent Optical Networks (ICTON)*, Coventry, UK, 2012, pp. 1–4.
- [107] M. Fiorani, M. Casoni, and S. Aleksic, "Hybrid optical switching for an energy-efficient internet core," *IEEE Internet Computing*, vol. 17, no. 1, pp. 14–22, 2013.
- [108] M. Fiorani, M. Casoni, and S. Aleksic, "Performance and power consumption analysis of a hybrid optical core node," *Journal of Optical Communications and Networking*, vol. 3, no. 6, pp. 502–513, 2011.
- [109] M. Fiorani, M. Casoni, and S. Aleksic, "Hybrid optical switching for energy-efficiency and QoS differentiation in core networks," *Journal of Optical Communications and Networking*, vol. 5, no. 5, pp. 484–497, 2013.
- [110] S. Aleksic, "Energy efficiency of electronic and optical network elements," *IEEE Journal of Selected Topics in Quantum Electronics*, vol. 17, no. 2, pp. 296–308, 2011.
- [111] F. Musumeci, M. Tornatore, and A. Pattavina, "A power consumption analysis for IP-over-WDM core network architectures," *Journal of Optical Communications and Networking*, vol. 4, no. 2, pp. 108–117, 2012.
- [112] F. Musumeci, D. Siracusa, G. Rizzelli, M. Tornatore, R. Fiandra, and A. Pattavina, "On the energy consumption of IP-over-WDM architectures," in *International Conference on Communications (ICC)*, Ottawa, Canada, 2012, pp. 3004–3008.
- [113] A. Autenrieth, A. K. Tilwankar, C. M. Machuca, and J.-P. Elbers, "Power consumption analysis of opaque and transparent optical core networks," in *13th International Conference on Transparent Optical Networks*, Stockholm, Sweden, 2011, pp. 1–5.
- [114] I. Tomkos, J. Leuthold, P. Petropoulos, D. Bimberg, and A. Ellis, "Multi-wavelength all-optical regeneration," in *Digest of the IEEE/LEOS Summer Topical Meetings*, Acapulco, Mexico, 2008, pp. 167–168.
- [115] P. G. Patki, M. Vasilyev, and T. I. Lakoba, "All-optical regeneration of multi-wavelength signals," in *IEEE/LEOS Winter Topicals Meeting Series*, Innsbruck, Tyrol, Austria, 2009, pp. 254–255.
- [116] J. Wang, J. Yu, T. Meng, W. Miao, and B. Sun, "Simultaneous 3R regeneration of 4 40-Gbit/s WDM signals in a single Fiber," *IEEE Photonics Journal*, vol. 4, no. 5, pp. 1816–1822, 2012.
- [117] L. Provost, F. Parmigiani, K. Mukasa, M. Takahashi, J. Hiroishi, M. Tadakuma, K. Petropoulos, and D. Richardson, "Simultaneous all-optical 2R regeneration of 4x10 Gbit/s wavelength division multiplexed channels," in *33rd European Conference and Exhibition on Optical Communication (ECOC)*, Berlin, Germany, 2007, pp. 451–451.
- [118] X. Dong, T. El-gorashi, and J. M. H. Elmirghani, "On the energy efficiency of physical topology design for IP over WDM networks," *Journal of Lightwave Technology*, vol. 30, no. 12, pp. 1931–1942, 2012.
- [119] C. J. A. Bastos-Filho, D. R. B. Araujo, E. A. Barboza, D. a. R. Chaves, and J. F. Martins-Filho, "Design of transparent optical networks considering physical impairments, CAPEX and energy consumption," in *13th International Conference on Transparent Optical Networks (ICTON)*, Stockholm, Sweden, 2011, pp. 1–4.

- 
- [120] W. Yang, J.-H. Jung, and Y.-C. Kim, "Performance evaluation of energy saving in core router architecture with low power idle for OBS networks," in *IEEE International Conference on Information Networking (ICOIN)*, Kuala Lumpur, Malaysia, 2012, pp. 318–323.
- [121] K. Zhu and B. Mukherjee, "A review of traffic grooming in WDM optical networks: architectures and challenges," *Optical Networks Magazine*, vol. 4, no. 2, pp. 55–64, 2003.
- [122] K. Zhu and B. Mukherjee, "Traffic grooming in an optical WDM mesh network," *IEEE Journal on Selected Areas in Communications*, vol. 20, no. 1, pp. 122–133, 2002.
- [123] E. Modiano, "Traffic grooming in WDM networks," *IEEE Communications Magazine*, vol. 39, no. 7, pp. 124–129, 2001.
- [124] R. Dutta and G. N. Rouskas, "Traffic grooming in WDM networks: past and future," *IEEE Network*, vol. 16, no. 6, pp. 46–56, 2002.
- [125] R. Parthiban, R. Tucker, and C. Leckie, "Waveband grooming and IP aggregation in optical networks," *Journal of Lightwave Technology*, vol. 21, no. 11, pp. 2476–2488, 2003.
- [126] W. Hou, L. Guo, and X. Wang, "A new multi-granularity traffic grooming routing algorithm in IP over WDM networks," *Optik-International Journal for Light and Electron Optics*, vol. 122, no. 11, pp. 1019–1029, 2011.
- [127] M. Xia, M. Tornatore, Y. Zhang, P. Chowdhury, C. Martel, and B. Mukherjee, "Greening the optical backbone network: a traffic engineering approach," in *IEEE International Conference on Communications*, Capetown, South Africa, 2010, pp. 1–5.
- [128] B. Ramamurthy, S. Member, and B. Mukherjee, "Wavelength Conversion in WDM networking," *IEEE Journal on Selected Areas in Communications*, vol. 16, no. 7, pp. 1061–1073, 1998.
- [129] F. Vismara, V. Grkovic, F. Musumeci, and M. Tornatore, "On the energy efficiency of IP-over-WDM networks," in *IEEE Latin-American Conference on Communications (LATIN-COM)*, Bogota, Colombia, 2010, pp. 1–6.
- [130] G. Shen and R. S. Tucker, "Energy-minimized design for IP over WDM networks," *Journal of Optical Communications and Networking*, vol. 1, no. 1, pp. 176–186, 2009.
- [131] I. Cerutti, L. Valcarenghi, and P. Castoldi, "Designing power-efficient WDM ring networks," in *Networks for Grid Applications, Lecture Notes of the Institute for Computer Sciences, Social Informatics and Telecommunications Engineering*, 2010, vol. 25, pp. 101–108.
- [132] E. Yetginer and G. N. Rouskas, "Power efficient traffic grooming in optical WDM networks," in *IEEE Global Telecommunications Conference (GLOBECOM)*, Honolulu, Hawaii, USA, 2009, pp. 1–6.
- [133] A. Coiro, M. Listanti, T. Squarcia, A. Valenti, and F. Matera, "Energy-minimised virtual topology design in IP over WDM backbone networks," *IET Optoelectronics*, vol. 6, no. 4, pp. 165–172, 2012.
- [134] M. Hasan, F. Farahmand, and J. Jue, "Energy-awareness in dynamic traffic grooming," in *Optical Fiber Communication Conference/National Fiber Optic Engineers Conference (OFC/NFOEC)*, San Diego, CA, USA, 2010, pp. 6–8.
- [135] F. Farahmand, I. Cerutti, M. M. Hasan, and J. P. Jue, "Energy-efficiency of drop-and-continue traffic grooming," in *Optical Fiber Communication Conference/National Fiber Optic Engineers Conference (OFC/NFOEC)*, Los Angeles, CA, USA, 2011, pp. 3–5.

- 
- [136] L. Guo, W. Hou, and X. Wei, "Power efficient grooming based on optical bypass reconfiguration in green optical networks," *Optik-International Journal for Light and Electron Optics*, vol. 124, no. 5, pp. 437–445, 2013.
- [137] S. Zhang and D. Shen, "Energy efficient time-aware traffic grooming in wavelength routing networks," in *IEEE Global Telecommunications Conference (GLOBECOM)*, Miami, Florida, USA, 2010, pp. 1–5.
- [138] S. Zhang and D. Shen, "Energy-efficient traffic grooming in WDM networks with scheduled time traffic," *Journal of Lightwave Technology*, vol. 29, no. 17, pp. 2577–2584, 2011.
- [139] S. Yang and F. Kuipers, "Energy-aware path selection for scheduled lightpaths in IP-over-WDM networks," in *18th IEEE Symposium on Communications and Vehicular Technology in the Benelux*, Ghent, Belgium, 2011, pp. 1–6.
- [140] F. Farahmand and X. Huang, "Efficient online traffic grooming algorithms in WDM mesh networks with drop-and-continue node architecture," in *First International Conference on Broadband Networks*, San Jose, CA, USA, 2004, pp. 180–189.
- [141] M. Jinno, H. Takara, B. Kozicki, Y. Tsukishima, Y. Sone, and S. Matsuoka, "Spectrum-efficient and scalable elastic optical path network : architecture , benefits , and enabling technologies," *IEEE Communications Magazine*, vol. 47, no. 11, pp. 66–73, 2009.
- [142] G. Zhang, M. D. Leenheer, A. Morea, and B. Mukherjee, "A survey on OFDM-based elastic core optical networking," *IEEE Communications Surveys and Tutorials*, vol. 15, no. 1, pp. 65–87, 2013.
- [143] S. Zhang and B. Mukherjee, "Energy-efficient dynamic provisioning for spectrum elastic optical networks," in *IEEE International Conference on Communications*, Ottawa, ON, Canada, 2012, pp. 3031–3035.
- [144] Y. Wang, X. Cao, and S. Member, "Multi-granular waveband assignment and protection in WDM networks," *Journal of Lightwave Technology*, vol. 28, no. 13, pp. 2004–2013, 2010.
- [145] X. Cao, Y. Xiong, and C. Qiao, "Performance evaluation of wavelength band switching in multifiber all-optical networks," in *Twenty-second Annual Joint Conference of the IEEE Computer and Communications Societies (INFOCOM)*, San Francisco, CA, USA, 2003, pp. 2251–2261.
- [146] C. Xiaojun, V. Anand, Y. Xiong, and C. Qiao, "A study of waveband switching with multilayer multigranular optical cross-connects," *IEEE Journal on Selected Areas in Communications*, vol. 21, no. 7, pp. 1081–1095, 2003.
- [147] H. Le, H. Hasegawa, and K.-i. Sato, "Cost evaluation of hybrid-hierarchical optical cross-connects based optical path networks," in *Third International Conference on Communications and Electronics*, Nha Trang, Vietnam, 2010, pp. 40–45.
- [148] X. Zhang and L. Li, "Robust routing algorithms based on valiant load balancing for wavelength-division-multiplexing mesh networks," *Optical Engineering*, vol. 45, no. 8, p. Art No. 085003, 2006.
- [149] W. Hou, L. Guo, X. Wei, and X. Gong, "Multi-granularity and robust grooming in power- and port-cost-efficient IP over WDM networks," *Computer Networks*, vol. 56, no. 10, pp. 2383–2399, 2012.

- 
- [150] Zhang, X, L. Li, and S. Wang, "Valiant load-balanced robust routing algorithm for multi-granularity connection requests in traffic-grooming WDM mesh networks," *Computer Communications*, vol. 30, no. 18, pp. 3498–3507, 2007.
- [151] Y. Yamada, H. Hasegawa, and K.-I. Sato, "Hierarchical optical path network design algorithm considering waveband protection," *Journal of Lightwave Technology*, vol. 27, no. 24, pp. 5736–5748, 2009.
- [152] W. Hou, L. Guo, X. Gong, and Z. Sun, "Survivable power efficiency oriented integrated grooming in green networks," *Computer Communications*, vol. 36, no. 3, pp. 420–428, 2013.
- [153] L. Guo, X. Wang, W. Hou, Y. Li, H. Wang, H. Li, and C. Wang, "A new integrated auxiliary graph based routing algorithm in waveband switching optical networks?," *AEU - International Journal of Electronics and Communications*, vol. 64, no. 1, pp. 87–91, 2010.
- [154] W. Hou, L. Guo, X. Wang, J. Cao, J. Wu, and Y. Li, "A new routing algorithm based on integrated grooming auxiliary graph in multi-granularity optical networks," in *Fifth International Joint Conference on INC, IMS and IDC*, Seoul, Korea, 2009, pp. 462–467.
- [155] X. Wang, W. Hou, L. Guo, J. Cao, and D. Jiang, "A new multi-granular grooming algorithm based on traffic partitioning in IP over WDM networks," *Computer Networks*, vol. 55, no. 3, pp. 676–688, 2011.
- [156] W. Hou, L. Guo, X. Wang, and J. Wu, "Energy efficient algorithm with considering port cost in hybrid hierarchical optical networks," in *IEEE 5th International ICST Conference on Communications and Networking in China (CHINACOM)*, Beijing, China, 2010, pp. 1–12.
- [157] X. Wang, W. Hou, L. Guo, J. Cao, and D. Jiang, "Energy saving and cost reduction in multi-granularity green optical networks?," *Computer Networks*, vol. 55, no. 3, pp. 676–688, 2011.
- [158] N. Naas, B. Kantarci, and H. Mouftah, "Design considerations for energy-efficient multi-granular optical networks," in *8th International Symposium on High Capacity Optical Networks and Enabling Technologies (HONET)*, Riyadh, KSA, 2011, pp. 137–141.
- [159] N. Naas, B. Kantarci, and H. Mouftah, "Power and cost reduction in optical transport networks by multi-granular switching with optical reach consideration," in *26th Biennial Symposium on Communications*, Kingston, ON, Canada, 2012, pp. 70–73.
- [160] N. Naas, B. Kantarci, and H. Mouftah, "Energy-efficient design for multi-granular optical transport networks with optical reach consideration," *Optical Switching and Networking*, vol. 13, pp. 76–93, 2014.
- [161] S. J. B. Yoo, "All-optical regeneration for ultra-long fiber links and its prospects for future applications with new modulation formats," in *Optical Fiber Communication Conference and National Fiber Optic Engineers Conference (OFC/NFOEC)*, Washington, DC, USA, 2009, p. OThS4.
- [162] R. Hulserman, M. Gunkel, C. Meusburger, and D. A. Schukpe, "Cost modeling and evaluation of capital expenditures in optical multilayer networks," *Journal of Optical Communications and Networking*, vol. 7, no. 9, pp. 814–833, 2008.
- [163] M. Murakami and K. Oda, "Power consumption analysis of optical cross-connect equipment for future large capacity optical networks," in *11th International Conference on Transparent Optical Networks (ICTON)*, Azores, Portugal, 2009, pp. 1–4.

- 
- [164] M. Vasilyev, T. I. Lakoba, and P. G. Patki, "Multi-wavelength all-optical regeneration," in *Conference on Optical Fiber Communication/National Fiber Optic Engineers Conference (OFC/NFOEC)*, San Diego, CA, USA, 2008, pp. 1–3.
- [165] C. Labovitz, "The Internet after dark," 2009. [Online]. Available: <http://ddos.arbornetworks.com/2009/08/the-internet-after-dark/>
- [166] AMS-IX, "AMS-IX traffic statistics," 2012. [Online]. Available: <http://www.ams-ix.net/statistics/>.
- [167] M. Gupta and S. Singh, "Greening of the internet," in *Conference on Applications, Technologies, Architectures, and Protocols for Computer Communications*, New York, USA, 2003, pp. 19–26.
- [168] M. Gupta and S. Singh, "Using low-power modes for energy conservation in Ethernet LANs," in *26th IEEE International Conference on Computer Communications*, Anchorage, Alaska, USA, 2007, pp. 2451–2455.
- [169] S. Nedeveschi, J. Chandrashekar, J. Liu, B. Nordman, S. Ratnasamy, and N. Taft, "Skilled in the art of being idle: reducing energy waste in networked systems," in *6th USENIX symposium on Networked systems design and implementation*, Boston, USA, 2009, pp. 381–394.
- [170] S. Nedeveschi, L. Popa, and G. Iannaccone, "Reducing network energy consumption via sleeping and rate-adaptation," in *5th USENIX Symposium on Networked Systems Design and Implementation*, San Francisco, CA, USA, 2008, pp. 323–336.
- [171] L. Chiaraviglio and M. Mellia, "Reducing power consumption in backbone networks," in *IEEE International Conference on Communications (ICC)*, Dresden, Germany, 2009, pp. 1–6.
- [172] F. Idzikowski, S. Orłowski, C. Raack, H. Woesner, and A. Wolisz, "Saving energy in IP-over-WDM networks by switching off line cards in low-demand scenarios," in *14th Conference on Optical Network Design and Modeling (ONDM)*, Kyoto, Japan, 2010, pp. 1–6.
- [173] J. Chabarek, J. Sommers, P. Barford, C. Estan, D. Tsiang, and S. Wright, "Power awareness in network design and routing," in *The 27th Conference on Computer Communications (INFOCOM)*, Phoenix, AZ, USA, 2008, pp. 457–465.
- [174] A. Coiro, M. Listanti, A. Valenti, and F. Matera, "Reducing power consumption in wavelength routed networks by selective switch off of optical links," *IEEE Journal of Selected Topics*, vol. 17, no. 2, pp. 428–436, 2011.
- [175] M. Caria, M. Chamania, and A. Jukan, "A comparative performance study of load adaptive energy saving schemes for IP-over-WDM networks," *Journal of Optical Communications and Networking*, vol. 4, no. 3, pp. 152–164, 2012.
- [176] M. Gupta, S. Grover, and S. Singh, "A feasibility study for power management in LAN switches," in *12th IEEE International Conference on Network Protocols*, Berlin, Germany, 2004, pp. 361–371.
- [177] C. Gunaratne, K. Christensen, and B. Nordman, "Managing energy consumption costs in desktop PCs and LAN switches with proxying, split TCP connections, and scaling of link speed," *International Journal of Network Management*, vol. 15, no. 5, pp. 297–310, 2005.
- [178] J. C. Cardona Restrepo, C. G. Gruber, and C. Mas Machuca, "Energy profile aware routing," in *IEEE International Conference on Communications Workshops*, Dresden, Germany, 2009, pp. 1–5.

- 
- [179] A. Bianzino, C. Chaudet, F. Larroca, D. Rossi, and J. Rougier, "Energy-aware routing : a reality check," in *IEEE GLOBECOM 2010 Workshops (GC Wkshps)*, Miami, Florida, USA, 2010, pp. 1422–1427.
- [180] F. Idzikowski, S. Orłowski, C. Raack, and H. Woesner, "Dynamic routing at different layers in IP-over- WDM networks?maximizing energy savings," *Optical Switching and Networking*, vol. 8, no. 3, pp. 181–200, 2011.
- [181] A. Cianfrani, V. Eramo, M. Listanti, M. Marazza, and E. Vittorini, "An energy saving routing algorithm for a green OSPF protocol," in *IEEE Conference on Computer Communications Workshops (INFOCOM)*, San Diego, CA, USA, 2010, pp. 1–5.
- [182] L. Chiaraviglio, M. Mellia, and F. Neri, "Energy-aware backbone networks: a case study," in *IEEE International Conference on Communications (ICC)*, Dresden, Germany, 2009, pp. 1–5.
- [183] L. Chiaraviglio, M. Mellia, and F. Neri, "Minimizing ISP network energy cost: formulation and solutions," *IEEE/ACM Transactions on Networking*, vol. 20, no. 2, pp. 463–176, 2012.
- [184] L. Wu, L. Chiaraviglio, M. Mellia, and F. Neri, "Power-aware routing and wavelength assignment in optical networks," in *European Conference of Optical Communications (ECOC)*, Vienna, Austria, 2009, pp. 1–2.
- [185] A. Coiro, M. Listanti, A. Valenti, and M. Francesco, "Power-aware routing and wavelength assignment in multi-fiber optical networks," *Journal of Optical Communications and Networking*, vol. 3, no. 11, pp. 816–829, 2011.
- [186] Y. Zhang, M. Tornatore, P. Chowdhury, and B. Mukherjee, "Energy optimization in IP-over-WDM networks," *Optical Switching and Networking*, vol. 8, no. 3, pp. 171–180, 2011.
- [187] L. Chiaraviglio and A. Cianfrani, "On the effectiveness of sleep modes in backbone networks with limited configurations," in *20th International Conference on Software, Telecommunications and Computer Networks (SoftCOM 2012)*, Croatia, 2012, pp. 1–6.
- [188] E. Bonetto, L. Chiaraviglio, D. Cuda, F. Idzikowski, and F. Neri, "Exploiting traffic dynamics in power-aware logical topology design," in *European Conference and Exposition on Optical Communications*, Geneva, Switzerland, 2011, pp. 1–3.
- [189] A. Ahmad, A. Bianco, E. Bonetto, D. Cuda, G. Castillo, and Fabio Neri, "Power-aware logical topology design heuristics in wavelength-routing networks," in *Optical Network Design and Modeling (ONDM)*, Bologna, Italy, 2011, pp. 1–6.
- [190] F. Idzikowski, E. Bonetto, and L. Chiaraviglio, "EWA: an adaptive algorithm using watermarks for energy saving in IP-over-WDM networks," in *17th European Conference on Networks and Optical Communications (NOC)*, Vilanova i la Geltru , Spain, 2012, pp. 1–6.
- [191] E. Bonetto, L. Chiaraviglio, F. Idzikowski, and E. Le Rouzic, "Algorithms for the multi-period power-aware logical topology design with reconfiguration costs," *Journal of Optical Communications and Networking*, vol. 5, no. 5, pp. 394–410, 2013.
- [192] A. Gencata and B. Mukherjee, "Virtual-topology adaptation for WDM mesh networks under dynamic traffic," *IEEE/ACM Transactions on Networking*, vol. 11, no. 2, pp. 236–247, 2003.
- [193] B. G. Bathula and J. M. H. Elmirghani, "Energy efficient optical burst switched (OBS) networks," in *IEEE Globecom Workshops*, Honolulu, Hawaii, USA, 2009, pp. 1–6.

- [194] W. Yang, M. Ahmed, K. Lee, and Y. Kim, "Analysis of energy consumption in edge router with sleep mode for green OBS networks," in *Grid and Pervasive Computing*, vol. 7861, pp. 873–879, 2013.
- [195] D.-k. Kang, W.-h. Yang, J.-y. Lee, and Y.-c. Kim, "Dynamic time based burst assemble scheme to reduce energy consumption in DBS network with low-power idle," in *IEEE 16th Asia-Pacific Conference on Communications (APCC)*, Seoul, Korea, 2010, pp. 183–187.
- [196] D.-k. Kang, W.-H. Yang, R. Xie, and Y.-C. Kim, "Impact of traffic patterns and burst assembly on energy consumption in OBS networks," in *12th International Conference on Computer Modelling and Simulation*, Cambridge, United Kingdom, 2010, pp. 609–614.
- [197] D. Kang, W. Yang, and J. Jung, "Wake transition decision algorithm for energy saving in OBS network with LPI," in *IEEE International Conference on Computing, Networking and Communications (ICNC)*, Maui, Hawaii, USA, 2012, pp. 527–531.
- [198] B. Nordman and K. Christensen, "Proxying: the next step in reducing IT energy use," *IEEE Computer*, vol. 43, no. 1, pp. 91–93, 2010.
- [199] S. Herreria-Alonso and M. Rodriguez-Perez, "A Power saving model for burst transmission in energy-efficient Ethernet," *IEEE Communications Letters*, vol. 15, no. 5, pp. 584–586, 2011.
- [200] M. Yamada, T. Yazaki, N. Matsuyama, and T. Hayashi, "Power efficient approach and performance control for routers," in *International Conference on Communications Workshops GreenComm*, Dresden, Germany, 2009, pp. 1–5.
- [201] R. Bolla, R. Bruschi, A. Cianfrani, and M. Listanti, "Enabling backbone networks to sleep," *IEEE Network*, vol. 25, no. 2, pp. 26–31, 2011.
- [202] Y. Wang, E. Keller, B. Biskeborn, J. van der Merwe, and J. Rexford, "Virtual routers on the move: live router migration as a network-management primitive," *ACM SIGCOMM Computer Communication Review*, vol. 38, no. 4, pp. 231–242, 2008.
- [203] Infinera, "Infinera introduces new line system, sets new standard for capacity," 2008. [Online]. Available: <http://www.infinera.com/j7/servlet/NewsItem?newsItemID=108>
- [204] Ciena, "Evolution to the 100G transport network," *Cienna white paper*, vol. -, no. -, pp. 1–7, 2007.
- [205] A. Klekamp, U. Gebhard, and F. Ilchmann, "Energy and cost efficiency of adaptive and mixed-line-rate IP over DWDM networks," *Journal of Lightwave Technology*, vol. 30, no. 2, pp. 215–221, 2012.
- [206] C. Gunaratne and K. Christensen, "Ethernet adaptive link rate: system design and performance evaluation," in *31st IEEE Conference on Local Computer Networks*, Tampa, Florida, USA, 2006, pp. 28–35.
- [207] C. Gunaratne, K. Christensen, B. Nordman, and S. Suen, "Reducing the energy consumption of Ethernet with adaptive link rate (ALR)," *IEEE Transactions on Computers*, vol. 57, no. 4, pp. 448–461, 2007.
- [208] B. Nordman, "Reducing the energy consumption of network devices," Tech. Rep., 2005. [Online]. Available: <http://scholar.google.com/scholar?hl=en&btnG=Search&q=intitle:Reducing+the+energy+consumption+of+network+devices\#1>

- 
- [209] S. Antonakopoulos, S. Fortune, L. Zhang, B. Laboratories, and M. H. Nj, "Power-aware routing with rate-adaptive network elements," in *GLOBECOM Workshops*, Miami, Florida, USA, 2010, pp. 1428–1432.
- [210] A. Klekamp, U. Gebhard, and F. Ilchmann, "Efficiency of adaptive and mixed-line-rate IP over DWDM networks regarding CAPEX and power consumption," *Journal of Optical Communications and Networking*, vol. 4, no. 11, pp. B11–B16, 2012.
- [211] A. Nag and M. Tornatore, "Transparent optical network design with mixed line rates," in *IEEE Advanced Networks and Telecommunications Systems*, Mumbai, India, 2008, pp. 1–3.
- [212] S. Chandrasekhar and X. Liu, "Impact of channel plan and dispersion map on hybrid DWDM transmission of 42.7Gb/s DQPSK and 10.7Gb/s OOK on 50Ghz grid," *IEEE Photonics Technology Letters*, vol. 19, no. 22, pp. 1801–1803, 2007.
- [213] B. Zhang, K. Sabhanatarajan, A. Gordon-Ross, and A. George, "Real-time performance analysis of adaptive link rate," in *33rd IEEE Conference on Local Computer Networks (LCN)*, Montreal, Quebec, Canada, 2008, pp. 282–288.
- [214] M. Jinno, B. Kozicki, H. Takara, A. Watanabe, and Y. Sone, "Distance-adaptive spectrum resource allocation in spectrum-sliced elastic optical path (SLICE) networks," *IEEE Communications Magazine*, vol. 48, no. 8, pp. 138–145, 2010.
- [215] R. Kubo, J.-i. Kani, Y. Fujimoto, N. Yoshimoto, and K. Kumozaki, "Sleep and adaptive link rate control for power saving in 10G-EPON systems," in *IEEE Global Telecommunications Conference (GLOBECOM)*, Hoboken, NJ, USA, 2009, pp. 1–6.
- [216] R. Kubo, J.-i. Kani, H. Ujikawa, T. Sakamoto, Y. Fujimoto, N. Yoshimoto, and H. Hadama, "Study and demonstration of sleep and adaptive link rate control mechanisms for energy efficient 10G-EPON," *Journal of Optical Communications and Networking*, vol. 2, no. 9, pp. 716–729, 2010.
- [217] A. Francini and D. Stiliadis, "Performance bounds of rate-adaptation schemes for energy-efficient routers," in *High Performance Switching and Routing (HPSR)*, TX, USA, 2010, pp. 175–182.
- [218] A. Klekamp, U. Gebhard, and F. Ilchmann, "Efficiency of adaptive and mixed-line-rate IP over DWDM networks regarding CAPEX and power consumption," in *Optical Fiber Communication Conference (OFC/NOFC)*, Los Angeles, CA, USA, 2012, pp. 1–3.
- [219] J. Vizcaino, Y. Ye, and I. Monroy, "Energy efficiency analysis for dynamic routing in optical transport networks," in *IEEE International Conference on Communications (ICC)*, Ottawa, ON, Canada, 2012, pp. 3009–3014.
- [220] J. Vizcaino, Y. Ye, and I. Monroy, "Energy efficiency analysis for flexible-grid OFDM-based optical networks," in *Computer Networks*, 2012, pp. 3042–4047.
- [221] J. Lopez, Y. Yabin, V. Lopez, F. Jimenez, R. Duque, P. Krummrich, F. Musumeci, M. Tornatore, and A. Pattavina, "Traffic and power-aware protection scheme in elastic optical networks," in *XVth International Telecommunications Network Strategy and Planning Symposium (NETWORKS)*, Rome, Italy, 2012, pp. 1–6.
- [222] IEE, "ICT core networks : towards a scalable , energy- efficient future," Tech. Rep., 2013. [Online]. Available: <http://iee.ucsb.edu/ICT2013/Report>
- [223] EConet, "Low energy consumption networks," 2013. [Online]. Available: <http://www.econet-project.eu/>

- [224] GreenTouch, "Greentouch green meter research study: reducing the net energy consumption in communications networks by up to 90% by 2020," 2013. [Online]. Available: <http://www.greentouch.org/uploads/documents/GreenTouch.Green.Meter.Research.Study.26.June.2013.pdf>
- [225] Alcatel Lucent, "Developing eco-sustainable networks," 2012. [Online]. Available: <http://www.alcatel-lucent.com/sustainability/developing-eco-sustainable-networks>
- [226] International Telecommunications Union, "NGNs and energy efficiency," Tech. Rep., 2008. [Online]. Available: [http://www.itu.int/dms\\_pub/itu-t/oth/23/01/T23010000070002PDFE.pdf](http://www.itu.int/dms_pub/itu-t/oth/23/01/T23010000070002PDFE.pdf)
- [227] Cisco, "Cisco honored by AT&T with 2012 supplier sustainability award in energy efficiency," 2013. [Online]. Available: <http://newsroom.cisco.com/release/1146256/Cisco-Honored-by-AT-T-With-2012-Supplier-Sustainability-Award-in-newline-Energy-Efficiency>
- [228] Juniper Networks, "Verizon to deploy Juniper networks PTX series in U.S. and European markets," 2012. [Online]. Available: <http://newsroom.juniper.net/manual-releases/2012/Verizon-to-Deploy-the-Industry?s-First-Eight-Terab>
- [229] Business Wire, "Japanese service provider increases performance and lowers power consumption with Juniper networks ethernet services routers," 2008. [Online]. Available: <http://www.thefreelibrary.com/Japanese+Service+Provider+Increases+Performance+and+Lowers+Power...-a0188341003>
- [230] Infinera, "Infinera's 400 Gb/s PIC sets new record for integration." [Online]. Available: <http://www.infinera.com/j7/servlet/NewsItem?newsItemID=150>
- [231] Fujitsu, "Fujitsu sets standard for energy efficiency in optical networks with FLASHWAVE 4500 platform," 2010. [Online]. Available: <http://www.fujitsu.com/us/news/pr/fnc.20100630.html>
- [232] Fujitsu, "Fujitsu develops world's first technology to increase efficiency of in-Service optical network resources," 2012. [Online]. Available: <http://www.fujitsu.com/global/news/pr/archives/month/2012/20120919-01.html>
- [233] MRV, "MRV lambda driver optical transport system meets service provider energy efficiency specification," 2010. [Online]. Available: <http://www.mrv.com/company/news/press-releases/newline/newlinemrv-lambdadriverr-optical-transport-system-meets-newline-provider-energy-efficiency-specification>
- [234] Huawei, "100G stands tall with a strong backbone," 2012. [Online]. Available: <http://www.huawei.com/en/about-huawei/publications/communicate/hw-079444.htm>
- [235] S. Alexander, "Transforming networks," 2013. [Online]. Available: <http://iee.ucsb.edu/files/01SteveAlexander2013-04-01UCSBEnergyConferenceSBA.pdf>
- [236] Multichannel-News, "Comcast paves way for 400-Gig backbone links," 2013. [Online]. Available: <http://www.multichannel.com/news/cable-operators/comcast-paves-way-400-gig-backbone-links/326052>
- [237] S. Ferdousi, A. Nag, and A. Reaz, "Mixed-Line-Rate (MLR) optical network design with wavebanding," in *IEEE 4th International Symposium on Advanced Networks and Telecommunication Systems*, Mumbai, India, 2010, pp. 46–48.

- 
- [238] S. Ferdousi, A. Nag, A. S. Reaz, M. Tornatore, and B. Mukherjee, "Mixed-line-rate optical network design with wavebanding," *Optical Switching and Networking*, vol. 9, no. 4, pp. 286–296, 2012.
- [239] A. Srinivasan and R. Parthiban, "Sparse grooming sites in all-optical networks," in *International Conference On Photonics*, Langkawi, Kedah, Malaysia, 2010, pp. 1–5.
- [240] B. Chen, G. N. Rouskas, and R. Dutta, "On hierarchical traffic grooming in WDM networks," *IEEE/ACM Transactions on Networking*, vol. 16, no. 5, pp. 1226–1238, 2008.
- [241] L. Cox, J. Sanchez, and L. Lu, "Cost savings from optimized packing and grooming optical circuits: Mesh versus ring comparisons," *Optical Networks Magazine*, vol. 2, no. 3, pp. 72–90, 2001.
- [242] S. Gangxiang, R. R. S. Tucker, and G. Shen, "Sparse Traffic Grooming in Translucent Optical Networks," *Journal of Lightwave Technology*, vol. 27, no. 20, pp. 4471–4479, 2009.
- [243] Y. Wang, M. Li, and B. Ramamurthy, "Performance analysis of sparse traffic grooming in WDM mesh networks," in *IEEE international Conference on Communications*, Seoul, Korea, 2005, pp. 1766–1770.
- [244] G. Shen, W. Grover, T. Cheng, and S. Bose, "Sparse placement of electronic switching nodes for low blocking in translucent optical networks," *Journal of Optical Networking*, vol. 1, no. 12, pp. 424–441, 2002.
- [245] G. Shen and R. Tucker, "Sparse traffic grooming in translucent optical networks," *Journal of Lightwave Technology*, vol. 27, no. 20, pp. 4471–4479, 2009.
- [246] K. Zhu, H. Zang, and B. Mukherjee, "Design of WDM mesh networks with sparse grooming capability," in *Global Telecommunications Conference (GLOBECOM)*, Taipei, Taiwan, 2002, pp. 2696–2700.
- [247] A. Srinivasan, "Optimization Techniques for All-Optical Networks." M.S. thesis, Dept. Elect. Comp. Sys. Eng., Monash. Univ., Malaysia. 2010
- [248] S. K. Korotky, "Semi-empirical description and projection of Internet traffic trends using hyperbolic compound annual growth rate," *Bell Labs Technical Journal*, vol. 18, no. 3, pp. 5–21, 2013.
- [249] A. Dwivedi and R. Wagner, "Traffic model for USA long-distance optical network," in *Optical Fiber Communication Conference*, Baltimore, MD, USA, 2000, pp. 156–158.
- [250] M. Vaughn and R. Wagner, "Metropolitan network traffic demand study," in *IEEE 13th Annual Lasers and Electro-Optics Society (LEOS) Meeting*, Rio Grande, USA, 2000, pp. 102–103.
- [251] Fujitsu Network Communications, "Fujitsu Flashwave 7700." [Online]. Available: <http://www.fujitsu.com/downloads/IN/fw7700.pdf>
- [252] A. Dacomo, S. D. Patre, G. Maier, A. Pattavina, and M. Martinelli, "Design of static resilient WDM mesh networks with multiple heuristic criteria," in *The 21st Annual Joint Conference of the IEEE Computer and Communications Societies (INFOCOM)*, 2002, New York, USA pp. 1793–1802.
- [253] A. Srinivasan and R. Parthiban, "A Heuristic Algorithm for Topological Optimization of All-Optical Networks," in *World Congress on Computer Science and Information Engineering*, Los Angeles, CA, USA, 2009, pp. 288–292.

- 
- [254] F. Rambach, B. Konrad, L. Dembeck, U. Gebhard, M. Gunkel, M. Quagliotti, L. Serra, and V. López, "A Multilayer Cost Model for Metro/Core Networks," *Journal of Optical Communications and Networking*, vol. 5, no. 3, p. 210, 2013.
- [255] Malcolm Turnbull, "The Coalition's plan for fast broadband and a fast NBN," Tech. Rep., 2013. [Online]. Available: <http://www.malcolmturnbull.com.au/wp-content/uploads/2013/04/Background.pdf>
- [256] BIS-Shrapnel, "Telecommunications infrastructure in Australia 2001," Tech. Rep., 2001. [Online] Available: <https://www.accc.gov.au/publications>
- [257] W. Fisher, M. Suchara, and J. Rexford, "Greening backbone networks : reducing energy consumption by shutting off cables in bundled links," in *Frst ACM SIGCOMM workshop on Green networking*, New Delhi, India, 2010, pp. 29–34.
- [258] K. Manousakis, A. Angeletou, and E. M. Varvarigos, "Energy Efficient RWA Strategies for WDM Optical Networks," *Journal of Optical Communications and Networking*, vol. 5, no. 4, p. 338, 2013.
- [259] Y. Miyao and H. Saito, "Optimal design and evaluation of survivable WDM trasport networks," *IEEE Journal on Selected Areas in Communications*, vol. 16, no. 7, pp. 1190–1198, 1998.
- [260] G. Maier, A. Pattavina, S. D. Patre, and M. Martinelli, "Optical network survivability : protection techniques in the WDM layer," *Photonic Network Communications*, vol. 4, no. 3–4, pp. 251–269, 2002.
- [261] M. Tornatore, G. Maier, and A. Pattavina, "WDM network optimization by ILP based on source formulation," in *INFOCOM 2002*, New York, USA, 2002, pp. 1813–1821.
- [262] N. Singhal and B. Mukherjee, "Architectures and algorithm for multicasting in WDM optical mesh networks using opaque and transparent optical cross-connects," in *Optical Fiber Communication Conference and Exhibition (OFC)*, Anaheim, CA, USA, 2001, p. TuG8 (1–3).
- [263] X. Wang, M. Chen, Q. Wang, M. Huang, and J. Cao, "Research on the virtual topology design methods in grid-computing-supporting IP/DWDM-based NGI," in *Grid and Cooperative Computing - GCC 2004*, 2004, pp. 277–284.
- [264] Ciena, "Dense Wavelength Division Multiplexing," Tech. Rep., [Online]. Available: <http://www.techguide.com>
- [265] R. Ramaswami, K. Sivarajan, and G. Sasaki, *Optical networks: A practical perspective*, 3rd ed. Burlington, Massachusetts: Morgan Kaufmann, 2010.
- [266] H. Zhu, H. Zang, K. Zhu, and B. Mukherjee, "A novel generic graph model for traffic grooming in heterogeneous WDM mesh networks," *IEEE/ACM Transactions on Networking*, vol. 11, no. 2, pp. 285–299, 2003.
- [267] A. Kakekhani and A. G. Rahbar, "A novel QoT-aware routing and wavelength assignment algorithm in all-optical networks," *Optical Fiber Technology*, vol. 17, no. 3, pp. 145–155, 2011.
- [268] X. Sun, Y. Li, I. Lambadaris, and Y. Q. Zhao, "Performance Analysis of First-Fit Wavelength Assignment Algorithm in Optical Networks." in *7th International Conference on Telecommunications*, Zagreb, Croatia, 2003, pp. 403–409.

- 
- [269] Infinera, "Infinera Optical Line Amplifier, EDFA," 2010. [Online]. Available: [http://www.infinera.com/pdfs/ola/infinera\\_ola\\_data\\_sheet.pdf](http://www.infinera.com/pdfs/ola/infinera_ola_data_sheet.pdf)
- [270] M. Ruffini, D. O'Mahony, and L. Doyle, "A cost analysis of Optical IP Switching in new generation optical networks," in *IEEE International Conference on Photonics in Switching*, Heraklion, Crete, 2006, pp. 1–3.
- [271] M. Gunkel, R. Leppla, and M. Wade, "A cost model for the WDM layer," *IEEE International Conference on Photonics in Switching*, Heraklion, Crete, 2006, pp. 3–8.
- [272] Kernel-Software-Inc, "CISCO price list as of 28 May 2013." [Online]. Available: <http://www.kernelsoftware.com/products/catalog/cisco.html>
- [273] Fiber Optics For Sale Co., "Fiber optics for sale co. complete supply solutions." [Online]. Available: <http://www.fiberoptics4sale.com/>
- [274] Fiber Store, "Source of Optic Communications." [Online]. Available: [www.fiberstore.com](http://www.fiberstore.com)
- [275] Ceragon Networks, "Mobile Backhaul : Fiber vs. Microwave (Case study analyzing various backhaul technology strategies)," *Ceragon white paper*, pp. 1–7, 2009.
- [276] X. Gaoxi, L. Yiu-Wing, and H. Kwok-Wak, "Two-stage cut saturation algorithm for designing all-optical networks," *IEEE Transactions on Communications*, vol. 49, no. 6, pp. 1102–1115, 2001.
- [277] R. Hulsermann, S. Bodamer, M. Berry, A. Betker, C. Guager, M. Jager, M. Kohn, and J. Spath, "A set of typical transport network scenarios for network modelling," in *5th ITG Workshop on Photonic Networks*, Leipzig, Germany, 2004, pp. 65–71.
- [278] A. Betker, C. Gerlach, R. Hulsermann, M. Jager, M. Barry, S. Bodamer, J. Spath, C. Gauger, and M. Kohn, "Reference transport network scenarios," Tech. Rep., 2003. [Online]. Available: [http://wall.ikr.uni-stuttgart.de/printable/Content/IKRSimLib/Usage/Referenz\\_Netze.v14\\_full.pdf](http://wall.ikr.uni-stuttgart.de/printable/Content/IKRSimLib/Usage/Referenz_Netze.v14_full.pdf)
- [279] J. Kowalski and B. Warfield, "Modelling traffic demand between nodes in a telecommunications network," in *Australasian Telecommunication Networks and Applications (ATNAC)*, 1995.
- [280] U.S. Energy Information Administration, "Electric power monthly May 2012," Tech. Rep., 2012. [Online]. Available: [http://www.eia.gov/electricity/monthly/current\\_year/may2012.pdf](http://www.eia.gov/electricity/monthly/current_year/may2012.pdf)
- [281] K. Harada, K. Shimizu, T. Kudou, and T. Ozeki, "Hierarchical optical path cross-connect systems for large scale WDM networks," *International Conference on Integrated Optics and Optical Fiber Communication (OFC/IOOC)*, San Diego, CA, USA, 1999, pp. 356–358.
- [282] X. Cao, V. Anand, and C. Qiao, "Framework for waveband switching in multigranular optical networks: part I-multigranular cross-connect architectures," *Journal of Optical Networking*, vol. 5, no. 12, pp. 1043–1055, 2006.
- [283] R. Izmailov, S. Ganguly, V. Kleptsyn, and A. Varsou, "Nonuniform waveband hierarchy in hybrid optical networks," in *22nd Annual Joint Conference of the IEEE Computer and Communications Societies (INFOCOM)*, San Francisco, CA, USA, 2003, pp. 1344–1354.
- [284] M. Li and B. Ramamurthy, "Integrated intermediate waveband and wavelength switching for optical WDM mesh networks," Barcelona, Spain, 2006, pp. 1–12

- [285] R. Izmailov, S. Ganguly, T. Wang, Y. Suemura, Y. Maeno, and S. Araki, "Hybrid hierarchical optical networks," *IEEE Communications Magazine*, vol. 40, no. 11, pp. 88–94, 2002.
- [286] J.-Y. Lai, Y.-J. Liu, H.-Y. Wu, Y.-H. Chen, and S.-D. Yang, "Engineered multiwavelength conversion using non periodic optical superlattice optimized by genetic algorithm" *Optics express*, vol. 18, no. 5, pp. 5328–37, 2010.
- [287] S. Varma and J. Jue, "Regenerator site selection in waveband optical networks supporting mixed line rates," in *IEEE Global Telecommunications Conference (GLOBECOM)*, Houston, TX, USA, 2011, pp. 1–5.
- [288] S. Varma and J. Jue, "Regenerator site selection in mixed line rate waveband optical networks," *Journal of Optical Communications and Networking*, vol. 5, no. 3, pp. 198–209, 2013.
- [289] J. Simmons, "On determining the optimal optical reach for a long-haul network," *Journal of Lightwave Technology*, vol. 23, no. 3, pp. 1039–1048, 2005.
- [290] G. Zhang, L. Nelson, Y. Pan, M. Birk, C. Skolnick, C. Rasmussen, M. Givhchi, B. Mikkelsen, T. Scherer, T. Downs, and W. Keil, "3760km, 100G SSMF transmission over commercial terrestrial DWDM ROADM systems using SD-FEC," in *Optical Fiber Communication Conference and National Fiber Optic Engineers Conference (OFC/NFOEC)*, Los Angeles, CA, 2012, pp. PDP5D (1–3).
- [291] B. Mukherjee, *Optical WDM networks*, New York: Springer Science & Business Media, 2006.
- [292] Y. Chen, C. Qiao, and X. Yu, "Optical burst switching : A new area in optical networking research," *IEEE Network*, vol. 18, no. 3, pp. 16–23, 2004.
- [293] P. V. Mieghem, *Performance analysis of communications networks and systems*, Melbourne, Australia: Cambridge Univ. Press, 2006.
- [294] P. Reviriego, J. Maestro, J. Hernandez, and D. Larrabeiti, "Burst transmission for energy-efficient ethernet," *IEEE Internet Computing*, vol. 14, no. 4, pp. 50–57, 2010.
- [295] Cisco, "Cisco CRS 4-Port OC-192c / STM-64c POS / DPT Interface Module," [Online]. Available: [http://www.cisco.com/c/en/us/products/collateral/routers/crs-1-16-slot-single-shelf-system/product\\_data\\_sheet09186a008022d5ef.html](http://www.cisco.com/c/en/us/products/collateral/routers/crs-1-16-slot-single-shelf-system/product_data_sheet09186a008022d5ef.html)
- [296] Cisco, "Cisco CRS-1 4-slot single-shelf system." [Online]. Available: [http://www.cisco.com/c/en/us/products/collateral/routers/carrier-routing-system/CRS-3.4-Slot\\_DS.pdf](http://www.cisco.com/c/en/us/products/collateral/routers/carrier-routing-system/CRS-3.4-Slot_DS.pdf)
- [297] K. Vlachos, "Optical Burst Switching," in *Encyclopedia of Internet Technologies and Applications*, Hershey, Pennsylvania: IGI Global, 2008. 375–382.
- [298] M. Duser, E. Kozlovski, R. I. Killey, and P. Bayvel, "Design trade-offs in optical burst switched networks with dynamic wavelength allocation," in *26th European Conference on Optical Communication*, Berlin, Germany, 2000, pp. 23–24.
- [299] M. Duser and P. Bayvel, "Analysis of wavelength-routed optical burst-switched network performance," *Fiber and Integrated Optics*, vol. 21, no. 6, pp. 471–477, 2002.
- [300] Z. Rosberg and M. Zukerman, "Burst segmentation benefit in optical switching," *IEEE Communications Letters*, vol. 7, no. 3, pp. 127–129, 2003.

- [301] V. Vokkarane, J. Jue, and S. Sitaraman, "Burst segmentation: an approach for reducing packet loss in optical burst switched networks," in *IEEE International Conference on Communications (ICC )*, 2002, pp. 2673–2677.